Aus dem
Institut für Pharmakologie und Toxikologie
des Universitätsklinikums Bonn
Direktor: Univ.-Prof. Dr. med. Alexander Pfeifer

Molekular-pharmakologische Ansätze zur Sensitivierung von Glioblastom-Zellen gegenüber Temozolomid

Habilitationsschrift
zur Erlangung der venia legendi
der Hohen Medizinischen Fakultät
der Rheinischen Friedrich-Wilhelms-Universität Bonn
für das Lehrgebiet
„Pharmakologie und Toxikologie“

Vorgelegt von
Dr. rer. nat. Bernd-Bodo Haas
Wissenschaftler am Bundesinstitut für Arzneimittel und
Medizinprodukte (BfArM), Bonn
Bonn 2026

Die folgenden aufgelisteten fünf Originalarbeiten liegen der kumulativen Habilitationsschrift zu Grunde, welche die wesentlichen Ergebnisse der Publikationen zusammenfasst und diskutiert.

1. **Haas B**, Klinger V, Keksel C, Bonigut V, Kiefer D, Caspers J, Walther J, Wos-Maganga M, Weickhardt S, Rohn G, Timmer M, Frotschl R, Eckstein N. Inhibition of the PI3K but not the MEK/ERK pathway sensitizes human glioma cells to alkylating drugs. Cancer Cell Int. 2018;18:69.
   DOI: https://doi.org/10.1186/s12935-018-0565-4
2. **Haas B**, Schutte L, Wos-Maganga M, Weickhardt S, Timmer M, Eckstein N. Thioredoxin Confers Intrinsic Resistance to Cytostatic Drugs in Human Glioma Cells. Int J Mol Sci. 2018;19(10).
   DOI: https://doi.org/10.3390/ijms19102874
3. Kaina B, Beltzig L, Piee-Staffa A, **Haas B**. Cytotoxic and Senolytic Effects of Methadone in Combination with Temozolomide in Glioblastoma Cells. Int J Mol Sci. 2020;21(19).
   DOI: https://doi.org/10.3390/ijms21197006
4. **Haas B**, Ciftcioglu J, Jermar S, Weickhardt S, Eckstein N, Kaina B. Methadone-mediated sensitization of glioblastoma cells is drug and cell line dependent. J Cancer Res Clin Oncol. 2021;147(3):779-792.
   DOI: https://doi.org/10.1007/s00432-020-03485-3
5. **Haas B**, Roth I, Sacker L, Wos-Maganga M, Beltzig L, Kaina B. Apoptotic and senolytic effects of hERG/Eag1 channel blockers in combination with temozolomide in human glioblastoma cells. Naunyn Schmiedebergs Arch Pharmacol. 2025;398(9):12267-12278.
   DOI: https://doi.org/10.1007/s00210-025-03955-w

Habilitationsdatum: 15.04.2026

1 Inhaltsverzeichnis

Für Niels †

Abkürzungsverzeichnis

AIC	5(4)-aminoimidazol-4(5)-carboxamid
ASK1	*Apoptosis Signal-regulated Kinase 1*
ATM	*Ataxia Telangiectasia Mutated*
ATR	*Ataxia Telangiectasia and Rad3-related*
BER	*Base Excision Repair*/Basenexzisionsreparatur
CBTRUS	*Central Brain Tumor Registry of the United States*
CDK	*Cyclin-dependent Kinase*
CUSP9	*Coordinated Undermining of Survival Paths with nine repurposed drugs*
DNA	*Deoxyribonucleic Acid*
E2F	*Transcription Factor E2F*
Eag1	*Human Ether-à-go-go Type 1*
EGFR	*Epidermal Growth Factor Receptor*
EMT	epithelial-mesenchymale Transition
ERK	*Extracellular Signal-regulated Kinase*
FACS	*Fluorescence-activated Cell Sorting*
GBR2	*Growth Factor Receptor-bound Protein*
γH2AX	*phosphorylated (Serin 139) Histon H2AX*
hERG	*Human Ether-à-go-go-related Gene*
IC_{50}	mittlere inhibitorische Konzentration
IDH	*Isocitrate Dehydrogenase*
JNK	*c-Jun N-terminal Kinase*
KCNH	*Potassium Voltage-Gated Channel Subfamily H*
KOF	Körperoberfläche
MAPK	*Mitogen-activated Protein Kinase*
MDM2	*Mouse Double Minute 2 Homolog*
MGMT	*O^6-methylguanin-DNA Methyltransferase*
MMR	*Mismatch repair/*Fehlpaarungsreparatur
MPG	*N-methylpurine-DNA Glycosylase*
MSH2/MSH6	*MutS Homolg 2 und 6*
MTIC	5-(3-N-methyltriazen-1-yl)-imidazol-4-carboxamid
mTOR	*Mammalian Target of Rapamycin*
MTT	3-(4,5-dimethylthiazol-2-yl)-2,5-diphenyltetrazolium bromid

NF1	*Neurofibromin 1*
NFκB	*Nuclear Factor κB*
N^3meA	*N^3-Methyladenine*
N^7meG	*N^7-Methylguanine*
O^6meG	*O^6-Methylguanine*
PARP1	*Poly(ADP-ribose)-Polymerase 1*
PDGFR	*Platelet-derived Growth Factor Receptor*
P-gp	*P-Glycoprotein*
PI3K	*Phosphoinositide-3-Kinase*
PIP_2	*Phosphatidylinositol 4,5-bisphosphate*
PIP_3	*Phosphatidylinositol (3,4,5)-trisphosphate*
PKA	*Protein kinase A*
pRB	*Retinoblastoma Protein*
PTEN	*Phosphatase and Tensin Homolog*
pTERT	*Telomerase Reverse Transcriptase Promotor*
RAF	*Rapidly Accelerated Fibrosarcoma*
RAS	*Rat Sarcoma*
RTK	Rezeptortyrosinkinase
SOS	*Son of Sevenless*
TCGA	*The Cancer Genome Atlas Program*
TMZ	Temozolomid
Trx	*Thioredoxin*
TrxR	*Thioredoxin Reductase*
VEGF	*Vascular Endothelial Growth Factor*
WHO	*World Health Organization*/Weltgesundheitsorganisation

2 Einleitung

Tumore des zentralen Nervensystems (ZNS) treten mit einer Inzidenz von etwa 25 von 100 000 Personen pro Jahr auf (Price et al., 2024). 95% dieser Tumore finden sich im Gehirn und zeichnen sich durch eine hohe Morbidität und Mortalität aus, da sie lokal begrenzt sind und invasiv wachsen. In Deutschland liegen die relativen 5-Jahres-Überlebensraten für bösartige ZNS-Tumore für Frauen bei 23 % und für Männer bei 21 % (RKI, 2020). Man unterscheidet zwischen primären Hirntumoren, die ihren Ursprung im Gehirn haben, und sekundären Hirntumoren, die durch Metastasierung außerhalb des Gehirns liegender Tumore entstanden sind und fünf- bis zehnmal häufiger sind als primäre Hirntumore (Lamba et al., 2021). Der bei weitem häufigste primäre Hirntumor ist ein gutartiger Hirnhauttumor (benignes Meningiom), Gliome machen etwa 30% aller primären Hirntumore aus. Allerdings sind 80 % der Gliome bösartig und für die meisten Todesfälle verantwortlich (Price et al., 2024).

2.1 Gliome

Gliome sind eine heterogene Gruppe von Tumoren, die sich aus dem Stützgewebe (Glia) des Gehirns entwickeln. Sie können aus drei verschiedenen glialen Zelltypen entstehen, den Astrozyten, den Oligodendrozyten und den Ependymozyten (Weller et al., 2024). Nach der Klassifikation der Weltgesundheitsorganisation (*World Health Organization*, WHO) werden sie nach ihren histologischen Merkmalen und definierten genetischen Markern diagnostiziert (Weller et al., 2022). Die WHO-Klassifikation unterscheidet drei Hauptgruppen von Gliomen basierend auf dem Erkrankungsalter, da sich pädiatrische und adulte Gliome sowohl genetisch als auch klinisch stark unterscheiden können: (1) diffuse Gliome vom adulten Typ, (2) diffuse niedriggradige Gliome vom pädiatrischen Typ und (3) diffuse hochgradige Gliome vom pädiatrischen Typ. Diffuse Gliome vom adulten Typ finden sich hauptsächlich oberhalb des Tentoriums und machen über 90 % der Gliome aus (Price et al., 2024). Neben histologischen Kriterien werden sie von der WHO auch genetisch wie folgt klassifiziert: Astrozytom *Isocitrate Dehydrogenase 1* oder *2* (*IDH*)-mutiert (Grad 2, 3 oder 4), Oligodendrogliom *IDH*-mutiert mit kombiniertem Verlust der Chromosomenarme 1p und 19q (1p/q19-Kodeletion) (Grad 2 oder 3) und das *IDH*-wildtyp-Glioblastom (Grad 4) (Komori, 2022; Louis et al., 2021).

Obwohl bei der Behandlung von Gliomen des Grades 2 und 3 mit einer Kombination aus Chemo- und Strahlentherapie mittlerweile sehr gute Fortschritte in Bezug auf die

Mortalität erzielt wurden, gab es in den letzten 20 Jahren kaum Fortschritte bei der Behandlung von Gliomen des Grades 4 insbesondere des Glioblastoms (Weller et al., 2024).

2.2 Glioblastome

Glioblastome machen etwa 50% der diffusen Gliome vom adulten Typ aus. Sie sind die aggressivste Form und werden von der WHO dem höchsten Grad 4 zugeordnet. Die jährliche Inzidenz liegt weltweit bei 3,1 von 100 000 Personen (Marenco-Hillembrand et al., 2020; Price et al., 2024), womit das Glioblastom zu den seltenen Erkrankungen (*Orphan Disease*)[1] gezählt wird. Die Inzidenz des Glioblastoms steigt mit dem Alter an von 0,15 von 100 000 Kindern bis zu einem Höchstwert von 15,03 von 100 000 Erwachsenen im Alter von 75-84 Jahren. Im Gegensatz dazu ist die Mortalität im Alter höher: 6,8% aller Patienten, bei denen ein Glioblastom diagnostiziert wurde, sind nach 5 Jahren noch am Leben, bei Patienten im Alter von 65 Jahren oder älter sind es lediglich noch etwa 2 % (Price et al., 2024). Nach der WHO-Klassifikation sind Glioblastome diffuse astrozytäre Gliome ohne Mutation in den Genen *IDH1* oder *IDH2* (*IDH*-wildtyp). Zusätzlich liegt keine Mutation in *Histone-G34-H3* vor (*H3*-wildtyp) (Komori, 2022; Louis et al., 2021). Histologisch zeichnen sich Glioblastome durch mikrovaskuläre Proliferation und Nekrose aus. Weitere Anzeichen für Malignität sind Anaplasie, hohe Mitoseraten und Invasivität, diese finden sich aber auch häufig bei Grad 3 Gliomen (Wirsching et al., 2016). Zur eindeutigen Charakterisierung sollten histologisch mikrovaskuläre Proliferation und Nekrose vorliegen oder eines der folgenden drei molekularen Merkmale: (1) Mutation des *Telomerase Reverse Transcriptase Promotors* (*pTERT*), (2) Amplifikation des *Epidermal Growth Factor Receptors* (*EGFR)* und (3) kombinierte Kopienzahlveränderungen der Chromosome 7 und 10 (+7/-10) (Park et al., 2023). Bei diffusen *IDH*-wildtyp Gliomen des Grades 2 oder 3 ohne Nekrose oder mikrovaskulärer Proliferation sollte ein Test auf *TERT*-Promotormutation, *EGFR*-Amplifikation und Chromosom +7/-10 durchgeführt werden. Das Vorhandensein eines oder mehrerer dieser genetischen Marker führt dann trotzdem zur Diagnose eines Glioblastoms (Grad 4), auch wenn sich histologisch keine Anzeichen von Nekrose oder mikrovaskulärer Proliferation zeigen (Park et al., 2023).

[1] Ein *Orphan Disease* (seltenes Leiden) ist in der der europäischen Union laut Verordnung (EG) Nr. 141/2000 definiert als eine Erkrankung die nicht mehr als 5 von 10 000 Personen betrifft.

Neben den oben bereits erwähnten diagnostischen genetischen Markern ist das Glioblastom durch eine Vielzahl weiterer Mutationen in Tumorsuppressor- und Onkogenen geprägt (Brennan et al., 2013; Dakal et al., 2024). Eine breit angelegte Studie des „*The Cancer Genome Atlas Program* (TCGA)“[2] hat drei eng miteinander verknüpfte intrazelluläre Signalwege identifiziert, die bei der Entstehung von Glioblastomen eine große Rolle spielen. Dabei handelt es sich um die zwei Tumorsuppressor-Signalwege p53 und *Retinoblastoma Protein* (pRb) und Rezeptortyrosinkinase-Signalwege wie die des *Platelet-derived Growth Factor Receptors* (PDGFR), des *Insulin-like Growth Factor Receptors* (IGFR) oder des EGFR (Comprehensive genomic characterization defines human glioblastoma genes and core pathways, 2008).

2.3 Leitlinien-Therapie des Glioblastoms

Die aktuelle Leitlinie zur Behandlung des Glioblastoms sieht ein Vorgehen basierend auf drei Säulen vor: (1) Chirurgische Resektion, (2) Strahlentherapie und (3) adjuvante Chemotherapie (Weller et al., 2021; Wick W, et al. 2021).

2.3.1 Operation und Strahlentherapie

Präoperativ können Kortikosteroide zur Reduktion von Ödemen eingesetzt werden, bei Krampfanfällen sind Antikonvulsiva indiziert. Aufgrund der Infiltration des Tumors in umliegende Gewebe ist eine vollständige Resektion meist nicht möglich und somit die Operation nicht kurativ (Cuddapah et al., 2014). Aus diesem Grunde sollte sich die Radikalität der Resektion immer an der Erhaltung neurologischer Funktionen orientieren. Mit der Strahlentherapie wird etwa 3 - 5 Wochen nach der Operation begonnen. Dabei sollte eine Dosierung von 50 – 60 Gy gewählt werden in Abhängigkeit von Alter und Morbidität der Patienten. Bei neu diagnostizierten erwachsenen Patienten im Alter bis zu 70 Jahren erfolgt eine Behandlung mit 60 Gy und 1,8 - 2 Gy-Fraktionen in 30 Einzeldosen an 5 Tagen pro Woche (Wick et al, 2021).

2.3.2 Chemotherapie

Bei Patienten mit gutem allgemeinem und neurologischem Zustand bis zu 70 Jahren wird zunächst gleichzeitig zur Strahlentherapie das Chemotherapeutikum

[2] Das TCGA ist eine vom *US National Institute of Health* (NIH) und der US-Regierung gefördertes Forschungsprojekt, welches das Ziel hat, durch Hochdurchsatz-Genomanalysen zu einem besseren Verständnis der genetischen Grundlagen der Krebsentstehung beizutragen und die Diagnose, Behandlung und Prävention zu verbessern: https://www.cancer.gov/ccg/research/genome-sequencing/tcga

Temozolomid (TMZ, Temodal®) täglich in einer oralen Dosis von 75 mg/m^2 Körperoberfläche (KOF) gegeben gefolgt von 28 Tagen mit 150 – 200 mg/m^2 KOF über 6 Zyklen. Dieses sogenannte Stupp-Schema basiert auf einer klinischen Phase III Studie, in der gezeigt werden konnte, dass die zusätzliche TMZ-Therapie die durchschnittliche Überlebenszeit um 2,5 Monate (von 12,1 Monaten auf 14,6 Monaten) verlängert und die 2-Jahres-Überlebensrate von 10,4 % auf 26,5 % erhöht (Stupp et al., 2005). Auch nach 5 Jahren war die Überlebensrate mit TMZ immer noch bei 9,8% im Vergleich zur Strahlentherapie mit nur 1,9% (Stupp et al., 2009). TMZ ist seit den Stupp-Studien essenzieller Bestandteil der Glioblastom-Therapie. Es handelt sich um ein alkylierendes Zytostatikum mit hoher Säurestabilität und kann aufgrund dessen oral verabreicht werden (Newlands et al., 1997). Nach der Einnahme wird TMZ schnell und fast vollständig resorbiert und die maximale Plasmakonzentration bereits nach 0,33 – 2 h erreicht, die Plasmahalbwertszeit liegt bei ca. 1,8 h. TMZ passiert schnell die Blut-Hirn-Schranke und liegt dadurch in der Zerebrospinalflüssigkeit und am Wirkort vor (Baker et al., 1999). Da es sich bei TMZ um ein Prodrug handelt, muss es erst zur eigentlichen Wirkform einem Methyl-Diazonium-Ion aktiviert werden (Denny et al., 1994). Der Aktivierungsmechanismus ist in der folgenden Abbildung gezeigt.

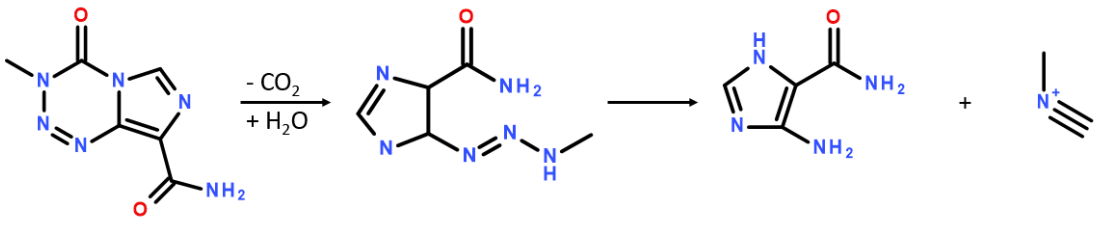

Abbildung 1: Aktivierung von TMZ zur eigentlichen Wirkform. Im alkalischen oder neutralen Milieu wird der Triazenring des TMZ (**1**) durch Hydrolyse geöffnet und es entsteht Methyl-(triazen-1-yl)imidazol-4-carboxamid (MTIC, **2**). MTIC zerfällt zu 5-Amino-imidazol-4-carboxamid (AIC, **3**) und einem Methyl-Diazonium-Ion (**4**). Modifiziert nach (Denny et al., 1994).

Dieses Methyl-Diazonium-Ion ist das eigentliche Alkylanz und methyliert die DNA hauptsächlich an N^7 des Guanins (N^{7}meG; >70% der Addukte) und an N^3 des Adenins (N^{3}meA; ~10% der Addukte) (Newlands et al., 1997). Dies ist jedoch nicht die Grundlage der therapeutischen Wirkung, da dieser Schaden durch DNA-Reparaturenzyme der Basenexzisionsreparatur (*Base Excision Repair*, BER) effektiv repariert wird. Die eigentliche antineoplastische Wirkung wird über die Methylierung

des Guanins an O^6 (O^6meG; ~5 % der Addukte) hervorgerufen (Kaina et al., 1997). Dies führt zu einer Fehlpaarung mit Thymin während der Replikation, die von der DNA-Fehlpaarungsreparatur (*Mismatch Repair*, MMR) erkannt wird (vergleiche 2.3.3.1). Der vergebliche Versuch der Reparatur führt im weiteren Verlauf zu DNA-Doppelstrangbrüchen und letztendlich zum Zelltod (Mojas et al., 2007; Quiros et al., 2010).

2.3.3 TMZ-Resistenz des Glioblastoms

Prinzipiell unterscheidet man zwei Arten von Resistenzen gegenüber Tumortherapien: die intrinsische und die erworbene Resistenz. Wenn eine Subpopulation von Tumorzellen intrinsisch resistent ist, kann es vorkommen, dass trotz Behandlung weiterhin unkontrollierte Zellproliferation stattfindet und der Tumor somit weiterwächst. Bei einer erworbenen Resistenz erwirbt eine bestimmte Zellpopulation eine Resistenz durch genetische Mutationen als Folge der Therapie. Im Allgemeinen werden bei der erworbenen Resistenz zunächst klinische Behandlungserfolge erzielt und der Tumor schrumpft. Nach einer gewissen Behandlungsdauer kommt es jedoch zu einem erneuten Wachstum des Tumors (Teraiya et al., 2023).

2.3.3.1 Einfluss von DNA-Reparatur-Mechanismen auf die Resistenz

Der weitaus wichtigste Grund für eine TMZ-Resistenz von Glioblastomen ist eine erhöhte Expression des DNA-Reparaturenzyms *O^6-Methylguanine-DNA Methyltransferase* (MGMT). Die TMZ-Behandlung oder Strahlentherapie selbst führt aber nicht zu einer gesteigerten MGMT-Expression (Aasland et al., 2018), es handelt sich also um eine intrinsische Resistenz. Es gibt jedoch auch Meta-Analysen die Änderungen in der *MGMT*-Promotormethylierung in Rezidiven zeigen konnten. Die klinische Relevanz der Methylierungen für die weitere Behandlung ist jedoch unklar (Feldheim et al., 2019). MGMT entfernt die Methylgruppen von den zytotoxischen O^6-Guanin-Addukten und überträgt sie auf einen Cysteinrest im katalytischen Zentrum und verhindert so den Zelltod (Pegg, 2000). Kaum ein anderes Reparaturgen ist so stark epigenetisch dereguliert wie *MGMT* (Christmann et al., 2019). Dies scheint insbesondere bei Glioblastomen der Fall zu sein, da etwa 20% der Tumore keine MGMT-Enzymaktivität aufweisen (Wiewrodt et al., 2008) und etwa 40% einen methylierten Promoter haben (Esteller et al., 2000). Bemerkenswert ist, dass bei den meisten Glioblastomen eine Kopie von Chromosom 10 fehlt, auf dem das *MGMT*-Gen liegt. Daher kann die Promotormethylierung der verbleibenden Kopie die MGMT-

Expression vollständig unterbinden (Kaina, 2023). Es zeigt sich, dass die *MGMT*-Promotormethylierung für das Gesamtüberleben von mit TMZ behandelten Patienten von Vorteil ist, was den Methylierungsstatus zu einem hilfreichen prädiktiven Marker für ein Ansprechen auf die Therapie macht (Hegi et al., 2005; Stupp et al., 2009; Switzeny et al., 2016).

Es gibt jedoch Zelllinien, die selbst trotz sehr niedriger MGMT-Expression nicht auf TMZ reagieren (Lee, 2016). Das bedeutet, dass es noch weitere Resistenzmechanismen geben muss, die hier eine Rolle spielen. Es konnte gezeigt werden, dass Mutationen in Enzymen des MMR-Systems eine klinische Relevanz haben. Eine verminderte Expression der MMR-Enzyme *MutS Homolg 2* und *6* (MSH2 und MSH6) verringern das Ansprechen auf die TMZ-Therapie (Cahill et al., 2007; McFaline-Figueroa et al., 2015; Dosch et al., 1998). Alkylanzien wie TMZ benötigen einen funktionierenden MMR-Signalweg, um ihre zytotoxische Wirkung zu entfalten. Eine Dysfunktionalität der MMR verhindert das Entstehen von DNA-Doppelstrangbrüchen, sodass weder Zellzyklusarrest noch Apoptose eingeleitet werden und die DNA-Replikation trotz DNA-Methylierungen fortgesetzt wird (Kaina, 2023). Neben dem MMR- ist auch das BER-System an der Reparatur der TMZ-induzierten DNA-Methylierungen beteiligt. Besonders N^3meA und N^7meG werden durch *N-Methylpurine-DNA Glycosylase* (MPG) und *Poly(ADP-ribose)-Polymerase 1* (PARP1) repariert, was ebenfalls zum Überleben der Zellen trotz TMZ-Behandlung beiträgt (Tentori et al., 2002). Bei Patienten, die eine erhöhte Expression von MPG in Glioblastomen zeigen, ist das Gesamtüberleben deutlich reduziert (Agnihotri et al., 2012). Der Einfluss der Aktivität der unterschiedlichen DNA-Reparaturmechanismen auf die Wirkung von TMZ ist in der folgenden Abbildung dargestellt.

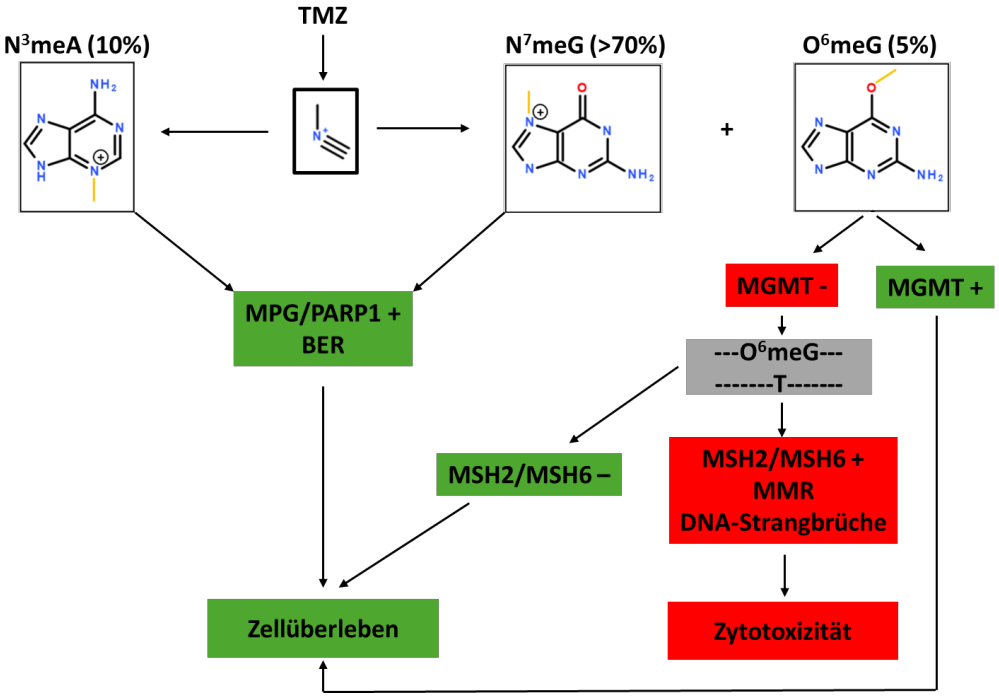

Abbildung 2: Einfluss von DNA-Reparaturmechanismen auf die Wirkung von TMZ. Abkürzungen: BER, *Base Excision Repair*; O^6meG, *O^6-Methylguanin*; MGMT, *O^6-Methylguanine-DNA Methyltransferase*; MMR, *Mismatch-Repair*; MPG, *N-methylpurine-DNA Glycosylase* (BER-Reparaturenzym); MSH2/MSH6, *MutS Homolg 2 und 6* (MMR-Reparaturenzyme); N^3meA, *N^3-Methyladenin*; N^7meG, *N^7-Methylguanin*; PARP1, *Poly(ADP-ribose)-Polymerase 1* (BER-Reparaturenzym); T, Thymin, TMZ, Temozolomid

2.3.3.2 Nachgeschaltete Signalwege der DNA-Reparatur

Die durch O^6meG ausgelösten Läsionen sowie die Hemmung der DNA-Replikation an O^6meG/Thymin-MMR-Clustern aktivieren die beiden PI3-Kinasen *Ataxia Telangiectasia and Rad3-related* (ATR) und *Ataxia Telangiectasia Mutated* (ATM). Ein Ziel der aktivierten Kinasen ist das p53-Tumorsuppressorprotein. Als „Wächter des Zellzyklus“ spielt p53 eine Hauptrolle bei der Zellteilung. p53 aktiviert als tetramerer Transkriptionsfaktor Gene, die Apoptose und DNA-Reparatur aber auch zelluläre Seneszenz steuern (Kaina, 2023). Die Rolle der Seneszenz bei der TMZ-Resistenz wird im folgenden Kapitel erläutert (siehe 2.3.3.3). In gesunden Zellen wird p53 durch die E3 Ubiquitin-Ligase *Mouse Double Minute 2 Homolog* (MDM2) reguliert. MDM2 bildet mit p53 einen Komplex und ubiquitiniert es, wodurch es durch das Proteasom abgebaut wird. In geschädigten Zellen wird p53 phosphoryliert, was die Bindung von MDM2 verhindert. Keine Bindung an MDM2 bedeutet keinen Abbau von p53 und damit eine erhöhte Verfügbarkeit (Huang et al., 2024). Die Phosphorylierung von p53 an Serin 15 aktiviert bevorzugt DNA-Reparaturenzyme, während die Phosphorylierung an

Serin 46 die Expression pro-apoptotischer Gene stimuliert (Roos et al., 2016). Das Protein $p14^{ARF}$ ist für die Neutralisierung von Ubiquitin-Ligasen verantwortlich und sorgt folglich für höhere p53-Spiegel in geschädigten Zellen (Knudsen et al., 2024). $p14^{ARF}$ wird von *CDKN2A* kodiert und ist eine verkürzte Variante des $p16^{INK4a}$ Tumorsuppressorproteins auch *Cyclin-dependent Kinase (CDK)-Inhibitor 2A* genannt, das in den pRB-Signalweg und die Zellzykluskontrolle involviert ist (Vergleiche Abbildung 4 zur Regulierung des pRB-Signalweges). Die folgende Abbildung gibt einen Überblick über die p53-regulierten Signalwege, die durch TMZ ausgelöst werden.

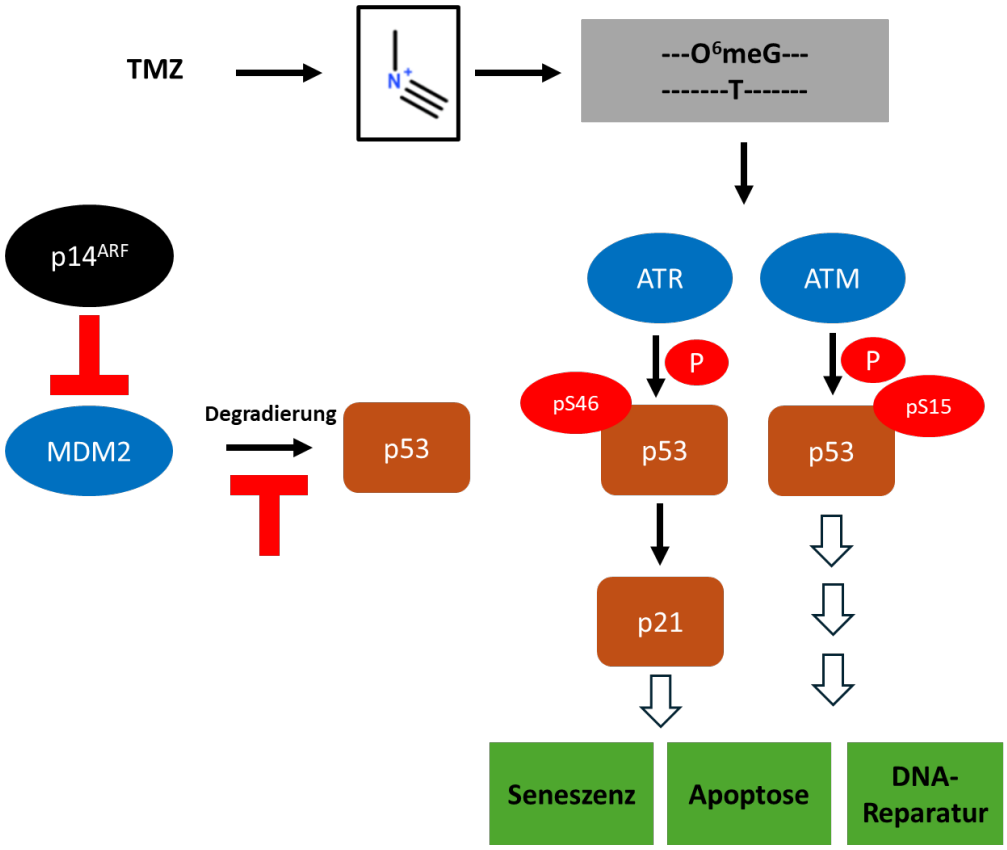

Abbildung 3: Effekte der durch TMZ ausgelösten DNA-Methylierung. Abkürzungen: ATM, *Ataxia Telangiectasia Mutated*; ATR, *Ataxia Telangiectasia and Rad3-related*; O^6meG, *O^6-Methylguanin*; MDM2, *Mouse Double Minute 2 Homolog*; $p14^{ARF}$ verkürzte Variante von $p16^{INK4}$ (*CDKN2A*); pS46, p53 Phosphoserin 46; pS15, p53 Phosphoserin 15; T, Thymin; TMZ, Temozolomid

Mutationen im *TP53*-Gen, Amplifikation von *MDM2* und Verlust von $p14^{ARF}$ werden häufig in Glioblastomen und Astrozytomen (Grad 4) beobachtet. *TP53*-Mutationen treten jedoch häufiger bei Astrozytomen (Grad 4) auf und sind bereits bei niedriggradigen Astrozytomen nachweisbar (Furnari et al., 2007). Die Studie des

Cancer Genome Atlas Research Network zeigte, dass der p53-Signalweg in 87 % der Glioblastome und Astrozytomen (Grad 4) verändert ist (Comprehensive genomic characterization defines human glioblastoma genes and core pathways, 2008). Der *TP53*-Mutationsstatus spielt auch eine Rolle für die Sensitivität von Glioblastom-Zellen gegenüber TMZ. Bei einem Fehlen des p53-Proteins löst die durch TMZ induzierte O^6meG-Läsion zwar noch weiterhin Apoptose über alternative Signalwege aus, dafür sind jedoch deutlich höhere Konzentrationen notwendig (Roos et al., 2007). Ähnlich wie p53 reguliert auch pRB den Übergang von der G1- in die S-Phase des Zellzyklus. Freies ungebundenes pRB bindet an den Transkriptionsfaktor E2F und hemmt dadurch die Replikation. In gesunden Zellen wird pRB durch einen Komplex aus CDK 4/6 und Cyclin D1 phosphoryliert, wodurch es keine Bindung mit E2F eingehen kann. Wenn zellulärer Stress zum Beispiel aufgrund von DNA-Schäden auftritt, bindet $p16^{INK4a}$ an CDK4/6, setzt den Komplex und damit pRB frei und der Zellzyklus hält an. Das Zusammenspiel ist in der folgenden Abbildung dargestellt.

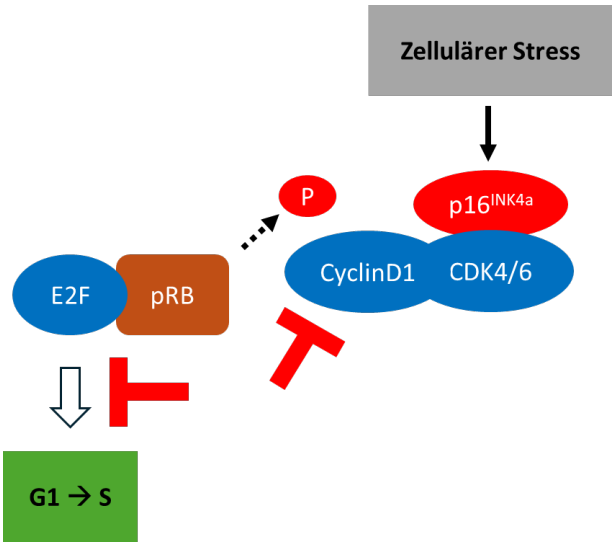

Abbildung 4: Regulierung des Zellzyklus durch den pRB-Signalweg. Abkürzungen: CDK4/6, *Cyclin-dependent Kinase 4/6*; E2F, *Transcription Factor E2F*; $p16^{INK4a}$, *Cyclin-dependent Kinase-Inhibitor 2A (CDKN2A)*; pRB, *Retinoblastoma Protein*

Der Verlust von $p16^{INK4a}$ oder Mutationen in *pRB*, *CDK4/6* oder *Cyclin D1* führen zu einer unkontrollierten Expression von anti-apoptotischen Genen und zur Zellproliferation (Witkiewicz et al., 2011). Mutationen in Genen des pRB-Signalweges werden in 78% der Glioblastome gefunden (Comprehensive genomic characterization defines human glioblastoma genes and core pathways, 2008).

Die DNA-Reparaturmechanismen und Apoptose-Signalwege werden durch übergeordnete Rezeptortyrosinkinasen reguliert. Über 60 % aller Glioblastome überexprimieren den EGFR, was in > 40 % durch eine Amplifikation des *EGFR*-Gens verursacht wird (Brennan et al., 2013). Darüber hinaus weisen etwa 50 % der Glioblastome mit *EGFR*-Amplifikation eine Deletion der Exone 2-7 auf. Diese Deletion resultiert in einem verkürzten EGFR (EGFRvIII). EGFRvIII ist konstitutiv aktiv, ohne aber selbst einen Liganden zu binden. Dies trägt zur hohen Proliferation und Invasivität von Glioblastom-Zellen bei (Ohgaki et al., 2009). Nach Bindung der Liganden wird der EGFR autophosphoryliert. Diese Phosphorylierung aktiviert die *Phosphoinositide-3-Kinase* (PI3K) und nachfolgend die *Proteinkinase B* (AKT). In der weiteren Kaskade werden durch AKT zahlreiche weitere Proteine beeinflusst, die maßgeblich an der Regulierung des Zellzyklus und der Apoptose beteiligt sind. So sorgt AKT durch eine nachgeschaltete Regulierung von *Nuclear Factor κB* (NFκB), *cAMP Response Element-binding Protein* (CREB) und MDM2/p53 für die Transkription proliferativer und anti-apoptotischer Gene. Ebenfalls wird p21 durch AKT phosphoryliert und seine inhibierende Wirkung auf den Zellzyklus aufgehoben. Zusätzlich aktiviert AKT das *Mammalian Target of Rapamycin* (mTOR), was dann zur Expression von angiogenen und zellzyklusfördernden Genen führt (Colardo et al., 2021). AKT hat aber auch einen direkten Einfluss auf die DNA-Reparatur. Zum einen unterdrückt es die MMR, zum anderen aktiviert es die BER (Liu et al., 2014). Beide Reparaturmechanismen spielen eine entscheidende Rolle für die Wirkung und Resistenzentwicklung von TMZ (vergleiche Abbildung 2). Mutationen mit Funktionsgewinn der PI3K finden sich in 15% aller Glioblastome (Comprehensive genomic characterization defines human glioblastoma genes and core pathways, 2008). Die Phosphatase *Phosphatase and Tensin homolog* (PTEN) fungiert als PI3K-Gegenspieler. Mutationen und homozygote Deletionen von *PTEN* zeigen 38 % aller Glioblastome (Koul, 2008; Comprehensive genomic characterization defines human glioblastoma genes and core pathways, 2008). Darüber hinaus korreliert die Aktivierung des PI3K-Signalwegs in Glioblastomen mit einer ungünstigen klinischen Prognose (Chakravarti et al., 2004). Der Signalweg der kleinen GTPase *Rat Sarcoma* (RAS) wird ebenfalls durch den EGFR reguliert und ist eng mit dem PI3K-Signalweg verknüpft. Eine Aktivierung der RAS nachgeschalteten *Extracellular-signal Regulated Kinase* (ERK) geht mit einer erhöhten Mortalität von Glioblastom-Patienten einher (Pelloski et al., 2006). Mutationen in *RAS*-Genen, die bei vielen Tumorentitäten beobachtet werden, sind

beim Glioblastom jedoch eher selten (Knobbe et al., 2004). Eine Überaktivierung des RAS-Signalwegs über vorgeschaltete Rezeptortyrosinkinasen oder homozygote Deletionen des negativen RAS-Regulators *Neurofibromin 1* (NF1) sind hingegen häufig (Brennan et al., 2013). Die folgende Abbildung gibt einen Überblick über Rezeptortyrosinkinase-Signalwege, die einen Einfluss auf die TMZ-Resistenz haben können.

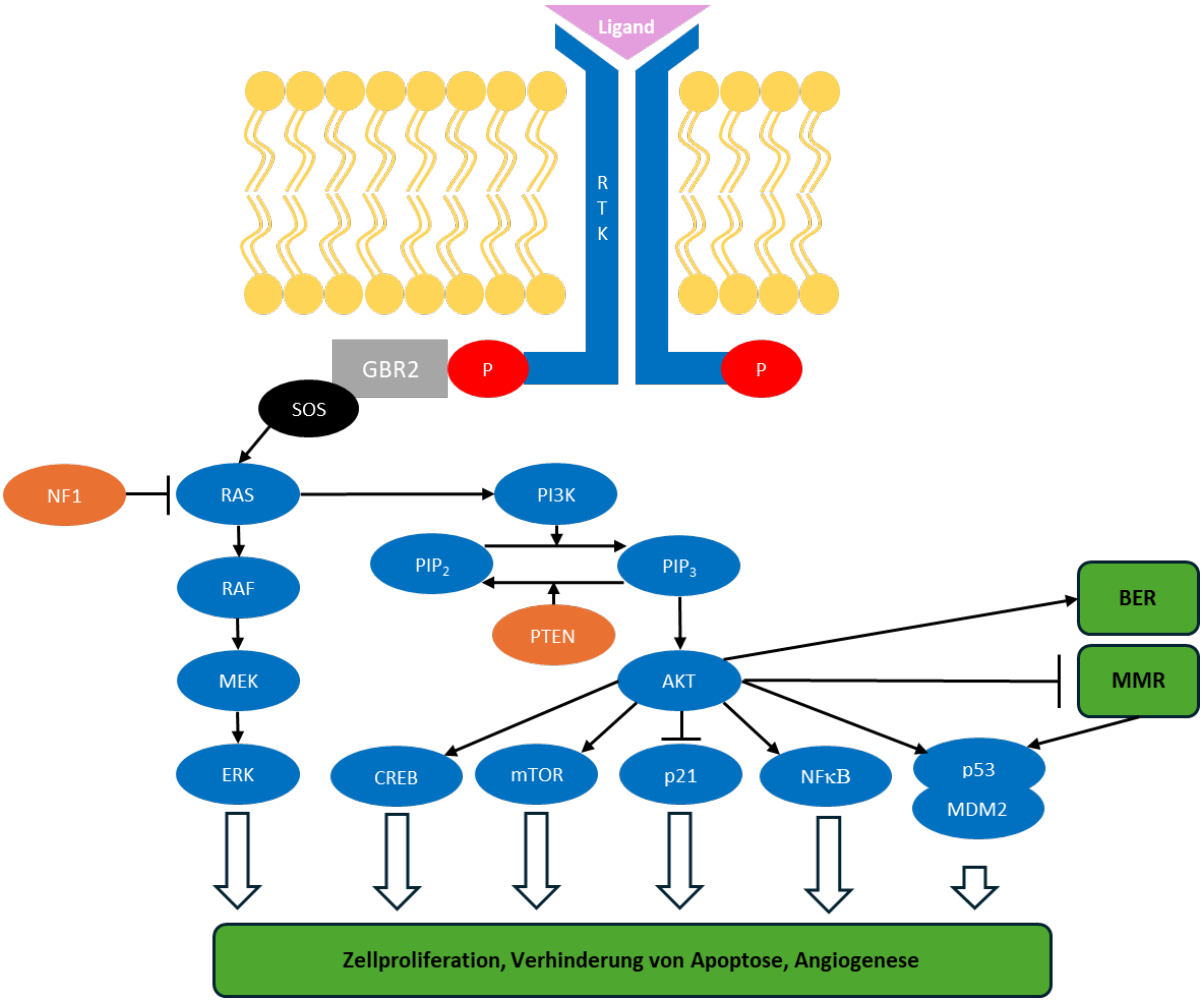

Abbildung 5: Aktivierung von Rezeptortyrosinkinase-Signalwegen in Glioblastomen mit Einfluss auf die TMZ-Resistenz. Abkürzungen: BER, *Base excision Repair*; CREB, *cAMP Response Element-binding Protein*; ERK, *Extracellular-signal Regulated Kinase*; GBR2, *Growth Factor Receptor-bound Protein*; MDM2, *Mouse Double Minute 2 Homolog*; MEK, *Mitogen-activated Protein Kinase*; MMR, *Mismatch Repair*; mTOR, *Mammalian Target of Rapamycin*; NF1, *Neurofibromin 1*; NFκB, *Nuclear Factor κB*; PI3K, *Phosphoinositide-3-Kinase*; PIP_2, *Phosphatidylinositol 4,5-bisphosphate*; PIP_3, *Phosphatidylinositol (3,4,5)-trisphosphate*; RAS, *Rat Sarcoma*; RAF, *Rapidly Accelerated Fibrosarcoma*; RTK, Rezeptortyrosinkinase; SOS, *Son of Sevenless*

2.3.3.3 Einfluss der zellulären Seneszenz auf die Resistenz

Unter zellulärer Seneszenz versteht man einen langanhaltenden Arrest des Zellzyklus, der unter anderem durch den p53/p21-Signalweg vermittelt wird (siehe 2.3.3.2 und Abbildung 3). In Tumoren wird Seneszenz durch zellulären Stress wie DNA-Schäden, Onkogenaktivierung, reaktive Sauerstoffspezies oder auch die Chemotherapie, die sogenannte Therapie-induzierte Seneszenz, ausgelöst (Gorgoulis et al., 2019). Charakteristisch für seneszente Zellen ist ein sekretorischer, proinflammatorischer Phänotyp, ein anti-apoptotisches Programm und ein erhöhter Gehalt an Lysosomen. Die gesteigerte Sekretion von Zytokinen, Chemokinen, Wachstumsfaktoren, Komponenten der extrazellulären Matrix und Proteasen kann die Angiogenese stimulieren und die epithelial-mesenchymale Transition (EMT) fördern (Coppe et al., 2010; Faget et al., 2019). Während der Tumorentstehung kann Seneszenz gegensätzliche Auswirkungen haben. In einigen Fällen verhindern seneszente Zellen die Vermehrung präneoplastischer Zellen, da die sekretierten Zytokine die Immunabwehr stimulieren können (Xue et al., 2007; Kang et al., 2011; Ruscetti et al., 2018). Umgekehrt kann die Sekretion jedoch auch das Tumorwachstum induzieren (Yoshimoto et al., 2013) oder zur Immunsuppression beitragen (Toso et al., 2014; Ruhland et al., 2016). Neuere Studien belegen, dass seneszente Zellen auch wieder in den normalen Zellzyklus zurückkehren können und dabei dann oft resistent gegenüber der vorangegangenen Therapie sind (Saleh et al., 2019).

TMZ induziert nicht nur Apoptose, sondern führt nach längerer Behandlungsdauer Glioblastom-Zellen in die Seneszenz (Knizhnik et al., 2013). In kultivierten Glioblastom-Zellen steigt nach 10 Tagen Behandlung mit TMZ die seneszente Zellpopulation auf bis zu 90% an. Diese Zellen bleiben in der G2-Phase des Zellzyklus stehen und zeigen sehr hohe oxidative Stresslevel, oxidative DNA-Schäden und DNA-Doppelstrangbrüche. Zusätzlich ist NF-kB aktiviert und die Sekretion proinflammatorischer Zytokine wie Interleukin-6 (IL-6) und Interleukin-8 (IL-8) gesteigert (Aasland et al., 2019; Beltzig et al., 2022b). Ein Vergleich von unbehandelten Glioblastomen mit Rezidiven, die nach Therapie auftraten, zeigte, dass in den Rezidiven die seneszente Zellpopulation erhöht, während gleichzeitig die Apoptoserate erniedrigt ist (Beltzig et al., 2022b). Somit ist ein großer Anteil der Glioblastom-Zellen auch nach Strahlen- und TMZ-Therapie im seneszenten Stadium und im rezidivierten Tumor noch vorhanden, wo sie erneut proliferieren und zu lokalen Entzündungen führen können (Salam et al., 2023).

2.4 Zielsetzung

Aufgrund der intrinsischen Resistenz des Glioblastoms ist die Ansprechrate auf die TMZ-Therapie nicht zufriedenstellend. Seit der Einführung von TMZ vor über 20 Jahren gab es keine grundlegenden pharmakologischen Neuentwicklungen mehr, die das Gesamtüberleben der Patienten signifikant verbessert haben (Weller et al., 2024). Das Ziel der in den folgenden Kapiteln beschriebenen fünf molekular-pharmakologischen Arbeiten war es, die Expression und den Aktivierungsstatus der für die TMZ-Resistenz relevanten Signalwege in Glioblastom-Biopsien und -Zellen zu untersuchen und durch gezielte pharmakologische Beeinflussung der aktivierten Signalwege ein verbessertes Ansprechen der Zellen auf TMZ zu erreichen.

Die erste Arbeit fokussiert sich dabei auf die Rezeptortyrosinkinase-Signalwege, die über PI3K und MEK/ERK signalisieren und regelmäßig in Glioblastomen mutiert sind (Comprehensive genomic characterization defines human glioblastoma genes and core pathways, 2008). Die Beeinflussung dieser Signalwege wird schon lange als molekularer Angriffspunkt von Tumortherapeutika auch für Glioblastome erforscht (Colardo et al., 2021; He et al., 2021). In der Studie werden seltene Biopsien von neu aufgetretenen Glioblastomen mit Biopsien von Rezidiven derselben Patienten auf ihren Aktivierungsstaus über *Proteom-Profiling* untersucht. Daraus lassen sich gezielt Angriffspunkte ableiten, die sich pharmakologisch in Glioblastom-Zellen beeinflussen lassen und mit Hinblick auf ein besseres Ansprechen der Chemotherapie untersucht werden können. Die zweite Arbeit greift diesen Aspekt auf und untersucht die Verbindung des PI3K/AKT-Signalweges mit dem bei der Redox-Homöostase beteiligten Thioredoxin (Trx)-Systems und dessen Einfluss auf die TMZ-Resistenz. Ausgangspunkt für die Untersuchungen waren Studien, die den Einfluss einer Aktivierung des Trx-Systems mit einem kürzeren Überleben von Glioblastom-Patienten in Verbindung brachten (Zhang et al., 2017b). Eine Rolle von Trx auf die TMZ-Resistenz in Glioblastomen war bis dato in der Literatur noch nicht beschrieben.

Im Jahr 2017 erlangte der μ-Opioidrezeptor-Agonist Methadon mediale Aufmerksamkeit durch eine intensive Berichterstattung in der Publikumspresse als mögliche adjuvante Therapieoption für Glioblastome (Hübner et al., 2017), nachdem in präklinischen Studien eine sensitivierende Wirkung gegenüber dem Chemotherapeutikum Doxorubicin beschrieben wurde (Friesen et al., 2014). Doxorubicin ist für die Therapie des Glioblastoms nicht indiziert und die Wirkung von Methadon in Kombination mit dem Therapie-Goldstandard TMZ war kaum untersucht.

Des Weiteren war der potenzielle Mechanismus der Methadon-Wirkung nicht eindeutig geklärt. Zwei Arbeiten widmen sich der Wirkung von Methadon auf Glioblastom-Zellen, beschreiben die Expression des μ-Opioidrezeptors in den Zellen und analysieren einen möglichen Einfluss dieses Signalweges auf die zytotoxische und Seneszenz-auslösende Wirkung von TMZ. Die Identifizierung senolytischer Arzneimittel, die gezielt die seneszente Zellpopulation abtöten, ist ein neuer Ansatz zur Behandlung der TMZ-induzierten Therapieresistenz des Glioblastoms (Beltzig et al., 2022a; Zhang et al., 2023). In den oben beschriebenen Arbeiten konnten keine Effekte von Methadon auf die Seneszenz nachgewiesen werden. Sie wurden jedoch zum Anlass genommen andere Signalwege zu untersuchen, die die Seneszenz regulieren. Eine Aktivierung der spannungsaktivierten Kalium-Kanäle aus der Familie der *Potassium Voltage-Gated Channel Subfamily H* (KCNH), *Human Ether-à-go-go Type 1* (Eag1) und *Human Ether-à-go-go-related Gene* (hERG), löst in Brustkrebszellen Seneszenz aus (Lansu et al., 2013). In Glioblastom-Patienten ist eine Überexpression der beiden Kanäle mit einer schlechten klinischen Prognose assoziiert (Martinez et al., 2015; Shugg et al., 2021; Zheng et al., 2023). Die pharmakologische Hemmung dieser Kanäle wird schon seit längerem als potenzielle Tumortherapie diskutiert (He et al., 2020) unter anderem auch für Gliome (Elias et al., 2023). Die fünfte Arbeit untersucht die Expression von hERG/Eag1-Kanälen in Glioblastomen und betrachtet den Einfluss einer pharmakologischen Hemmung der Kanäle auf die Apoptose und die TMZ-induzierte Seneszenz. Der Einfluss einer hERG/Eag1-Hemmung auf die Seneszenz von Glioblastom-Zellen wurde bisher in der Literatur noch nicht beschrieben.

3 Ergebnisteil

3.1 **Haas B**, Klinger V, Keksel C, Bonigut V, Kiefer D, Caspers J, Walther J, Wos-Maganga M, Weickhardt S, Rohn G, Timmer M, Frotschl R, Eckstein N. Inhibition of the PI3K but not the MEK/ERK pathway sensitizes human glioma cells to alkylating drugs. Cancer Cell Int. 2018;18:69.

Zielsetzung der Arbeit: Für die Chemoresistenz und hohe Rezidivrate des Glioblastoms sind unter anderem aktivierte PI3K- und MEK/ERK-Signalwege verantwortlich (Colardo et al., 2021). Diese Signalkaskaden sind eng miteinander verbunden, der quantitative Beitrag beider zur intrinsischen Resistenz war jedoch noch nicht geklärt. In dieser Arbeit sollte der Aktivierungsstatus dieser Signalwege in humanen Glioblastom-Biopsien und *PTEN*-mutierten Zellen bestimmt und der Einfluss auf die Chemoresistenz durch gezielte Hemmung der Signalwege untersucht werden. Methoden und Ergebnisse: *Proteom-Profiling* von Biopsien TMZ-naiver und TMZ-resistenter Patienten zeigten eine erhebliche Aktivierung der PI3K- und MEK/ERK-Signalwege in beiden Gruppen. Die AKT- und CREB-Phosphorylierung war jedoch in Biopsien resistenter Tumore reduziert, während die ERK-Phosphorylierung unverändert hoch blieb. Zusätzlich zeigte sich eine verringerte Expression der Pro-Caspase 3 in den Rezidiven. *Proteom-Profiling* bestätigte auch eine starke Aktivierung mehrere Rezeptortyrosinkinasen und nachgeschalteter Signalwege in drei humanen Glioblastom-Zelllinien. In MTT-Versuche mit dem Alkylanz Cisplatin, welches zunächst als Modelsubstanz verwendet wurde, wurde eine intrinsische Resistenz der Glioblastom-Zellen festgestellt, die mit Cisplatin-adaptierten Ovarialkarzinom und Brustkrebszellen vergleichbar war. Cisplatin-Zyklen über 24 Wochen vermochten es nicht, die Resistenz weiter zu steigern. Keiner der untersuchten Inhibitoren der vorgeschalteten Rezeptortyrosinkinasen konnte die Zellen gegenüber Cisplatin sensitivieren. In weiteren MTT-Versuchen und durch Messung der Apoptoseraten über Annexin-V-FACS Assays konnte gezeigt werden, dass das Ansprechen der Zellen auf TMZ und Cisplatin durch Hemmung der PI3K mit spezifischen Inhibitoren verbessert werden konnte. Im Gegensatz dazu führte eine Hemmung der MEK/ERK-Signalkaskade mit zwei verschiedenen Inhibitoren zu einer verringerten Wirkung von TMZ. Die PI3K-Hemmung in Kombination mit TMZ resultierte in Comet Assays in vermehrten DNA-Schäden und reduzierte die Phosphorylierung von p53 an Serin 15 und die Expression von Claspin.

Schlussfolgerung: In TMZ-naiven und TMZ-resistenten Glioblastom-Biopsien wurde ein eindeutiges Aktivierungsmuster der MEK/ERK- und PI3K-Signalkaskaden festgestellt, was auf eine Rolle dieser Signalwege bei der Resistenzentwicklung hindeutet. Beide Signalwege sind auch in intrinsisch resistenten Glioblastom-Zelllinien aktiviert, jedoch scheint nur der PI3K-Signalweg eine entscheidende Rolle bei der Resistenz gegenüber Alkylanzien zu spielen. Mechanistisch steigert eine PI3K-Hemmung die TMZ-induzierten DNA-Schäden durch Beeinflussung des p53-Signalweges und der DNA-Reparatur. Somit könnte die PI3K ein lohnender Angriffspunkt neuer Arzneimittel zur Verbesserung der TMZ-Therapie in Glioblastomen sein.

Haas et al. Cancer Cell Int (2018) 18:69
https://doi.org/10.1186/s12935-018-0565-4

Cancer Cell International

PRIMARY RESEARCH

Open Access

Inhibition of the PI3K but not the MEK/ERK pathway sensitizes human glioma cells to alkylating drugs

Bodo Haas[1*], Veronika Klinger[1,2], Christina Keksel[1,3], Verena Bonigut[1,3], Daniela Kiefer[1,3], Julia Caspers[1,4], Julia Walther[1,2], Maria Wos-Maganga[1], Sandra Weickhardt[1], Gabriele Röhn[5], Marco Timmer[5], Roland Frötschl[1] and Niels Eckstein[3]

Abstract

Background: Intrinsic chemoresistance of glioblastoma (GBM) is frequently owed to activation of the PI3K and MEK/ERK pathways. These signaling cascades are tightly interconnected however the quantitative contribution of both to intrinsic resistance is still not clear. Here, we aimed at determining the activation status of these pathways in human GBM biopsies and cells and investigating the quantitative impact of both pathways to chemoresistance.

Methods: Receptor tyrosine kinase (RTK) pathways in temozolomide (TMZ) treatment naive or TMZ resistant human GBM biopsies and GBM cells were investigated by proteome profiling and immunoblotting of a subset of proteins. Resistance to drugs and RTK pathway inhibitors was assessed by MTT assays. Apoptotic rates were determined by Annexin V staining and DNA damage with comet assays and immunoblotting.

Results: We analyzed activation of RTK pathways by proteome profiling of tumor samples of patients which were diagnosed a secondary GBM and underwent surgery and patients which underwent a second surgery after TMZ treatment due to recurrence of the tumor. We observed substantial activation of the PI3K and MEK/ERK pathways in both groups. However, AKT and CREB phosphorylation was reduced in biopsies of resistant tumors while ERK phosphorylation remained unchanged. Subsequent proteome profiling revealed that multiple RTKs and downstream targets are also activated in three GBM cell lines. We then systematically describe a mechanism of resistance of GBM cell lines and human primary GBM cells to the alkylating drugs TMZ and cisplatin. No specific inhibitor of the upstream RTKs sensitized cells to drug treatment. In contrast, we were able to restore sensitivity to TMZ and cisplatin by inhibiting PI3K in all cell lines and in human primary GBM cells. Interestingly, an opposite effect was observed when we inhibited the MEK/ERK signaling cascade with two different inhibitors.

Conclusions: Temozolomide treatment naive and TMZ resistant GBM biopsies show a distinct activation pattern of the MEK/ERK and PI3K signaling cascades indicating a role of these pathways in resistance development. Both pathways are also activated in GBM cell lines, however, only the PI3K pathway seems to play a crucial role in resistance to alkylating agents and might serve as drug target for chemosensitization.

Keywords: Glioblastoma, Drug resistance, PI3K, Temozolomide, Cisplatin

*Correspondence: bodo.haas@bfarm.de
[1] Federal Institute for Drugs and Medical Devices, Kurt-Georg-Kiesinger-Allee 3, 53175 Bonn, Germany
Full list of author information is available at the end of the article

Background

Gliomas are divided into four grades with grade IV glioblastoma multiforme (GBM) as the most aggressive form with highest incidence [1, 2]. The high aggressive potential is revealed by a median survival of 14.6 months under therapy, the 5-year survival rate only is at 5.1% [3–5]. The vast majority of GBM occur de novo (primary GBM) while only 5% develop from lower grade II–III astrocytoma forming secondary GBM. Secondary and primary GBM can hardly be distinguished histopathologically but differ from mutations e.g. in the isocitrate dehydrogenase 1 (*IDH1*) gene. While secondary GBM are largely *IDH1* mutant, primary GBM carry the *IDH1* wild-type gene. *IDH1* mutations have been shown to be an independent positive prognostic marker of patient survival [1, 6, 7]. Another important predictor of response to therapy involves O^6-methylguanine-DNA-methyltransferase (*MGMT*) promoter methylation. There is growing evidence that the combination of *IDH1* mutation and *MGMT* promoter methylation is associated with longer survival under therapy [8, 9]. Three main difficulties aggravate GBM therapy. (i) GBM cells spread as single cells rather than building an encapsulated, operable tumor. This infiltrative growth is making GBM virtually incurable by surgery alone. (ii) GBM cells are beyond the blood brain barrier, making them usually unreachable for anti-cancer drugs with affinity to *P*-glycoprotein (*P*-gp) or multi-drug resistance proteins (MRPs) [10]. (iii) GBM cells are intrinsically resistant to chemo- and radiotherapy [11]. This may be owed to frequently mutated tumor suppressor genes known to mediate chemoresistance after loss of function like P53, retinoblastoma protein (RB) and phosphatase and tensin homolog (PTEN) and alterations in receptor tyrosine kinase (RTK) signaling pathways [12, 13]. RTKs such as epidermal growth factor receptor (EGF-R), platelet-derived growth factor receptor (PDGF-R) and insulin-like growth factor 1 receptor (IGF1-R) involved in proliferation, survival and invasiveness of GBM are frequently altered and over-activated [14]. GBM is treated with adjuvant radiotherapy after surgery, while chemotherapy for a long time was not a primary option. In fact, only one chemotherapy-regime results in a significant overall survival benefit: adjuvant temozolomide (TMZ) following radiotherapy [3, 4].

The phosphatidylinositide 3-kinase (PI3K) pathway is a complex, multi-armed signaling network, mediating proliferation, differentiation, migration, metabolism, and survival [15]. Prevention of apoptosis mediated by aberrant PI3K activation or deregulated upstream RTKs is observed in many drug-resistant tumors [16, 17]. The PI3K pathway is frequently over-activated in GBM due to increased RTK signaling or loss of PTEN function [18–23]. In addition, activation of the PI3K pathway in GBM has been correlated with adverse clinical outcome [24, 25]. On the other hand, it has been reported that PTEN and AKT (protein kinase B, PKB) activation status of GBM is irrelevant for prognostic development while activation of extracellular signal-regulated kinase (ERK) is associated with poor patient survival [26, 27]. Mutations in genes of the RAS family of small GTPases commonly observed in many tumor entities are rare for GBM [28]. However, over-activation of the RAS pathway via upstream RTKs or homozygous deletions of the negative RAS regulator neurofibromin 1 (NF1) are common [23]. It has been demonstrated that inhibition of RAS by several miRNAs is able to enhance TMZ-induced apoptosis in GBM cell lines [29, 30]. Mitogen-activated protein kinase kinase (MAPKK/MEK) inhibition however only reduced growth of a small subset of NF1-deficient GBM cell lines [31] and the multi-kinase inhibitor sorafenib failed to enhance radio- and chemosensitivity of GBM cell lines [32].

An array of reports from the literature suggests that inhibition of aberrant PI3K pathway activation may serve to reverse acquired multi-drug resistance in human tumors [33–35]. Consequently, the PI3K pathway has emerged as a promising treatment modality, with the potential to act synergistically with chemotherapy [36–39]. To this end, it has been shown that inhibition of PI3K by small molecules can sensitize tumor cells to various DNA damaging drugs by induction of apoptosis [40–44]. In contrast, another study has shown that inhibition of PI3K in primary GBM stem cells and differentiated GBM cells did not substantially chemosensitize cells to drug treatment [45]. Despite encouraging pre-clinical results, positive clinical outcome with PI3K inhibitors in GBM is limited. Thus, solely inhibiting the PI3K arm of RTK signaling cascades as the magic bullet appears questionable. Several reasons for the lack of efficacy are discussed [46]. Among others blocking PI3K and in particular downstream targets such as AKT and mammalian target of rapamycin (mTOR) counter regulatory activate RTKs and downstream signaling such as the RAS cascade allowing the cell to bypass PI3K/AKT blockade [47–50].

Therefore, we aimed at further disentangling the quantitative contribution of the PI3K/AKT and MEK/ERK pathways to intrinsic resistance to alkylating drugs in GBM. We investigate the activation status of RTK pathways in GBM tumor biopsies and GBM cell lines and subsequently elaborate the molecular mechanism of resistance to the DNA-alkylating anti-cancer drugs cisplatin and TMZ in three *PTEN* mutated GBM cell lines and primary GBM cells derived from tumor biopsies.

Methods

Materials

Temozolomide (Temodal®), LY294002, U0126, AG1024, AG1296, erlotinib (Tarceva®), wortmannin, U0126, and PD98059 were purchased from Sigma-Aldrich.

Tumor samples

Human tissue specimens of secondary GBM were taken from the tumor tissue bank of the Clinic of Neurosurgery, University Hospital Cologne. The collection of samples was approved by the University's Institutional Ethical Board. Informed consent of the patients was obtained according to the Helsinki declaration of ethical requirements.

Tissue samples were obtained directly from neurosurgery between 1990 and 2015, immediately snap-frozen in liquid nitrogen and stored at − 80 °C. 10 µm cryostat sections were taken from each sample, stained with HE for histological examination by a neuropathologist in order to assure that representative tissues were used for biochemical analysis. Histopathological diagnosis and grading was based on the WHO classification 2007 [51]. Mutation analysis was performed as previously described [52].

Cell culture

U87-MG, U251-MG, and U373-MG (Uppsala) GBM cell lines were obtained by Sigma-Aldrich (HPA Culture Collections) in 2015 and not used beyond passage 20. U251 Cells were cultivated in RPMI 1640 (Biochrom) containing 10% FCS (Biochrome), 100 IU/ml penicillin, and 100 µg/ml streptomycin (Biowest). All other cells and cell lines were cultivated in DMEM low Glucose (Biowest) containing 10% FCS, 100 IU/ml penicillin, and 100 µg/ml streptomycin. Primary GBM cells derived from a primary GBM tumor biopsy were obtained from the University Hospital Cologne. *IDH1* mutation and *MGMT* promoter methylation status [52] of all primary cells and cell lines used is displayed in Table 1.

Table 1 *IDH1* mutation and *MGMT* promoter methylation status of GBM cell lines and primary cells

Cells	IDH1	MGMT promoter
U251-MG	Wild-type	Methylated
U373-MG	Wild-type	Methylated
U87-MG	Wild-type	Methylated
Primary culture	Wild-type	Methylated

Proteome profiling

The functional status of signaling pathways was measured by Proteome Profiler™ human phospho-RTK, human apoptosis and human phospho-MAPK antibody arrays (R&D Systems). Tissue samples were disrupted with ice cold lysis buffer and a tissue homogenizer. Cells were lysed after incubation with respective inhibitors and TMZ by addition of ice cold lysis buffer to PBS washed culture plates. After centrifugation the protein content of the supernatant was determined and 200–300 µg of total protein was used for proteome profiling according to the manufactures protocol and as described previously [53].

Western blot analysis

For immunoblotting standard procedures using the following antibodies were used as previously described [53, 54]. Anti-EGF-R (AF-231), anti-IGF-R (AF-305-NA), anti-PDGF-Rβ (AF-385) combined with donkey anti-goat IgG-HRP (HAF 109; all R&D systems). Anti-MRP-2 (M2 III-6), Anti-P-gp (D-11; both Santa Cruz Biotechnology) combined with goat anti-mouse IgG (H + L)-HRP (Thermo Scientific). Anti-P53-phospho-S15 (A7180; Assay Biotechnology Company), P21 (C-19, Santa Cruz Biotechnology) combined with goat anti-rabbit IgG (H + L)-HRP (Thermo Scientific). P53-HRP (DO-1) and β-Actin-HRP (C-4; both Santa Cruz Biotechnology). Immunoblots were developed with the enhanced chemoluminescence system (Amersham Biosciences).

MTT assay

For MTT assays we followed a published protocol [55]. Briefly, cell survival after exposure to cisplatin or TMZ and in the presence of signaling inhibitors was determined by MTT assays. Signaling inhibitors 1 µM AG1024, 10 ng/ml AG1296, 3 µM Erlotinib, 2–20 µM LY294002, 30 nM Wortmannin, 5–20 µM U0126, and 5–20 µM PD98059 were added to culture medium prior to addition of cisplatin or TMZ for 72 h.

Annexin V apoptosis assay

For apoptosis measurements the BD Pharmingen™ FITC Annexin V Apoptosis Detection Kit (BD Biosciences) was used according to the manufacturer's protocol. Briefly, 2.5×10^5 cells were seeded into 6-well plates and incubated at 37 °C and 5% CO_2 overnight. After compound treatment for 72 h, cells were trypsinized and centrifuged for 4 min at 1500×*g*. Medium supernatant was removed and cells were resuspended in 500 µl binding buffer. 5 µl PI and 5 µl Annexin V-FITC were mixed with 100 µl of cells in binding buffer. After 15 min of incubation on ice,

samples were analyzed on a flow cytometry (FACSCalibur™, BD Bioscience).

Alkaline comet assay

1.25×10^5 cells were seeded into 6-well plates. After 24 h cells were treated with 20 µM LY294002 and TMZ for 1 h and washed with PBS. Cells were released from the culture plate by Accutase. Comet assays were performed as previously described [56]. For analysis of comets, 50 cells were selected randomly by image analyzing (Comet Assay IV, Perceptive instruments) using a Zeiss Axioskop 2 (Carl Zeiss, Jena).

Data analysis and statistical methods

Concentration effect curves were fitted to data points by nonlinear regression analysis using the four-parameter logistic equation (GraphPad™ Prism). Statistical differences between two groups were determined by unpaired 2-tailed Student's *t* test. Comparisons among several groups were performed by ANOVA followed by Turkey post hoc test. Data are presented as mean ± SEM.

Results

Glioblastoma multiforme are reported to have various deregulated signaling pathways which drive resistance towards radio- and chemotherapy [23, 57]. In order to investigate the activation of RTK pathways in vivo, we performed human proteome profiler arrays with a subset of proteins of tumor biopsies of four patients, which were diagnosed a secondary GBM and underwent surgery before TMZ treatment and of four patients which underwent a second surgery later on after TMZ treatment due to recurrence of the tumor. Due to time of sampling of the biopsies between years 1990 and 2015, grading of tumors was based on histopathological analysis and clinical observations according to the 2007 WHO classification [51]. Additional *IDH1* mutation analysis revealed that all GBM samples with one exception (P8) were *IDH1* mutant (Table 2) and could therefore also be classified as secondary GBM according to the recent 2016 WHO classification [1]. P8 was clinically judged as secondary GBM due to a previously diagnosed precursor lesion (low-grade glioma) and was therefore included in the analysis despite lack of *IDH1* mutation.

Table 2 *IDH1* mutation status of secondary GBM samples

Patient ID	Treatment	IDH1
P1	–	Mutated
P2	–	Mutated
P3	–	Mutated
P4	–	Mutated
P5	TMZ	Mutated
P6	TMZ	Mutated
P7	TMZ	Mutated
P8	TMZ	Wild-type

We found that several kinases were phosphorylated in all eight patients (Additional file 1: Figure S1a). Strikingly, there was a trend ($P < 0.05$) towards reduced phosphorylation of AKT and its downstream target cAMP response element-binding protein (CREB) in GBM of patients resistant to TMZ therapy while ERK activation remained unchanged on a high level (Fig. 1a and Additional file 1: Figure S1a) indicating a role of these kinase in resistance development. It is also interesting to note that several apoptotic proteins were expressed in GBM biopsies but only small differences were observed between untreated and TMZ treated and resistant patients (Additional file 1: Figure S1b). Only reduction in pro-caspase-3 expression in TMZ treated patients reached statistical significance ($P < 0.05$).

This led us to further elucidate these findings in vitro. As *IDH1* mutant cell lines are rare we focused our study on *IDH1* wild-type GBM cell lines and cells (Table 1). GBM cells are reported to be intrinsically resistant to anti-cancer drugs and different sensitivities to TMZ are reported in the literature. Thus, we initially characterized RTK signaling pathway expression and activation in U87, U251, and U373 GBM cell lines. EGF-R, IGF1-R, and PDGF-Rβ RTKs are overexpressed (Fig. 1b, left panel) and activated (Fig. 1b, middle panel) in all GBM cell lines. All of these growth factor receptors converge on MEK/ERK and PI3K pathway activation, which is reflected by phosphorylation of ERK, AKT and the downstream target CREB (Fig. 1b, right panel). Thus, as observed in vivo the MEK/ERK and PI3K pathways are also active in GBM cells and might be responsible for drug resistance.

Yet TMZ is the only substance for which a statistically significant and clinically relevant benefit in both, overall survival and progression free survival was demonstrated. Thus, TMZ was approved by both, EMA and US-FDA, for orally active cytostatic therapy of GBM. However, it is very difficult to handle in the laboratory setting as it must be given to cell culture assays in concentrations as high as or even beyond its solubility. In addition, TMZ is a prodrug with a highly complex pharmacokinetic bioactivation pattern and intracellular distribution. Thus, as many other groups, we also used cisplatin as a model substance with a similar molecular mechanism of action: both substances are DNA-alkylating agents.

We first characterized the status of cisplatin resistance in GBM cell lines U87, U251, and U373 by MTT cell survival assays (Fig. 2a). Intrinsic resistance of the cells is also demonstrated in Fig. 2b, where cisplatin IC_{50} concentrations of GBM cell lines are compared to

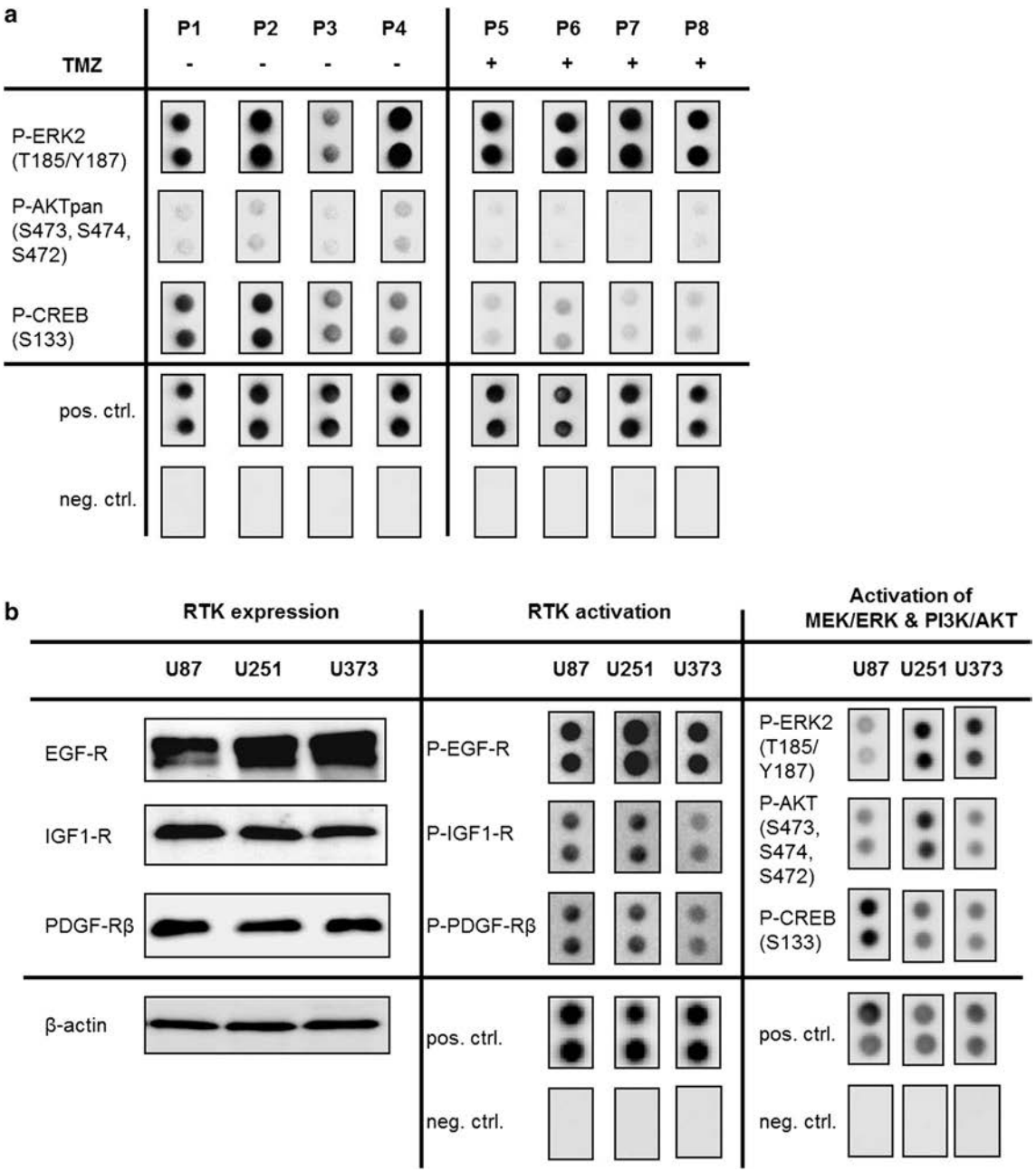

Fig. 1 The MEK/ERK and PI3K pathways are activated in GBM in vivo and in vitro. **a** Human proteome-profiler phospho-MAPkinase arrays of GBM tumor biopsies before and after TMZ treatment. Shown are biopsies derived from patients, who were newly diagnosed a secondary GBM and underwent surgery before TMZ treatment (P1–P4) and of patients which underwent a second surgery after TMZ treatment due to recurrence of the tumor (P5–P8). Phosphorylated ERK2 (T185/Y187, AKTpan (S473, S474, S472) and CREB (S133) were detected in all biopsies. **b** Western blotting reveals that EGF-R, IGF1-R, and PDGF-Rβ RTKs are constitutively overexpressed. β-actin Western blot was performed to control for loading (left panel). Human proteome-profiler phospho-antibody arrays were used to assess the activation status of RTKs (middle panel) and downstream targets ERK2 (T185/Y187), AKTpan (S473, S474, S472) and CREB (S133) (right panel)

non-resistant and cisplatin resistant breast and ovarian cancer cell lines as previously reported by us [53, 55]. GBM cell lines showed cisplatin tolerance comparable to cells with acquired cisplatin resistance and exhibit an average IC_{50} concentration of 10 μM, representing about threefold the concentration maximally achieved in plasma of patients treated with cisplatin. We then wished to investigate, whether the intrinsic resistance in

(See figure on next page.)

Fig. 2 GBM cell lines show high intrinsic tolerance to alkylating cytostatics cisplatin and TMZ. **a** Cisplatin resistance status of U87, U251, and U373 cell lines was assessed by MTT assays (n = 4). **b** Intrinsic resistance of GBM cell lines is demonstrated in comparison to cell pairs of non-resistant and cells with acquired resistance. GBM cell line IC_{50} concentrations of cisplatin parallel the ones of resistant MCF-7 breast-, and A2780 ovarian cancer cell lines (determined by MTT assays; n = 3). **c** GBM cell lines were treated by weekly cycles of cisplatin and IC_{50} values were assayed after each treatment cycle in MTT assays. IC_{50} values were obtained from sigmoidal concentration–response curves and dotted in a time-dependent manner. **d** Western blots showing MRP-2 and *P*-gp expression in GBM cell lines untreated and after 24 cycles of weekly intermittent cisplatin exposure. β-actin Western blot was performed to control for loading. **e** TMZ resistance status in U87, U251 and U373 cells was assessed by MTT assays (upper graph; n ≥ 6). The respective IC_{50} values for each cell line are shown in the table below the graph

GBM cells can be strengthened by long-term intermittent application of cisplatin in a way the drug is administered to patients. Therefore, we used a 6-month protocol of weekly intermittent cisplatin exposure, which we have used previously to generate cisplatin-resistant breast- and ovarian cancer cells [53, 55]. Interestingly, no gain in cisplatin tolerance could be observed in either of the three cell lines (Fig. 2c). We conclude that no intracellular pathway alteration emerged after 6 months of weekly intermittent cisplatin treatment. In addition, we assumed that no transport protein expression has occurred over the 24 weekly treatment cycles, which is also demonstrated by low to undetectable *P*-gp and MRP-2 expression (Fig. 2d). In addition, GBM cell lines displayed high resistance towards TMZ (Fig. 2e) with calculated IC_{50} values at around 1 mM TMZ (table in Fig. 2e). We were not able to determine the bottom of the concentration response curve for U87 and U373 cells in MTT assays at feasible TMZ concentrations. To determine IC_{50} values curves were extrapolated to zero.

To inhibit RTKs and downstream signaling pathways, we used small molecule inhibitors, each of them targeting specifically one protein of the activated network. However, no specific inhibitor of any of the RTKs was able to overcome resistance (Additional file 2: Figure S2). Due to their relevance in drug resistance, we used two structurally different substances to inhibit MEK/ERK, and PI3K/AKT signaling, respectively. All cell lines under investigation show pronounced PI3K/AKT pathway activation (Fig. 1b), which one would expect to be caused by *PTEN* mutation. Therefore, we tested initially if inhibition of PI3K mediated AKT phosphorylation was capable of sensitizing the cell lines to TMZ. Inhibition of this survival pathway with the PI3K inhibitor LY294002 triggered capability of the cells to apoptotic stimuli like TMZ (Fig. 3a). Reduction of AKT phosphorylation after LY294002 treatment for 72 h in U251 cells is shown in Additional file 3: Figure S3. The sensitizing effect of LY294002 was most pronounced in U251 cells. Therefore, in further experiments with TMZ we focused on this cell line. In order to quantitatively characterize the concentration response relationship we recorded concentration response curves with increasing LY294002 and TMZ concentrations (Fig. 3b). We observed a systematic left shift of the TMZ concentration response curve at increasing LY294002 concentrations becoming significant at 12 µM LY294002 (table in Fig. 3b). LY294002 and wortmannin, another PI3K inhibitor, also significantly left-shifted cisplatin concentration response curves in all cell lines. Cisplatin IC_{50} values derived from respective curves are displayed in Fig. 3c.

Annexin V apoptosis assays of U251 cells confirmed an increase in apoptotic rates after combination treatment when compared to TMZ or LY294002 treatment alone (Fig. 4a, b). Furthermore, combination treatment also resulted in significantly increased DNA damage as determined by comet assays (Fig. 4c). These data confirm findings from Westhoff et al. [42] who have shown that inhibition of PI3K and DNA-dependent protein kinase (DNA-PK), a kinase involved in DNA repair and also inhibited by LY294002, sensitize GBM cells to cytostatic drugs by interfering with DNA damage repair. In order to gain insight into the molecular mechanisms we performed proteome profiler arrays with cell lysates from TMZ and LY294002 treated U251 cells. TMZ induced phosphorylation of AKT and P53 and expression of a variety of apoptotic and anti-apoptotic proteins. Notably, concomitant LY294002 treatment abolished TMZ-induced effects such as P53 phosphorylation or claspin expression indicating that DNA damage repair is disturbed by LY294002 (Additional file 3: Figure S3). Western blotting of P53 and phosphorylated P53 (S15) confirmed these findings. Interestingly despite P53 activation, P21 protein abundance was not affected by TMZ or LY294002 treatment (Fig. 4d).

In a next step we targeted MEK with two specific inhibitors, U0126 and PD98059, respectively. Cell lines U373 and U251 have been reported to be both NF1-deficient and to display different sensitivities for MEK inhibition [31]. Concentration response experiments with TMZ in both cell lines revealed no significant left shift of the curves after concomitant U0126 or PD98059 treatment at 5 and 20 µM, respectively. Conversely, MEK inhibition even tended to desensitize cells for TMZ treatment and this effect was more pronounced in U373 cells which have been reported to be more sensitive to

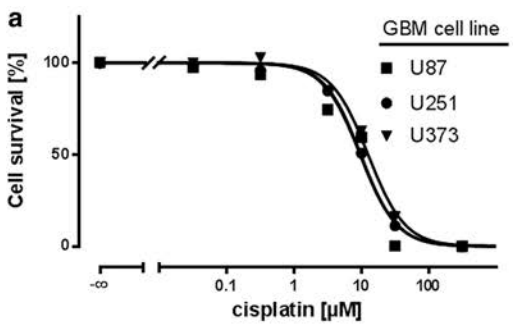

b

cell line	*cisplatin IC_{50} [μM]*
U87	11.7
U251	10.3
U373	13.0
MCF-7	3.0
MCF-7 CisR	10.0
A2780	2.4
A2780 CisR	12.8

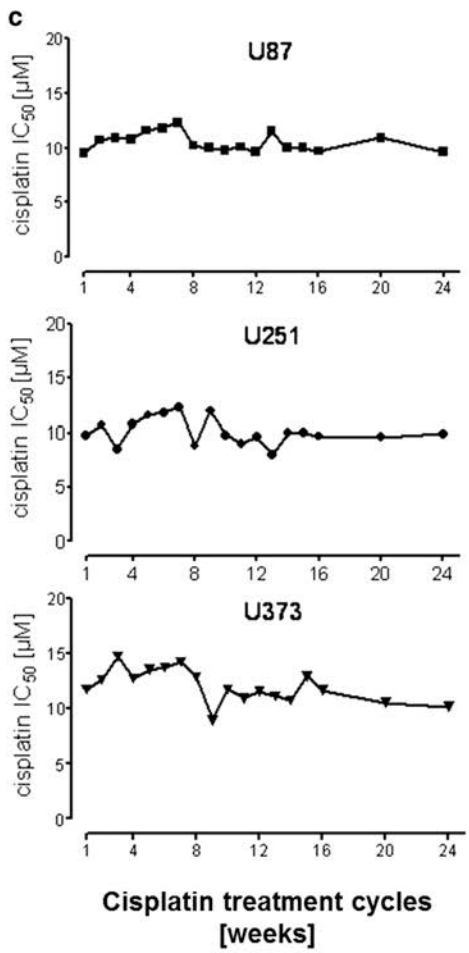

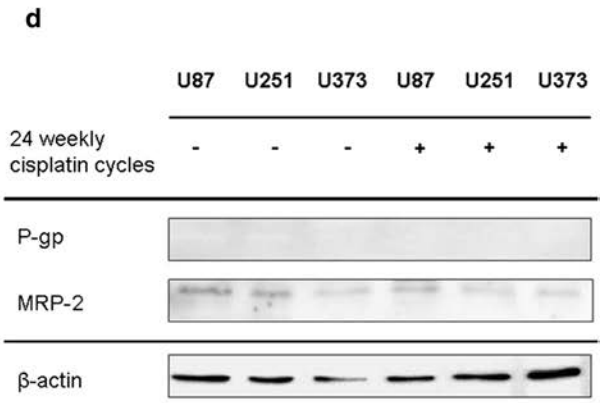

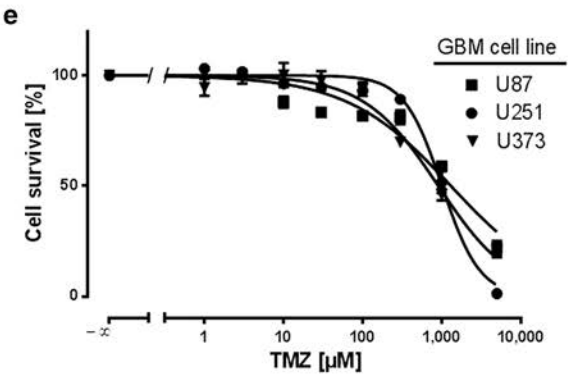

cell line	*TMZ IC_{50} [μM]*
U87	1309
U251	1008
U373	907

MEK inhibition (Fig. 5a–d) [31]. This might be owed to reduced proliferation velocity and subsequent reduced ability of TMZ to alkylate DNA during mitosis. Indeed, U0126 and PD98059, respectively, almost completely block proliferation of U373 and U251 cells (Additional file 4: Figure S4). Similar results were obtained for

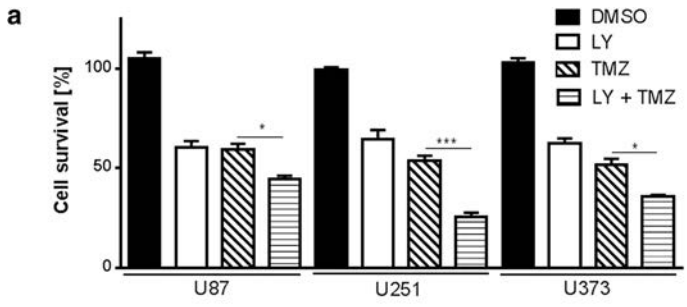

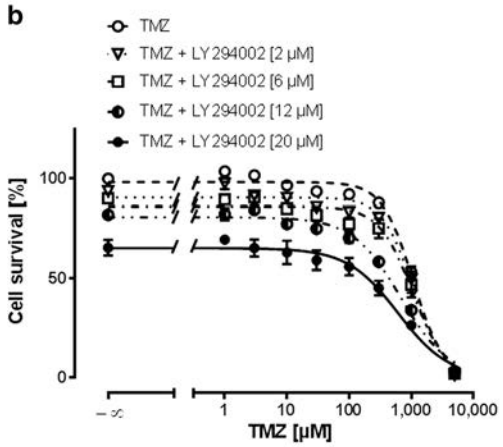

LY294002 [µM]	*TMZ IC_{50} [µM]*
0	1067
2	1065
6	1048
12	677*
20	610*

c

		cisplatin IC_{50} [µM]		
Inhibitor	***Function***	***U87***	***U251***	***U373***
DMSO	control	9.5	9.8	12.6
LY294002	PI3K inhibitor	4.0*	3.2*	5.4*
Wortmannin	PI3K inhibitor	3.7*	3.0*	4.4*

Fig. 3 PI3K as a key component of TMZ resistance in GBM cells. **a** PI3K inhibition (20 µM LY294002) sensitizes all GBM cells to TMZ (1000 µM) (n = 3). **b** MTT concentration response curve showing concentration dependency of sensitization by LY294002 in U251 cells (upper graph). Respective TMZ IC_{50} values at increasing LY294002 concentrations are displayed in the table below the graph (n ≥ 3). **c** Both, LY294002 (5 µM) and Wortmannin (30 nM), sensitize GBM cell lines to cisplatin. Presented IC_{50} values were derived from MTT assays (n = 3). *$P < 0.05$, ***$P < 0.001$

cisplatin in all other cell lines (Fig. 5e). These data indicate that the MEK/ERK pathway is negatively associated to GBM intrinsic chemoresistance.

Finally, we asked whether our findings can be translated to a more clinically relevant scenario. Therefore, we isolated human primary GBM cells from a tumor biopsy. In line with our findings in GBM cell lines, inhibition of PI3K also sensitized primary cells to TMZ. In addition, MEK inhibition with U0126 or PD98059 did not affect cellular resistance of these cells (Fig. 6a–d) indicating that inhibition of PI3K signaling to enhance chemotherapy might also be relevant in patients.

(See figure on next page.)

Fig. 4 LY290042 increases apoptosis and DNA damage of TMZ treated U251 cells. **a** Representative FACS blots of U251 cells treated with either vehicle (DMSO), TMZ (1000 µM), LY294002 (20 µM) or the combination for 72 h. Annexin V positive cells were regarded as apoptotic cells. **b** Quantification of apoptotic cells from Annexin V assays (n = 5). **c** DNA damage was assayed by comet assay and is displayed as tail moment in U251 cells treated with LY290042, TMZ or vehicle (DMSO) for 1 h as indicated. **d** Representative Western blots showing P–P53 (S15), P53 and P21 expression in U251 cells treated with LY290042 (20 µM), TMZ (1000 µM) or vehicle (DMSO) for 24 h as indicated. β-actin Western blot was performed to control for loading (left panels). Densitometric analysis of the respective (phospho-) proteins relative to β-actin (right bars, n = 3). *$P < 0.05$, ***$P < 0.001$

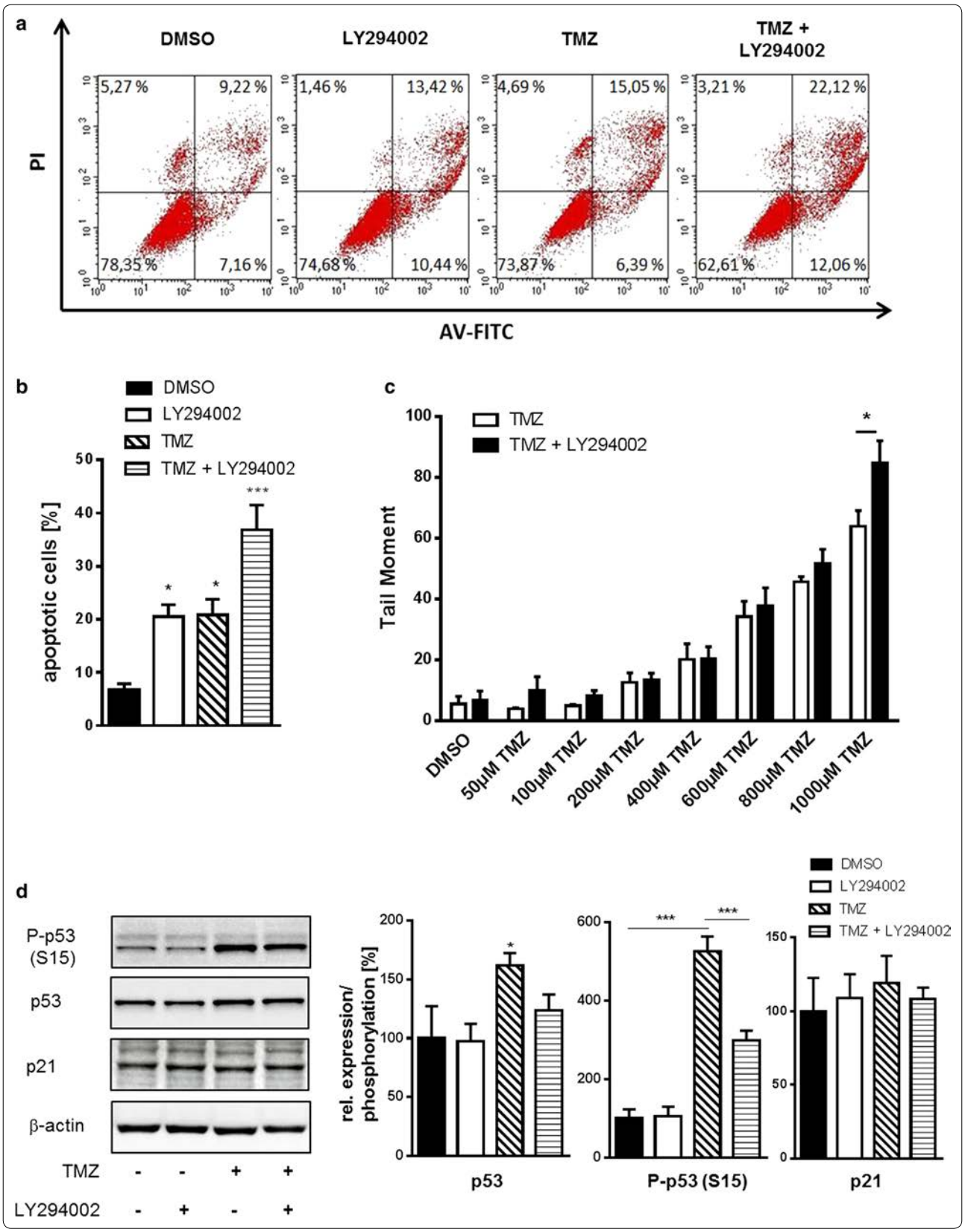
a
DMSO
LY294002
TMZ
TMZ + LY294002
PI
AV-FITC
5,27 %
9,22 %
78,35 %
7,16 %
1,46 %
13,42 %
74,68 %
10,44 %
4,69 %
15,05 %
73,87 %
6,39 %
3,21 %
22,12 %
62,61 %
12,06 %
b
DMSO
LY294002
TMZ
TMZ + LY294002
apoptotic cells [%]
c
TMZ
TMZ + LY294002
Tail Moment
DMSO
50µM TMZ
100µM TMZ
200µM TMZ
400µM TMZ
600µM TMZ
800µM TMZ
1000µM TMZ
d
P-p53 (S15)
p53
p21
β-actin
TMZ
LY294002
rel. expression/ phosphorylation [%]
p53
P-p53 (S15)
p21

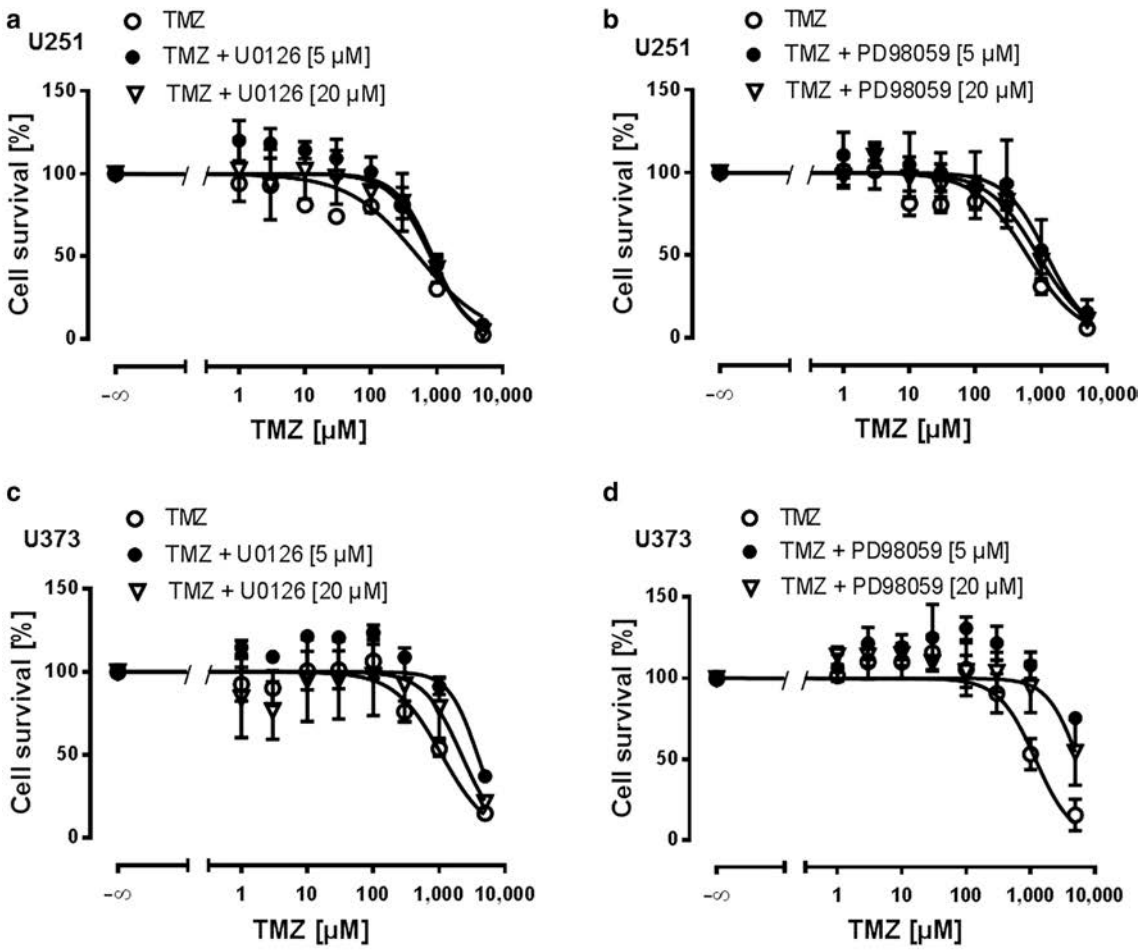

e

	cisplatin IC_{50} [µM]		
Inhibitor	**U87**	**U251**	**U373**
DMSO	9.5	9.8	12.6
U0126	14.2	11.1	9.1
PD98059	9.3	9.8	13.2

Fig. 5 MEK inhibition negatively impacts on intrinsic chemoresistance. MTT assays showing that **a** U0126 (5 and 20 µM) and **b** PD98059 (5 and 20 µM) desensitize U251 cells for TMZ treatment (n = 3). **c** U0126 (5 and 20 µM) and **d** PD98059 (5 and 20 µM) lead to a strong right shift of TMZ concentration response curves in U373 cells (n = 3). **e** U0126 (10 µM) and PD98059 (20 µM) do not sensitize GBM cell lines to cisplatin. Presented IC_{50} values were derived from MTT assays (n = 3)

Discussion

An important mechanism of chemoresistance of GBM is an intrinsic high activation status of the PI3K/AKT survival pathway due to frequent mutations in the *PTEN* gene [19–21]. It appears logical that inhibition of this pathway should enhance chemosensitivity and prone cells to apoptosis. Pre-clinical results are encouraging but, clinical evidence of efficacy of inhibitors of the PI3K/AKT pathway is still lacking [46]. Several reasons might be responsible. Targeting the brain beyond the blood brain barrier is often not feasible leading to failure of drug development due to pharmacokinetic reasons. In addition, PI3K is a ubiquitous enzyme and inhibition is frequently associated with adverse events leading to

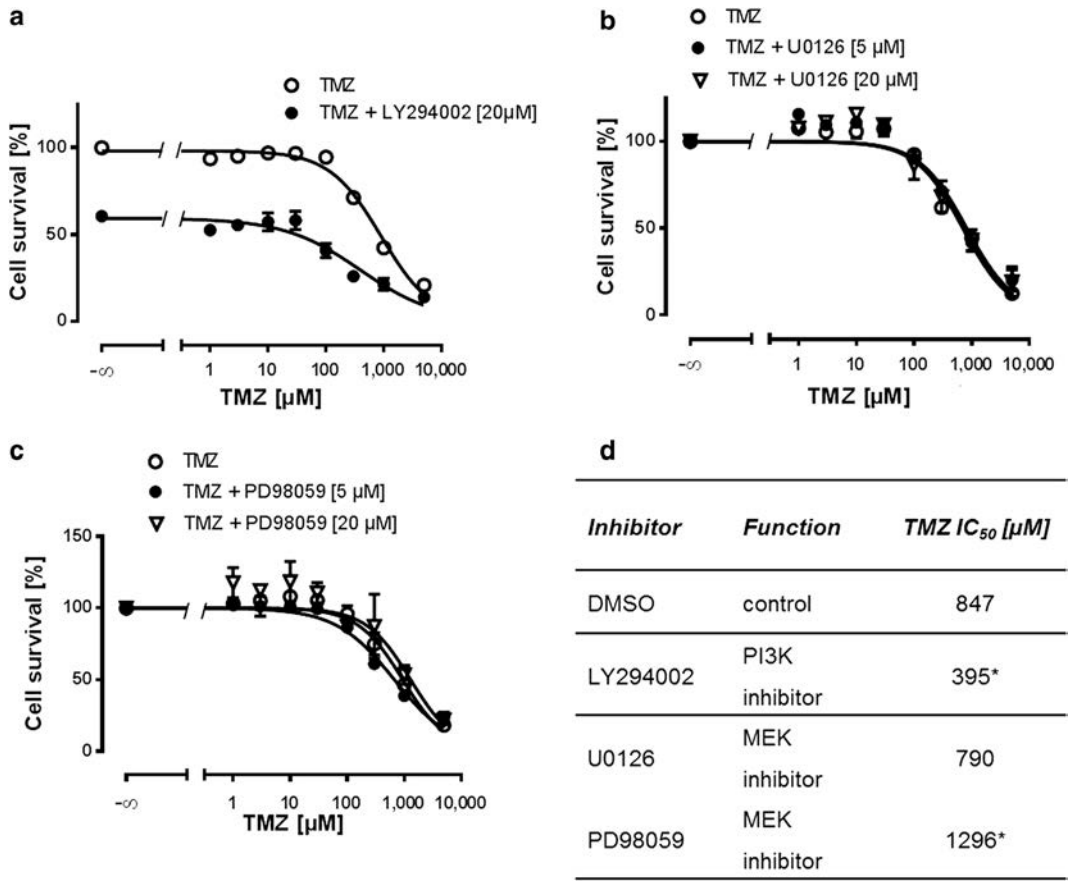

d

Inhibitor	*Function*	*TMZ IC_{50} [μM]*
DMSO	control	847
LY294002	PI3K inhibitor	395*
U0126	MEK inhibitor	790
PD98059	MEK inhibitor	1296*

Fig. 6 PI3K but not MEK inhibition sensitizes human primary GBM cells to TMZ. **a** PI3K inhibition (20 μM LY294002) leads to a left shift of the TMZ concentration response curve (n = 3). **b** Neither, U0126 (5 and 20 μM; n ≥ 3) **c** nor PD98059 (5 and 20 μM; n ≥ 3) sensitize primary cells to TMZ. **d** Derived mean IC_{50} values for TMZ of respective primary GBM cells treated with LY294002 and MEK inhibitors (20 μM each; n ≥ 3). *$P < 0.05$

termination of clinical trials for safety reasons despite efficacy. On a molecular level counter regulatory mechanisms involving upregulation of RTKs or the RAS pathway have also been described to be involved in limiting PI3K inhibitor efficacy [47–50]. We found a strong phosphorylation of proteins of the PI3K and MEK/ERK pathways in very rare biopsies of secondary GBM naive to TMZ and resistant to TMZ treatment. Secondary GBM itself do only constitute a very small subgroup of GBM accounting for not more than 5% in total. Thus, to gain these very rare biopsies *before* and *after* TMZ treatment took great effort. Interestingly, phosphorylation of AKT and its downstream effector CREB was reduced in TMZ-resistant tumors indicating that these pathways are deregulated and are probably involved in resistance development while no changes were observed in ERK phosphorylation status. These findings however have to be interpreted with caution as secondary GBM are highly heterogeneous and only a small number of biopsies from eight different patients was analyzed. Thus, it was even more remarkable that significant differences were observed between groups despite the limitations described above. These findings encouraged us to further elaborate the quantitative impact of these pathways on chemoresistance in in vitro experiments. Due to the scarcity of available material, we were not able to obtain secondary GBM cells with an *IDH1* mutation and based our study on *IDH* wild-type cells. Despite histopathological similarities, primary and secondary GBM derive from different precursor cells and are distinct tumor entities [7] what makes translation of our results difficult. In addition, *MGMT* promoter methylation status was only available for cells but not for tumor samples. As both, *IDH1* mutation and MGMT expression, can predict outcome of therapy [8, 9] obtained in vitro results cannot directly be translated to the clinical situation of our tumor sample analysis.

We found that GBM cell lines were highly resistant to cisplatin comparable to resistant breast (MCF-7 CisR) and ovarian cancer cells (A2780 CisR) [53]. IC_{50} values

for TMZ were in the range of 1 mM for all cell lines indicating high intrinsic resistance also to TMZ.

Since, PI3K and MEK/ERK signaling cascades operate downstream of membrane-spanning growth-factor receptors, it is intuitive that inhibition of receptors for EGF, IGF-1, and PDGF did not impact on cisplatin resistance. This is in line with clinical data that small molecule RTK inhibitors or monoclonal antibodies designed to target RTKs failed to improve GBM therapy [50, 51]. It has previously been reported that PI3K inhibition sensitizes tumor cells to extrinsic TRAIL-induced apoptosis as well as apoptosis induced by DNA damaging agents [40–44, 58] while another study suggests that PI3K inhibition in GBM stem cells and differentiated primary cells only leads to poor or negative chemosensitization [45]. These discrepancies drove us to investigate these findings in more detail in a quantitative manner and finally—to generalize our findings—in primary human GBM cells. A systematic and statistically significant left shift of concentration response curves and approximately twofold reduction of TMZ and cisplatin IC_{50} values was observed upon PI3K inhibition in all three cell lines and most importantly also in primary cells. Investigating the molecular mechanism of this chemosensitization we found that PI3K inhibition induced DNA damage which is probably mediated by inhibition of DNA repair after TMZ treatment. This is further strengthened by the fact, that TMZ-induced P53 phosphorylation and claspin expression, which both are involved in DNA damage response, were reversed by LY294002 treatment. These data confirm findings from Westhoff et al. [42] who have shown that LY294002 sensitize GBM cells to cytostatic drugs by interfering with DNA damage repair. Nevertheless, it cannot finally be concluded from these experiments if inhibition of DNA repair by LY294002 is solely due to inhibition of PI3K or also inhibition of other members of the PI3K family such as DNA-PK, ataxia-telangiectasia-mutated kinase (ATM) and Rad3-related kinase (ATR). However, data from other groups suggest, that inhibition of ATR/ATM and DNA-PK by LY294002 does not occur at the concentrations tested here (20 µM) and that effects on DNA damage repair are probably mediated by PI3K inhibition [53–55].

We found a negative impact of the MEK/ERK pathway on chemosensitivity upon inhibition with two different inhibitors in all cell lines and primary cells. Both MEK inhibitors led to an almost complete growth arrest. As TMZ is an agent which damages DNA by forming *O*6-alkylguanine [59], a process which requires cell proliferation, it might explain why MEK inhibition was not successful in sensitizing cells to TMZ and cisplatin. These findings are in line with Riedel et al. who have shown that the RAF inhibitor sorafenib reduced proliferation but failed to enhance chemosensitivity of GBM cells [32].

Conclusion

Taken together, our data indicate that the PI3K pathway is one of the main pathways involved in GBM chemoresistance. Combination of TMZ with PI3K inhibitors might therefore result in clinical benefit for GBM patients when problems of pharmacokinetics and safety of these compounds can be addressed. This is underlined by the fact that several inhibitors of the PI3K/mTOR axis are currently undergoing clinical development for GBM [39]. A further implication of our study is that simply combining an inhibitor of the MEK/ERK signaling cascade with chemotherapy in GBM is probably not a recommendable strategy.

Additional files

Additional file 1: Figure S1. Densitometric analysis of (**a**) human proteome profiler phospho-MAPkinase and (**b**) human apoptosis arrays of GBM tumor biopsies of patients which were newly diagnosed a secondary GBM and underwent surgery before TMZ treatment (n=4) and of patients which underwent a second surgery after TMZ treatment due to recurrence of the tumor (n=4). Phosphorylation was normalized to positive control spots. $*P < 0.05$, $**P < 0.01$.**Additional file 2: Figure S2.** Impact of RTK inhibitors on cisplatin resistance in GBM cell lines. RTK inhibitors erlotinib (3 µM), AG1024 (1 µM), and AG1296 (10 ng/mL) do not sensitize GBM cell lines to cisplatin. Presented IC_{50} values were derived from MTT assays (n=3).**Additional file 3: Figure S3.** Human proteome-profiler (**a**) phospho-MAPKkinase and (**b**) apoptosis arrays of U251 cells treated with LY290042 (20 µM), TMZ (1000 µM) or vehicle (DMSO) for 72 hours.**Additional file 4: Figure S4.** MEK inhibition blocks cell proliferation of U251 and U373 cells. (**a**) U251 cells and (**b**) U373 cells were treated with vehicle (DMSO), U0126 or PD98059 as indicated (n=3). Cells were trypsinized at 24, 48 and 72 hours post treatment and counted. Cell number at time point 0 hours was set to 1.

Abbreviations

AKT: protein kinase B (PKB); ATM: ataxia-telangiectasia-mutated kinase; ATR : Rad3-related kinase; GBM: glioblastoma multiforme; CREB: cAMP response element-binding protein; DNA-PK: DNA-dependent protein kinase; EGF-R: epidermal growth factor receptor; ERK: extracellular signal-regulated kinase; IDH: isocitrate dehydrogenase; IGF1-R: insulin-like growth factor 1 receptor; MEK: mitogen-activated protein kinase kinase (MAPKK); MGMT: O^6-methylguanine-DNA-methyltransferase; MRP: multi-drug resistance proteins; mTOR: mammalian target of rapamycin; NF1: neurofibromin 1; PDGF-R: platelet-derived growth factor receptor; *P*-gp: *P*-glycoprotein; PI3K: phosphatidylinositide 3-kinase; PTEN: phosphatase and tensin homolog; RB: retinoblastoma protein; RTK: receptor tyrosine kinase; TMZ: temozolomide.

Authors' contributions

BH, NE, RF designed and performed experiments, analyzed data and wrote the manuscript. VK, CK, VB, DK, JC, JW, MW-M, SW performed experiments and analyzed data. GR, MT prepared human tissue specimens and isolated human primary cells. All authors read and approved the final manuscript.

Author details

[1] Federal Institute for Drugs and Medical Devices, Kurt-Georg-Kiesinger-Allee 3, 53175 Bonn, Germany. [2] Institute of Pharmacy, University of Bonn, 53121 Bonn, Germany. [3] Applied Pharmacy, University of Applied Sciences Kaiserslautern, Campus Pirmasens, Carl-Schurz-Str. 10-16, 66953 Pirmasens,

Germany. [4] Faculty of Applied Natural Sciences, Cologne University of Applied Sciences, Kaiser-Wilhelm-Allee, 51368 Leverkusen, Germany. [5] Department of General Neurosurgery, Center for Neurosurgery, University Hospital Cologne, 50937 Cologne, Germany.

Acknowledgements
We thank Julia Stingl and Dirk von Mallek for support and expert scientific advice.

Competing interests
The authors declare that they have no competing interests.

Availability of data and materials
The datasets used and/or analyzed during the current study are available from the corresponding author on reasonable request.

Consent for publication
Not applicable.

Disclaimer
The opinions mentioned throughout the following article are personal views of the authors and do not reflect an official position of the Federal Institute for Drugs and Medical Devices or an EMA-committee or working party, respectively.

Ethics approval and consent to participate
Human tissue specimens of secondary glioblastoma were taken from the tumor tissue bank of the Clinic of Neurosurgery, University of Cologne. The collection of samples was approved by the University's Institutional Ethical Board. Informed consent of the patients was obtained according to the Helsinki declaration of ethical requirements.

Funding
This article was supported by an intramural funding of the Federal Institute for Drugs and Medical Devices (BfArM) and the University of Applied Sciences Kaiserslautern.

Publisher's Note

Received: 8 November 2017 Accepted: 14 March 2018
Published online: 04 May 2018

References

1. Louis DN, Perry A, Reifenberger G, von Deimling A, Figarella-Branger D, Cavenee WK, Ohgaki H, Wiestler OD, Kleihues P, Ellison DW. The 2016 World Health Organization classification of tumors of the central nervous system: a summary. Acta Neuropathol. 2016;131(6):803–20.
2. Siegel RL, Miller KD, Jemal A. Cancer statistics, 2016. CA Cancer J Clin. 2016;66(1):7–30.
3. Stupp R, Mason WP, van den Bent MJ, Weller M, Fisher B, Taphoorn MJ, Belanger K, Brandes AA, Marosi C, Bogdahn U, et al. Radiotherapy plus concomitant and adjuvant temozolomide for glioblastoma. N Engl J Med. 2005;352(10):987–96.
4. Stupp R, Hegi ME, Mason WP, van den Bent MJ, Taphoorn MJ, Janzer RC, Ludwin SK, Allgeier A, Fisher B, Belanger K, et al. Effects of radiotherapy with concomitant and adjuvant temozolomide versus radiotherapy alone on survival in glioblastoma in a randomised phase III study: 5-year analysis of the EORTC-NCIC trial. Lancet Oncol. 2009;10(5):459–66.
5. Ostrom QT, Gittleman H, Xu J, Kromer C, Wolinsky Y, Kruchko C, Barnholtz-Sloan JS. CBTRUS statistical report: primary brain and other central nervous system tumors diagnosed in the United States in 2009–2013. Neuro Oncol. 2016;18(suppl_5):v1–75.
6. Ohgaki H, Kleihues P. Genetic pathways to primary and secondary glioblastoma. Am J Pathol. 2007;170(5):1445–53.
7. Ohgaki H, Kleihues P. The definition of primary and secondary glioblastoma. Clin Cancer Res. 2013;19(4):764–72.
8. Molenaar RJ, Verbaan D, Lamba S, Zanon C, Jeuken JW, Boots-Sprenger SH, Wesseling P, Hulsebos TJ, Troost D, van Tilborg AA, et al. The combination of IDH1 mutations and MGMT methylation status predicts survival in glioblastoma better than either IDH1 or MGMT alone. Neuro Oncol. 2014;16(9):1263–73.
9. Yang P, Zhang W, Wang Y, Peng X, Chen B, Qiu X, Li G, Li S, Wu C, Yao K, et al. IDH mutation and MGMT promoter methylation in glioblastoma: results of a prospective registry. Oncotarget. 2015;6(38):40896–906.
10. Gottesman MM, Fojo T, Bates SE. Multidrug resistance in cancer: role of ATP-dependent transporters. Nat Rev Cancer. 2002;2(1):48–58.
11. Wen PY, Kesari S. Malignant gliomas in adults. N Engl J Med. 2008;359(5):492–507.
12. Ishii N, Maier D, Merlo A, Tada M, Sawamura Y, Diserens AC, Van Meir EG. Frequent co-alterations of TP53, p16/CDKN2A, p14ARF, PTEN tumor suppressor genes in human glioma cell lines. Brain Pathol. 1999;9(3):469–79.
13. Iwadate Y, Fujimoto S, Tagawa M, Namba H, Sueyoshi K, Hirose M, Sakiyama S. Association of p53 gene mutation with decreased chemosensitivity in human malignant gliomas. Int J Cancer. 1996;69(3):236–40.
14. Carrasco-Garcia E, Saceda M, Martinez-Lacaci I. Role of receptor tyrosine kinases and their ligands in glioblastoma. Cells. 2014;3(2):199–235.
15. Manning BD, Cantley LC. AKT/PKB signaling: navigating downstream. Cell. 2007;129(7):1261–74.
16. Tokunaga E, Oki E, Egashira A, Sadanaga N, Morita M, Kakeji Y, Maehara Y. Deregulation of the Akt pathway in human cancer. Curr Cancer Drug Targets. 2008;8(1):27–36.
17. Vivanco I, Sawyers CL. The phosphatidylinositol 3-Kinase AKT pathway in human cancer. Nat Rev Cancer. 2002;2(7):489–501.
18. Martini M, De Santis MC, Braccini L, Gulluni F, Hirsch E. PI3K/AKT signaling pathway and cancer: an updated review. Ann Med. 2014;46(6):372–83.
19. Eyler CE, Foo WC, LaFiura KM, McLendon RE, Hjelmeland AB, Rich JN. Brain cancer stem cells display preferential sensitivity to Akt inhibition. Stem Cells. 2008;26(12):3027–36.
20. Hirose Y, Katayama M, Mirzoeva OK, Berger MS, Pieper RO. Akt activation suppresses Chk2-mediated, methylating agent-induced G2 arrest and protects from temozolomide-induced mitotic catastrophe and cellular senescence. Cancer Res. 2005;65(11):4861–9.
21. Molina JR, Hayashi Y, Stephens C, Georgescu MM. Invasive glioblastoma cells acquire stemness and increased Akt activation. Neoplasia. 2010;12(6):453–63.
22. Haas-Kogan D, Shalev N, Wong M, Mills G, Yount G, Stokoe D. Protein kinase B (PKB/Akt) activity is elevated in glioblastoma cells due to mutation of the tumor suppressor PTEN/MMAC. Curr Biol. 1998;8(21):1195–8.
23. Brennan CW, Verhaak RG, McKenna A, Campos B, Noushmehr H, Salama SR, Zheng S, Chakravarty D, Sanborn JZ, Berman SH, et al. The somatic genomic landscape of glioblastoma. Cell. 2013;155(2):462–77.
24. Chakravarti A, Zhai G, Suzuki Y, Sarkesh S, Black PM, Muzikansky A, Loeffler JS. The prognostic significance of phosphatidylinositol 3-kinase pathway activation in human gliomas. J Clin Oncol. 2004;22(10):1926–33.
25. Koul D. PTEN signaling pathways in glioblastoma. Cancer Biol Ther. 2008;7(9):1321–5.
26. Carico C, Nuno M, Mukherjee D, Elramsisy A, Dantis J, Hu J, Rudnick J, Yu JS, Black KL, Bannykh SI, et al. Loss of PTEN is not associated with poor survival in newly diagnosed glioblastoma patients of the temozolomide era. PLoS ONE. 2012;7(3):e33684.
27. Pelloski CE, Lin E, Zhang L, Yung WK, Colman H, Liu JL, Woo SY, Heimberger AB, Suki D, Prados M, et al. Prognostic associations of activated mitogen-activated protein kinase and Akt pathways in glioblastoma. Clin Cancer Res. 2006;12(13):3935–41.
28. Knobbe CB, Reifenberger J, Reifenberger G. Mutation analysis of the Ras pathway genes NRAS, HRAS, KRAS and BRAF in glioblastomas. Acta Neuropathol. 2004;108(6):467–70.
29. Shi Z, Chen Q, Li C, Wang L, Qian X, Jiang C, Liu X, Wang X, Li H, Kang C, et al. MiR-124 governs glioma growth and angiogenesis and enhances chemosensitivity by targeting R-Ras and N-Ras. Neuro Oncol. 2014;16(10):1341–53.
30. Wang L, Shi ZM, Jiang CF, Liu X, Chen QD, Qian X, Li DM, Ge X, Wang XF, Liu LZ, et al. MiR-143 acts as a tumor suppressor by targeting N-RAS and enhances temozolomide-induced apoptosis in glioma. Oncotarget. 2014;5(14):5416–27.

31. See WL, Tan IL, Mukherjee J, Nicolaides T, Pieper RO. Sensitivity of glioblastomas to clinically available MEK inhibitors is defined by neurofibromin 1 deficiency. Cancer Res. 2012;72(13):3350–9.
32. Riedel M, Struve N, Muller-Goebel J, Kocher S, Petersen C, Dikomey E, Rothkamm K, Kriegs M. Sorafenib inhibits cell growth but fails to enhance radio- and chemosensitivity of glioblastoma cell lines. Oncotarget. 2016;7(38):61988–95.
33. Jia J, Zhu F, Ma X, Cao Z, Li Y, Chen YZ. Mechanisms of drug combinations: interaction and network perspectives. Nat Rev Drug Discov. 2009;8(2):111–28.
34. McDowell KA, Riggins GJ, Gallia GL. Targeting the AKT pathway in glioblastoma. Curr Pharm Des. 2011;17(23):2411–20.
35. Rodon J, Dienstmann R, Serra V, Tabernero J. Development of PI3K inhibitors: lessons learned from early clinical trials. Nat Rev Clin Oncol. 2013;10(3):143–53.
36. Courtney KD, Corcoran RB, Engelman JA. The PI3K pathway as drug target in human cancer. J Clin Oncol. 2010;28(6):1075–83.
37. Engelman JA. Targeting PI3K signalling in cancer: opportunities, challenges and limitations. Nat Rev Cancer. 2009;9(8):550–62.
38. Porta C, Paglino C, Mosca A. Targeting PI3K/Akt/mTOR signaling in cancer. Front Oncol. 2014;4:64.
39. Wen PY, Lee EQ, Reardon DA, Ligon KL, Alfred Yung WK. Current clinical development of PI3K pathway inhibitors in glioblastoma. Neuro Oncol. 2012;14(7):819–29.
40. Chen L, Han L, Shi Z, Zhang K, Liu Y, Zheng Y, Jiang T, Pu P, Jiang C, Kang C. LY294002 enhances cytotoxicity of temozolomide in glioma by down-regulation of the PI3K/Akt pathway. Mol Med Report. 2011;5:575–9.
41. Carminati PO, Donaires FS, Marques MM, Donadi EA, Passos GA, Sakamoto-Hojo ET. Cisplatin associated with LY294002 increases cytotoxicity and induces changes in transcript profiles of glioblastoma cells. Mol Biol Rep. 2014;41(1):165–77.
42. Westhoff MA, Kandenwein JA, Karl S, Vellanki SH, Braun V, Eramo A, Antoniadis G, Debatin KM, Fulda S. The pyridinylfuranopyrimidine inhibitor, PI-103, chemosensitizes glioblastoma cells for apoptosis by inhibiting DNA repair. Oncogene. 2009;28(40):3586–96.
43. Prasad G, Sottero T, Yang X, Mueller S, James CD, Weiss WA, Polley MY, Ozawa T, Berger MS, Aftab DT, et al. Inhibition of PI3K/mTOR pathways in glioblastoma and implications for combination therapy with temozolomide. Neuro Oncol. 2011;13(4):384–92.
44. Sinnberg T, Lasithiotakis K, Niessner H, Schittek B, Flaherty KT, Kulms D, Maczey E, Campos M, Gogel J, Garbe C, et al. Inhibition of PI3K-AKT-mTOR signaling sensitizes melanoma cells to cisplatin and temozolomide. J Invest Dermatol. 2009;129(6):1500–15.
45. Strobele S, Schneider M, Schneele L, Siegelin MD, Nonnenmacher L, Zhou S, Karpel-Massler G, Westhoff MA, Halatsch ME, Debatin KM. A potential role for the inhibition of PI3K signaling in glioblastoma therapy. PLoS ONE. 2015;10(6):e0131670.
46. Westhoff MA, Karpel-Massler G, Bruhl O, Enzenmuller S, La Ferla-Bruhl K, Siegelin MD, Nonnenmacher L, Debatin KM. A critical evaluation of PI3K inhibition in glioblastoma and neuroblastoma therapy. Mol Cell Ther. 2014;2:32.
47. Will M, Qin AC, Toy W, Yao Z, Rodrik-Outmezguine V, Schneider C, Huang X, Monian P, Jiang X, de Stanchina E, et al. Rapid induction of apoptosis by PI3K inhibitors is dependent upon their transient inhibition of RAS-ERK signaling. Cancer Discov. 2014;4(3):334–47.
48. Rodrik-Outmezguine VS, Chandarlapaty S, Pagano NC, Poulikakos PI, Scaltriti M, Moskatel E, Baselga J, Guichard S, Rosen N. mTOR kinase inhibition causes feedback-dependent biphasic regulation of AKT signaling. Cancer Discov. 2011;1(3):248–59.
49. Serra V, Scaltriti M, Prudkin L, Eichhorn PJ, Ibrahim YH, Chandarlapaty S, Markman B, Rodriguez O, Guzman M, Rodriguez S, et al. PI3K inhibition results in enhanced HER signaling and acquired ERK dependency in HER2-overexpressing breast cancer. Oncogene. 2011;30(22):2547–57.
50. Chandarlapaty S, Sawai A, Scaltriti M, Rodrik-Outmezguine V, Grbovic-Huezo O, Serra V, Majumder PK, Baselga J, Rosen N. AKT inhibition relieves feedback suppression of receptor tyrosine kinase expression and activity. Cancer Cell. 2011;19(1):58–71.
51. Louis DN, Ohgaki H, Wiestler OD, Cavenee WK, Burger PC, Jouvet A, Scheithauer BW, Kleihues P. The 2007 WHO classification of tumours of the central nervous system. Acta Neuropathol. 2007;114(2):97–109.
52. Werner JM, Kuhl S, Stavrinou P, Rohn G, Krischek B, Blau T, Goldbrunner R, Timmer M. Expression of FAS-L differs from primary to relapsed low-grade gliomas and predicts progression-free survival. Anticancer Res. 2017;37(12):6639–48.
53. Eckstein N, Servan K, Girard L, Cai D, von Jonquieres G, Jaehde U, Kassack MU, Gazdar AF, Minna JD, Royer HD. Epidermal growth factor receptor pathway analysis identifies amphiregulin as a key factor for cisplatin resistance of human breast cancer cells. J Biol Chem. 2008;283(2):739–50.
54. Haas B, Mayer P, Jennissen K, Scholz D, Diaz MB, Bloch W, Herzig S, Fassler R, Pfeifer A. Protein kinase G controls brown fat cell differentiation and mitochondrial biogenesis. Sci Signal. 2009;2(99):ra78.
55. Eckstein N, Servan K, Hildebrandt B, Politz A, von Jonquières G, Wolf-Kummeth S, Napierski I, Hamacher A, Kassack MU, Budczies J, et al. Hyperactivation of the insulin-like growth factor receptor I signaling pathway is an essential event for cisplatin resistance of ovarian cancer cells. Cancer Res. 2009;69(7):2996–3003.
56. Frotschl R, Weickardt S, Staszewski S, Kaufmann G, Kasper P. Effects of chlorpromazine with and without UV irradiation on gene expression of HepG2 cells. Mutat Res. 2005;575(1–2):47–60.
57. Cancer Genome Atlas Research Network. Comprehensive genomic characterization defines human glioblastoma genes and core pathways. Nature. 2008;455(7216):1061–8.
58. Opel D, Westhoff MA, Bender A, Braun V, Debatin KM, Fulda S. Phosphatidylinositol 3-kinase inhibition broadly sensitizes glioblastoma cells to death receptor- and drug-induced apoptosis. Cancer Res. 2008;68(15):6271–80.
59. Tisdale MJ. Antitumour imidazotetrazines–XI: effect of 8-carbamoyl-3-methylimidazo[5,1-d]-1,2,3,5-tetrazin-4(3H)-one [CCRG 81045; M and B 39831 NSC 362856] on poly(ADP-ribose) metabolism. Br J Cancer. 1985;52(5):789–92.

Supplementary Figure 1

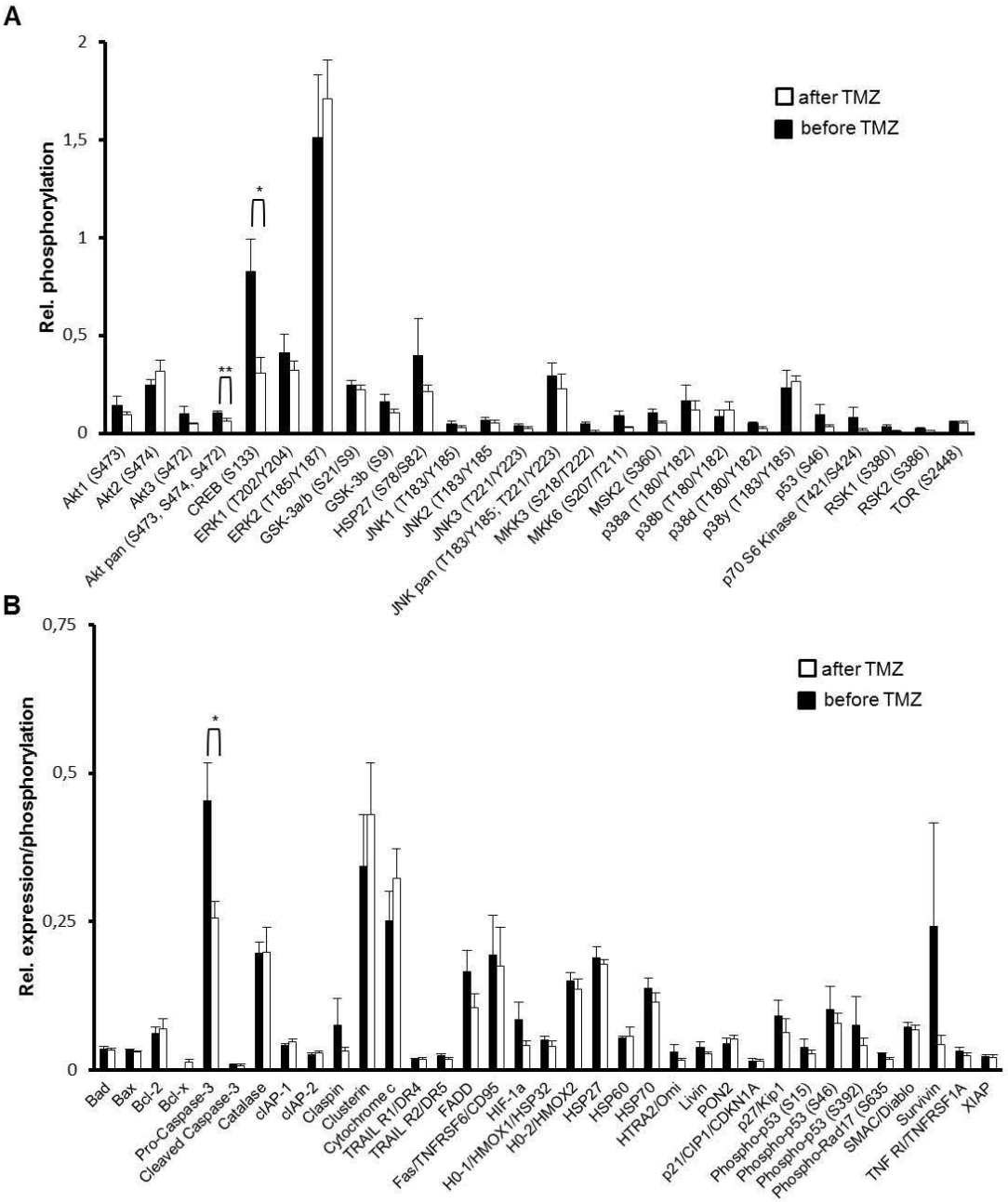

Additional file 1: Figure S1. Densitometric analysis of (**a**) human proteome profiler phospho-MAPkinase and (**b**) human apoptosis arrays of GBM tumor biopsies of patients, which were newly diagnosed a secondary GBM and underwent surgery before TMZ treatment (n=4) and of patients which underwent a second surgery after TMZ treatment due to recurrence of the tumor (n=4). Phosphorylation was normalized to positive control spots. **P* < 0.05, ***P* < 0.01.

Supplementary Figure 2

		cisplatin IC_{50} [µM]		
Inhibitor	***Function***	***U87***	***U251***	***U373***
DMSO	control	9.5	9.8	12.6
Erlotinib	EGF-R inhibitor	10.2	12.1	9.7
AG1024	IGF-1R inhibitor	9.3	7.6	15.2
AG1296	PDGF-Rβ inhibitor	7.4	9.4	15.0

Additional file 2: Figure S2. Impact of RTK inhibitors on cisplatin resistance in GBM cell lines. RTK inhibitors erlotinib (3 µM), AG1024 (1 µM), and AG1296 (10 ng/mL) do not sensitize GBM cell lines to cisplatin. Presented IC_{50} values were derived from MTT assays (n=3).

Supplementary Figure 3

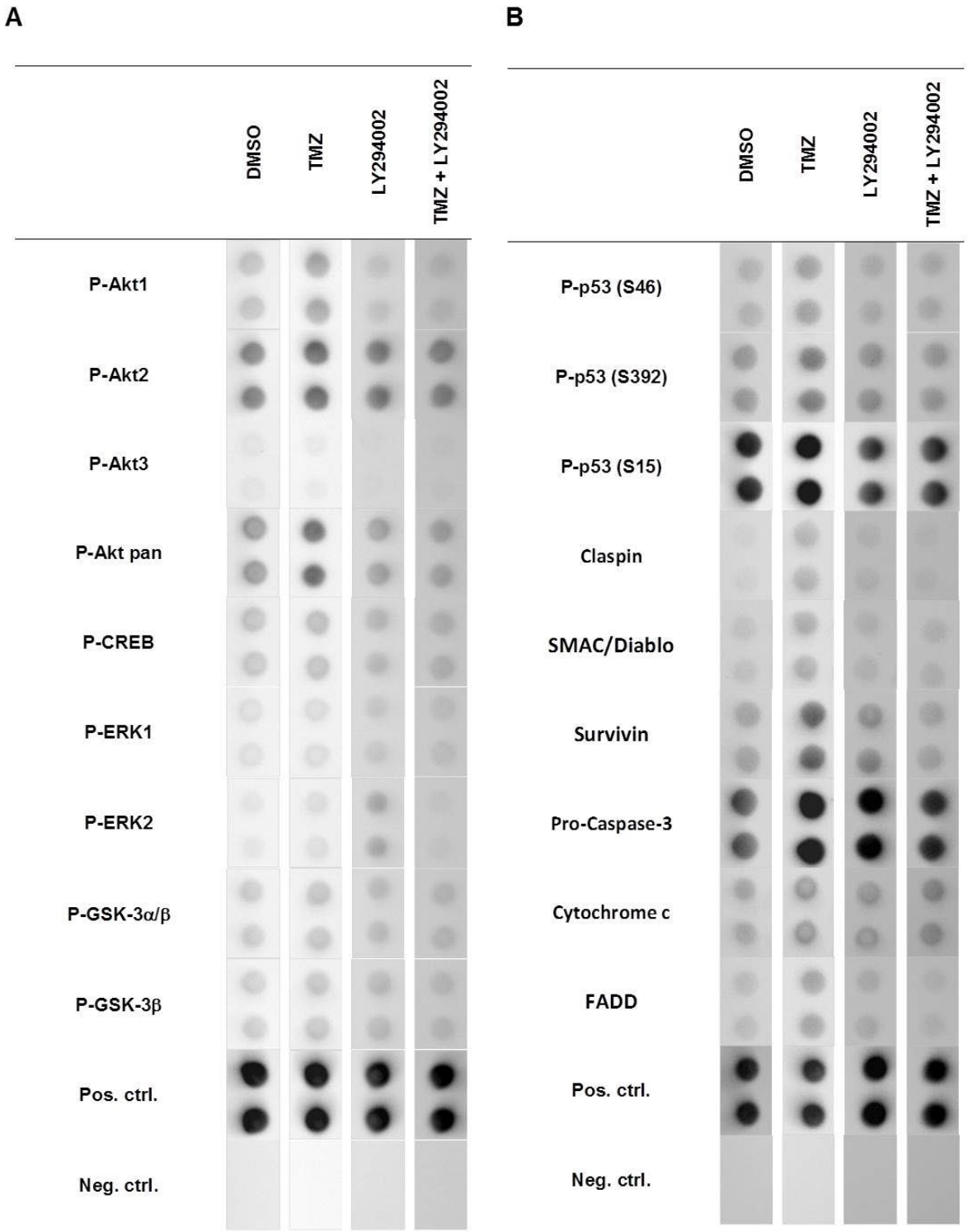

Additional file 3: Figure S3. Human proteome-profiler (**a**) phospho-MAPKkinase and (**b**) apoptosis arrays of U251 cells treated with LY290042 (20 µM), TMZ (1000 µM) or vehicle (DMSO) for 72 hours.

Supplementary Figure 4

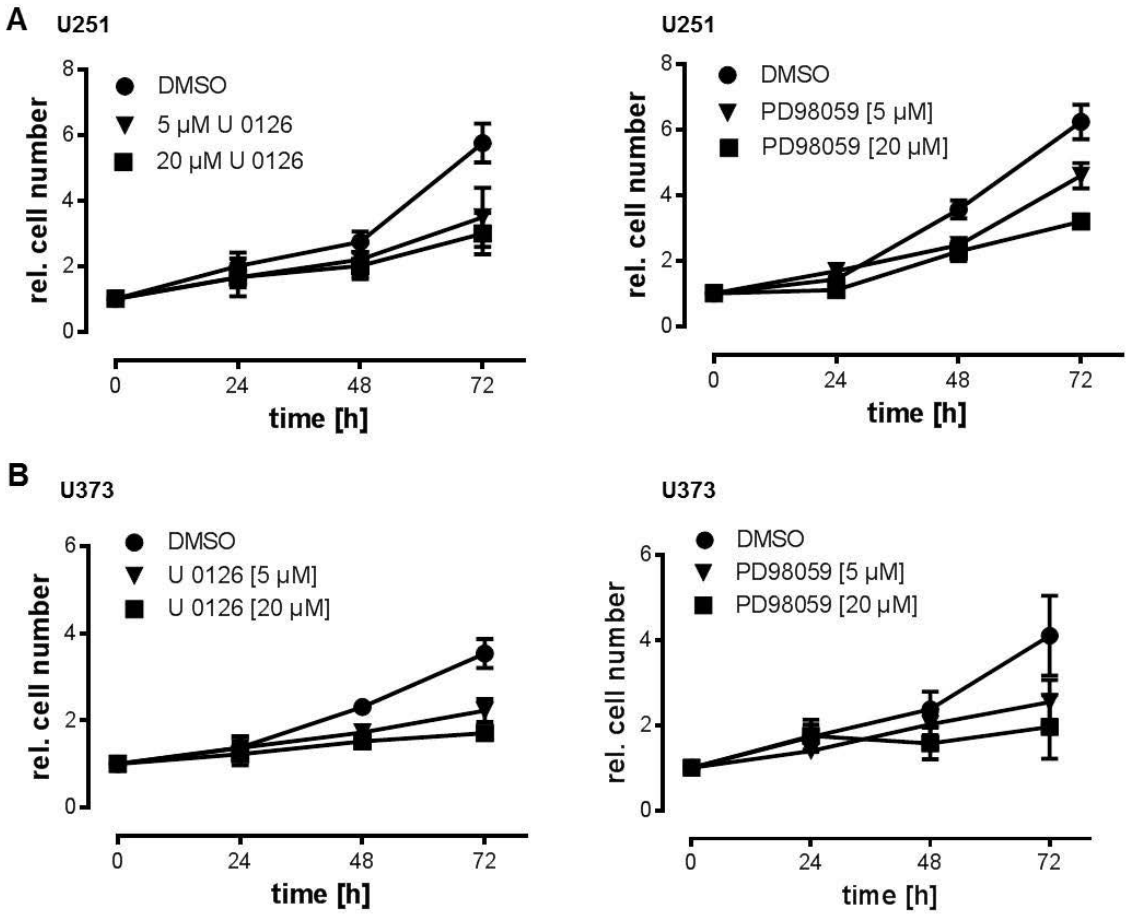

Additional file 4: Figure S4. MEK inhibition blocks cell proliferation of U251 and U373 cells. (**a**) U251 cells and (**b**) U373 cells were treated with vehicle (DMSO), U0126 or PD98059 as indicated (n=3). Cells were trypsinized at 24, 48 and 72 hours post treatment and counted. Cell number at time point 0 hours was set to 1.

3.2 **Haas B**, Schutte L, Wos-Maganga M, Weickhardt S, Timmer M, Eckstein N. Thioredoxin Confers Intrinsic Resistance to Cytostatic Drugs in Human Glioma Cells. Int J Mol Sci. 2018;19(10).

Zielsetzung der Arbeit: Die Überexpression des in der Redox-Homöostase involvierten Thioredoxins (Trx) ist als eine mögliche Ursache für eine Chemoresistenz bei verschiedenen Tumorentitäten beschrieben (Powis et al., 2001; Zhang et al., 2017a). Der Tumorsuppressor *Trx-interacting Protein* (TXNIP) reguliert die Aktivität des Trx-Systems und eine verringerte Expression ist mit einem kürzerem Gesamtüberleben von Glioblastom-Patienten assoziiert (Zhang et al., 2017b). Das Trx-System interagiert auch mit den in der vorangegangenen Arbeit beschriebenen PI3K-Signalweg (Ray et al., 2012). Aus diesem Grund sollte in der vorliegenden Studie die Auswirkungen des Trx-Systems auf die intrinsische Chemoresistenz von humanen Glioblastom-Zellen und eine mögliche Interaktion mit dem PI3K-Signalweg untersucht werden.

Methoden und Ergebnisse: Mit Hilfe von Immunoblotting konnte gezeigt werden, dass sowohl Trx als auch TXNIP in humanen Glioblastom-Zelllinien und in primären Glioblastom-Zellen exprimiert sind. Die pharmakologische Hemmung von Trx mit dem spezifischen Inhibitor PX-12 induzierte Apoptose in Annexin-V-FACS Assays und steigerte die Expression von aktiver Caspase-3, verringerte die Phosphorylierung von AKT und die Expression von β-Catenin. In Kombination mit TMZ oder Cisplatin führte PX-12 zu einer synergistischen Induktion der Apoptose und einem verringerten Zellüberleben in MTT-Versuchen. Ähnliche synergistische Effekte wurden auch durch Transfektion und Überexpression der Zellen mit TXNIP erzielt. Eine gleichzeitige Hemmung von Trx mit PX12 und dem PI3K-Inhibitor LY294002 in nicht zytotoxischen Konzentrationen, führte zu einem massiven Zelltod.

Schlussfolgerung: Diese Arbeit zeigte, dass sowohl eine pharmakologische als auch eine genetische Hemmung von Trx Glioblastom-Zellen gegenüber einer Chemotherapie sensitivieren kann, was so bisher noch nicht beschrieben war. Zusätzlich wurde postuliert, dass Trx und PI3K in einer sequenziellen Signalkaskade miteinander verbunden sind und eine duale Hemmung additive Effekte hat und einen klinischen Benefit für Glioblastom-Patienten haben könnte. Der Zusammenhang der beiden Signalwege und die Einflüsse ihrer Hemmung auf die Chemoresistenz, die in den ersten beiden Arbeiten untersucht wurden, zeigt **Figure 4** (Haas et al., Int J Mol Sci 2018).

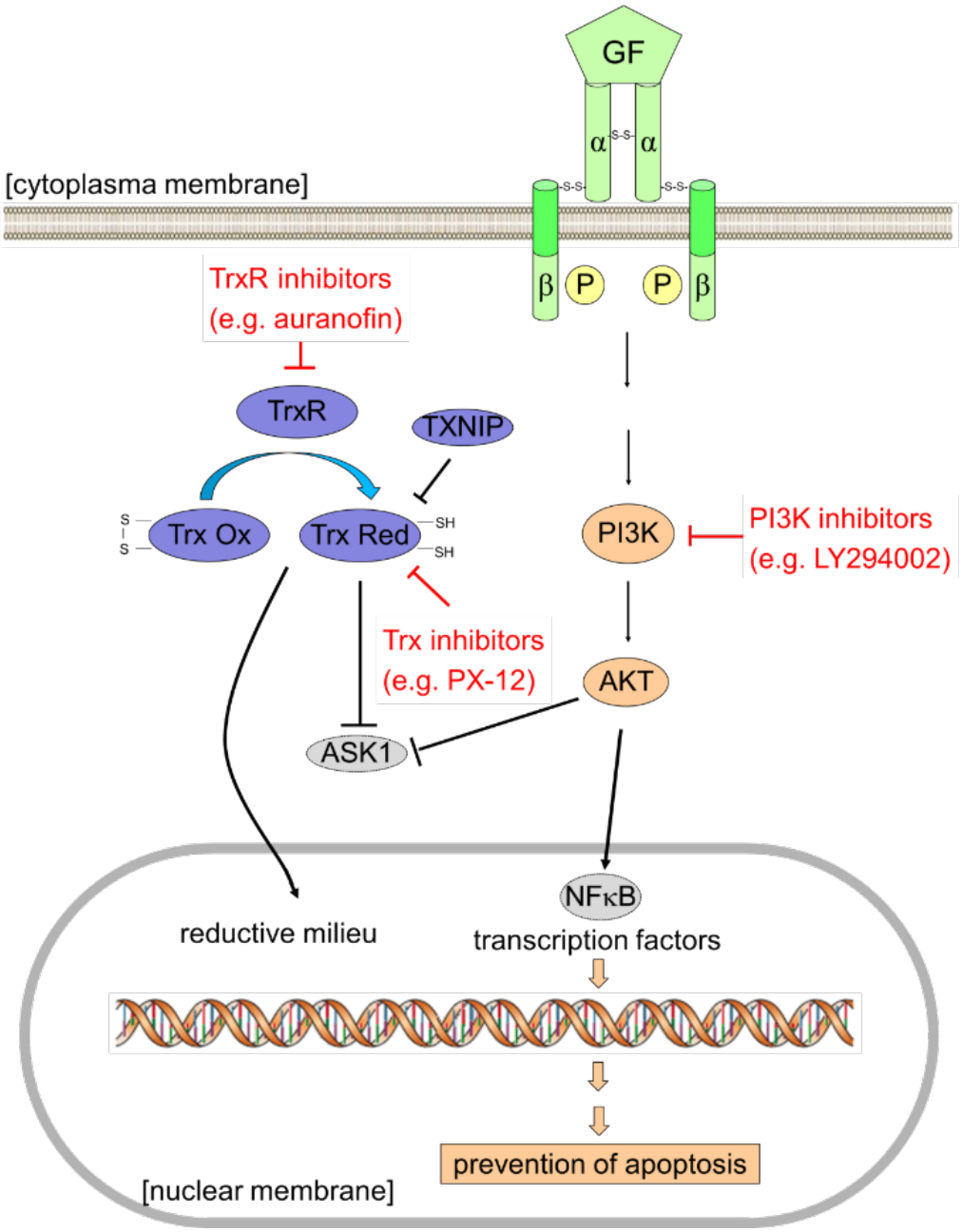

Figure 4. Schematic overview of the Trx system and tentative pathways involved in drug resistance of GBM cells. Potential drug insult to overcome resistance is presented in red. Abbreviations: AKT, protein kinase B (PKB); ASK1, apoptosis signal-regulating kinase 1; GF, growth factor; NF κB, nuclear factor kappa-light-chain-enhancer of activated B cells; PI3K, phosphatidylinositide 3-kinase; Trx, thioredoxin; TrxR, Trx-reductase TXNIP, Trx-interacting protein.

International Journal of
Molecular Sciences

MDPI

Article

Thioredoxin Confers Intrinsic Resistance to Cytostatic Drugs in Human Glioma Cells

Bodo Haas [1,*], Lena Schütte [1,2], Maria Wos-Maganga [1], Sandra Weickhardt [1], Marco Timmer [3] and Niels Eckstein [4]

1 Federal Institute for Drugs and Medical Devices, Kurt-Georg-Kiesinger-Allee 3, 53175 Bonn, Germany; lenaschuette@gmx.net (L.S.); maria.wos-maganga@bfarm.de (M.W.-M.); sandra.weickhardt@bfarm.de (S.W.)
2 Faculty of Applied Natural Sciences, Cologne University of Applied Sciences, Kaiser-Wilhelm-Allee, 51368 Leverkusen, Germany
3 Department of General Neurosurgery, Center for Neurosurgery, University Hospital Cologne, 50937 Cologne, Germany; marco.timmer@uk-koeln.de
4 Applied Pharmacy, University of Applied Sciences Kaiserslautern, Campus Pirmasens, Carl-Schurz-Str. 10-16, 66953 Pirmasens, Germany; niels.eckstein@hs-kl.de
* Correspondence: bodo.haas@bfarm.de; Tel.: +49-228-99307-3476

Received: 14 August 2018; Accepted: 18 September 2018; Published: 21 September 2018

Abstract: Thioredoxin (Trx) overexpression is known to be a cause of chemotherapy resistance in various tumor entities. However, Trx effects on resistance are complex and depend strictly on tissue type. In the present study, we analyzed the impact of the Trx system on intrinsic chemoresistance of human glioblastoma multiforme (GBM) cells to cytostatic drugs. Resistance of GBM cell lines and primary cells to drugs and signaling inhibitors was assessed by 3-(4,5-dimethylthiazol-2-yl)-2,5-diphenyltetrazolium bromide (MTT) assays. Impact of Trx inhibition on apoptosis was investigated by proteome profiling of a subset of proteins and annexin V apoptosis assays. Trx-interacting protein (TXNIP) was overexpressed by transfection and protein expression was determined by immunoblotting. Pharmacological inhibition of Trx by 1-methyl-2-imidazolyl-disulfide (PX-12) reduced viability of three GBM cell lines, induced expression of active caspase-3, and reduced phosphorylation of AKT-kinase and expression of β-catenin. Sensitivity to cisplatin could be restored by both PX-12 and recombinant expression of the upstream Trx inhibitor TXNIP, respectively. In addition, PX-12 also sensitized primary human GBM cells to temozolomide. Combined inhibition of Trx and the phosphatidylinositide 3-kinase (PI3K) pathway resulted in massive cell death. We conclude that the Trx system and the PI3K pathway act as a sequential cascade and could potentially present a new drug target.

Keywords: glioblastoma; drug resistance; thioredoxin; TXNIP; PX-12

1. Introduction

Gliomas are the most common primary brain tumors in humans, with glioblastoma multiforme (GBM, WHO grade IV) as the most aggressive form with the highest incidence [1,2]. GBM is treated with adjuvant radiotherapy and chemotherapy after surgery, but still, the median survival is only 14.6 months and the 5-year survival rate is 6% under therapy. Actually, the only chemotherapy regime resulting in a significant benefit in overall survival is adjuvant temozolomide (TMZ) following radiotherapy [3–5]. GBM therapy is aggravated by eventual development of intrinsic resistance of the tumor to radio- and chemotherapy. Resistance is frequently driven by mutated tumor suppressor genes after loss of function like *P53*, retinoblastoma protein (*RB*), and phosphatase and tensin homolog (*PTEN*) but also alterations in upstream receptor tyrosine kinase (RTK) signaling pathways [6–8].

Thioredoxin (Trx) is a 12 kDa ubiquitous protein of 104 amino acids with reducing activity. Trx is involved in cellular redox homeostasis, maintaining the balance between reactive oxygen species (ROS) generation and elimination [9]. Its active site comprises two cysteine residues which serve as a general disulfide oxidoreductase. Trx-interacting protein (TXNIP), a 46 kDa tumor suppressor protein, is also known as vitamin-D_3-upregulated protein 1 (VDUP1) [10]. TXNIP is an upstream, negative regulator of the Trx-reducing activity. This functional antagonism comprises both suppression of Trx expression and direct protein interaction. Like other thiol-containing proteins, Trx overexpression has been suspected as a cause of chemotherapy resistance [11]. Hence, Trx overexpression in several tumor-derived cell lines is associated with resistance to cisplatin [12]. However, Trx effects on anticancer drug resistance are complex and depend strictly on the tissue type. For instance, cisplatin resistance in bladder and prostate cancer cell lines is triggered by Trx overexpression [13]. In contrast, cisplatin resistance in ovarian cancer cell lines is associated with high Trx levels, but recombinant Trx overexpression in nonresistant cells does not confer resistance to cisplatin [14]. Interestingly, it has been demonstrated that low TXNIP expression in glioma is associated with higher histopathological glioma grade and shorter overall patient survival. Furthermore, knockdown of TXNIP in the U251 GBM cell line promoted cell invasion, migration, and proliferation [15]. In this context, it is interesting to note that Trx expression correlates with glioma grade [16] and high Trx levels in breast cancer are associated with poor patient survival [17].

Another important player in the regulation of Trx function is Trx reductase (TrxR), which reduces oxidized disulfide-containing Trx back to the dithiol form. Inhibition of TrxR by specific inhibitors leads to an increase in oxidized, nonfunctional Trx. Consequently, targeting the Trx system, either by inhibition of Trx or TrxR, has been proposed as a promising strategy for cancer treatment [18,19]. This is reflected in anticancer clinical trials currently ongoing with the TrxR inhibitor auranofin (NCT03456700, NCT01737502, NCT01747798, NCT02770378). Auranofin is an organic gold complex clinically used as antiarthritic drug. In various cancer cells, auranofin has been shown to elicit strong cytotoxicity through diverse mechanisms such as overproduction of ROS, inhibition of glycolysis and the proteasome, and activation of apoptotic pathways [20–26]. Furthermore, auranofin treatment has been described to overcome cisplatin resistance in ovarian cancer cells [27].

There is currently one ongoing clinical trial combining TMZ treatment with auranofin in recurrent glioblastoma (NCT02770378). However, the exact role of the Trx system in GBM and more specifically in chemoresistance is still not clear at present.

Here, we present data confirming a substantial impact of the Trx/TXNIP system on intrinsic chemoresistance of GBM cells to cytostatic drugs which could pave the way to alternative treatment modalities.

2. Results

2.1. Trx-Inhibition Triggers Apoptosis in Human GBM Cell Lines

GBM cell lines and high-grade glioma tissue have been reported to express significant amounts of Trx [16,28,29]. In order to confirm this, we determined Trx and TXNIP expression in three established GBM cell lines—U87, U251, and U373—and primary GBM cells, which have previously been shown by us to be intrinsically resistant to TMZ and cisplatin [30]. Trx-1 and TXNIP protein was expressed in all cells as determined by Western blotting (Figure 1a). To investigate whether GBM cell lines are responsive to Trx-inhibition, 1-methyl-2-imidazolyl-disulfide (PX-12), a pharmacological inhibitor of Trx, was applied. First, we investigated the effect of PX-12 at increasing concentrations on cell survival in 3-(4,5-dimethylthiazol-2-yl)-2,5-diphenyltetrazolium bromide (MTT) assays (Figure 1b, upper graph). An IC_{50} concentration of around 10 μM was determined for all three cell lines (Figure 1b, lower table). This concentration was used to assess the effect of PX-12 on apoptosis-related proteins such as (pro-)caspase-3, AKT-kinase (protein kinase B), and β-catenin (Figure 1c). PX-12 strongly induced expression of active caspase-3 and reduced phosphorylation of AKT-kinase and expression of β-catenin

in a similar fashion in all three cell lines. These findings are in line with a concentration-dependent increase of apoptotic rates of U251 cells after PX-12 exposure as determined by annexin-V/propidium iodide staining (Figure 1d). Similar results were obtained with U87 and U373 cells (Figure S1).

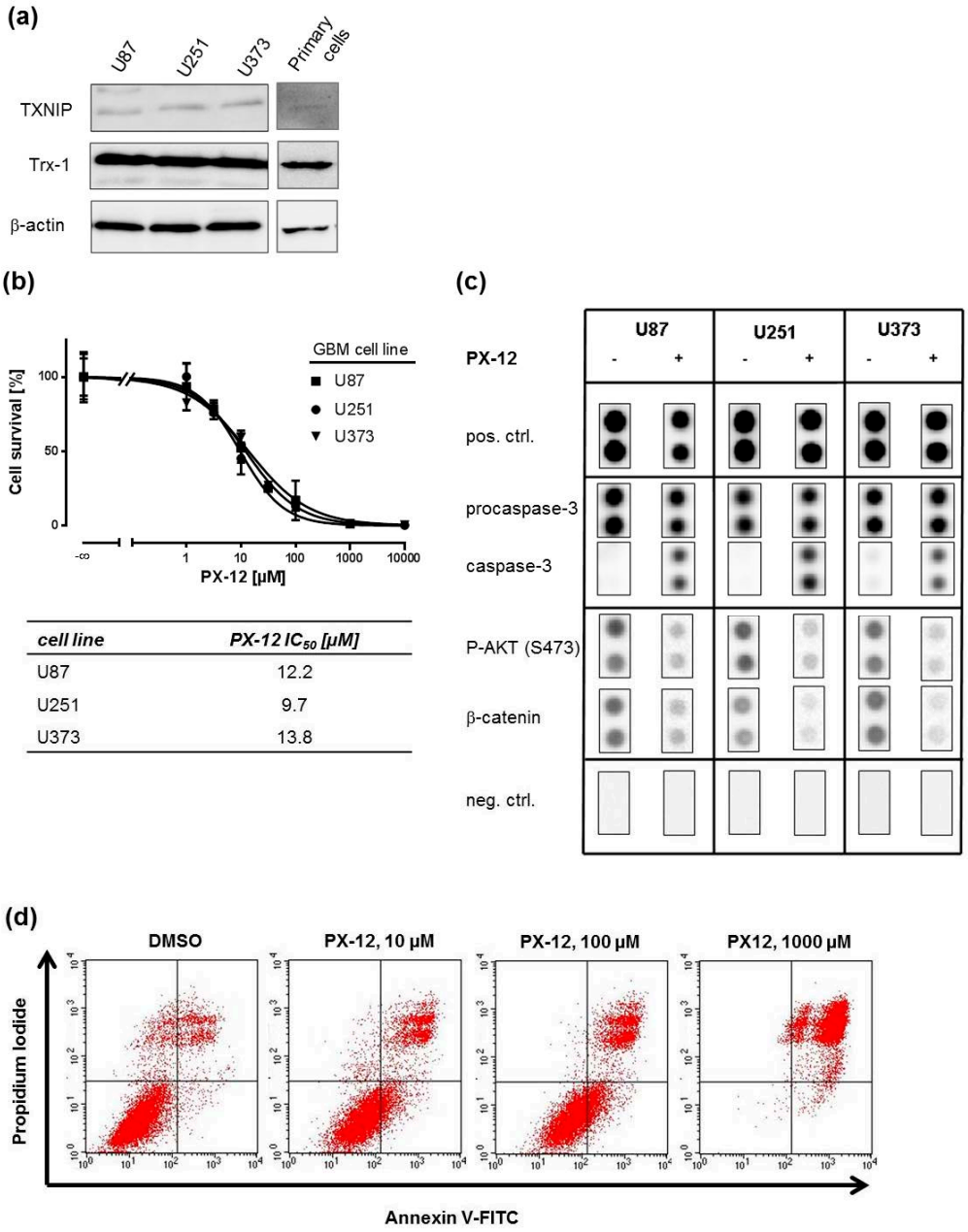

cell line	*PX-12 IC_{50} [µM]*
U87	12.2
U251	9.7
U373	13.8

Figure 1. Pharmacological inhibition of thioredoxin (Trx) increases cell death via induction of apoptosis in human glioblastoma multiforme (GBM) cell lines. (**a**) Representative Western blots showing endogenous Trx-1 and Trx-interacting protein (TXNIP) expression in U87, U251, U373, and primary GBM cells. β-actin Western blot was performed to control for loading; (**b**) 3-(4,5-dimethylthiazol-2-yl)-2,5-diphenyltetrazolium bromide (MTT) concentration-response curves after 1-methyl-2-imidazolyl-disulfide (PX-12) exposure for 72 h in U87, U251, and U373 cells (upper graph). Respective PX-12 IC_{50} values are displayed in the table below the graph (n = 4); (**c**) Human proteome-profiler antibody arrays were used to assess the expression/phosphorylation of AKT (S473), procaspase-3, caspase-3, and β-catenin 72 h after PX-12 exposure; (**d**) Representative FACS blots of U251 cells treated with either vehicle (DMSO) or increasing PX-12 concentrations for 72 h as indicated. Annexin V positive cells were regarded as apoptotic cells.

2.2. Pharmacological Trx Inhibition Sensitizes Human GBM Cells to Cytostatic Drugs

Next, we investigated whether Trx inhibition by PX-12 sensitizes GBM cell lines to the cytostatic drug cisplatin in MTT assays. Yet, TMZ is the only substance for which a statistically significant and clinically relevant benefit in both overall survival and progression-free survival has been demonstrated [4]. However, it is very difficult to handle in the laboratory setting as it must be given to GBM cells in concentrations as high as or even beyond its solubility [30]. Thus, we also used cisplatin as a model substance with a similar molecular mechanism of action: both substances interfere with DNA, resulting in strand breaks and apoptosis. Therefore, we treated cells with an IC_{50} concentration of PX-12 and increasing concentrations of cisplatin. Treatment with 10 µM PX-12 sensitized all GBM cell lines significantly to cisplatin when administered 1 h prior to cisplatin exposure. The sensitizing effect was concentration dependent, since 20 µM PX-12 triggered a more pronounced effect (Figure 2a). Next, we asked if our findings can be translated to a more clinically relevant scenario of primary GBM cells derived from a tumor biopsy. Initially, we determined the IC_{50} concentration of PX-12 in these cells (Figure 2b). Thereafter, we treated primary cells with this IC_{50} concentration and increasing TMZ concentrations. As observed with cisplatin in GBM cell lines, PX-12 was also capable of sensitizing primary GBM cells to TMZ as assessed by MTT assays (Figure 2c). This was paralleled by an increase in apoptotic rates after concomitant treatment of IC_{50} concentrations of PX-12 and TMZ as compared to single treatment alone (Figure 2d and Figure S2).

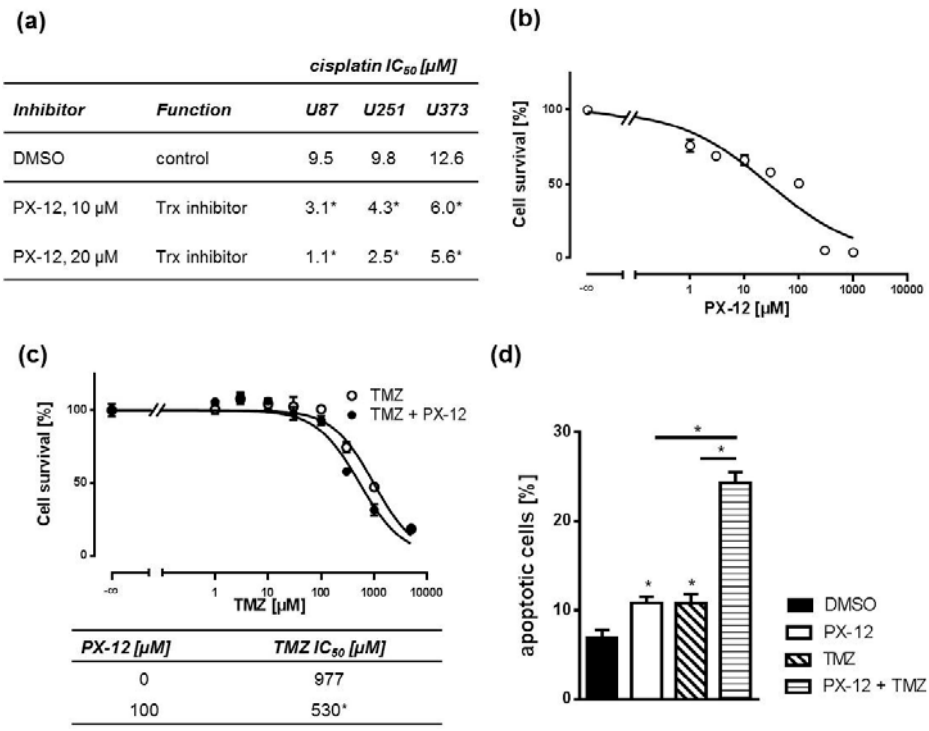

Figure 2. PX-12 treatment sensitizes human GBM cells to cytostatic drug treatment. (**a**) PX-12 causes a concentration-dependent reversal of cisplatin resistance. IC_{50} concentrations of cisplatin in the absence and presence of 10 µM and 20 µM PX-12 for 72 h, respectively, were obtained from sigmoidal concentration-response curves (0.03–300 µM cisplatin) of MTT assays ($n = 3$, * $p < 0.05$); (**b**) MTT assays with a concentration-response curve of PX-12 in primary human GBM cells treated for 72 h ($n = 3$); (**c**) Temozolomide (TMZ) concentration-response curves showing sensitization of primary GBM cells at 100 µM PX-12 incubated for 72 h (upper graph). Respective TMZ IC_{50} values are depicted in the table below the graph ($n = 3$, * $p < 0.05$); (**d**) Apoptotic rates as determined by annexin-V assays of primary GBM cells treated with either vehicle (DMSO), TMZ (1000 µM), PX-12 (100 µM), or a combination of both for 48 h as indicated. Annexin V positive cells were regarded as apoptotic cells ($n = 3$, * $p < 0.05$).

2.3. TXNIP Overexpression Chemosensitizes Human GBM Cell Lines

In order to confirm our data, we overexpressed TXNIP in GBM cell lines as a genetic tool to inhibit Trx function and expression. We were not able to achieve sufficient expression of TXNIP in primary GBM cells after transfection. Therefore, we focused our experiments with TXNIP on GBM cells lines. Trx-1 expression was nearly abrogated after *TXNIP* transfection as exemplarily depicted for U87 cells (Figure 3a). Overexpression of TXNIP and consequently reduced Trx-1 expression significantly sensitized cells towards cisplatin when compared to empty vector transfected cells (Figure 3b–e). It has previously been shown by us and others that pharmacological inhibition of phosphatidylinositide 3-kinase (PI3K) sensitizes GBM cells to cisplatin and TMZ [30]. Reports from the literature indicate that PI3K/AKT signaling and the Trx system can be interconnected on various levels [31]. Therefore, we sought to combine both mechanisms and measure the impact on cisplatin resistance status of GBM cell lines. However, combining PI3K inhibition with anti-Trx treatment did not yield a window large enough to record a cisplatin concentration-response curve. Thus, we assessed the impact of the PI3K inhibitor LY294002 and PX-12 and a combination of both on cell survival in GBM cells. Both substances show an additive behavior in MTT assays (Figure 3f). We conclude that both mechanisms are closely interconnected (Figure 4).

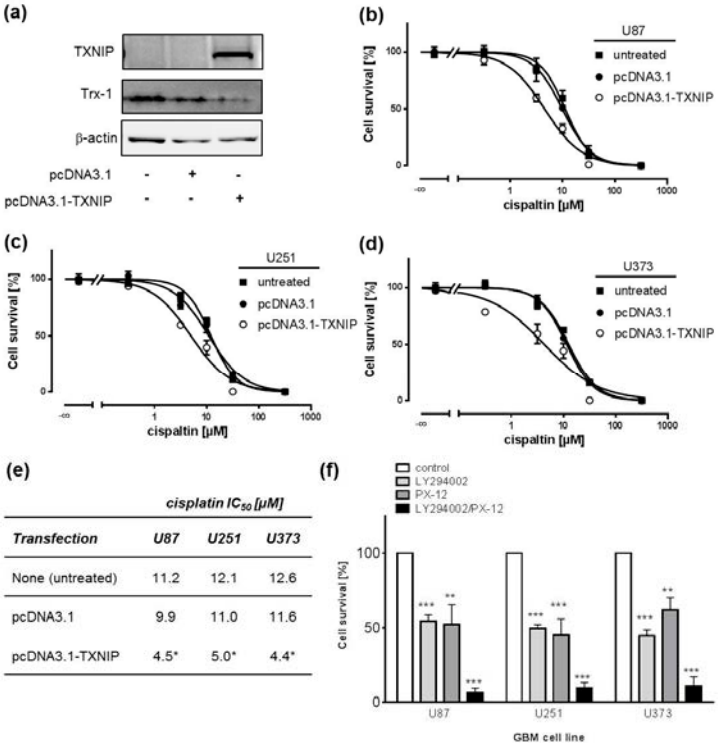

Figure 3. Overexpression of the tumour suppressor TXNIP inhibits Trx expression and sensitizes GBM cell lines to cisplatin. (**a**) Representative Western blots of U87 cells showing overexpression of TXNIP and downregulation of Trx-1 protein expression after transient transfection with pcDNA3.1-TXNIP or empty vector (pcDNA3.1) 48 h post-transfection. β-actin Western blot was performed to control for loading; (**b**–**d**) MTT assays with cisplatin concentration-response curves showing sensitization of U87 (**b**), U251 (**c**), and U373 (**d**) cells after transient transfection with empty vector (pcDNA3.1) or pcDNA3.1-TXNIP. Cells were incubated with cisplatin for 72 h at 24 h post-transfection; (**e**) Respective cisplatin IC_{50} values derived from curves presented in **b**–**d** ($n = 4$, * $p < 0.05$); (**f**) Prevention of AKT kinase signaling and Trx deactivation triggers cell death in GBM cell lines. U87, U251, and U373 cells were treated with control (DMSO) or 5 µM of the phosphatidylinositide 3-kinase (PI3K) inhibitor LY294002, 10 µM PX-12, and a combination of both, respectively. After 72 h, cell viability was assessed by MTT assays ($n = 3$, ** $p < 0.01$, *** $p < 0.001$).

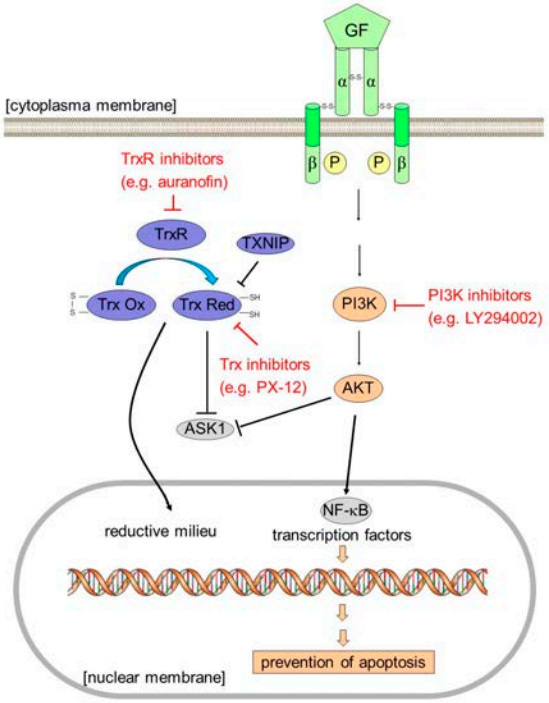

Figure 4. Schematic overview of the Trx system and tentative pathways involved in drug resistance of GBM cells. Potential drug insult to overcome resistance is presented in red. Abbreviations: AKT, protein kinase B (PKB); ASK1, apoptosis signal-regulating kinase 1; GF, growth factor; NF-κB, nuclear factor kappa-light-chain-enhancer of activated B cells; PI3K, phosphatidylinositide 3-kinase; Trx, thioredoxin; TrxR, Trx-reductase TXNIP, Trx-interacting protein.

3. Discussion

Despite its low incidence of about 30,000 new diagnoses per year, GBM is one of the deadliest cancer types, with a 5-year survival of 6% [1,5]. Drug resistance, radio resistance, and inoperability result in a useless medical armamentarium. The only improvement in GBM therapy, which leads to prolonged overall survival, is adjuvant administration of TMZ following radiotherapy [4]. Here, we present a mechanism of how resistance to cytostatic drugs is brought about in GBM cells. The mechanism we discovered operates on Trx overexpression. High Trx levels can be regarded as a marker for increased tumor aggressiveness in general [18]. In addition, in glioma downregulation of the negative Trx regulator TXNIP has been shown to be associated with higher histopathological glioma grade and shorter overall patient survival [15]. In line with that, Trx expression increases with glioma grade [16]. Trx overexpression was demonstrated to provoke vascular endothelial growth factor (VEGF) secretion and angiogenesis [32]. In invasive cervical carcinomas, Trx upregulation was detected in tumor microregions suffering from hypoxia, suggesting hypoxia-inducible factor-1 α (HIF-1α) induction, which is entailed by PI3K/AKT pathway activation [33]. Consistently, hypoxia was also linked to increased Trx levels and sensitivity to TrxR inhibition in cancer cells cultured in monolayers and 3D spheroid-based culture models [34]. Additionally, *TRX* gene transfection of lymphoid and breast cancer cells or Trx protein supplemented to tissue culture medium has been reported to prevent apoptosis and increase cell invasion [11,17]. With respect to anticancer drug resistance, *TRX* transfected murine WEHI7.2 lymphoma cells show significantly lower apoptosis rates when exposed to the anticancer drug etoposide, a topoisomerase-II inhibitor [35]. In this context, it is noteworthy that the TrxR inhibitor auranofin is currently evaluated in clinical trials as an anticancer agent alone or in combination with other drugs (NCT03456700, NCT01737502, NCT01747798, NCT02770378). There is strong evidence that the cytostatic activity of auranofin and other TrxR inhibitors on various cancer cells is mediated via an increase in cellular ROS, subsequently leading to apoptosis [17,19–22,26]. Other mechanisms discussed are inhibition of the PI3K/AKT

pathway in lung cancer cells [23,36], inhibition of the proteasome in rhabdomyosarcoma and hepatoma cells [25,37], and adenosine triphosphate (ATP) depletion by inhibition of glycolysis in stem-like cancer cells [24]. The sensitivity of gastric cancer cells to auranofin could be increased by the silencing of genes involved in autophagy [38], and *BRCA1* deficiency has further been implicated to increase sensitivity of ovarian cancer cells to auranofin [39]. Synergistic activity on cancer cell growth in preclinical models is reported for the combination of auranofin with many anticancer agents and is in line with the use of auranofin as combination therapy in current clinical trials [24,25,36,40,41]. The sensitizing activity of auranofin is further supported by studies showing an enhancement of radiation response in breast cancer cells [42,43]. Furthermore, auranofin treatment has been described to overcome cisplatin resistance in ovarian cancer cells [27].

Thus, with respect to tailored medicine, Trx and TrxR are promising markers and emerging drug targets—if not alone, then at least in combination with cytostatic drugs or radiation as a chemosensitizer. In our study we confirmed Trx-1 and TXNIP expression in three GBM cell lines and primary cells. It has previously been shown by us that these cell lines are intrinsically resistant to TMZ and cisplatin [30]. This further drove us to investigate the role of Trx in chemoresistance. To this end, we applied PX-12, a small-molecule inhibitor which has already been demonstrated to overcome drug resistance in multiple myeloma [44,45], alone and in combination with cisplatin or TMZ. PX-12 chemically belongs to the group of alkylated 2-imidazolyl disulfide Trx inhibitors. On the molecular level, it covalently binds Cys-73 of Trx, thus thioalkylating the protein [46].

PX-12 treatment, just like genetic TXNIP overexpression, restored sensitivity to cytostatic drug treatment. Thus, we present a new treatment modality to overcome Trx-mediated ineffectiveness of drug therapy in GBM.

It is noteworthy that we and others have demonstrated that PI3K inhibition sensitizes GBM cells to alkylating drugs [30]. Reports from the literature provide evidence of a crosstalk of PI3K/AKT and the Trx system on various levels depending on the cell type [31]. Trx was observed to inhibit PTEN lipid phosphatase activity, thereby leading to unbraked PI3K-stimulated AKT-kinase activation [47]. This is underlined by the fact that TrxR inhibition by auranofin inhibited the PI3K/AKT pathway in lung cancer cells [23,36]. However, this mechanism might not operate in GBM, since all cell lines under investigation carry *PTEN* mutations. Apart from that, it is known that AKT-kinase functions in concert with Trx upstream of nuclear factor kappa-light-chain-enhancer of activated B cells (NF-κB). In this doublet, Trx preserves a reductive nuclear condition, which is a prerequisite for the transcription factor to bind DNA [48]. To this end, it is noteworthy that NF-κB is overexpressed frequently in GBM and is associated with chemoresistance [49]. Finally, Trx binds and inactivates apoptosis signal-regulating kinase 1 (ASK1). ASK1 is released from Trx binding upon oxidative stress to interact directly with AKT-kinase [50], which negatively regulates ASK1 activity by phosphorylation [51]. Consequently, oxidation or inactivation of Trx and reduced AKT activity lead to ASK1 activation, which in turn activates c-Jun N-terminal kinase (JNK) and p38 mitogen-activated protein (MAP) kinase pathways resulting in apoptosis [52].

Thus, we investigated whether both mechanisms are interconnected in GBM. If a sequential cascade would lead from Trx overexpression to AKT-kinase activation, inhibition of both principles should act in an additive manner. This would clear the path to so-called sequential therapy, a treatment modality where two sequential steps in a certain cascade are targeted simultaneously to ultimately block the pathway. In the context of this report, treatment of GBM cell lines with both a PI3K inhibitor and a Trx inhibitor should yield a high sensitivity to cytostatic drugs. However, we did not yield a window large enough to record a cisplatin concentration-response curve. However, cell survival assays under either inhibition alone and in combination revealed an additive interaction of both approaches in triggering cell death. Additionally, AKT-kinase phosphorylation and β-catenin protein expression were substantially reduced under the action of the Trx blocker PX-12, which also suggests that the AKT-kinase pathway is closely interconnected with Trx. We conclude that both principles act as a sequential cascade and could potentially present a new drug target (Figure 4). Combination of

cytostatic drugs with Trx and/or PI3K inhibitors might thus result in clinical benefit for glioma patients. However, it has to be taken into account that the ability to cross the blood brain barrier is not common to all PI3K inhibitors and only a handful have entered into clinical trials so far [53]. No information could be retrieved regarding the ability of PX-12 to penetrate into the brain, leaving the question if PX-12 is a feasible option for glioma treatment.

4. Materials and Methods

4.1. Cell Culture, Transfection, and Preparation of Cell Lysates

All chemicals and cell lines—U87-MG, U251-MG, and U373-MG (Uppsala)—were obtained from Sigma-Aldrich (St. Louis, MO, USA), (HPA Culture Collections). Cell lines were not used beyond passage 20. U251 cells were cultivated in Roswell Park Memorial Institute (RPMI) 1640 Medium (Biochrom, Berlin, Germany) containing 10% fetal calf serum (FCS; Biochrom, Berlin, Germany), 100 IU/mL penicillin, and 100 µg/mL streptomycin (Biowest, Nuaillé, France) at 37 °C and 5% CO_2. All other cell lines were cultivated in Dulbecco's Modified Eagle Medium (DMEM) low Glucose (Biowest, Nuaillé, France) containing 10% FCS, 100 IU/mL penicillin, and 100 µg/mL streptomycin. Primary GBM cells were obtained from the University Hospital Cologne from a tumor biopsy of one patient with primary GBM (grade 4) according to the 2007 WHO classification [54]. The collection of tissue samples was approved by the University's Institutional Ethical Board (project number: 03-170, approve date: 23.04.2012). Informed consent of the patient was obtained according to the Helsinki declaration of ethical requirements. Tissue specimens were obtained during neurosurgery, directly put on DMEM (+glucose, +glutamine, +pyruvate) on ice in the operation theatre, and immediately transported to the lab for further processing under sterile conditions. Specimens were cut into approximately 1-mm^3 pieces with a scalpel and separately placed into 25-mm^2 culture flasks with DMEM containing 10% FCS, 100 IU/mL penicillin, and 100 µg/mL streptomycin. Pieces were cultured for about 2–3 weeks at 37 °C, 5% CO_2 until cells reached approx. 80% confluence. Thereafter, remaining tissue and debris was removed and only adherent cells were transferred into 75-mm^2 culture flasks (passage 1), expanded again, and frozen (passage 2). For experiments, cells were thawed, expanded, and split for experiments (passage 3).

Full-length human TXNIP cDNA was subcloned in the mammalian expression vector pcDNA3.1 (Invitrogen, Carlsbad, CA, USA). Transient transfections were performed using Lipofectamin®2000 (Invitrogen, Carlsbad, CA, USA) according to the manufacturer's instructions. Cells were grown to 70–90% confluence and transfected with a mixture of 3.5 µg (6-well) or 1 µg (24-well) plasmid, Lipofectamine®2000, and Opti-MEM® Medium (Invitrogen, Carlsbad, CA, USA). Whole cell lysates were isolated 48 h after transfection to confirm TXNIP and Trx-1 expression by Western blotting.

In order to prepare whole cell lysates, cells were washed with ice cold phosphate-buffered saline (PBS) and lysed with ice cold Denaturing Cell Extraction Buffer (FNN00091, Thermo Fisher Scientific, Waltham, MA, USA), incubated on ice for 30 min, and centrifuged for 15 min at 4 °C. The supernatant was used for protein content determination and subsequent immunoblotting.

4.2. Proteome Profiling

The functional status of the signaling pathways was measured by Proteome Profiler® human apoptosis and human phosphokinase arrays (R&D Systems ARY003B and ARY009, respectively, Minneapolis, MN, USA). Only membranes of the same lot numbers were used for comparison. Cells were lysed after incubation with PX-12 by addition of ice-cold lysis buffer to PBS washed culture plates. After centrifugation, the protein content of the supernatant was determined and 300 µg of total protein was used for proteome profiling according to the manufacturer´s protocol and as described previously [55].

4.3. Western Blot Analysis

For immunoblotting, standard procedures were used as previously described [55]. Thirty micrograms of total protein were loaded onto Criterion® Tris-HCL protein gels (Biorad, Hercules, CA, USA). After electrophoresis, gels were blotted onto polyvinylidene fluoride (PVDF) membranes (Merck Millipore, Burlington, MA, USA) and blocked with 5% milk/Tris-buffered saline-Tween (TBS-T). The following antibodies were used: Anti-Trx-1 (1:2000; AF 1970) combined with donkey anti-goat IgG-HRP (1:10,000; HAF 109; both R&D systems, Minneapolis, MN, USA), anti-VDUP1 (1:500; D2, Santa Cruz Biotechnology, Dallas, TX, USA) combined with goat anti-mouse IgG (H + L)-HRP (1:10,000; Thermo Scientific, Waltham, MA, USA), and anti-β-actin-HRP (1:10,000; C-4, Santa Cruz Biotechnology, Dallas, TX, USA). Primary antibodies were applied in 1% milk/TBS-T at 4 °C overnight and secondary antibodies in 1% milk/TBS-T for 1 h. Immunoblots were developed with the enhanced chemoluminescence system (Amersham Biosciences, Little Chalfont, UK).

4.4. MTT Assay

Cell survival after exposure to cisplatin or TMZ and in the presence of signaling inhibitors was determined by MTT assays as previously described [55]. Briefly, 5000 (U251, U87, U373) or 15,000 (primary) cells were plated on 96 wells and grown at 37 °C and 5% CO_2 overnight. Thereafter, signaling inhibitors PX-12 (1–10.000 μM) and LY294002 (5 μM) were added to culture media 1 h prior to addition of cisplatin or TMZ for 72 h as indicated. Final DMSO concentrations in media did not exceed 1%. For the analysis of TXNIP overexpressing cells, 1×10^4 cells were seeded into individual wells of a 24-well plate and transfected with Lipofectamine®2000 as described above. After 24 h, cells were exposed to increasing concentrations of cisplatin for 72 h.

4.5. Annexin V Apoptosis Assay

For apoptosis measurements, the BD Pharmingen® FITC Annexin V Apoptosis Detection Kit (BD Biosciences, Franklin Lakes, NJ, USA) was used according to the manufacturer's protocol. Briefly, 2.5×10^5 cells were seeded into six-well plates and incubated at 37 °C and 5% CO_2 overnight. After compound treatment for 48–72 h, cells were trypsinized and centrifuged for 4 min at 1500× *g*. Supernatant was removed and cells were resuspended in 500 μL binding buffer. Five microliters of propidium iodide and 5 μL Annexin V-FITC were mixed with 100 μL of cells in binding buffer. After 15 min of incubation on ice, samples were analyzed by flow cytometry (FACSCalibur®, BD Bioscience Franklin Lakes, NJ, USA).

4.6. Data Analysis and Statistical Methods

Concentration effect curves were fitted to data points by nonlinear regression analysis using the four-parameter logistic equation (GraphPad® Prism, https://www.graphpad.com/scientific-software/prism/). Statistical differences between two groups were determined by unpaired two-tailed Student's *t*-test. Comparisons among several groups were performed by ANOVA followed by Tukey's post hoc test. Data are presented as means ± SEM.

Supplementary Materials: Supplementary materials can be found at http://www.mdpi.com/1422-0067/19/10/2874/s1.

Author Contributions: Conceptualization, B.H. and N.E.; Investigation, B.H., L.S., M.W.-M., S.W., M.T., and N.E.; Methodology, B.H., L.S., M.W.-M., S.W., M.T., and N.E.; Supervision, B.H. and N.E.; Visualization, B.H., L.S., and N.E.; Writing original draft, N.E.; Writing review & editing, B.H.

Funding: This research received no external funding.

Acknowledgments: We thank G. Röhn for help with glioma sample preparation and Julia Stingl for support and expert scientific advice.

Conflicts of Interest: The authors declare no conflict of interest.

Disclaimer: The opinions mentioned throughout the following article are personal views of the authors and do not reflect an official position of the Federal Institute for Drugs and Medical Devices.

Abbreviations

AKT	protein kinase B (PKB)
ATP	adenosine triphosphate
ASK1	apoptosis signal-regulating kinase 1
GBM	glioblastoma multiforme
GF	growth factor
HIF-1 α	hypoxia-inducible factor-1 α
JNK	c-Jun N-terminal kinase
MAP kinase	mitogen-activated protein kinase
PI3K	phosphatidylinositide 3-kinase
PTEN	phosphatase and tensin homolog
ROS	reactive oxygen species
TMZ	temozolomide
Trx	thioredoxin
TrxR	thioredoxin reductase
TXNIP	Trx-interacting protein
VDUP1	vitamin-D_3-upregulated protein 1
VEGF	vascular endothelial growth factor

References

1. Siegel, R.L.; Miller, K.D.; Jemal, A. Cancer statistics, 2016. *CA Cancer J. Clin.* **2016**, *66*, 7–30. [CrossRef] [PubMed]
2. Louis, D.N.; Perry, A.; Reifenberger, G.; von Deimling, A.; Figarella-Branger, D.; Cavenee, W.K.; Ohgaki, H.; Wiestler, O.D.; Kleihues, P.; Ellison, D.W. The 2016 World Health Organization Classification of Tumors of the Central Nervous System: A summary. *Acta Neuropathol.* **2016**, *131*, 803–820. [CrossRef] [PubMed]
3. Stupp, R.; Hegi, M.E.; Mason, W.P.; van den Bent, M.J.; Taphoorn, M.J.; Janzer, R.C.; Ludwin, S.K.; Allgeier, A.; Fisher, B.; Belanger, K.; et al. Effects of radiotherapy with concomitant and adjuvant temozolomide versus radiotherapy alone on survival in glioblastoma in a randomised phase III study: 5-Year analysis of the EORTC-NCIC trial. *Lancet. Oncol.* **2009**, *10*, 459–466. [CrossRef]
4. Stupp, R.; Mason, W.P.; van den Bent, M.J.; Weller, M.; Fisher, B.; Taphoorn, M.J.; Belanger, K.; Brandes, A.A.; Marosi, C.; Bogdahn, U.; et al. Radiotherapy plus concomitant and adjuvant temozolomide for glioblastoma. *N. Engl. J. Med.* **2005**, *352*, 987–996. [CrossRef] [PubMed]
5. Ostrom, Q.T.; Gittleman, H.; Xu, J.; Kromer, C.; Wolinsky, Y.; Kruchko, C.; Barnholtz-Sloan, J.S. CBTRUS Statistical Report: Primary Brain and Other Central Nervous System Tumors Diagnosed in the United States in 2009–2013. *Neuro Oncol.* **2016**, *18*, v1–v75. [CrossRef] [PubMed]
6. Carrasco-Garcia, E.; Saceda, M.; Martinez-Lacaci, I. Role of receptor tyrosine kinases and their ligands in glioblastoma. *Cells* **2014**, *3*, 199–235. [CrossRef] [PubMed]
7. Ishii, N.; Maier, D.; Merlo, A.; Tada, M.; Sawamura, Y.; Diserens, A.C.; van Meir, E.G. Frequent co-alterations of TP53, p16/CDKN2A, p14ARF, PTEN tumor suppressor genes in human glioma cell lines. *Brain Pathol.* **1999**, *9*, 469–479. [CrossRef] [PubMed]
8. Iwadate, Y.; Fujimoto, S.; Tagawa, M.; Namba, H.; Sueyoshi, K.; Hirose, M.; Sakiyama, S. Association of p53 gene mutation with decreased chemosensitivity in human malignant gliomas. *Int. J. Cancer* **1996**, *69*, 236–240. [CrossRef]
9. Holmgren, A. Thioredoxin structure and mechanism: Conformational changes on oxidation of the active-site sulfhydryls to a disulfide. *Structure* **1995**, *3*, 239–243. [CrossRef]
10. Nishinaka, Y.; Nishiyama, A.; Masutani, H.; Oka, S.; Ahsan, K.M.; Nakayama, Y.; Ishii, Y.; Nakamura, H.; Maeda, M.; Yodoi, J. Loss of thioredoxin-binding protein-2/vitamin D3 up-regulated protein 1 in human T-cell leukemia virus type I-dependent T-cell transformation: Implications for adult T-cell leukemia leukemogenesis. *Cancer Res.* **2004**, *64*, 1287–1292. [CrossRef] [PubMed]

11. Powis, G.; Montfort, W.R. Properties and biological activities of thioredoxins. *Annu. Rev. Pharmacol. Toxicol.* **2001**, *41*, 261–295. [CrossRef] [PubMed]
12. Sasada, T.; Nakamura, H.; Ueda, S.; Sato, N.; Kitaoka, Y.; Gon, Y.; Takabayashi, A.; Spyrou, G.; Holmgren, A.; Yodoi, J. Possible involvement of thioredoxin reductase as well as thioredoxin in cellular sensitivity to cis-diamminedichloroplatinum (II). *Free Radic. Biol. Med.* **1999**, *27*, 504–514. [CrossRef]
13. Yokomizo, A.; Ono, M.; Nanri, H.; Makino, Y.; Ohga, T.; Wada, M.; Okamoto, T.; Yodoi, J.; Kuwano, M.; Kohno, K. Cellular levels of thioredoxin associated with drug sensitivity to cisplatin, mitomycin C, doxorubicin, and etoposide. *Cancer Res.* **1995**, *55*, 4293–4296. [PubMed]
14. Yamada, M.; Tomida, A.; Yoshikawa, H.; Taketani, Y.; Tsuruo, T. Overexpression of thioredoxin does not confer resistance to cisplatin in transfected human ovarian and colon cancer cell lines. *Cancer Chemother. Pharmacol.* **1997**, *40*, 31–37. [CrossRef] [PubMed]
15. Zhang, P.; Gao, J.; Wang, X.; Wen, W.; Yang, H.; Tian, Y.; Liu, N.; Wang, Z.; Liu, H.; Zhang, Y.; et al. A novel indication of thioredoxin-interacting protein as a tumor suppressor gene in malignant glioma. *Oncol. Lett.* **2017**, *14*, 2053–2058. [CrossRef] [PubMed]
16. Gollapalli, K.; Ghantasala, S.; Atak, A.; Rapole, S.; Moiyadi, A.; Epari, S.; Srivastava, S. Tissue Proteome Analysis of Different Grades of Human Gliomas Provides Major Cues for Glioma Pathogenesis. *OMICS* **2017**, *21*, 275–284. [CrossRef] [PubMed]
17. Bhatia, M.; McGrath, K.L.; Di Trapani, G.; Charoentong, P.; Shah, F.; King, M.M.; Clarke, F.M.; Tonissen, K.F. The thioredoxin system in breast cancer cell invasion and migration. *Redox Biol.* **2016**, *8*, 68–78. [CrossRef] [PubMed]
18. Zhang, J.; Li, X.; Han, X.; Liu, R.; Fang, J. Targeting the Thioredoxin System for Cancer Therapy. *Trends Pharmacol. Sci.* **2017**, *38*, 794–808. [CrossRef] [PubMed]
19. Stafford, W.C.; Peng, X.; Olofsson, M.H.; Zhang, X.; Luci, D.K.; Lu, L.; Cheng, Q.; Tresaugues, L.; Dexheimer, T.S.; Coussens, N.P.; et al. Irreversible inhibition of cytosolic thioredoxin reductase 1 as a mechanistic basis for anticancer therapy. *Sci. Transl. Med.* **2018**, *10*, 428. [CrossRef] [PubMed]
20. Fiskus, W.; Saba, N.; Shen, M.; Ghias, M.; Liu, J.Y.; Das Gupta, S.; Chauhan, L.; Rao, R.; Gunewardena, S.; Schorno, K.; et al. Auranofin Induces Lethal Oxidative and Endoplasmic Reticulum Stress and Exerts Potent Preclinical Activity against Chronic Lymphocytic Leukemia. *Cancer Res.* **2014**, *74*, 2520–2532. [CrossRef] [PubMed]
21. Hwang-Bo, H.; Jeong, J.W.; Han, M.H.; Park, C.; Hong, S.H.; Kim, G.Y.; Moon, S.K.; Cheong, J.; Kim, W.J.; Yoo, Y.H.; et al. Auranofin, an inhibitor of thioredoxin reductase, induces apoptosis in hepatocellular carcinoma Hep3B cells by generation of reactive oxygen species. *Gen. Physiol. Biophys.* **2017**, *36*, 117–128. [CrossRef] [PubMed]
22. Shin, D.W.; Kwon, Y.J.; Ye, D.J.; Baek, H.S.; Lee, J.E.; Chun, Y.J. Auranofin Suppresses Plasminogen Activator Inhibitor-2 Expression through Annexin A5 Induction in Human Prostate Cancer Cells. *Biomol. Ther.* **2017**, *25*, 177–185. [CrossRef] [PubMed]
23. Li, H.; Hu, J.; Wu, S.; Wang, L.; Cao, X.; Zhang, X.; Dai, B.; Cao, M.; Shao, R.; Zhang, R.; et al. Auranofin-mediated inhibition of PI3K/AKT/mTOR axis and anticancer activity in non-small cell lung cancer cells. *Oncotarget* **2016**, *7*, 3548–3558. [CrossRef] [PubMed]
24. Hou, G.X.; Liu, P.P.; Zhang, S.; Yang, M.; Liao, J.; Yang, J.; Hu, Y.; Jiang, W.Q.; Wen, S.; Huang, P. Elimination of stem-like cancer cell side-population by auranofin through modulation of ROS and glycolysis. *Cell. Death Dis.* **2018**, *9*, 89. [CrossRef] [PubMed]
25. Habermann, K.J.; Grunewald, L.; van Wijk, S.; Fulda, S. Targeting redox homeostasis in rhabdomyosarcoma cells: GSH-depleting agents enhance auranofin-induced cell death. *Cell. Death Dis.* **2017**, *8*, e3067. [CrossRef] [PubMed]
26. Raninga, P.V.; Di Trapani, G.; Vuckovic, S.; Tonissen, K.F. Cross-talk between two antioxidants, thioredoxin reductase and heme oxygenase-1, and therapeutic implications for multiple myeloma. *Redox Biol.* **2016**, *8*, 175–185. [CrossRef] [PubMed]
27. Marzano, C.; Gandin, V.; Folda, A.; Scutari, G.; Bindoli, A.; Rigobello, M.P. Inhibition of thioredoxin reductase by auranofin induces apoptosis in cisplatin-resistant human ovarian cancer cells. *Free Radic Biol. Med.* **2007**, *42*, 872–881. [CrossRef] [PubMed]

28. Long, J.; Manchandia, T.; Ban, K.; Gao, S.; Miller, C.; Chandra, J. Adaphostin cytoxicity in glioblastoma cells is ROS-dependent and is accompanied by upregulation of heme oxygenase-1. *Cancer Chemother. Pharmacol.* **2007**, *59*, 527–535. [CrossRef] [PubMed]
29. Sharma, V.; Joseph, C.; Ghosh, S.; Agarwal, A.; Mishra, M.K.; Sen, E. Kaempferol induces apoptosis in glioblastoma cells through oxidative stress. *Mol. Cancer Ther.* **2007**, *6*, 2544–2553. [CrossRef] [PubMed]
30. Haas, B.; Klinger, V.; Keksel, C.; Bonigut, V.; Kiefer, D.; Caspers, J.; Walther, J.; Wos-Maganga, M.; Weickhardt, S.; Rohn, G.; et al. Inhibition of the PI3K but not the MEK/ERK pathway sensitizes human glioma cells to alkylating drugs. *Cancer Cell Int.* **2018**, *18*, 69. [CrossRef] [PubMed]
31. Ray, P.D.; Huang, B.W.; Tsuji, Y. Reactive oxygen species (ROS) homeostasis and redox regulation in cellular signaling. *Cell Signal.* **2012**, *24*, 981–990. [CrossRef] [PubMed]
32. Welsh, S.J.; Bellamy, W.T.; Briehl, M.M.; Powis, G. The redox protein thioredoxin-1 (Trx-1) increases hypoxia-inducible factor 1alpha protein expression: Trx-1 overexpression results in increased vascular endothelial growth factor production and enhanced tumor angiogenesis. *Cancer Res.* **2002**, *62*, 5089–5095. [PubMed]
33. Hedley, D.; Pintilie, M.; Woo, J.; Nicklee, T.; Morrison, A.; Birle, D.; Fyles, A.; Milosevic, M.; Hill, R. Up-regulation of the redox mediators thioredoxin and apurinic/apyrimidinic excision (APE)/Ref-1 in hypoxic microregions of invasive cervical carcinomas, mapped using multispectral, wide-field fluorescence image analysis. *Am. J. Pathol.* **2004**, *164*, 557–565. [CrossRef]
34. Bhatia, M.; Lovitt, C.J.; Raninga, P.V.; Avery, V.M.; Di Trapani, G.; Tonissen, K.F. Expression of the thioredoxin system in an in vivo-like cancer cell environment upon auranofin treatment. *Eur. J. Cell Biol.* **2016**, *95*, 378–388. [CrossRef] [PubMed]
35. Powis, G.; Kirkpatrick, D.L.; Angulo, M.; Baker, A. Thioredoxin redox control of cell growth and death and the effects of inhibitors. *Chem. Biol. Interact.* **1998**, *111*, 23–34. [CrossRef]
36. Hu, J.; Zhang, H.; Cao, M.; Wang, L.; Wu, S.; Fang, B. Auranofin Enhances Ibrutinib's Anticancer Activity in EGFR-Mutant Lung Adenocarcinoma. *Mol. Cancer Ther.* **2018**. [CrossRef] [PubMed]
37. Huang, H.; Liao, Y.; Liu, N.; Hua, X.; Cai, J.; Yang, C.; Long, H.; Zhao, C.; Chen, X.; Lan, X.; et al. Two clinical drugs deubiquitinase inhibitor auranofin and aldehyde dehydrogenase inhibitor disulfiram trigger synergistic anti-tumor effects in vitro and in vivo. *Oncotarget* **2016**, *7*, 2796–2808. [CrossRef] [PubMed]
38. Kim, T.W.; Lee, S.J.; Kim, J.T.; Kim, S.J.; Min, J.K.; Bae, K.H.; Jung, H.; Kim, B.Y.; Lim, J.S.; Yang, Y.; et al. Kallikrein-related peptidase 6 induces chemotherapeutic resistance by attenuating auranofin-induced cell death through activation of autophagy in gastric cancer. *Oncotarget* **2016**, *7*, 85332–85348. [CrossRef] [PubMed]
39. Oommen, D.; Yiannakis, D.; Jha, A.N. BRCA1 deficiency increases the sensitivity of ovarian cancer cells to auranofin. *Mutat. Res.* **2016**, *784*, 8–15. [CrossRef] [PubMed]
40. Lee, J.E.; Kwon, Y.J.; Baek, H.S.; Ye, D.J.; Cho, E.; Choi, H.K.; Oh, K.S.; Chun, Y.J. Synergistic induction of apoptosis by combination treatment with mesupron and auranofin in human breast cancer cells. *Arch. Pharm. Res.* **2017**, *40*, 746–759. [CrossRef] [PubMed]
41. Roh, J.L.; Jang, H.; Kim, E.H.; Shin, D. Targeting of the Glutathione, Thioredoxin, and Nrf2 Antioxidant Systems in Head and Neck Cancer. *Antioxid. Redox Signal.* **2017**, *27*, 106–114. [CrossRef] [PubMed]
42. Rodman, S.N.; Spence, J.M.; Ronnfeldt, T.J.; Zhu, Y.; Solst, S.R.; O'Neill, R.A.; Allen, B.G.; Guan, X.; Spitz, D.R.; Fath, M.A. Enhancement of Radiation Response in Breast Cancer Stem Cells by Inhibition of Thioredoxin- and Glutathione-Dependent Metabolism. *Radiat. Res.* **2016**, *186*, 385–395. [CrossRef] [PubMed]
43. Wang, H.; Bouzakoura, S.; de Mey, S.; Jiang, H.; Law, K.; Dufait, I.; Corbet, C.; Verovski, V.; Gevaert, T.; Feron, O.; et al. Auranofin radiosensitizes tumor cells through targeting thioredoxin reductase and resulting overproduction of reactive oxygen species. *Oncotarget* **2017**, *8*, 35728–35742. [CrossRef] [PubMed]
44. Raninga, P.V.; Di Trapani, G.; Vuckovic, S.; Bhatia, M.; Tonissen, K.F. Inhibition of thioredoxin 1 leads to apoptosis in drug-resistant multiple myeloma. *Oncotarget* **2015**, *6*, 15410–15424. [CrossRef] [PubMed]
45. Raninga, P.V.; Di Trapani, G.; Vuckovic, S.; Tonissen, K.F. TrxR1 inhibition overcomes both hypoxia-induced and acquired bortezomib resistance in multiple myeloma through NF-small ka, Cyrillicbeta inhibition. *Cell. Cycle* **2016**, *15*, 559–572. [CrossRef] [PubMed]
46. Kirkpatrick, D.L.; Kuperus, M.; Dowdeswell, M.; Potier, N.; Donald, L.J.; Kunkel, M.; Berggren, M.; Angulo, M.; Powis, G. Mechanisms of inhibition of the thioredoxin growth factor system by antitumor 2-imidazolyl disulfides. *Biochem. Pharmacol.* **1998**, *55*, 987–994. [CrossRef]

47. Meuillet, E.J.; Mahadevan, D.; Berggren, M.; Coon, A.; Powis, G. Thioredoxin-1 binds to the C2 domain of PTEN inhibiting PTEN's lipid phosphatase activity and membrane binding: A mechanism for the functional loss of PTEN's tumor suppressor activity. *Arch. Biochem. Biophys.* **2004**, *429*, 123–133. [CrossRef] [PubMed]
48. Toledano, M.B.; Leonard, W.J. Modulation of transcription factor NF-kappa B binding activity by oxidation-reduction in vitro. *Proc. Natl. Acad. Sci. USA* **1991**, *88*, 4328–4332. [CrossRef] [PubMed]
49. Wang, C.Y.; Guttridge, D.C.; Mayo, M.W.; Baldwin, A.S. NF-kappaB induces expression of the Bcl-2 homologue A1/Bfl-1 to preferentially suppress chemotherapy-induced apoptosis. *Mol. Cell. Biol.* **1999**, *19*, 5923–5929. [CrossRef] [PubMed]
50. Saitoh, M.; Nishitoh, H.; Fujii, M.; Takeda, K.; Tobiume, K.; Sawada, Y.; Kawabata, M.; Miyazono, K.; Ichijo, H. Mammalian thioredoxin is a direct inhibitor of apoptosis signal-regulating kinase (ASK) 1. *EMBO J.* **1998**, *17*, 2596–2606. [CrossRef] [PubMed]
51. Kim, A.H.; Khursigara, G.; Sun, X.; Franke, T.F.; Chao, M.V. Akt phosphorylates and negatively regulates apoptosis signal-regulating kinase 1. *Mol. Cell. Biol.* **2001**, *21*, 893–901. [CrossRef] [PubMed]
52. Ichijo, H.; Nishida, E.; Irie, K.; ten Dijke, P.; Saitoh, M.; Moriguchi, T.; Takagi, M.; Matsumoto, K.; Miyazono, K.; Gotoh, Y. Induction of apoptosis by ASK1, a mammalian MAPKKK that activates SAPK/JNK and p38 signaling pathways. *Science* **1997**, *275*, 90–94. [CrossRef] [PubMed]
53. Zhao, H.F.; Wang, J.; Shao, W.; Wu, C.P.; Chen, Z.P.; To, S.T.; Li, W.P. Recent advances in the use of PI3K inhibitors for glioblastoma multiforme: Current preclinical and clinical development. *Mol. Cancer* **2017**, *16*, 100. [CrossRef] [PubMed]
54. Louis, D.N.; Ohgaki, H.; Wiestler, O.D.; Cavenee, W.K.; Burger, P.C.; Jouvet, A.; Scheithauer, B.W.; Kleihues, P. The 2007 WHO classification of tumours of the central nervous system. *Acta Neuropathol.* **2007**, *114*, 97–109. [CrossRef] [PubMed]
55. Eckstein, N.; Servan, K.; Girard, L.; Cai, D.; von Jonquieres, G.; Jaehde, U.; Kassack, M.U.; Gazdar, A.F.; Minna, J.D.; Royer, H.D. Epidermal growth factor receptor pathway analysis identifies amphiregulin as a key factor for cisplatin resistance of human breast cancer cells. *J. Biol. Chem.* **2008**, *283*, 739–750. [CrossRef] [PubMed]

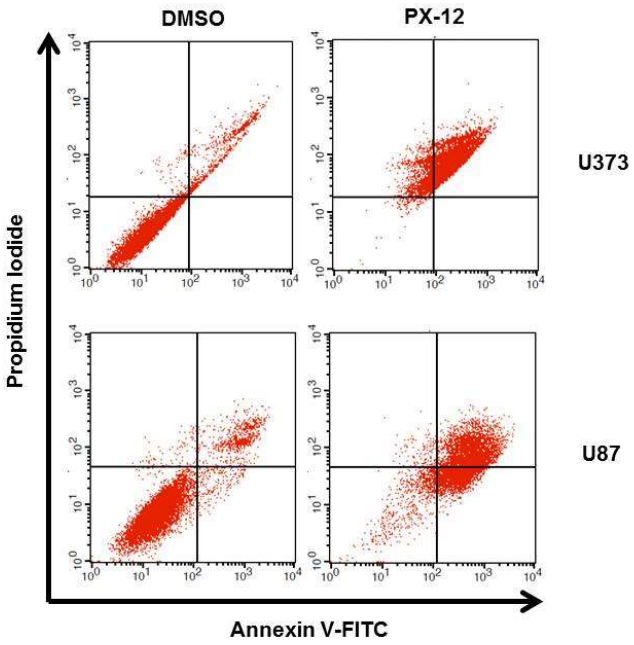

Figure S1. Representative FACS blots of U373 and U87 cells treated with either vehicle (DMSO) or 1000 μM PX-12 for 72 hours as indicated. Annexin V positive cells were regarded as apoptotic cells.

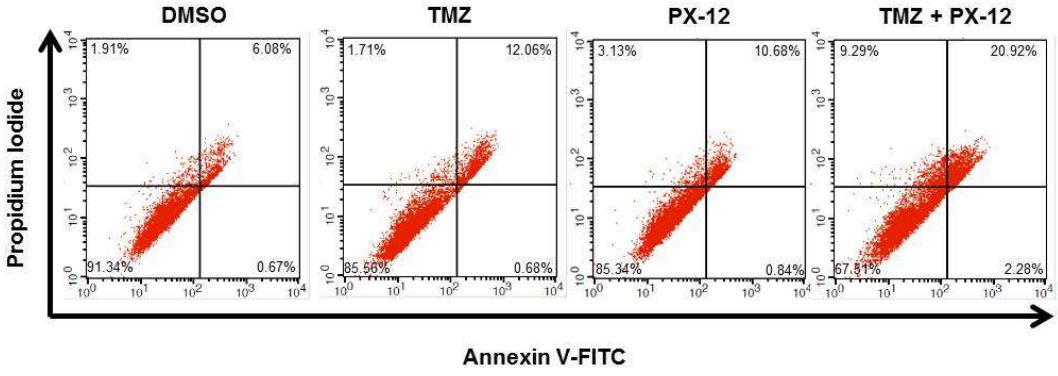

Figure S2. Representative FACS blots of primary GBM cells treated with either vehicle (DMSO) or 100 μM PX-12, 1000 μM TMZ, or a combination of both for 48 hours as indicated. Annexin V positive cells were regarded as apoptotic cells.

3.3 Kaina B, Beltzig L, Piee-Staffa A, **Haas B**. Cytotoxic and Senolytic Effects of Methadone in Combination with Temozolomide in Glioblastoma Cells. Int J Mol Sci. 2020;21(19).

Zielsetzung der Arbeit: Das Opioid Methadon wird zur Schmerzbehandlung und Heroinsubstitution eingesetzt. Studien mit Methadon an Glioblastom-Zellen zeigten eine vielversprechende zytotoxische Aktivität in Kombination mit Doxorubicin (Friesen et al., 2014), was zu einer großen medialen Aufmerksamkeit und Verunsicherung von Patienten führte, da es sich nur um präklinische Versuche handelte und es zu dieser Zeit nur wenige Daten zur Wirkung von Methadon mit dem Therapie-Goldstandard TMZ gab (Hübner et al., 2017). Um zur Aufklärung beizutragen, wurden in dieser Arbeit die Wirkung von Methadon alleine und in Kombination mit TMZ in zwei humanen Glioblastom-Zelllinien und in humane Fibroblasten untersucht.

Methoden und Ergebnisse: Annexin-V-FACS Assays ergaben, dass Methadon ab einer Konzentration von 20 µg/ml (60 µM) zytotoxisch ist und Apoptose und Nekrose in Glioblastom-Zellen induziert. Methadon war in MGMT-exprimierenden und nicht-exprimierenden Glioblastom-Zellen und humanen Fibroblasten ähnlich toxisch. Weiterhin zeigte sich, dass die Apoptoseinduktion nicht über den µ-Opioidrezeptor vermittelt wird, da der Antagonist Naloxon die Wirkung von Methadon nicht aufhob. Bei gleichzeitiger Inkubation der Zellen mit TMZ hatte Methadon nur additive, jedoch keine synergistischen Effekte auf die TMZ-induzierte Apoptose. Methadon war weder genotoxisch in Comet- und γH2AX-Assays, noch hatte es synergistischen Effekte auf die Genotoxizität von TMZ. Darüber hinaus induzierte Methadon keine Seneszenz und hatte auch keinen Einfluss auf die TMZ-induzierte Seneszenz, die über FACS-Messungen der lysosomalen β-Galaktosidase quantifiziert wurde. Schließlich ergaben PCR-Experimente, dass Methadon die MGMT-Promotormethylierung in Zellen nicht beeinflusst.

Schlussfolgerung: Methadon induzierte in Glioblastom-Zellen Apoptose und Nekrose, allerdings erst ab Konzentrationen >60 µM, die keine klinisch Relevanz haben, denn die Plasmakonzentration von mit Methadon behandelten Schmerzpatienten liegt bei etwa 1 µM (Inturrisi et al., 1987). Methadon war nicht genotoxisch und steigerte auch nicht synergistisch die zytotoxische oder Seneszenz-induzierende Wirkung von TMZ, was darauf hindeutet, dass Methadon keinen Einfluss auf TMZ-induzierten Signalwege hat. Die Daten stützen somit nicht die Hypothese, dass eine gleichzeitige Methadon-Behandlung die TMZ-Therapie des Glioblastoms unterstützen könnte.

International Journal of
Molecular Sciences

MDPI

Article

Cytotoxic and Senolytic Effects of Methadone in Combination with Temozolomide in Glioblastoma Cells

Bernd Kaina [1,*], Lea Beltzig [1], Andrea Piee-Staffa [1] and Bodo Haas [2]

[1] Institute of Toxicology, University Medical Center, Obere Zahlbacher Str. 67, 55131 Mainz, Germany; lea.beltzig@uni-mainz.de (L.B.); pieean01@uni-mainz.de (A.P.-S.)
[2] Federal Institute for Drugs and Medical Devices, Kurt-Georg-Kiesinger-Allee 3, 53175 Bonn, Germany; bodo.haas@bfarm.de
* Correspondence: kaina@uni-mainz.de

Received: 11 July 2020; Accepted: 17 September 2020; Published: 23 September 2020

Abstract: Methadone is an analgesic drug used for pain treatment and heroin substitution. Recently, methadone has been proposed to be useful also for cancer therapy, including glioblastoma multiforme (GBM), the most severe form of brain cancer, because experiments on cultured glioma cells treated with doxorubicin showed promising results. Doxorubicin, however, is not used first-line in GBM therapy. Therefore, we analyzed the cytotoxic effect of methadone alone and in combination with temozolomide, a DNA-alkylating drug that is first-line used in GBM treatment, utilizing GBM-derived cell lines and a human fibroblast cell line. We show that methadone is cytotoxic on its own, inducing apoptosis and necrosis, which was observed at a concentration above 20 μg/mL. Methadone was similar toxic in isogenic MGMT expressing and non-expressing cells, and in LN229 glioblastoma and VH10T human fibroblasts. The apoptosis-inducing activity of methadone is not bound on the opioid receptor (OR), since naloxone, a competitive inhibitor of OR, did not attenuate methadone-induced apoptosis/necrosis. Administrating methadone and temozolomide together, temozolomide had no impact on methadone-induced apoptosis (which occurred 3 days after treatment), while temozolomide-induced apoptosis (which occurred 5 days after treatment) was unaffected at low (non-toxic) methadone concentration (5 μg/mL), and at high (toxic) methadone concentration (20 μg/mL) the cytotoxic effects of methadone and temozolomide were additive. Methadone is not genotoxic, as revealed by comet and γH2AX assay, and did not ameliorate the genotoxic effect of temozolomide. Further, methadone did not induce cellular senescence and had no effect on temozolomide-induced senescence. Although methadone was toxic on senescent cells, it cannot be considered a senolytic drug since cytotoxicity was not specific for senescent cells. Finally, we show that methadone had no impact on the MGMT promoter methylation. Overall, the data show that methadone on glioblastoma cells in vitro is cytotoxic and induces apoptosis/necrosis at doses that are above the level that can be achieved in vivo. It is not genotoxic, and does not ameliorate the cell killing or the senescence-inducing effect of temozolomide (no synergistic effect), indicating it has no impact on temozolomide-induced signaling pathways. The data do not support the notion that concomitant methadone treatment supports temozolomide-based chemotherapy.

Keywords: glioblastoma; methadone; temozolomide; apoptosis; drug resistance; cancer therapy; senescence

1. Introduction

Glioblastoma (WHO grade IV, glioblastoma multiforme, GBM) accounting for ~70% of high- grade malignant gliomas, have a dismal prognosis. The median overall survival time of newly diagnosed

GBM is maximally 14 months, and the median overall 2-year survival rate is 26%, with a wide range of outcomes [1]. An important prognostic marker is the DNA repair protein O^6-methylguanine-DNA methyltransferase (MGMT), and patients harboring the methylated (silenced) MGMT promoter have a better prognosis than patients with the tumor-unmethylated (active) MGMT promoter, with overall survival times of 12.2 and 18.2 months, respectively [2]. Standard therapy includes resection of the tumor with maximum safe margin, followed by radiotherapy and concomitant chemotherapy with temozolomide (TMZ) [3]. Taken the bad prognosis of patients suffering from glioblastoma, it is obvious that there is an urgent need for supporting therapeutic strategies.

It has been reported that D,L-methadone (MTD), an opioid agonist used for heroin substitution and a widely used analgesic in pain therapy, induces cell death and supports the cytotoxic effect of doxorubicin in leukemia cells [4]. Extending this work, the same group studied MTD on glioblastoma cell lines and reported that the opioid is able to enhance the apoptosis-inducing effect of doxorubicin in this cell system [5]. This was explained by assuming that MTD impacts doxorubicin uptake and attenuates its efflux, which would enhance the intracellular level of doxorubicin and, consequently, its cytotoxic activity [5]. Based on this work, a trial has been initiated treating glioma patients (grade II–IV) with MTD, which occurred independent of their neuro-oncological treatment [6]. In view of the patient heterogeneity, small group size and lacking stratification of the control group, a conclusion as to the therapeutic benefit of MTD in mono- or combined therapy could not be drawn.

Although a beneficial effect of MTD in glioblastoma therapy cannot per se be neglected, it is important to note that glioblastoma is not treated first-line with the topoisomerase II-inhibitor doxorubicin, which has been used in previous studies. First-line chemotherapeutics for glioma (grade III and IV) is the DNA alkylating agent temozolomide (TMZ) [3] and, therefore, it is desirable to study the interaction of MTD with TMZ. This genotoxic anticancer drug is a triazene derivative that does not need metabolic activation and methylates DNA at various sites [7]. One of the methylation products, O^6-methylguanine, is the preponderant killing lesion, inducing apoptosis, autophagy, and senescence [8]. The survival pathways, including DNA repair by MGMT [7,9], and death pathways activated upon TMZ treatment were described in detail [8–10]. Cell death is based on DNA mismatch repair-mediated processing of O^6-methylguanine/thymine mispairs in the DNA, formation of DNA double-strand breaks (DSB), activation of the DNA damage response and downstream cell death pathways. Here, we set out to determine whether MTD has an impact on the well-known cytotoxic effect of TMZ on glioblastoma cells in an in vitro setting. Our data do not support the hypothesis that MTD has a synergistic effect on glioblastoma cells, ameliorating apoptosis, necrosis, and cellular senescence following TMZ treatment, although MTD itself, at high dose levels (>20 µg/mL), was apoptosis/necrosis-inducing, irrespective of the MGMT status of glioblastoma cells. We also report that MTD does not induce cellular senescence, is not genotoxic, and has no impact on epigenetic MGMT regulation.

2. Results

2.1. Viability Assays

First, in dose-finding experiments, we set out to determine whether MTD is cytotoxic in LN229 glioblastoma cells. As shown in Figure 1A, MTD reduced the viability of LN229 cells dose dependently. Already with a concentration of 5 µg/mL, viability was significantly reduced (by ~30%), and with 100 µg/mL, all cells in the population died. The data shows that MTD itself reduces the viability of GBM cells.

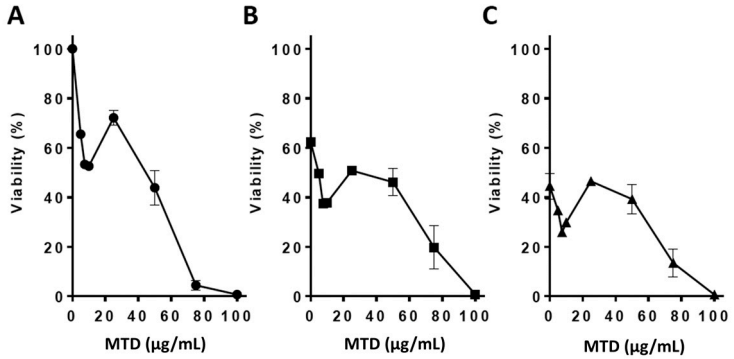

Figure 1. Cytotoxicity of methadone (MTD) on LN229 cells without and with co-treatment with temozolomide (TMZ). (**A**) Viability of LN229 cells, measured by the MTT assay, as a function of MTD concentration in the medium. (**B**) Viability of LN229 cells treated with 20 µM TMZ and (**C**) 75 µM TMZ and increasing concentrations of MTD. The MTT assay was performed 96 h after the addition of MTD to the medium. Data are the mean of three independent experiments.

Next, we addressed the possibility that MTD exerts a supportive effect on the viability brought about by TMZ in LN229 cells. Treatment of exponentially growing LN229 cells occurred first with TMZ and, 2 h later, by the addition of MTD to the medium. TMZ treatment with a dose of 20 and 75 µM reduced the viability by about 40 and 60%, respectively, and MTD further reduced the viability (Figure 1B,C).

In another experimental series, we measured the viability in a dose range of up to 40 µg/mL MTD in the absence and presence of TMZ. In this case, cells were treated simultaneously with both drugs. The viability curves displayed a nearly parallel course up to a dose level of 20 µg/mL MTD, indicating an additive mode of action. At high MTD concentrations (>20 µg/mL), TMZ seems to be even less effective than expected (Figure 2A), which was also observed in other experiments (see below). We should note that the viability curves for MTD have a biphasic shape with an initial nadir at 7.5 µg/mL, which was observed in all cell viability assays performed. In the viability assays, inhibition of proliferation and cell death reduce MTT metabolic activity, which might explain the first nadir, resulting from proliferation inhibition.

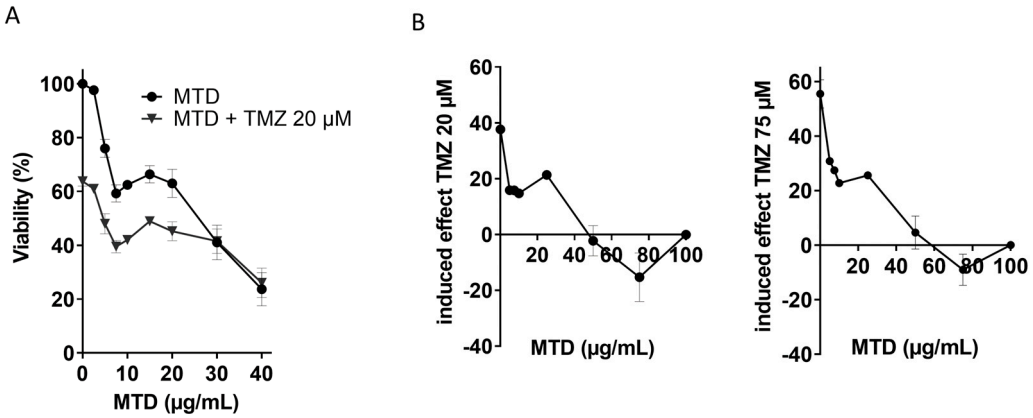

Figure 2. Cytotoxicity of TMZ measured in the MTT assay in the absence and presence of MTD. (**A**) Exponentially growing cells were treated with TMZ and increasing concentrations of MTD. Data are the mean of three separate experiments. (**B**) Induced effect of TMZ (20 and 75 µM, left and right panel, respectively) on the viability of LN229 cells co-treated with MTD. The toxic effect induced by MTD was subtracted from the effect obtained after combined treatment, shown in panel A for 20 µM TMZ. Viability was measured 120 h after addition of the drugs to the medium.

The effect of MTD on TMZ-induced cell death was further assessed by subtracting the cytotoxic effect of MTD from the effect observed in the combination treatment, which represents the effect induced by TMZ. The cytotoxic effect of TMZ was completely abrogated if cells were co-treated with MTD with a concentration >40 µg/mL (Figure 2B). This is likely a result of proliferation inhibition since TMZ requires cell cycle progression for the conversion of critical DNA adducts into toxic lesions [11].

2.2. Apoptosis and Necrosis Induced by MTD

The cytotoxic effect of MTD on glioblastoma cells was substantiated by measuring apoptosis and necrosis (annexin V and propidium iodine (AV/PI) flow cytometry). As shown in Figure 3, apoptosis and necrosis increased concentration-dependently. Glioblastoma A172 cells were clearly more sensitive than LN229. For comparison, we included human diploid fibroblasts, the line VH10T [11], which also showed concentration-dependent apoptosis. The fibroblasts (MGMT proficient) displayed a response similar to LN229 (MGMT deficient), while A172 was more sensitive, showing significant apoptosis/necrosis at a concentration >20 µg/mL MTD. Interestingly, MTD was also effective in inducing apoptosis and necrosis in LN229 cells expressing the DNA repair protein MGMT (LN229-MGMT-c12), indicating that the cytotoxic effect of MTD is independent on O^6-DNA alkylation lesions.

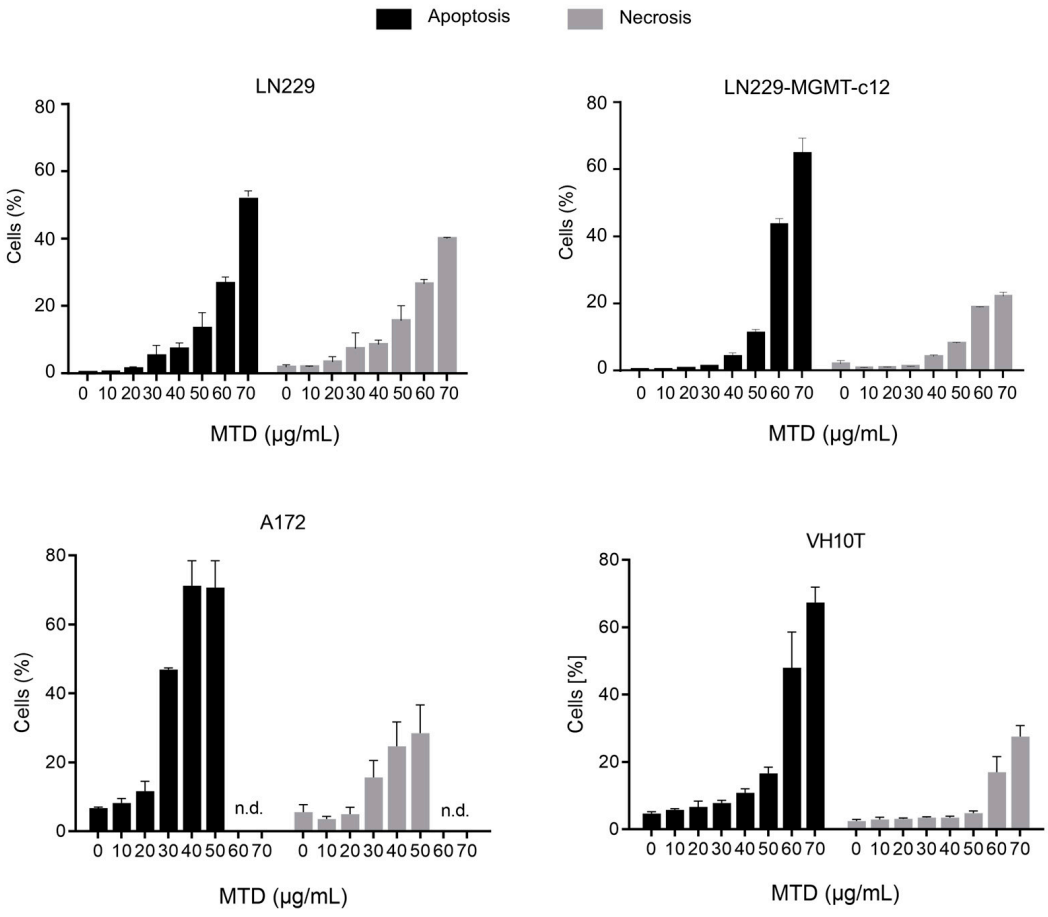

Figure 3. Apoptosis and necrosis induced in different glioblastoma cell lines and human fibroblasts VH10T. Exponentially growing cells were cultivated in medium with increasing concentrations of MTD, harvested, annexin V and propidium iodine (annexin V/PI) stained and measured by flow cytometry. Cells were analyzed 72 h after addition of MTD to the medium. Data are the mean of three independent experiments. n.d., not detectable.

2.3. Is MTD a Senescence Inducing Drug?

Previously, we have shown that glioblastoma cells undergo apoptosis and cellular senescence, if they were treated with DNA damaging agents [8,11]. Therefore, we were interested in assessing whether the cells enter the senescent state upon treatment with MTD. Surprisingly, although cells undergo apoptosis 3 days after the onset of MTD treatment, cellular senescence was not induced under these treatment conditions. The spontaneous level of senescence (as measured by c12FDG flow cytometry) was about 3%, which even declined following treatment, which is likely a result of death of spontaneously occurring senescent cells in the population (Figure 4).

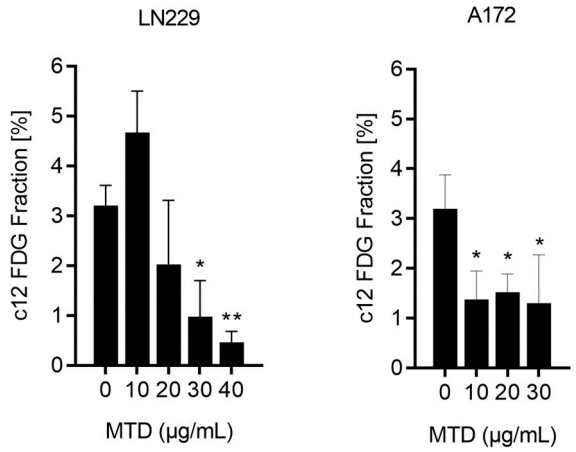

Figure 4. Level of cellular senescence in LN229 and A172 glioblastoma cells treated with MTD. Cells were harvested and measured 72 h after addition of MTD to the medium of exponentially growing cells. Data are the mean of three independent experiments. * $p < 0.05$; ** $p < 0.01$.

2.4. Is the Opioid Receptor Involved?

LN229 and A172 express the μ-opioid receptor (MOR-1), as human fibroblasts VH10T (used as a control) do (Figure 5A). Interestingly, TMZ treatment reduced the amount of MOR-1, and a lower basal expression level of MOR-1 was observed in A172 cells compared to LN229 (Figure 5A), although this line was more sensitive to apoptosis induction by MTD than LN229 (Figure 3). This may be taken to indicate that the toxic effect of MTD is not mediated by the opioid receptor. This is supported by the finding that naloxone, a competitive inhibitor of opioid receptors, had no effect on MTD-induced apoptosis (Figure 5B). We should note that we used naloxone concentrations that were non-toxic and equimolar to the MTD concentration or even higher (100 and 200 μM). We conclude that cytotoxicity induced by MTD in glioblastoma cells is not mediated by the opioid receptor.

2.5. Is MTD-Induced Apoptosis/Necrosis Affected by TMZ?

To elucidate whether TMZ has an impact on apoptosis and necrosis induced by MTD, we treated cells with MTD and immediately thereafter with TMZ. As shown in Figure 6, MTD (30 and 40 μg/mL) induced apoptosis/necrosis effectively whereas TMZ (25 μM) was ineffective when measured 3 days after treatment. Co-exposure of MTD and TMZ did not ameliorate the toxic effect of MTD.

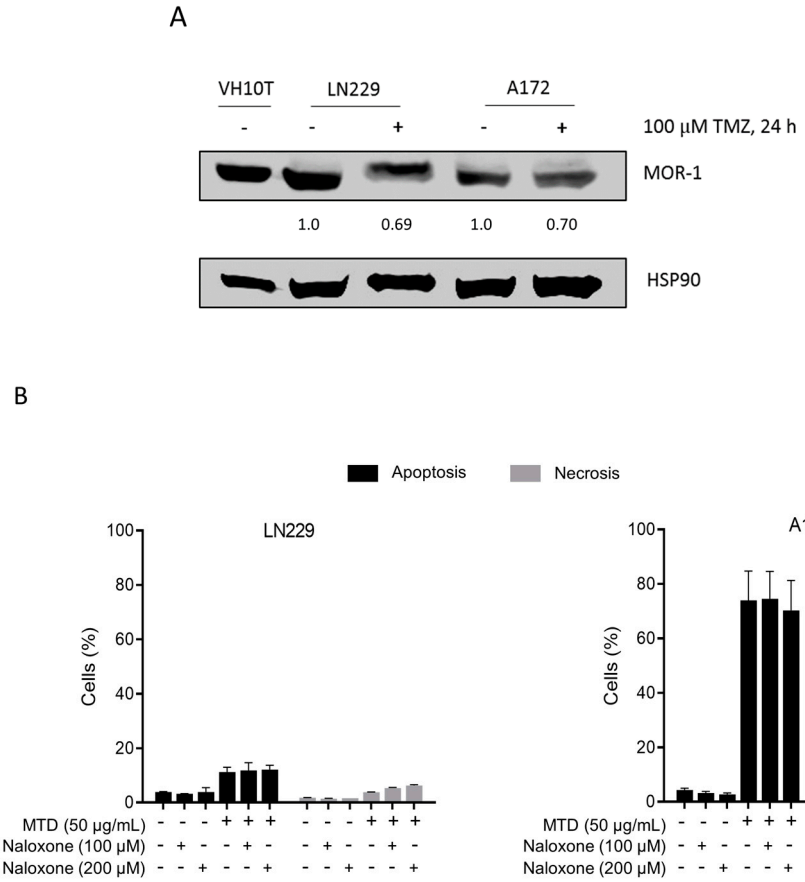

Figure 5. Expression of µ-opioid receptor MOR-1 in LN229 and A172 cells and effect of naloxone. (**A**) For comparison the level in human diploid fibroblasts VH10T are shown. The effect of TMZ on the receptor expression level was quantified in relation to the non-treated control, which was set to 1.0. (**B**) Effect of naloxone on MTD-induced cell death. Naloxone was administered 30 min before the addition of MTD to the medium. Data are the mean of three independent experiments.

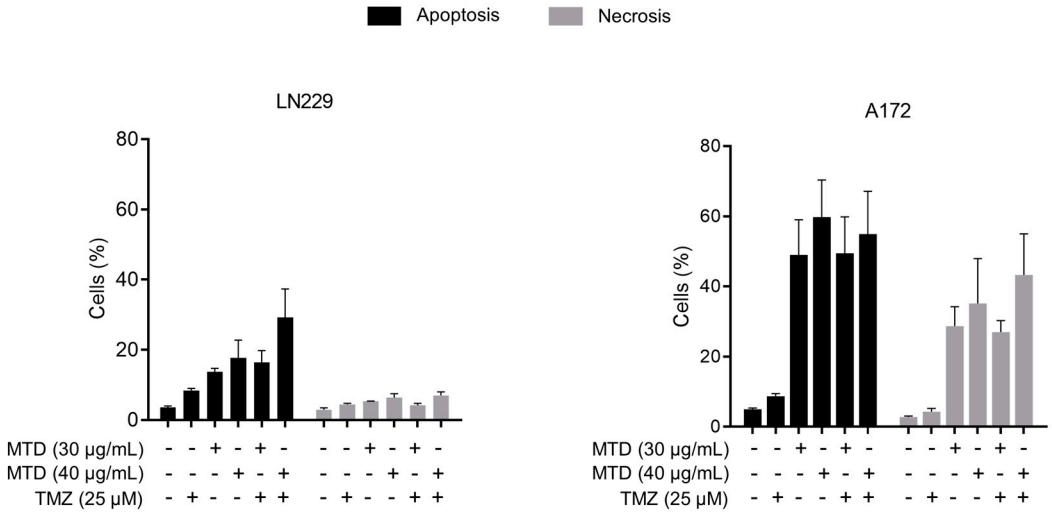

Figure 6. Effect of TMZ on MTD-induced apoptosis/necrosis in LN229 and A172 cells, measured 72 h after treatment. Data are the mean of three independent experiments. The differences between MTD and MTD-TMZ were in both cell lines not significant.

2.6. Is TMZ-Induced Apoptosis/Necrosis Affected by MTD?

While glioblastoma cells undergo apoptosis/necrosis already 2–3 days after addition of MTD to the medium, the onset of apoptosis following TMZ is much later, starting 4–5 days after treatment [11]. TMZ-induced apoptosis is obviously a late effect, resulting from DNA damage processing and the activation of a complex signaling cascade [12]. To analyze whether MTD has an impact on these processes triggered by O^6MeG, LN229 cells were treated with TMZ, and 3 h later post-treated with MTD until harvest 96 h later. As shown in Figure 7, MTD was ineffective in inducing apoptosis and necrosis up to a dose of 10 µg/mL. In this dose range, MTD did not enhance the cytotoxic response of TMZ. With a higher concentration of 20 µg/mL, MTD induced apoptosis and ameliorated the effect of TMZ, which was, however, merely additive (Figure 7).

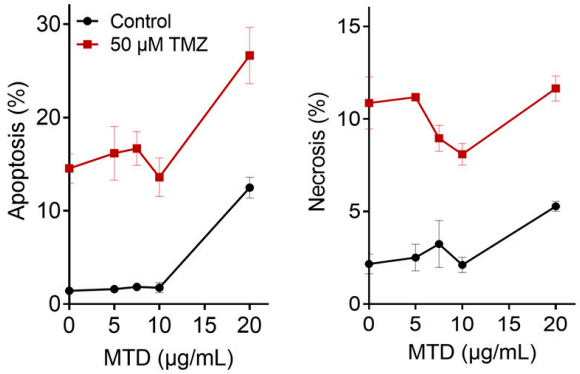

Figure 7. Effect of MTD alone (control) and in combination with TMZ (20 µM) on TMZ-induced apoptosis and necrosis, measured by AV/PI flow cytometry. Cells were harvested and analyzed 96 h after the addition of TMZ and MTD to the medium.

In another experimental series, LN229 and A172 cells were treated with TMZ and post-treated with MTD. Again, a subtoxic concentration of MTD (5 µg/mL) had no impact while a cytotoxic MTD concentration (20 µg/mL) ameliorated the apoptotic effect of TMZ (Figure 8A). The measured combined effects and the effects expected on the basis of additivity revealed that cell death induced by TMZ (25 µM) plus a toxic dose of MTD (20 µg/mL) is additive (Figure 8B and Table S1) supporting the data shown above (Figure 7). In conclusion, the data indicate that MTD has no impact on TMZ-induced cell death pathways.

2.7. Is TMZ-Induced Senescence Affected by MTD?

As outlined above, TMZ is a potent inducer of cellular senescence [8] and, thus, the possibility remained that MTD has an impact on this process. Therefore, we measured the level of TMZ-induced senescence in the absence or presence of MTD. As shown in Figure 9A, 8 days after addition of TMZ to the medium, about 80% of the population was tested positive for the senescence marker c12FDG, and MTD (5 and 20 µg/mL) neither enhanced nor reduced the senescence level. Obviously, MTD has no impact on TMZ-induced senescence pathways.

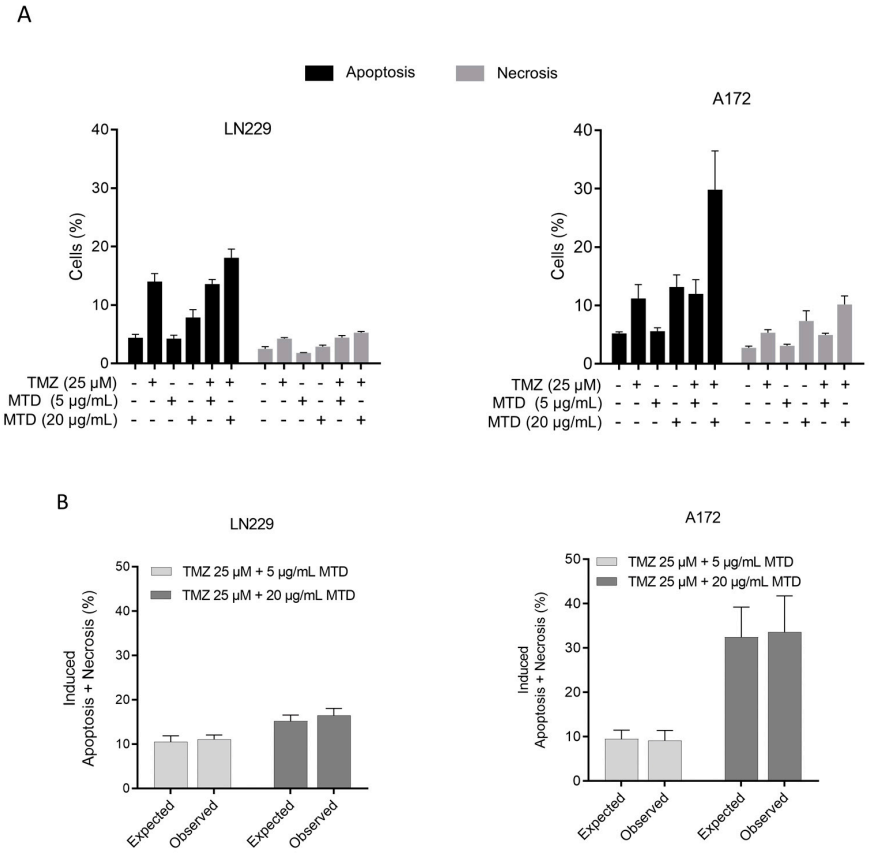

Figure 8. Effect of MTD on TMZ-induced apoptosis and necrosis, measured by AV/PI flow cytometry. (**A**) Percentage of apoptotic and necrotic cells in the population, determined 120 h after treatment. Data are the mean of three independent experiments. (**B**) TMZ-MTD induced cell death (apoptosis/necrosis). Observed levels after combined treatment and expected frequencies on the basis of additivity of single-drug treatment.

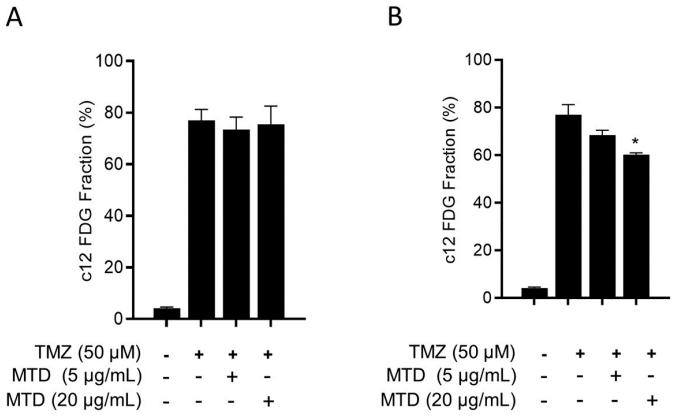

Figure 9. Effect of MTD on TMZ-induced senescence. (**A**) Induction of senescence by TMZ in LN229 cells and effect of MTD co-treatment on senescence induction. (**B**) Effect of MTD on the TMZ-induced senescent cell level. Data are the mean of three independent experiments +/-SEM. * $p \leq 0.05$.

2.8. Is MTD a Senolytic Drug?

Senescent cells can be killed by specific agents through a process called senolysis. To elucidate whether MTD acts as a senolytic drug, we treated the senescent population with MTD and measured the senescent fraction 48h later. As shown in Figure 9B, a subtoxic concentration of MTD had no significant effect on the senescent population while a toxic MTD concentration significantly reduced

the senescence level. This, however, was not specific for senescent cells since 20 µg/mL MTD was also toxic for non-senescent (exponentially growing) cells. Obviously, MTD is able to kill senescent and non-senescent cells (see also Figure S1); therefore, it cannot be considered as a senolytic drug, which acts specifically on senescent cells.

2.9. Is MTD a DNA Damaging Agent and Does It Impact TMZ-Induced DNA Damage?

TMZ is a genotoxic anticancer drug that methylates DNA bases in different positions. The N-methylation purines N7-methylguanine, N3-methyladenine, and N3-methylguanine are major alkylation products, and their formation can indirectly be monitored by the alkaline comet assay, which is a sensitive method for the detection of alkali labile and apurinic sites, as well as DNA single-strand breaks. As shown in Figure 10A,B, MTD was not genotoxic in LN229 cells. It also did not ameliorate the genotoxic effect of TMZ. There was even a reduction in tail intensity, which was, however, not statistically significant (Figure 10B). Therefore, MTD appears to have no significant impact on the DNA-damaging capacity of TMZ.

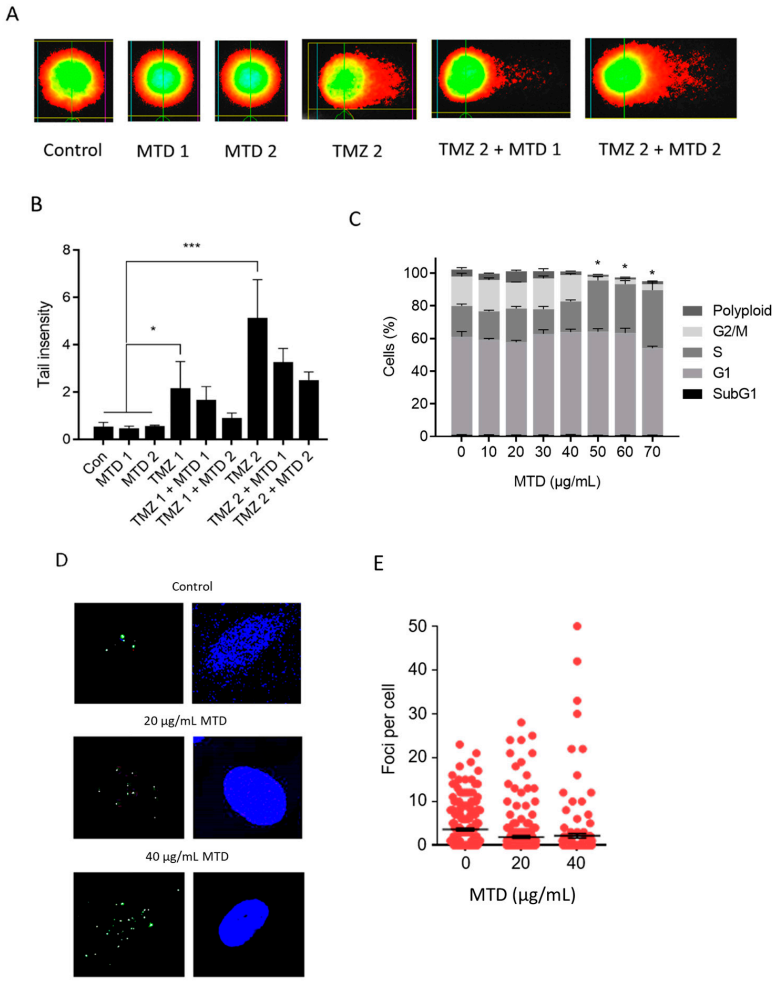

Figure 10. Effect of MTD on genotoxicity of TMZ and cell cycle distribution. (**A**) Comet assay, MTD alone (control) and in combination with TMZ, measured by the alkaline comet assay. Representative pictures are shown. (**B**) Quantification: TMZ 1, 100 µM; TMZ 2, 200 µM; MTD 1, 10 µg/mL, MTD 2, 30 µg/mL. Data represent the mean of three independent experiments ± SEM. * $p < 0.05$; *** $p < 0.001$. (**C**) Cell cycle distribution of LN229 cells treated with increasing concentrations of MTD. * indicates significant difference ($p > 0.05$) of S and G2 fraction from control. (**D**) Representative pictures of γH2AX foci and (**E**) foci levels in LN229 cells measured 24 h after addition of MTD to the medium. The differences in the mean foci number between control and MTD are statistically not significant.

The observed trend of lower tail intensity in the TMZ + MTD treatment schedule could be a result of inhibition of proliferation following MTD treatment since genotoxicity of TMZ is enhanced if cells replicate [12]. Indeed, high concentrations of MTD (>40 μg/mL) significantly enhanced the fraction of S-phase and reduced the fraction of G2-phase cells (Figure 10C). Obviously, at high MTD concentrations, cells do not enter G2 because they became arrested in the S-phase. Therefore, it is reasonable to conclude that cell cycle inhibition upon MTD treatment reduces the genotoxic and toxic effects of TMZ.

A sensitive indicator for DNA damage are γH2AX foci, whereby each focus represents either blocked and collapsed replication forks or free DSBs that trigger the DNA damage response (DDR) [13]. It has further been shown that γH2AX foci are tightly linked to cytotoxic DNA damage [14]. To elucidate whether MTD has the capacity to induce the DDR, we measured the γH2AX level following MTD exposure. There was no significant difference in the mean γH2AX foci level between control and MTD (Figure 10D,E). This supports the notion that MTD, even at cytotoxic concentration, is not genotoxic.

2.10. MTD and MGMT Promoter Methylation

Finally, we considered the possibility that MTD has an impact on MGMT promoter methylation, which is tightly linked to MGMT expression and alkylating drug resistance [15]. Therefore, we measured MGMT promoter methylation by MS-PCR, as described previously [16]. Cultivation of cells in medium containing MTD had no impact on the MGMT promoter methylation status. Thus, neither the unmethylated MGMT promoter of TMZ-resistant LN18 glioblastoma cells was converted into a methylated promoter, nor the methylated promoter of TMZ-sensitive LN229 cells was converted into an unmethylated one (Figure 11). Thus, it appears that MTD has no impact on MGMT promoter methylation.

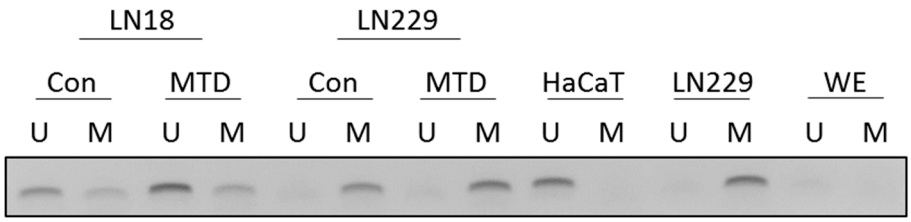

Figure 11. MGMT promoter methylation in glioma cells cultivated in the absence and presence of methadone. Con, control without MTD; MTD, 10 μg/mL for a period of 72 h. Separately harvested extracts of non-treated human HaCaT cells were used as a control for the unmethylated promoter, and LN229 for the methylated promoter. WE, without cell extract. U, unmethylated; M, methylated.

3. Discussion

MTD, an opioid and μ-receptor agonist commonly used for pain treatment of cancer patients, was shown to be cytotoxic first on human leukemia cell lines. Apoptosis was induced in doxorubicin resistant and sensitive lines, which was taken to indicate that the mechanism of cell death is different from the mechanisms leading to doxorubicin resistance [4]. Thereafter, it was reported that MTD-induced cytotoxicity is dependent on the opioid receptor level, regulating doxorubicin influx and efflux [17]. Extending this concept, authors stepped into the glioblastoma cell system and confirmed the findings obtained with leukemia cells, i.e., MTD is cytotoxic and sensitizes glioma cells to doxorubicin [5]. Other anti-cancer drugs were not tested. The findings led to the notion that MTD is useful for GBM therapy and opened a heated debate about the general use of MTD in cancer treatment. Doxorubicin is frequently used in veterinary medicine; thus, the question arose whether MTD is useful also for increasing the effectiveness of therapy of animals. In a recent study with μ-receptor expressing canine cell lines, authors did not observe a potentiation of doxorubicin-induced growth inhibition by MTD and, overall, were unable to confirm the data summarized above [18].

Although doxorubicin is not brain-permeable and not primarily used in glioma therapy (except the pegylated liposomal drug, Caelyx®®, used off-label), the findings were taken to indicate that MTD might be useful for monotherapy or as a supportive drug in glioma treatment. Therefore, a first trial was conducted with glioma patients (grade II-IV) that received standard therapy, including TMZ, together with MTD. Although no final conclusions can be drawn from this retrospective study of small group size [6], the regime based on MTD as therapeutic has been widely discussed and propagated in social media. It, thus, became obvious that there is a strong need for more background data on MTD and its impact on TMZ-induced responses.

Aimed at addressing these questions, we conducted a study using the glioblastoma cell lines LN229 and A172 (both are p53 functionally active and MGMT lacking) and a MGMT transfected derivative of LN229 (LN229-MGMT-c12) as well as human fibroblasts (the telomerase immortalized, non-tumorigenic line VH10T). The cells were previously well characterized by us, and others, as to TMZ-induced responses [8,11,19,20]. We observed that MTD is cytotoxic and induces apoptosis and, to a much lesser extent, necrosis in LN229 and A172 cells. A172 was more sensitive than LN229, whereas VH10T showed a response similar to LN229. All cell lines expressed the opioid receptor MOR−1. Interestingly, the expression level did not correlate with their sensitivity to MTD. Experiments with naloxone showed that competitive inhibition of the opioid receptors was without effect on MTD-induced cell death, indicating that opioid receptor-triggered pathways are not involved in MTD-induced cell death.

MTD induces apoptosis/necrosis early (i.e., 2–3 days) after treatment, while TMZ needs a much longer time for lesion processing and activating the cell death pathways (5 to 8 days in glioma cells, dependent on their cell cycle progression [21]). Therefore, we studied in two experimental settings whether MTD and TMZ are interacting. Firstly, we elucidated the effect of TMZ on MTD-induced apoptosis and found that MTD-induced death was not affected by TMZ. Secondly, we elucidated whether MTD has an impact on TMZ-induced apoptosis/necrosis and again, with low (non-toxic) dose of MTD we did not observe drug interaction. At higher (cytotoxic) MTD concentration, the killing effects of MTD and TMZ were additive. The data suggests that the cell death pathways triggered by MTD and TMZ are not converging and involve different mechanisms. We should note that at high MTD concentration (>40 μg/mL) the TMZ-induced decrease in viability (measured in the MTT assay) was even attenuated, presumably due to cell cycle inhibition following MTD, which counteracts TMZ-induced cell death responses [12].

We further show that MTD, even at cytotoxic concentration, was negative in the alkaline comet assay and in the γH2AX foci assay, which strongly indicates that MTD is not a genotoxic drug. This disproves the hypothesis that MTD-induced cytotoxicity is merely a result of oxidative stress generated in MTD exposed cells, which damages the nuclear DNA. We cannot exclude, however, that oxidative stress is provoked in the mitochondria, which causes cell death. Interestingly, we observed equal levels of MTD-induced apoptosis and necrosis in MGMT lacking and MGMT expressing LN229 cells, indicating that MTD induces death irrespective of the MGMT status and thus is able to kill cells that are highly resistant to TMZ and other O^6-alkylating anticancer drugs, such as nimustine, carmustine, lomustine and others [9]. Cell death induced by these drugs in highly sensitive MGMT lacking cells is a result of activation of complex signaling pathways triggered by the specific DNA lesion O^6-alkylguanine [10,20,22]. Thus, it can be concluded that the MTD-induced death pathway does not interfere with O^6-alkylguanine-triggered cell death pathways.

TMZ is not only an apoptosis-inducing agent, it also triggers with high efficiency cellular senescence in glioblastoma cells [8]. The pathways involved were previously described [11]. Having this in mind, we set out to determine whether MTD has an impact on TMZ-induced senescence, which is a late response following TMZ exposure. MTD itself did not induce senescence. We also did not observe an impact of MTD on the capacity of TMZ to induce senescence. This is in line with the notion that the signaling pathways triggered by MTD and TMZ are essentially different. It is important to note that MTD was able to kill LN229 cells arrested in a TMZ-induced senescent state. Agents

having this ability are considered senolytic drugs. However, to elicit this response, a concentration of MTD was required that was cytotoxic on proliferating cells and, thus, the effect was obviously not specific for senescent cells. Therefore, we do not consider MTD as a senolytic agent.

The MTD concentration resulting in reduction of viability and induction of apoptosis was in the range of 10–100 μg/mL (significant apoptosis was induced in the most sensitive line LN229 at a concentration >20 μg/mL). This is far above the serum concentration that can be achieved in patients. Thus, the clinical tolerable serum level in humans was reported to be between 0.3 and 1.3 μg/mL [23]. In most studies the plasma levels in maintenance patients were <1 μg/mL (for a compilation of published data see Table S2). Therefore, a cytotoxic MTD concentration sufficiently high enough to exert a therapeutic anticancer effect is unlikely to be achieved in a therapeutic setting. Conclusions in line with this were drawn from studies using a panel of glioblastoma cell lines expressing the μ-opioid receptor. The authors found no interaction of MTD with TMZ [24]. Similar observations were made in an independent study with glioblastoma cells and MTD administered together with TMZ or IR (4 Gy) [25]. It should be noted that in this study TMZ was used at high dose of 200 μM, which causes mainly cytotoxic N-alkylations in the DNA. In our cytotoxicity studies, we used TMZ at lower doses (25 and 50 μM). Although under these conditions apoptosis is triggered exclusively by O^6-methylguanine [26], we also observed that MTD and TMZ do not act synergistically, supporting the notion that MTD is not useful for enhancing the anticancer effect of TMZ.

It is important to note that the TMZ serum concentration in a therapeutic setting with a single dose of 150 mg/m^2 is in the range of 20–30 μM [27] and following oral 200 mg/m^2 TMZ, a plasma peak level of 72 μM and a cerebrospinal fluid level of 9.9 μM were determined [28]. This is close to the TMZ concentration that induces cell death in vitro (this study and ref. [21] where it is shown that apoptosis increases, without a threshold, linearly with dose of TMZ in LN229 cells). Moreover, TMZ in GBM therapy is administered repeatedly with daily doses of 50–130 mg/m^2 or even higher [29,30]. This causes accumulation of toxic O^6-methylguanine adducts in tumors not able to repair the lesion (MGMT promoter methylated) and, therefore, cytotoxic effects brought about by cumulative doses should be taken into account. In contrast to this, methadone as a non-genotoxic agent has likely a threshold for eliciting cytotoxicity (see dose-response curves). However, if methadone accumulates in the tumor, the critical target concentration might be higher than anticipated from the plasma level. Whether, under these conditions, toxic concentrations can be achieved without side effects on the normal tissue is, however, doubtful. It would be interesting to determine the tumor-MTD concentration and to elucidate whether locoregional administration of MTD elicits a tumor-specific effect.

The usefulness of MTD as an adjuvant in cancer therapy has been addressed recently in studies with malignant melanoma. Moreover, in this case, no interaction was found between MTD and TMZ (as well as cisplatin) and no benefit was observed following concomitant treatment in a single-case report [31]. Although these studies cannot exclude the possibility that there are subgroups of tumors that are highly sensitive to MTD and, therefore, respond at MTD concentrations that are achievable in patients, including addicted cases tolerating dose escalation, the data obtained so far are not encouraging, leading to the conclusion that MTD cannot be recommended as monotherapy or adjuvant radio-chemotherapy of gliomas.

4. Material and Methods

4.1. Cell Lines and Culture Conditions

The human glioblastoma cell lines LN-229 and A172 were purchased from American Type Culture Collection (ATCC). LN-229-MGMTc.12 was generated by stable transfection of LN-229 with a human MGMT cDNA expression vector and described previously [11,20]. VH10T were a kind gift of Prof. L. Mullenders, Leiden. Cells were cultured in DMEM with GlutaMAX (Gibco, Life Technologies Corporation, Paisley, UK) and 10% fetal calf serum. Cells were maintained at 37 °C in a humidified 6% CO_2 atmosphere. Cells were seeded 24 up to 48 h before treatment when they reached exponential

growth. For short term experiments (harvest 3 days after treatment), 2×10^5 cells were seeded per 5-cm or 6-well dish (in 5 or 4 mL medium, respectively), for long-term experiments (apoptosis and senescence following TMZ) 5×10^4 cells were seeded per dish. Under these conditions, cells were kept in exponential growth for the whole experimental period.

4.2. Drugs and Drug Treatment

D,L-methadone (MTD) and naloxone were purchased from Sigma-Aldrich (Taufkirchen, Germany). Temozolomide (TMZ) was obtained from Dr. Geoff Margison (University of Manchester, Manchester, UK). MTD and naloxone were dissolved in phosphate buffered saline (PBS; stock solution 5 mg/mL) and stored in batches at −20 °C. TMZ was dissolved in DMSO (150 mM) and stored in 50 µL batches at −80 °C until use. Immediately before treatment, it was diluted 1:10 in sterile distilled water and added to the cell culture medium at the desired final concentration. The amount of DMSO in the medium did not exceed 0.05% and was without any toxic effect (controls). Naloxone was added 30 min before MTD was added to the medium.

4.3. Western Blotting and MS-PCR

Protein extracts and immunoblotting occurred according to standard procedures as described previously [19]. Antibodies used were Anti-MOR1 D-12 (1:1000, Santa Cruz Biotechnology, Heidelberg, Germany) combined with goat anti-mouse IgG-HRP (1:5000, Santa Cruz Biotechnology) and HSP90 (Santa Cruz Biotechnology) as loading control. Immunoblots were developed with enhanced chemiluminescence (Amersham Biosciences, Freiburg, Germany).

For methylation-specific PCR (MS-PCR), 2×10^5 cells were seeded and treated 2 days later with MTD at a subtoxic concentration (10 µg/mL). Cells were harvested by trypsinization 72 h later and subjected to MS-PCR, which occurred essentially as described previously [32].

4.4. Viability Assay

The MTT assays was performed according to the manufacturer's instructions. MTT reagent (thiazolyl blue tetrazolium bromide) was obtained from BIOMOL (Hamburg, Germany).

4.5. Quantification of Apoptosis and Necrosis

The fraction of apoptotic and necrotic cells was determined using annexin V and propidium iodine (A/PI) staining of cells and measured by flow cytometry. For analysis, trypsinized cells including the supernatant were collected, transferred into 15 mL falcon tubes, washed with PBS and stored on ice. For labeling, cells were incubated for 15 min at RT in 50 µL 1× annexin binding buffer containing 2.5 µL annexin V/FITC (Miltenyi Biotec GmbH, Bergisch Gladbach, Germany) on ice. For PI staining, 10 µL PI from a 1 mg/mL stock solution (Sigma-Aldrich, Steinheim, Germany) and annexin binding buffer were added to each sample. Cells were incubated for additional 10 min. Cells were kept in the dark until measurement. Data acquisition was performed using the FACS Canto II flow cytometer (Becton Dickinson GmbH, Heidelberg, Germany) and the data was analyzed using the BD FACSDiva software. Apoptotic cells were defined as annexin V^+/PI^- cells, whereas necrotic cells were defined as annexin V^+/PI^+ cells (see Figure S2). Experiments were performed in duplicate and repeated at least twice.

4.6. Quantification of Cellular Senescence

Senescence was determined by the amount of SA-β-galactosidase within the cells. To inhibit endogenous β-galactosidase activity, cells were pre-incubated with 300 µM chloroquine for 30 min in the incubator after which C12FDG was added to each sample to a final concentration of 33 µM. Following a 90 min incubation period in the incubator, cells were washed once with cold PBS and collected by trypsinization. Cell pellets were washed once with cold PBS, then resuspended in an adjusted amount of cold PBS and stored on ice. Cell were kept in the dark from the addition of c12FDG

to the measurement. Data acquisition was performed using the FACS Canto II flow cytometer (Becton Dickinson GmbH, Heidelberg, Germany) and the data was analyzed using the Flowing Software 2 program (Perttu Terho, Turku Center for Biotechnology, University of Turku, Finland). Untreated, proliferating cells were measured, and the gate was set accordingly. Cells with a fluorescence higher than the control were defined as senescent.

4.7. Quantification of γH2AX Foci

The γH2AX foci assay we conducted essentially as described in detail before [21]. Evaluation of γH2AX stained nuclei of cells grown on coverslips occurred by laser scanning microscopy (LSM). At least 75 cells were assessed per experiment and experiments were performed twice.

4.8. Comet Assay

Cells were seeded in 6-well plates and treated 2 days later with the drugs. Moreover, 24 h thereafter, cells were harvested by trypsinization and embedded in low-melting point agarose. The alkaline comet assay was essentially performed as previously described [33]. The experiments were repeated twice.

4.9. Statistics

Data are presented as the mean of at least three independent experiments, ± SEM, and were treated statistically by the unpaired t-test and the two-way ANOVA test.

Supplementary Materials: Supplementary Materials can be found at http://www.mdpi.com/1422-0067/21/19/7006/s1.

Author Contributions: B.K. and B.H. designed the study and provided materials and reagents, B.K., L.B., and A.P.-S. performed the experiments; L.B. made drawings; B.K. wrote the manuscript, and B.K. and B.H. corrected and approved the submitted version. All authors have read and agreed to the published version of the manuscript.

Funding: The research of BK has been supported by Deutsche Forschungsgemeinschaft (DFG KA724).

Acknowledgments: We gratefully acknowledge technical assistance regarding the MS-PCR assay by Birgit Rasenberger.

Conflicts of Interest: The authors declare no conflict of interest. The funders had no role in the design of the study; in the collection, analyses, or interpretation of data; in the writing of the manuscript, or in the decision to publish the results. The opinions mentioned throughout the following article are personal views of the authors and do not reflect an official position of the Federal Institute for Drugs and Medical Devices or an EMA-committee or working party, respectively.

References

1. Stupp, R.; Mason, W.P.; Van Den Bent, M.J.; Weller, M.; Fisher, B.; Taphoorn, M.J.; Belanger, K.; Brandes, A.A.; Marosi, C.; Curschmann, J.; et al. Radiotherapy plus concomitant and adjuvant temozolomide for glioblastoma. *N. Engl. J. Med.* **2005**, *352*, 987–996. [CrossRef]
2. Hegi, M.E.; Diserens, A.C.; Gorlia, T.; Hamou, M.F.; De Tribolet, N.; Weller, M.; Kros, J.M.; Hainfellner, J.A.; Mason, W.; Bromberg, J.E.; et al. MGMT gene silencing and benefit from temozolomide in glioblastoma. *N. Engl. J. Med.* **2005**, *352*, 997–1003. [CrossRef]
3. Anton, K.; Baehring, J.M.; Mayer, T. Glioblastoma multiforme: Overview of current treatment and future perspectives. *Hematol. Oncol. Clin. N. Am.* **2012**, *26*, 825–853. [CrossRef]
4. Friesen, C.; Roscher, M.; Alt, A.; Miltner, E. Methadone, commonly used as maintenance medication for outpatient treatment of opioid dependence, kills leukemia cells and overcomes chemoresistance. *Cancer Res.* **2008**, *68*, 6059–6064. [CrossRef]
5. Friesen, C.; Hormann, I.; Roscher, M.; Fichtner, I.; Alt, A.; Hilger, R.; Debatin, K.-M.; Miltner, E. Opioid receptor activation triggering downregulation of cAMP improves effectiveness of anti-cancer drugs in treatment of glioblastoma. *Cell Cycle* **2014**, *13*, 1560–1570. [CrossRef]
6. Onken, J.; Friesen, C.; Vajkoczy, P.; Misch, M. Safety and Tolerance of D,L-Methadone in Combination with Chemotherapy in Patients with Glioma. *Anticancer Res.* **2017**, *37*, 1227–1235.

7. Kaina, B.; Christmann, M.; Naumann, S.; Roos, W.P. MGMT: Key node in the battle against genotoxicity, carcinogenicity and apoptosis induced by alkylating agents. *DNA Repair* **2007**, *6*, 1079–1099. [CrossRef]
8. Knizhnik, A.V.; Roos, W.P.; Nikolova, T.; Quiros, S.; Tomaszowski, K.H.; Christmann, M.; Kaina, B. Survival and death strategies in glioma cells: Autophagy, senescence and apoptosis triggered by a single type of temozolomide-induced DNA damage. *PLoS ONE* **2013**, *8*, e55665. [CrossRef]
9. Kaina, B.; Christmann, M. DNA repair in personalized brain cancer therapy with temozolomide and nitrosoureas. *DNA Repair (Amst.)* **2019**, *78*, 128–141. [CrossRef]
10. Kaina, B. Temozolomide in Glioblastoma Therapy: Role of Apoptosis, Senescence and Autophagy. Comment on Strobel et al., Temozolomide and Other Alkylating Agents in Glioblastoma Therapy. *Biomedicines* **2019**, *7*, 69. [CrossRef]
11. Aasland, D.; Götzinger, L.; Hauck, L.; Berte, N.; Meyer, J.; Effenberger, M.; Schneider, S.; Reuber, E.E.; Roos, W.P.; Kaina, B.; et al. Temozolomide Induces Senescence and Repression of DNA Repair Pathways in Glioblastoma Cells via Activation of ATR-CHK1, p21, and NF-kappaB. *Cancer Res.* **2019**, *79*, 99–113. [CrossRef]
12. Roos, W.; Baumgartner, M.; Kaina, B. Apoptosis triggered by DNA damage O6-methylguanine in human lymphocytes requires DNA replication and is mediated by p53 and Fas/CD95/Apo-1. *Oncogene* **2004**, *23*, 359–367. [CrossRef]
13. Lukas, J.; Lukas, C.; Bartek, J. More than just a focus: The chromatin response to DNA damage and its role in genome integrity maintenance. *Nat. Cell Biol.* **2011**, *13*, 1161–1169. [CrossRef] [PubMed]
14. Nikolova, T.; Dvorak, M.; Jung, F.; Adam, I.; Krämer, E.; Gerhold-Ay, A.; Kaina, B. The gammaH2AX assay for genotoxic and nongenotoxic agents: Comparison of H2AX phosphorylation with cell death response. *Toxicol. Sci.* **2014**, *140*, 103–117. [CrossRef]
15. Christmann, M.; Kaina, B. Epigenetic regulation of DNA repair genes and implications for tumor therapy. *Mutat. Res.* **2019**, *780*, 15–28. [CrossRef] [PubMed]
16. Christmann, M.; Nagel, G.; Horn, S.; Krahn, U.; Wiewrodt, D.; Sommer, C.; Kaina, B. MGMT activity, promoter methylation and immunohistochemistry of pretreatment and recurrent malignant gliomas: A comparative study on astrocytoma and glioblastoma. *Int. J. Cancer* **2010**, *127*, 2106–2118. [CrossRef]
17. Friesen, C.; Roscher, M.; Hormann, I.; Fichtner, I.; Alt, A.; Hilger, R.A.; Miltner, E. Cell death sensitization of leukemia cells by opioid receptor activation. *Oncotarget* **2013**, *4*, 677–690. [CrossRef] [PubMed]
18. Cueni, C.; Nytko, K.J.; Thumser-Henner, P.; Weyland, M.S.; Rohrer Bley, C. Methadone does not potentiate the effect of doxorubicin in canine tumour cell lines. *Vet. Med. Sci.* **2020**, *6*, 283–289. [CrossRef] [PubMed]
19. Hermisson, M.; Klumpp, A.; Wick, W.; Wischhusen, J.; Nagel, G.; Roos, W.; Weller, M. MGMT and p53 status predict temozolomide sensitivity in human malignant glioma cells. *J. Neurochem.* **2006**, *96*, 766–776. [CrossRef] [PubMed]
20. He, Y.; Roos, W.P.; Wu, Q.; Hofmann, T.G.; Kaina, B. The SIAH1-HIPK2-p53ser46 Damage Response Pathway is Involved in Temozolomide-Induced Glioblastoma Cell Death. *Mol. Cancer Res.* **2019**, *17*, 1129–1141. [CrossRef] [PubMed]
21. He, Y.; Kaina, B. Are There Thresholds in Glioblastoma Cell Death Responses Triggered by Temozolomide? *Int. J. Mol. Sci.* **2019**, *20*, 1562. [CrossRef] [PubMed]
22. Roos, W.P.; Kaina, B. DNA damage-induced cell death: From specific DNA lesions to the DNA damage response and apoptosis. *Cancer Lett.* **2013**, *332*, 237–248. [CrossRef] [PubMed]
23. Inturrisi, C.E.; Colburn, W.A.; Kaiko, R.F.; Houde, R.W.; Foley, K.M. Pharmacokinetics and pharmacodynamics of methadone in patients with chronic pain. *Clin. Pharmacol. Ther.* **1987**, *41*, 392–401. [CrossRef] [PubMed]
24. Brawanski, K.; Brockhoff, G.; Hau, P.; Vollmann-Zwerenz, A.; Freyschlag, C.; Lohmeier, A.; Riemenschneider, M.J.; Thomé, C.; Brawanski, A.; Proescholdt, M.A. Efficacy of D,L-methadone in the treatment of glioblastoma in vitro. *CNS Oncol.* **2018**, *7*, CNS18. [CrossRef]
25. Oppermann, H.; Matusova, M.; Glasow, A.; Dietterle, J.; Baran-Schmidt, R.; Neumann, K.; Meixensberger, J.; Gaunitz, F. D,L-Methadone does not improve radio- and chemotherapy in glioblastoma in vitro. *Cancer Chemother. Pharmacol.* **2019**, *83*, 1017–1024. [CrossRef]
26. Roos, W.P.; Batista LF, Z.; Naumann, S.C.; Wick, W.; Weller, M.; Menck CF, M.; Kaina, B. Apoptosis in malignant glioma cells triggered by the temozolomide-induced DNA lesion O6-methylguanine. *Oncogene* **2007**, *26*, 186–197. [CrossRef]

27. Marzolini, C.; Decosterd, L.A.; Shen, F.; Gander, M.; Leyvraz, S.; Bauer, J.; Buclin, T.; Biollaz, J.; Lejeune, F. Pharmacokinetics of temozolomide in association with fotemustine in malignant melanoma and malignant glioma patients: Comparison of oral, intravenous, and hepatic intra-arterial administration. *Cancer Chemother. Pharmacol.* **1998**, *42*, 433–440. [CrossRef]
28. Portnow, J.; Badie, B.; Chen, M.; Liu, A.; Blanchard, S.; Synold, T.W. The neuropharmacokinetics of temozolomide in patients with resectable brain tumors: Potential implications for the current approach to chemoradiation. *Clin. Cancer Res.* **2009**, *15*, 7092–7098. [CrossRef]
29. Wick, W.; Steinbach, J.P.; Küker, W.M.; Dichgans, J.; Bamberg, M.; Weller, M. One week on/one week off: A novel active regimen of temozolomide for recurrent glioblastoma. *Neurology* **2004**, *62*, 2113–2115. [CrossRef]
30. Strik, H.M.; Marosi, C.; Kaina, B.; Neyns, B. Temozolomide dosing regimens for glioma patients. *Curr. Neurol. Neurosci. Rep.* **2012**, *12*, 286–293. [CrossRef]
31. Brüggen, M.C.; Mangana, J.; Irmisch, A.; French, L.E.; Levesque, M.P.; Cheng, P.F.; Dummer, R. Methadone-Not a magic bullet in melanoma therapy. *Exp. Dermatol.* **2018**, *27*, 694–696. [CrossRef] [PubMed]
32. Switzeny, O.J.; Christmann, M.; Renovanz, M.; Giese, A.; Sommer, C.; Kaina, B. MGMT promoter methylation determined by HRM in comparison to MSP and pyrosequencing for predicting high-grade glioma response. *Clin. Epigenetics* **2016**, *8*, 49. [CrossRef] [PubMed]
33. Nikolova, T.; Marini, F.; Kaina, B. Genotoxicity testing: Comparison of the gammaH2AX focus assay with the alkaline and neutral comet assays. *Mutat. Res.* **2017**, *822*, 10–18. [CrossRef] [PubMed]

Cytotoxic and senolytic effects of methadone in combination with temozolomide in glioblastoma cells

Bernd Kaina, Lea Beltzig, Andrea Piee-Staffa, Bodo Haas

Supplementary material

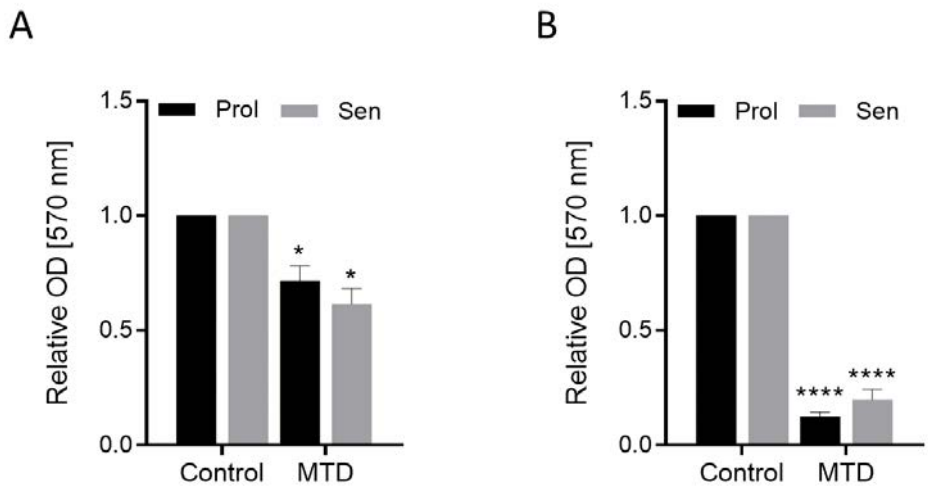

Figure S1
Viability of LN229 (A) and A172 (B) cells that were in the proliferating (Prol) or senescent (Sen) state when treated with methadone (40 µg/mL). Cellular senescence was achieved by TMZ treatment (50 µM, 8 days post-incubation at 37°C). Proliferating and senescent cells were reseeded for MTT assay. Two days after addition of MTD to the medium (96-well dishes) cells were processed for MTT staining according to the manufacturer‘s protocol and measured at OD 570. Data are set in relation to the corresponding non-treated controls. Each measure points represents the mean of quadruplicates. * $p<0.05$; **** $p<0.001$

Supplementary material

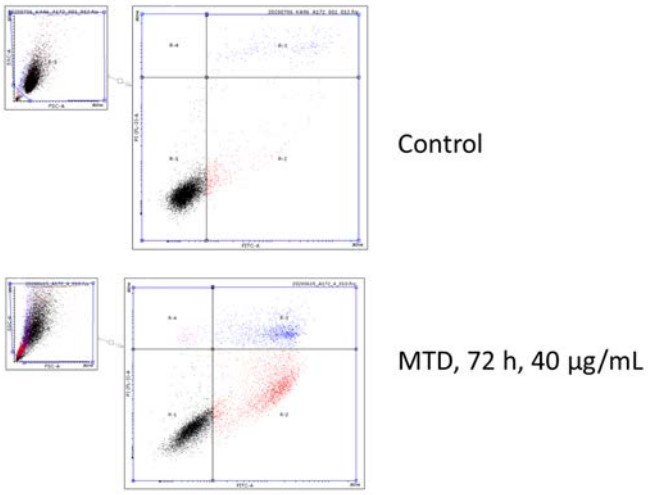

Figure S2
Flow cytometry of A172 cells not treated (control) and treated with methadone.
Ordinate: propidium iodide staining intensity, abscissa: annexin V staining intensity;
Black, life cells; red, apoptotic population; blue, necrotic population.

Supplementary material

A

	Apotosis						Necrosis					
Control	5.1	2.98	5.43	6.06	4.34	2.58	3.7	2.34	3.54	2.35	1.56	1.54
TMZ 25 µM	11.63	10.08	17.11	18.94	13.41	12.89	4.0	4.34	5.09	4.1	4.36	3.63
5 µg/mL MTD	4.67	2.83	6.04	5.37	4.23	2.43	1.96	1.5	2.05	1.84	1.84	1.68
20 µg/mL MTD	9.7	13.48	6.94	7.37	4.74	4.99	2.53	3.08	3.95	3.02	2.49	2.36
TMZ 25 µM + 5 µg/mL MTD	12.29	12.06	12.55	17.22	12.99	14.31	4.85	4.86	5.28	4.83	3.11	3.75
TMZ 25 µM + 20 µg/mL MTD	13.7	20.61	18.05	23.48	18.12	14.64	5.71	5.33	5.63	5.67	4.89	4.48

	Expected induced cell death						Observed induced cell death					
TMZ 25 µM + 5 µg/mL MTD	4.66	8.11	12.35	13.43	12.04	12.39	8.34	11.6	8.86	13.64	10.2	13.94
TMZ 25 µM + 20 µg/mL MTD	10.26	20.34	15.15	16.61	13.2	15.63	10.61	20.62	14.71	20.74	17.11	15.0

B

	Apotosis						Necrosis					
Control	6.01	4.97	6.04	4.96	4.88	4.58	2.09	2.27	3.45	3.59	3.06	2.1
TMZ 25 µM	7.66	8.13	22.6	12.07	6.77	9.86	5.14	4.62	5.53	7.6	5.37	3.81
5 µg/mL MTD	7.19	5.74	6.21	5.66	5.9	2.93	2.48	2.38	3.77	3.76	3.47	2.71
20 µg/mL MTD	10.09	9.21	16.58	16.87	40.83	38.71	3.53	3.77	5.46	5.95	13.53	11.81
TMZ 25 µM + 5 µg/mL MTD	9.08	9.03	22.69	15.62	7.43	7.97	4.42	4.95	4.6	6.24	5.25	4.37
TMZ 25 µM + 20 µg/mL MTD	16.09	15.94	27.5	19.43	46.87	53.1	7.6	7.45	8.3	8.25	15.05	14.43

	Expected induced cell death						Observed induced cell death					
TMZ 25 µM + 5 µg/mL MTD	6.46	7.37	19.19	10.21	7.09	6.35	6.46	6.39	19.33	11.81	5.2	5.58
TMZ 25 µM + 20 µg/mL MTD	45.14	12.61	18.97	20.85	45.24	51.53	58.6	16.48	26.64	19.32	46.65	60.51

Table S1
Apoptosis and necrosis frequencies in cells treated with TMZ and MTD. Expected induced cell death: Sum of induced apoptosis and necrosis measured after singe agent treatment. Observed induced cell death: Induced apoptosis and necrosis measured in the population concomitantly treated with TMZ and MTD. Induced frequencies: controls (untreated population) were subtracted from the treated population.
A, LN229; B, A172.

Supplementary material

Reference	Dose	Route	Plasma level	Patients
Dole et al, 1973	100 mg/day	oral	0.58 - 0.91 µg/mL	Maintenance patients
Foster et al, 2000	7.5 – 130 mg/day	oral	L-methadone: 0.251 µg/mL D-methadone: 0.303 µg/mL	Maintenance patients
Inturrisi et al, 1987	10 – 30 mg	IV	0.3 – 1.3 µg/mL	Chronic use, pain patients
Lehotay et al, 2005	20 – 205 mg/day	oral	L-methadone: 0.06 – 2.84 µM (0.018 - 0.85 µg/mL) D-methadone: 0.12 – 2.04 µM (0.036 – 0.61 µg/mL)	Maintenance patients
Linares et al, 2015	10 mg single dose	oral	up to ~0.04 µg/mL	Methadone treatment naïve patients
Mohamad et al, 2013	30 – 160 mg/day	oral	0.03 – 0.7 µg/mL	Maintenance patients
Wolff et al, 1993	10 – 60 mg/day	oral	0.13 – 0.68 nM (0.04 - 0.2 ng/mL)	Opioid addicts

Dole VP, Kreek MJ: Methadone plasma level: sustained by a reservoir of drug in tissue. *Proc Natl Acad Sci U S A* 1973, 70(1):10.

Foster DJ, Somogyi AA, Dyer KR, White JM, Bochner F. Steady-state pharmacokinetics of (R)- and (S)-methadone in methadone maintenance patients. Br. J. Clin. Pharmacol. 50(5), 427–440 (2000).

Inturrisi, C.E., et al., Pharmacokinetics and pharmacodynamics of methadone in patients with chronic pain. Clin Pharmacol Ther, 1987. 41(4): p. 392-401.

Lehotay DC, George S, Etter ML, Graybiel K, Eichhorst JC, Fern B, Wildenboer W, Selby P, Kapur B. Free and bound enantiomers of methadone and its metabolite, EDDP in methadone maintenance treatment: relationship to dosage?, 2005, Clin Biochem 38:1088–1094.

Linares OA, Fudin J, Daly A, Schiesser WE, Boston RC: Methadone Recycling Sustains Drug Reservoir in Tissue. *J Pain Palliat Care Pharmacother* 2015, 29(3):261-271.

Mohamad N, Salehuddin RM, Ghazali B et al. Plasma methadone level monitoring in methadone maintenance therapy: a personalized methadone therapy. In: New Insights into Toxicity and Drug Testing. Gowder S (Ed.) InTech, Rijeka, Croatia (2013).

Wolff K, Hay AW, Raistrick D, Calvert R: Steady-state pharmacokinetics of methadone in opioid addicts. *Eur J Clin Pharmacol* 1993, 44(2):189-194

Table S2

3.4 **Haas B**, Ciftcioglu J, Jermar S, Weickhardt S, Eckstein N, Kaina B. Methadone-mediated sensitization of glioblastoma cells is drug and cell line dependent. J Cancer Res Clin Oncol. 2021;147(3):779-792.

Zielsetzung der Arbeit: Die in der obigen Arbeit gewonnen Erkenntnisse zur Wirkung von Methadon in Kombination mit TMZ sollten an einer erweiterten Reihe von humanen Glioblastom-Zelllinien und primären Zellen vertieft und quantifiziert werden. Des Weitern sollte der Einfluss des μ-Opioidrezeptors und eine mögliche Wirkung in Kombination mit Doxorubicin untersucht werden, da es hierzu widersprüchliche Angaben in der Literatur gab (Cueni et al., 2020; Friesen et al., 2014).

Methoden und Ergebnisse: Immunfluoreszenz- und Immunoblotting-Experimente belegten eine hohe Expression des μ-Opioidrezeptors in allen vier getesteten humanen Glioblastom-Zellen. In MTT-Versuchen war Methadon alleine in hohen mikromolaren Konzentrationen (IC_{50}: 60–130 μM) zytotoxisch und induzierte Apoptose und Nekrose in Annexin-V-FACS Assays. Im Gegensatz dazu zeigten zwei andere μ-Opioidrezeptor-Agonisten Morphin und Oxycodon in diesem Konzentrationsbereich keine Zytotoxizität. Der μ-Opioidrezeptor-Antagonist Naloxon konnte die Methadon-Effekte nicht aufheben. In MTT-Versuchen verstärkte Methadon die Doxorubicin-induzierte Zytotoxizität nur in einer Zelllinie. In primären Zellen wurde dies nur in einem bestimmten Methadon-Konzentrationsbereich beobachtet. Methadon hatte keine sensitivierenden Effekte auf eine Behandlung mit TMZ in den verwendeten Zellen und verringertet sogar die Empfindlichkeit gegenüber TMZ in zwei Zelllinien.

Schlussfolgerung: Die zytotoxischen Effekte bei hohen Konzentrationen von Methadon, die in der vorangegangenen Arbeit beobachtet wurden, wurden an weiteren Zelllinien und primären Zellen bestätigt. Da die potenten μ-Opioidrezeptor-Agonisten Morphin und Oxycodon nicht zytotoxisch waren und die Methadon-Effekte auch nicht durch Naloxon aufgehoben wurde, ist davon auszugehen, dass Methadon über andere molekulare Zielstrukturen zytotoxisch wirkt. Sensitivierende Effekte wurden nur in Kombination mit Doxorubicin nicht aber mit TMZ beobachtet. Die Doxorubicin-Effekte waren zudem abhängig von der Zelllinie und der angewandten Wirkstoffkonzentration. Wie schon die Ergebnisse der vorangegangenen Arbeit zeigten, kann die Verwendung von Methadon in Kombination mit TMZ zur Behandlung des Glioblastoms basierend auf unseren Daten nicht empfohlen werden.

Journal of Cancer Research and Clinical Oncology (2021) 147:779–792
https://doi.org/10.1007/s00432-020-03485-3

ORIGINAL ARTICLE – CANCER RESEARCH

Methadone-mediated sensitization of glioblastoma cells is drug and cell line dependent

Bodo Haas[1] · Janine Ciftcioglu[1,2] · Sanja Jermar[1,2] · Sandra Weickhardt[1] · Niels Eckstein[3] · Bernd Kaina[4]

Received: 17 September 2020 / Accepted: 24 November 2020 / Published online: 14 December 2020

Abstract

Purpose D,L-methadone (MET), an analgesic drug used for pain treatment and opiate addiction, has achieved attention from oncologists and social media as possible chemoensitizing agent in cancer therapy, notably brain cancer (glioblastoma multiforme, GBM). MET has been reported to enhance doxorubicin-induced cytotoxicity in GBM cells via activation of the μ-opioid receptor (MOR). Here, we extended this work and quantified the toxic effect of MET in comparison to other opioids alone and in combination with doxorubicin and the clinically more relevant alkylating drug temozolomide (TMZ), using a set of GBM cell lines and primary GBM cells.

Methods MOR expression in GBM cells was investigated by immunofluorescence and immunoblotting. Resistance to drugs alone and in combination with anticancer drugs was assessed by MTT assays. Concentration effect curves were fitted by nonlinear regression analysis and IC_{50} values were calculated. Apoptosis and necrosis rates were determined by annexin V/propidium iodide (PI)-flow cytometry.

Results MET alone was cytotoxic in all GBM cell lines and primary GBM cells at high micromolar concentrations (IC_{50} ~ 60–130 μM), observed both in the metabolic MTT assay and by quantifying apoptosis and necrosis, while morphine and oxycodone were not cytotoxic in this concentration range. Naloxone was not able to block MET-induced cytotoxicity, indicating that cell death-inducing effects of MET are not MOR-dependent. We recorded doxorubicin and TMZ concentration- response curves in combination with fixed MET concentrations. MET enhanced doxorubicin-induced cytotoxicity in only one cell line, and in primary cells it was observed only in a particular MET concentration range. In all assays, MET was not effective in sensitizing cells to TMZ. In two cell lines, MET even decreased the cell's sensitivity to TMZ.

Conclusion MET was found to be cytotoxic in GBM cells in vitro only at high, clinically not relevant concentrations, where it was effective in inducing apoptosis and necrosis. Sensitizing effects were only observed in combination with doxorubicin, but not with TMZ, and are dependent on cell line and the applied drug concentration. Therefore, our findings do not support the use of MET in the treatment of GBM in combination with TMZ, as no sensitizing effect of MET was observed.

Keywords Glioblastoma · Methadone · Temozolomide · Doxorubicin · Apoptosis · Chemosensitizer

Abbreviations

DOXO	Doxorubicin
GBM	Glioblastoma multiforme
Gi	Inhibitory G-protein
MET	D,L-methadone
MOR	μ-Opioid receptor
MTT	3-(4,5-dimethylthiazol-2-yl)-2,5-diphenyltetrazolium bromide
NAL	Naloxone

Supplementary Information The online version contains supplementary material available at https://doi.org/10.1007/s00432-020-03485-3.

✉ Bodo Haas
bodo.haas@bfarm.de

[1] Federal Institute for Drugs and Medical Devices, Kurt-Georg-Kiesinger-Allee 3, 53175 Bonn, Germany

[2] Faculty of Applied Natural Sciences, Cologne University of Applied Sciences, Kaiser-Wilhelm-Allee, 51368 Leverkusen, Germany

[3] Applied Pharmacy, University of Applied Sciences Kaiserslautern, Campus Pirmasens, Carl-Schurz-Str. 10-16, 66953 Pirmasens, Germany

[4] Institute of Toxicology, University Medical Center, Obere Zahlbacher Strasse 67, 55131 Mainz, Germany

OXY	Oxycodone
P-gp	P-Glycoprotein
PKA	cAMP-dependent protein kinase
PI	propidium idodide
TMZ	Temozolomide

Background

Grade IV glioma (glioblastoma multiforme, GBM) is the most aggressive form of brain cancer with the highest incidence among adults (Louis et al. 2016; Siegel et al. 2020). Median survival is 14.6 months under therapy, the 5-year survival rate is only less than 6% (Ostrom et al. 2016), indicating that there is high need for new therapeutic options. Therapeutic standard of care in GBM treatment is radiotherapy with concomitant temozolomide (TMZ) treatment (Stupp et al. 2005, 2009). Previous studies indicate that D,L-methadone (MET), an analgesic drug used for pain treatment and opiate addiction (Krantz and Mehler 2004; Parsons et al. 2010), increases apoptosis of leukemia cells and the cytotoxic effects of the topoisomerase II-inhibitor doxorubicin (Friesen et al. 2008, 2013; Singh et al. 2011). In a follow-up study, the same group showed that the opioid has also the potential to enhance apoptosis induced by doxorubicin in GBM cells (Friesen et al. 2014). The proposed mechanism of action involves activation of the μ-opioid receptor (MOR) and subsequent suppression of cAMP/protein kinase A (PKA) signaling via inhibitory G-proteins (Gi), which finally activates caspases and induces apoptosis. However, cAMP displays pro- and anti-apoptotic effects depending on cell type (Insel et al. 2012), raising the question if all GBM cells respond equally to MET treatment. In addition, it was shown that MET increases intracellular doxorubicin levels probably by inhibiting P-glycoproteins (P-gp) in GBM cells (Friesen et al. 2014). On the other hand, data published by others indicate no sensitizing effect of MET on various doxorubicin-treated canine tumor cells (Cueni et al. 2020).

It is important to note that the first-line therapy in GBM treatment is TMZ in combination with radiotherapy, while doxorubicin in first place has no indication for GBM because of its poor blood–brain barrier penetration and neurologic side effects (Merker et al. 1978; Neuwelt et al. 1981). A liposomal formulation of doxorubicin (Caelyx®) is sometimes used off-label with marginal benefit (Fabel et al. 2001; Fiorillo et al. 2004). Despite the lack of preclinical and clinical data on any beneficial effects of MET on TMZ therapy, it has been promoted as promising therapeutic option for GBM treatment.

Considering the importance of TMZ in GBM therapy, we aimed at investigating, first, the cytotoxic effect of MET in a variety of GBM cell lines differing in their p53 status and primary GBM cells and, secondly, to assess the contribution of MET to doxorubicin and TMZ-induced cytotoxicity in these cells. We recorded concentration–response curves in 3-(4,5-dimethylthiazol-2-yl)-2,5-diphenyltetrazolium bromide (MTT) assays of MET alone and doxorubicin or TMZ in combination with MET to quantify effects and determine IC_{50} values. Furthermore, we compared MET with morphine and oxycodone, other opioids used in oncology, and assessed the effect of the MOR inhibitor naloxone to determine if the opioid-induced cytotoxicity is mediated via MOR. Although MET was cytotoxic at high, clinically not relevant concentrations in all GBM cells, we only observed a weak MET-induced sensitization to doxorubicin in one established cell line and in primary cells, while no effect of MET was observed on TMZ-induced cell death.

Methods

Materials

All compounds were purchased from Sigma-Aldrich (St. Louis, MO, USA). Temozolomide (Temodal®) was dissolved in dimethyl sulfoxide (DMSO), doxorubicin hydrochloride, D,L-methadone hydrochloride, morphine sulfate salt pentahydrate, oxycodone, naloxone hydrochloride dehydrate were dissolved in sterile water.

Cell culture

U87-MG, U251-MG, and U373-MG (Uppsala) GBM cell lines were obtained by Sigma-Aldrich (St. Louis, MO, USA) (HPA Culture Collections). The A172 GBM cell line was obtained by American Type Culture Collection (ATCC, Manassas, VA, USA). Cell lines were not used beyond passage 20. U251 Cells were cultivated in Roswell Park Memorial Institute (RPMI) 1640 medium (Biochrom, Berlin, Germany) containing 10% fetal calf serum (FCS; Biochrom, Berlin, Germany), 100 IU/ml penicillin, and 100 µg/ml streptomycin (Biowest, Nuaillé, France). All other cells and cell lines were cultivated in Dulbecco's Modified Eagle Medium (DMEM) low glucose (Biowest, Nuaillé, France) containing 10% FCS (Biochrom, Berlin, Germany), 100 IU/ml penicillin, and 100 µg/ml streptomycin (Biowest, Nuaillé, France). Primary GBM cells derived from a primary GBM tumor biopsy were obtained from the University Hospital Cologne, genetically characterized and cultured as previously described (Haas et al. 2018).

Western blot analysis

In order to prepare whole cell lysates, cells were washed with ice-cold phosphate-buffered saline (PBS; Biowest, Nuaillé, France) and lysed with ice-cold Denaturing Cell

Extraction Buffer (FNN00091, Thermo Fisher Scientific, Waltham, MA, USA), incubated on ice for 30 min, and centrifuged for 15 min at 4 °C. The supernatant was used for protein content determination and subsequent immunoblotting. For immunoblotting standard procedures using the following antibodies were used as previously described (Haas et al. 2009). Anti-MOR-1 (D-12; 1:1000, Santa Cruz Biotechnology, TX, USA) combined with goat antimouse IgG-HRP (1:5000, Santa Cruz Biotechnology, TX, USA) and β-Actin-HRP (C-4; Santa Cruz Biotechnology, TX, USA). Immunoblots were developed with the enhanced chemoluminescence system (Amersham Biosciences, Little Chalfont, United Kingdom).

MTT assay

For MTT assays, we followed a published protocol (Eckstein et al. 2009). Briefly, 5000 (A172, U251, U87, U373) or 15,000 (primary) cells were plated on 96 wells and grown at 37 °C and 5% CO_2 overnight. Cell survival after exposure to either opioids alone or doxorubicin/TMZ in the presence of MET as indicated was determined by MTT assays after 72 h. In combination experiments MET or naloxone were added to culture medium 1 h prior to addition of compounds for 72 h. Controls were treated with vehicle (DMSO or water). Final DMSO concentrations in media did not exceed 1%.

Annexin V/propidium iodide (PI) apoptosis assay

For apoptosis measurements the BD Pharmingen™ FITC Annexin V Apoptosis Detection Kit (BD Biosciences, Franklin Lakes, NJ, USA) was used according to the manufacturer's protocol. Briefly, 2.5×10^5 cells were seeded into 6-well plates and incubated at 37 °C and 5% CO_2 overnight. After compound treatment for 72 h, cells were trypsinized and centrifuged for 4 min at $1500 \times g$. Supernatant was removed, and cells were resuspended in 500 µL binding buffer. 5 µL PI and 5 µL Annexin V-FITC were mixed with 100 µL of cells in binding buffer. After 15 min of incubation on ice, samples were analyzed by flow cytometry (FACSCaliburTM, BD Bioscience, Franklin Lakes, NJ, USA).

Fluorescence microscopy

75,000 cells/mL were seeded on cover glasses and incubated at 37° C and 5% CO_2 for 48 h before staining. Thereafter, cells were washed twice for 1 min with PBS and fixed with 4% paraformaldehyde/PBS for 10 min. Fixed cells were washed for 3 times with PBS and blocked in 2% bovine serum albumin (BSA; Sigma-Aldrich, St. Louis, MO, USA) including 0.2% Triton X-100 for 30 min. Thereafter, cells were incubated with MOR-1-antibody (D12, Santa Cruz Biotechnology, TX, USA) in 2% BSA (1:50) at 4° C overnight. The next day cells were washed incubated with antimouse IgG (H + L) DyLight™ 680 Conjugate (Cell Signalling Technology, Danvers, MA, USA) in 2% BSA (1:500) for 1 h. Finally, stained cells were washed for 3 times with PBS and covered with a coverslip using 1 drop of mounting medium. Cells stained with secondary antibody only were used as negative control. MOR expression was visualized using a Zeiss LSM 780 microscope (Carl Zeiss AG, Oberkochen, Germany) and 40 × magnification.

Data analysis and statistical methods

Concentration effect curves were fitted to data points by nonlinear regression analysis using the four-parameter logistic equation (GraphPad™ Prism). Top of each curve was defined as 100% and bottom as 0%. Statistical differences between two groups were determined by paired 2-tailed Student's *t* test. Comparisons among several groups were performed by ANOVA followed by Tukey post-hoc test. The data are presented as mean ± SEM or ± SD as indicated.

Results

It has previously been shown that MOR is expressed in human GBM cell lines and primary cells (Brawanski et al. 2018; Friesen et al. 2014; Oppermann et al. 2019; Vatter et al. 2020). Here, we demonstrate the expression of MOR in commonly used GBM cell lines (U87, U251, U373) and primary GBM cells isolated from a patient biopsy by Western blotting (Fig. 1a) and immunocytochemistry (Fig. 1b), confirming and extending the finding that MOR is expressed in a wide range of GBM cells to a similar extent.

We next asked whether MET is cytotoxic in these MOR-expressing cells, including the A172 cell line in which beneficial effects of MET on doxorubicin-induced cytotoxicity were reported (Friesen et al. 2014). In MTT viability assays, we obtained very similar IC_{50} values for MET in all GBM cell lines, which were in the range of 62–130 µM, measured 72 h after the onset of treatment. MET displayed a steep concentration response in all cells (Hill slopes ranging from − 3.3 to − 4.4). The lowest IC_{50} of 62 µM was obtained for A172 cells (Fig. 2a). Despite differences in p53 status (Table S1), all cell lines were uniformly responding to MET. Annexin V/propidium iodide (AV/PI) flow cytometry analysis of cell lines treated with the previously determined IC_{50} MET concentrations revealed that approximately 50% of cell deaths each account for apoptosis and necrosis (Fig. 2b).

In order to test if MET-induced cytotoxicity is mediated via MOR, we co-treated A172, U373 and primary cells with the MOR antagonist naloxone and MET. Naloxone treatment alone did not affect cell viability and, most importantly, it was not capable of abolishing MET-induced cytotoxicity

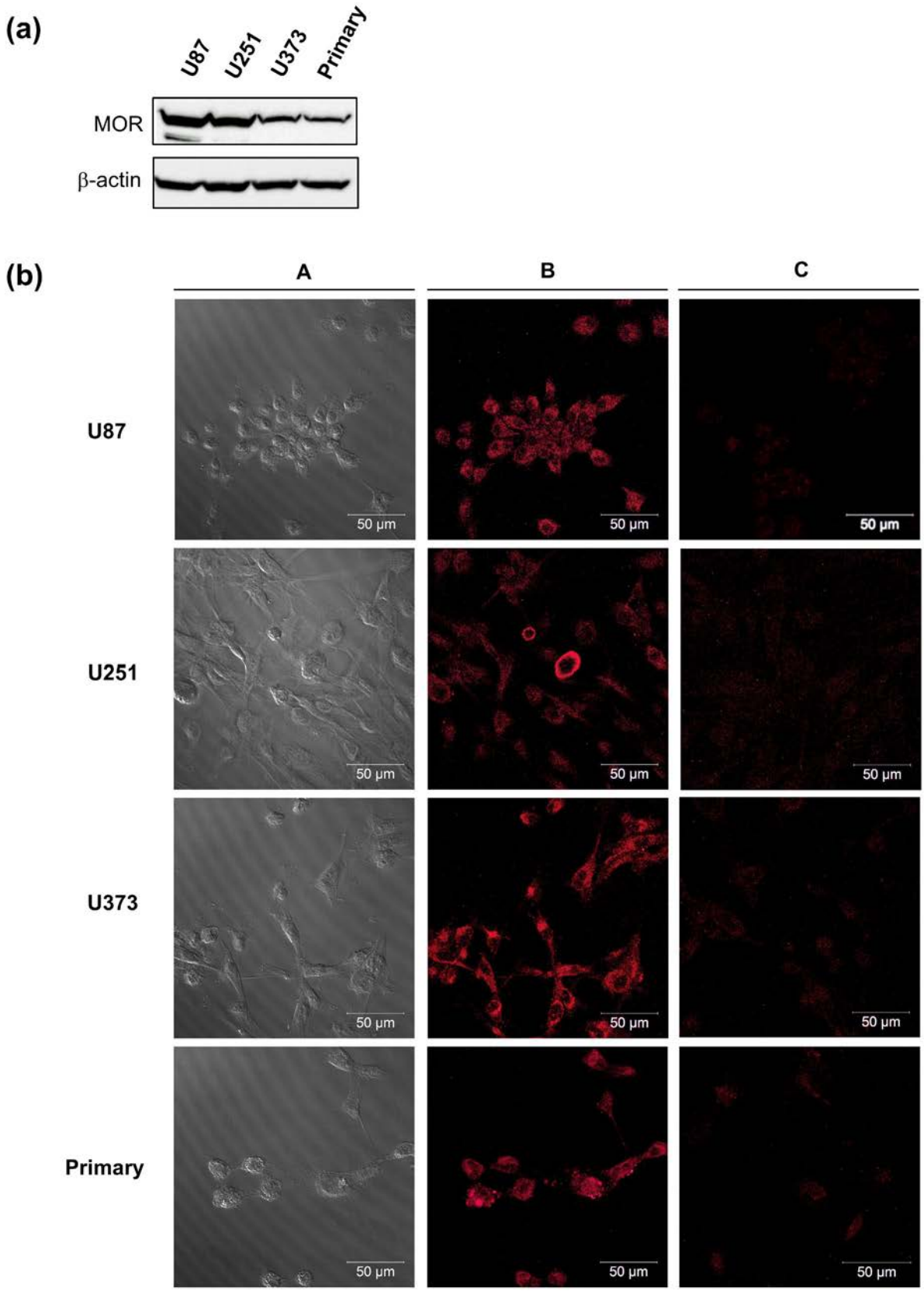
(a)
U87
U251
U373
Primary
MOR
β-actin
(b)
A
B
C
U87
U251
U373
Primary
50 µm

◂**Fig. 1** μ-Opioid receptor (MOR) expression in glioblastoma cells. **a** Representative Western blot showing protein expression of MOR in U87, U251, U373 GBM cell lines, and primary cells. β-actin blots were performed for loading control. **b** Representative immune fluorescence images showing expression of MOR in U87, U251, U373 GBM cell lines, and primary GBM cells. A, bright field images of respective cell lines; B, staining with primary and secondary antibody; C, treatment with secondary antibody only (negative control)

(Fig. 2c–e). The opposite was true, naloxone even significantly increased MET toxicity in A172 and primary cells (Fig. 2f), indicating that MET does not require MOR for its cytotoxic action.

To further verify these findings, we treated cells with other MOR agonists used in clinical practice for pain management such as morphine and oxycodone. Strikingly, both compounds showed very weak cytotoxicity in supra-therapeutic concentrations in all GBM cell lines and primary cells (Fig. 3a–e). The determined IC_{50} values were in the millimolar range or could not be established because of very low cytotoxicity (Fig. 3f).

Previously, it was reported that various MET concentrations (e.g. 10, 3, 1 μg/mL corresponding to ~ 30, 10, 3 μM, respectively) were capable of sensitizing A172 cells to a fixed doxorubicin concentration (0.3 μg/mL = 0.5 μM) in apoptosis assays (Friesen et al. 2014). In order to determine a concentration relationship, we treated A172, U87, and primary cells with ascending doxorubicin concentrations combined with 10 μM MET, a concentration which was not cytotoxic, but close to what might be reached in plasma of patients. We chose U87 cells because they do not express P-gp (Haas et al. 2018), while A172 cells likely express P-gp as its inhibtion by MET was reported to be responsible for doxorubicin accumulation (Friesen et al. 2014). MTT concentration–response curves overlapped in both tested GBM cell lines and, interestingly also in primary GBM cells (Fig. 4a–c); respective IC_{50} values showing no significant differences are displayed in Fig. 4d. Of note, in A172 cells at 0.3 μM doxorubicin, combination treatment with 10 μM MET slighly reduced cell viability as compared to doxorubicin treated cells alone (red circle in Fig. 4a). This is close to the concentrations tested in a previous work (0.5 μM doxorubicin combined with 3–30 μM MET), where effects on apoptosis were observed (Friesen et al. 2014).

Next, we repeated this experiment with previously determined IC_{50} concentrations of MET (Fig. 2a). High dose MET treatment (60 μM) resulted in a slight left shift of the doxorubicin concentration–response curve in A172 cells (Fig. 5a), while curves overlapped in U87 cells at 100 μM MET (Fig. 5b). Also in primary GBM cells at 100 μM MET curves largely overlapped independently of treatment (Fig. 5c). Statistical analysis revealed that MET treatment significantly reduced doxorubicin IC_{50} values in A172 and primary GBM cells indicating a sensitization (Fig. 5d). Looking closer at the curves of primary GBM cells, the data revealed at both curves overlap at most data points except at 1 μM (~ 0.5 μg/mL) doxorubicin (red circle in Fig. 5c), which explains the difference in IC_{50} values and indicates that a potential synergism of MET and doxorubicin highly depends on cell line and applied drug concentrations.

Doxorubicin is not used in the first-line treatment for GBM. Therefore, we studied the effect of MET on the toxicity of TMZ, which is the clinically relevant drug used in GBM therapy. We treated four GBM cell lines and primary GBM cells with ascending TMZ concentrations in combination with 10 μM MET and performed MTT assays. In A172 cells MET even reduced the sensitivity to TMZ (Fig. 6a) while in all other cells no effect was observed (Fig. 6b–e). The only statistical difference in IC_{50} values was obtained for A172 cells (Fig. 6f) confirming the negative impact of MET on TMZ treatment in this cell line. Similar results were obtained when cells were treated with an IC_{50} MET concentration in combination with TMZ (Fig. 7). At this high MET concentrations, both A172 and U373 (Fig. 7a, d, respectively) cells responded in a less sensitive way to TMZ.

Discussion

MET is a widely used therapeutic opioid in narcotic addiction and neuropathic pain syndromes. In oncological settings, it is regularly used as a long-lasting analgesic. Recently, it has also been proposed as a chemosensitzing agent in leukemia and GBM therapy based on the results of in vitro studies and a xenograft mouse model (Friesen et al. 2014, 2008, 2013). In these studies, fixed doxorubicin concentrations combined with MET were applied and MET was found to be capable of sensitizing cells to doxorubicin in terms of apoptosis induction. The proposed mechanism of action rests on activation of MOR, inhibition of P-gp by MET leading to increased intracellular doxorubicin levels, and subsequent induction of apoptosis (Friesen et al. 2014). In another study, the data were not reproduced in doxorubicin and MET-treated canine tumor cells (Cueni et al. 2020), indicating a need for further in vitro studies. MET has also been implicated in enhancing cytotoxic effects of other chemotherapeutics in cancer cell lines of different origins, such as bladder cancer, squamous cell carcinoma and head and neck cancer, albeit with varying efficacy, greatly depending on cell type, the chemotherapeutic agent and applied concentrations (Landgraf et al. 2019; Michalska et al. 2018; Shi et al. 2019). Also for GBM, conflicting results were reported. Thus, a sensitization to acid-based photodynamic therapy (ALA-PDT) by MET was observed in the GBM cell line A172 (Shi et al. 2019, 2020), indicating that MET might also be effective in GBM in combination with other treatments apart from doxorubicin. When MET

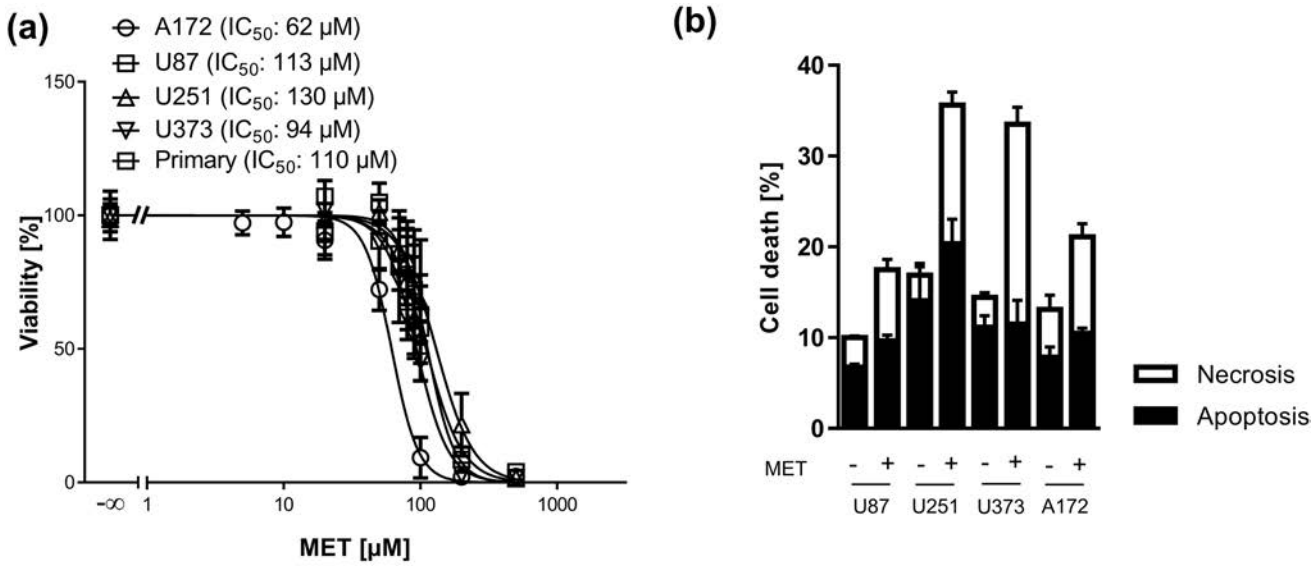

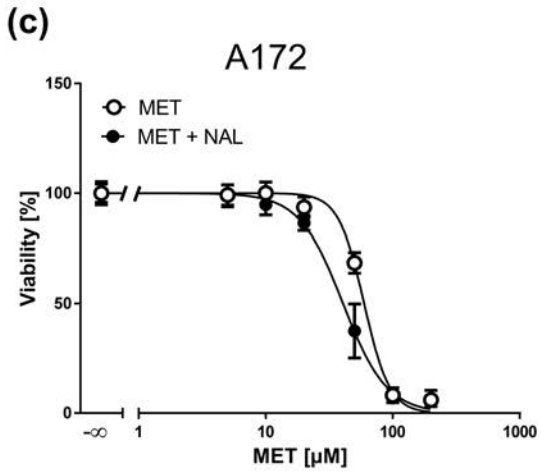

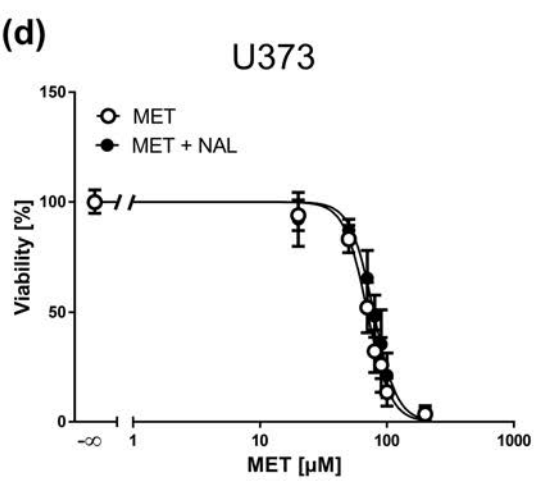

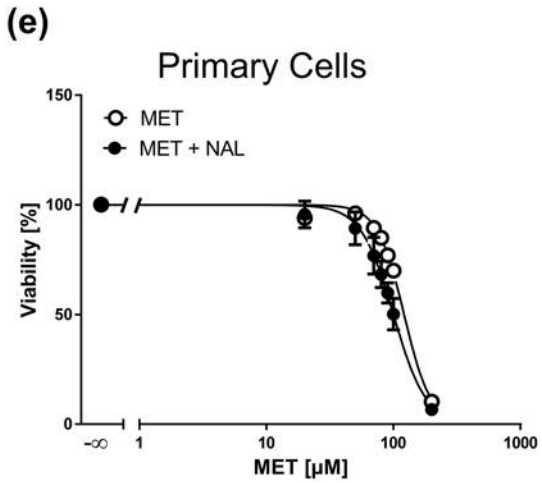

(f)

	MET IC_{50} [µM]		
Cell line	***A172***	***U373***	***Primary***
Vehicle	59	79	121
NAL	**41***	70	**100***

was combined with the more relevant treatment TMZ and irradiation (up to 8 Gy), no beneficial effect was observed in vitro (Oppermann et al. 2019; Vatter et al. 2020), while another study reported agonistic and antagonistic effects at high MET concentrations (> 15 µg/mL) on TMZ, which was cell line-dependent (Brawanski et al. 2018). Interestingly, in

◂**Fig. 2** Cytotoxicity of methadone (MET) in GBM cells. **a** 3-(4,5-Dimethylthiazol-2-yl)-2,5-diphenyltetrazolium bromide (MTT) assays of four GBM cell lines and primary cells treated with increasing concentrations of MET for 72 h as indicated. Values are displayed as mean ± SD ($n = 3$). **b** AnnexinV/propidium iodide (AV/PI) FACS analysis of GBM cell lines U87, U251, U373, and A172 treated with an IC_{50} MET concentration for 72 h. AV positive cells were considered apoptotic and PI positive/AV negative cells necrotic. Values are displayed as mean ± SEM ($n = 4$). MTT assays of A172 (**c**), U373 (**d**) GBM cell lines and primary cells (**e**) treated with increasing concentrations of MET for 72 h pretreated with 300 µM naloxone (NAL) for 1 h. Values are displayed as mean ± SD ($n = 3$). **f** IC_{50} values of MET in GBM cells derived from MTT assays; $^*p < 0.05$

these studies, MET effects on GBM cells were independent of MOR expression levels raising the question if MOR alone mediates the cytotoxic action of MET.

In our work presented here, we wished to quantify first whether MET alone is cytotoxic in GBM cells. MET induced cell death in a similar concentration range in various cell lines and primary cells. We also found that at high dose levels of MET (IC_{50} concentrations) apoptosis and necrosis were induced to a similar extend in most cell lines, except for U373 cells where about two thirds of cell deaths accounted for necrosis. This is in line with what has been shown by others, i.e., MET is able to induce apoptosis (Friesen et al. 2014) or necrotic-like cell death in cells of neuronal origin (Perez-Alvarez et al. 2010, 2011). Interestingly, we observed that naloxone was not able to block MET-induced cytotoxicity and other MOR agonists, morphine and oxycodone, were hardly cytotoxic at clinically relevant concentrations. This implies that MET's cytotoxic action on GBM cells is not MOR-dependent. MET might interfere with other cellular targets, which are responsible for its cytotoxicity. For instance, MET, in contrast to oxycodone and morphine, inhibits at low micromolar concentrations members of the voltage-gated potassium channel family (Fanoe et al. 2009; Katchman et al. 2002; Zunkler and Wos-Maganga 2010). Pharmacological inhibition of these channels leads to cell death in various tumor cells, including GBM cell lines (Sales et al. 2016) and thus the channels were proposed to be promising targets for cancer treatment (Wang et al. 2017). Whether MET-induced inhibition of voltage-gated potassium channels at the concentrations used in our work leads to cytotoxicity in GBM cells needs further investigation.

As conflicting results have been reported on the capability of MET to sensitize tumor cells to doxorubicin, we tested the combination of doxorubicin and MET in our cellular system. We used an approach commonly applied to determine sensitizing effects of a compound on cytostatic drugs. We treated cells with a wide range of doxorubicin combined with low (10 µM) and high concentrations (determined IC_{50} concentration for each cell line) of MET for 72 h because at this time point MET already induced cell death. We found a sensitizing effect only for the A172 cell line and to some extent in primary GBM cells, but not for the U87 cell line. We have previously shown that P-gp is not expressed in U87 cells (Haas et al. 2018), which might explain that these cells cannot be sensitized to doxorubicin by MET. Whether inhibition of doxorubicin efflux, as reported for the A172 cell line (Friesen et al. 2014), or inhibition of voltage-gated potassium channels is the underlying reason of MET-induced apoptosis/necrosis remains an open question.

Another important finding of our study is that the sensitizing effect of MET in A172 and primary cells was highly dependent on the applied drug concentrations. Although a complete left shift of the doxorubicin concentration–response curve upon MET treatment only was observed at high, clinically not relevant MET concentrations (60 µM) in A172 cells, lower MET concentrations (10 µM) only further increased doxorubicin cytotoxicity at one single doxorubicin/MET concentration combination but not over the whole concentration range. This might have clinical implications as it is challenging to exactly achieve the needed doxorubicin and MET levels in vivo where synergistic cell death-inducing effects might occur. In addition, tolerable MET plasma levels in addicts are between 0.3 and 1.3 µg/ml (corresponding to ~ 1–4 µM) after a dose of 60–120 mg/day (Dole and Kreek 1973; Inturrisi et al. 1987) which is much lower as compared to effective in vitro MET concentrations reported previously (Friesen et al. 2014) and in our present study. When a blood–brain barrier penetration of only 42% for MET is assumed (Oldendorf et al. 1972), sufficient brain levels can hardly be reached in GBM patients at feasible MET doses. It could be argued that MET accumulates in tissue stores and also in brain and corresponding tumors (Linares et al. 2015). However, if sufficient MET levels are actually reached in brain tumor tissue at clinically achievable doses warrants further investigation, apart from the fact that doxorubicin is not the indicated treatment option for GBM due to its low blood–brain barrier penetration and neurological side effects (Merker et al. 1978; Neuwelt et al. 1981). Although pegylated and liposomal-encapsulated formulations of doxorubicin (Caelyx®) with increased brain uptake and less side effects are available, GBM is rarely treated with doxorubicin and its liposomal formulations in clinical practice (Fabel et al. 2001; Fiorillo et al. 2004).

Because of these shortcomings, we also tested the clinically more relevant drug TMZ in combination with MET. We did not observe an effect of MET on TMZ-induced

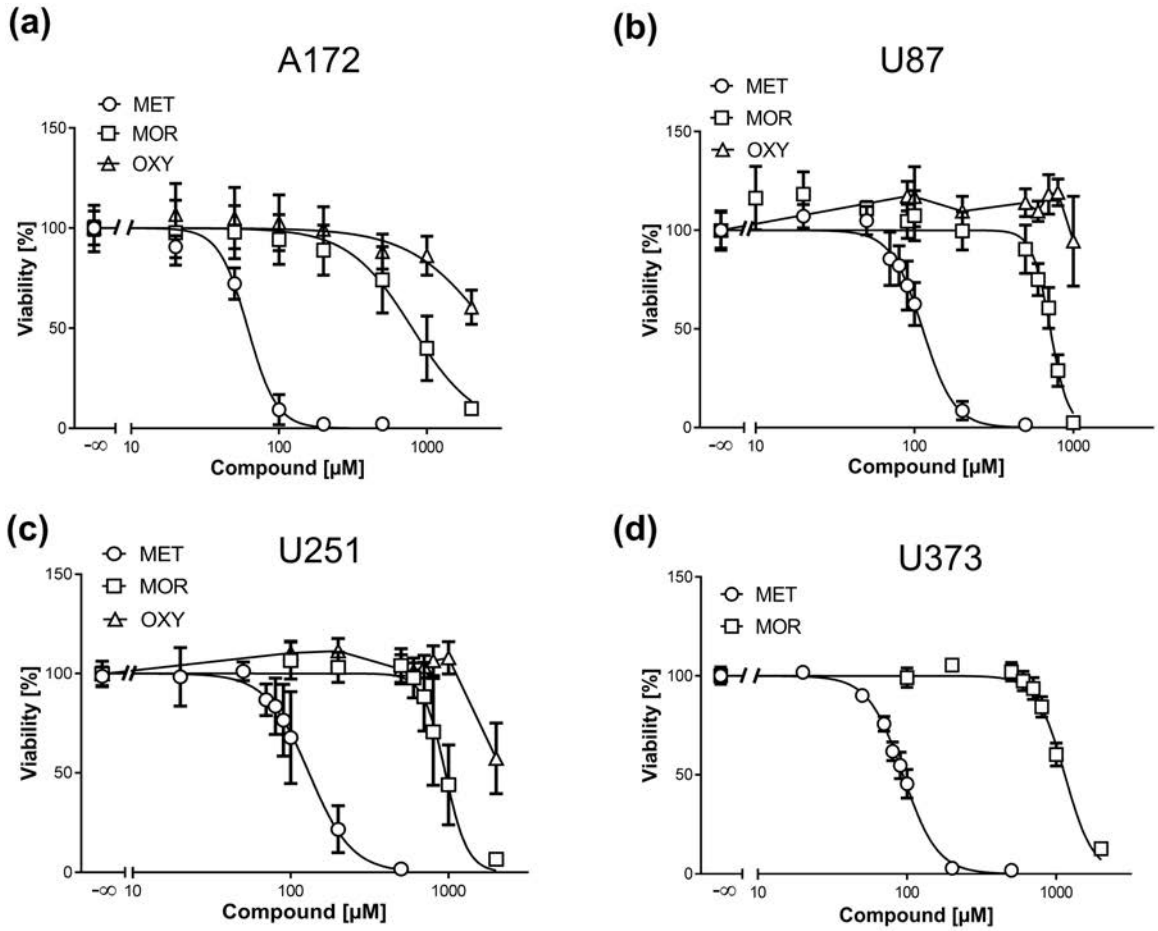

(f)

Compound IC_{50} [µM]					
Cell line	*A172*	*U87*	*U251*	*U373*	*Primary*
MET	62	113	130	94	122
MOR	796	714	953	1140	1458
OXY	2654	N.C.	N.C.	-	1570

Fig. 3 Comparison of opioid-induced cytotoxicity in GBM cell lines and primary cells. MTT assays of A172 (**a**), U87 (**b**), U251 (**c**), U373 (**d**), GBM cell lines and primary cells (**e**) treated with increasing concentrations of MET, morphine (MOR), and oxycodone (OXY) for 72 h as indicated. Values are displayed as mean ± SD ($n = 3$–4). **f** IC_{50} values of MET, MOR, and OXY in GBM cells derived from MTT assays, *NC* not calculated, – not determined

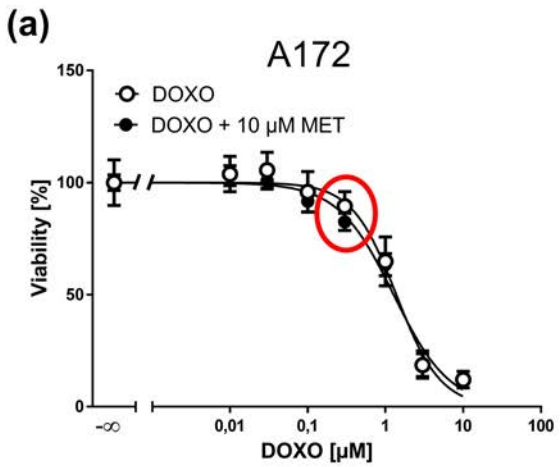

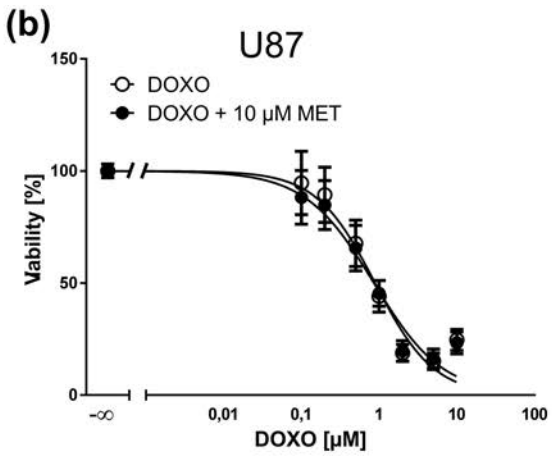

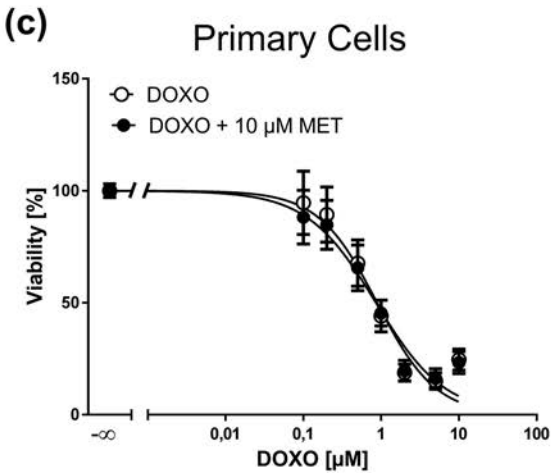

(d)

DOXO IC_{50} [µM]			
Cell line	**A172**	**U87**	**Primary**
Vehicle	1.4	0.937	1.8
MET, 10 µM	1.3	0.907	1.9

Fig. 4 MET (10 µM) does not sensitize GBM cell lines and primary cells to doxorubicin (DOXO). MTT assays of A172 (**a**), U87 (**b**) GBM cell lines and primary cells (**c**) treated with increasing concentrations of DOXO for 72 h pretreated with vehicle or 10 µM MET for 1 h. **d** IC_{50} values derived from MTT assays of doxorubicin treated GBM cells with or without 10 µM MET. Values are displayed as mean ± SD ($n = 3$). Note: in A172 at one data point of combination treatment differed from DOXO treatment [0.3 µM, red circle in (**a**)]

cytotoxicity in none of the tested GBM cell lines and primary cells, which is in line with a previous study (Oppermann et al. 2019). Importantly, in U373 and A172 cells MET even reduced sensitivity to TMZ, an effect that has also been demonstrated by others in different GBM cell lines (Brawanski et al. 2018). This might be due to cell cycle inhibition following MET treatment especially at high cytotoxic concentrations, which counteracts TMZ-induced cell death responses (Roos et al. 2004). In contrast to other studies where MET and TMZ were applied for 6 days (Brawanski et al. 2018; Kaina et al. 2020; Oppermann et al. 2019), we applied a 72-h MTT protocol as at this time MET already displayed high cytotoxicity and, therefore, we considered it sufficient to observe an effect on TMZ. As a consequence, the determined TMZ IC_{50} values in our study are in the higher micromolar range, as TMZ requires repeated cell cycles to process lesions and activate cell death pathways (He and Kaina 2019). Despite these differences in treatment protocols we yielded similar results, which strengthen the conclusion also drawn by other groups that MET is not capable to synergistically sensitize GBM cell to TMZ. Similar data were obtained on glioblastoma cells and TMZ-induced

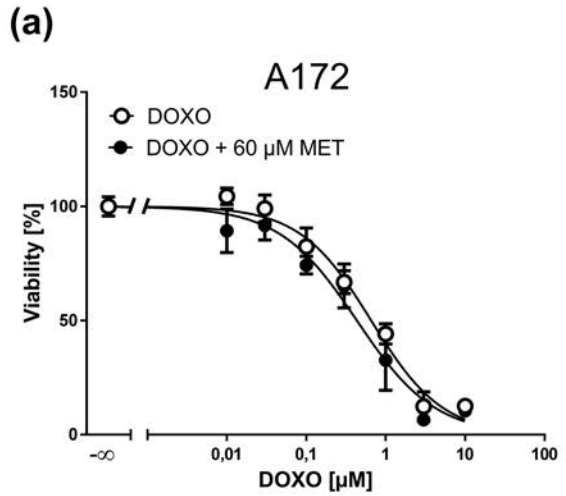

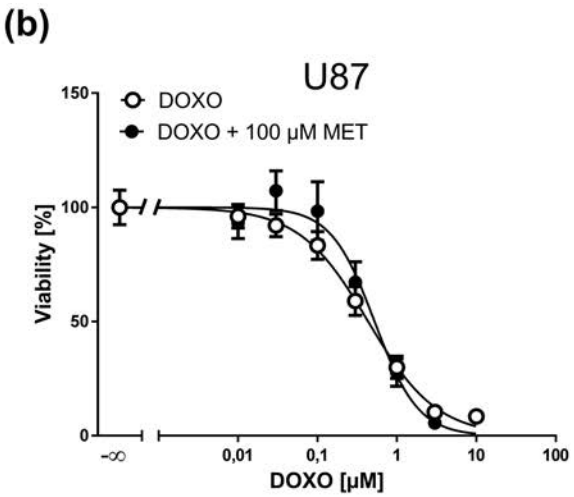

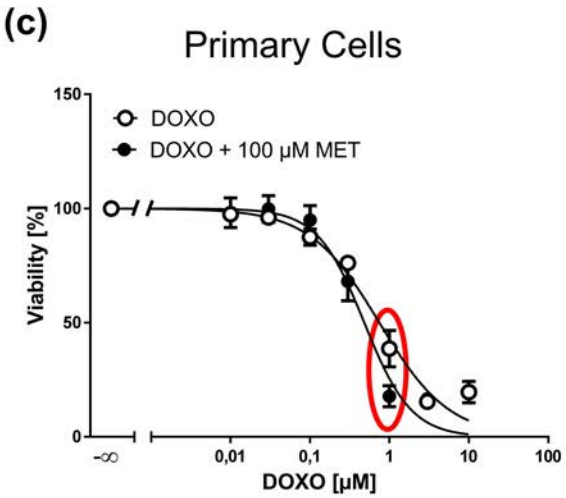

(d)

	DOXO IC_{50} [µM]		
Cell line	**A172**	**U87**	**Primary**
Vehicle	0.657	0.435	0.749
MET, IC_{50}	**0.434***	0.523	**0.483***

Fig. 5 Sensitization of GBM cells by high MET concentrations to DOXO is cell line-dependent. MTT assays of A172 (**a**), U87 (**b**) GBM cell lines, and primary cells (**c**), treated with increasing concentrations of DOXO for 72 h pretreated with vehicle or the corresponding IC_{50} concentration of MET for 1 h. Values are displayed as mean ± SD ($n = 3$) (**d**) IC_{50} values derived from MTT assays of DOXO-treated GBM cells with or without an IC_{50} concentration of MET; $^*p < 0.05$. Note: Combination treatment in primary GBM cells was only statistically different from DOXO alone treated cells due to one data point [red circle in (**c**)]

apoptosis and cellular senescence, demonstrating that MET does not impact pathways involved in these endpoints (Kaina et al. 2020).

Conclusions

We conclude that the cytotoxic effect of MET alone on GBM cells is not mediated via the opioid receptor MOR. This implicates that other cellular targets, including voltage-gated potassium channels, are involved, which warrants further investigation. Furthermore, our findings do not support the use of MET in the treatment of GBM in combination with TMZ, as no sensitizing effect of MET was observed. In GBM therapy, treatment with doxorubicin is not the rule. Although we observed in two cell lines (out of 3) a supportive effect of MET on doxorubicin-induced cytotoxicity, we doubt that critical MET concentration levels might be reached in the brain of patients to achieve a potential

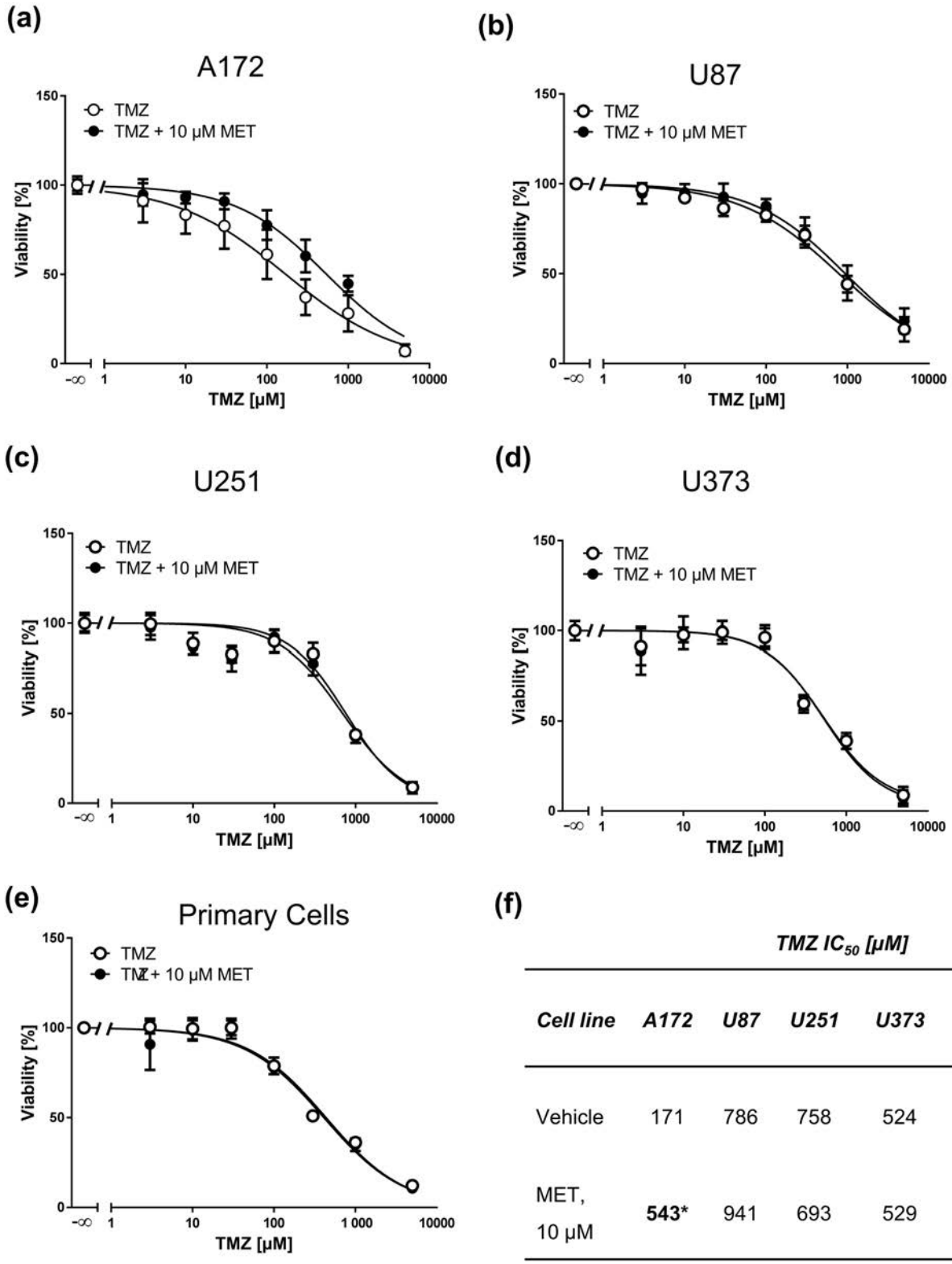

(f)

	TMZ IC_{50} [µM]				
Cell line	**A172**	**U87**	**U251**	**U373**	**Primary**
Vehicle	171	786	758	524	435
MET, 10 µM	**543***	941	693	529	410

Fig. 6 MET (10 µM) does not sensitize GBM cell lines and primary cells to TMZ. MTT assays of A172 (**a**), U87 (**b**), U251 (**c**), U373 (**d**) GBM cell lines and primary cells (**e**) treated with increasing concentrations of TMZ for 72 h pretreated with vehicle or 10 µM MET for 1 h. Values are displayed as mean ± SD ($n = 3$–4). (**f**) IC_{50} values of TMZ (vehicle) and TMZ + MET-treated GBM cells derived from MTT assays; *$p < 0.05$

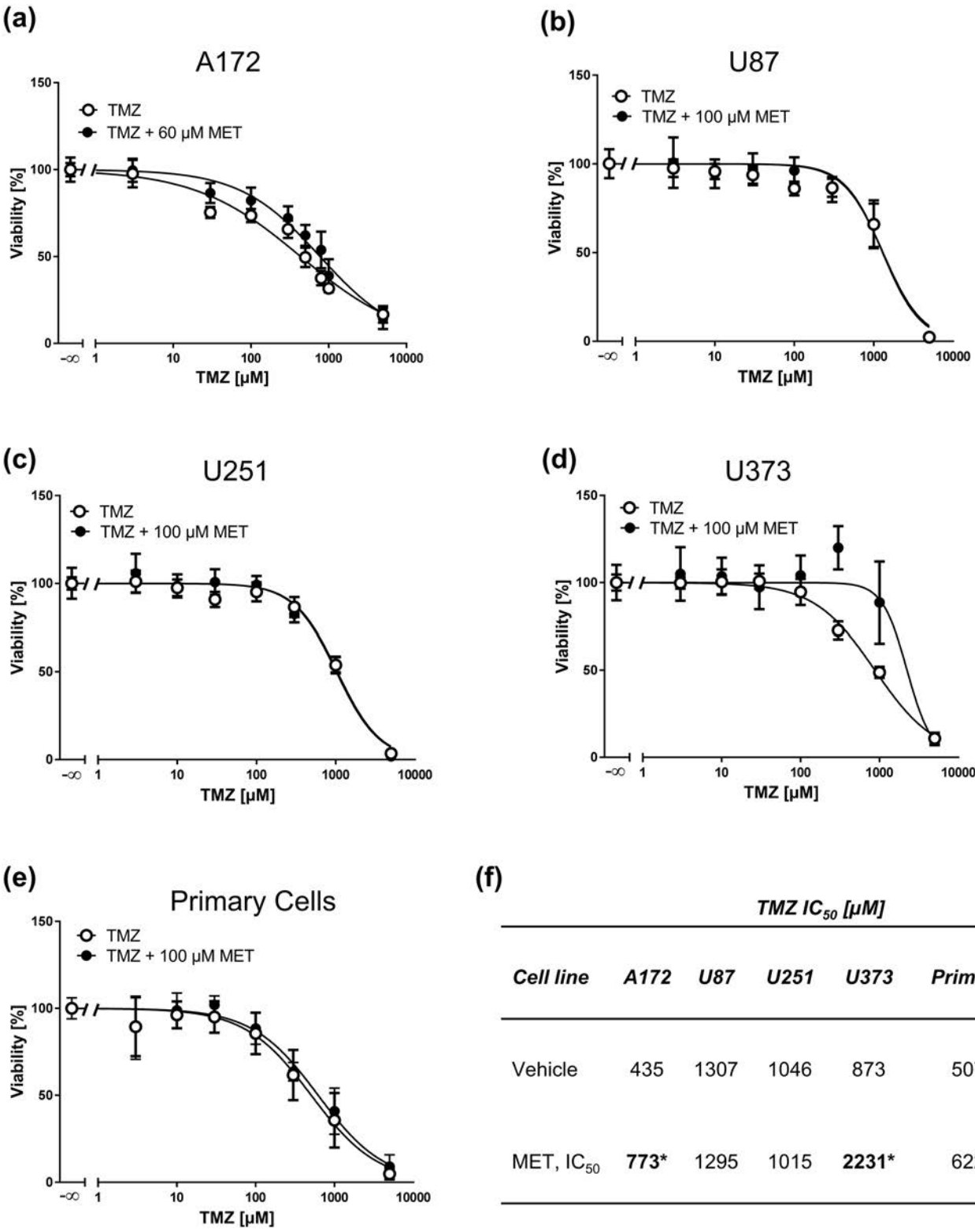

(f)

	TMZ IC_{50} [µM]				
Cell line	**A172**	**U87**	**U251**	**U373**	**Primary**
Vehicle	435	1307	1046	873	507
MET, IC_{50}	**773***	1295	1015	**2231***	622

Fig. 7 High MET concentrations do not sensitize GBM cell lines and primary cells to TMZ. MTT assays of A172 (**a**), U87 (**b**), U251 (**c**), U373 (**d**) GBM cell lines and primary cells (**e**) treated with increasing concentrations of TMZ pretreated with vehicle or the corresponding IC_{50} concentration of MET for 1 h. Values are displayed as mean ± SD ($n = 3$–4). **b** IC_{50} values of TMZ (vehicle) and TMZ + MET-treated GBM cells derived from MTT assays; *$p < 0.05$

synergistic effect with doxorubicin. It is obvious that further clinical studies are warranted.

Acknowledgements We thank Marco Timmer and Gabriele Röhn of the tumor tissue bank of the Clinic of Neurosurgery, University of Cologne for providing primary GBM cells.

Author contributions BH, NE designed and performed experiments. BH, NE, BK analyzed data and wrote the manuscript. JC, SJ, SW performed experiments and analyzed data. All authors read and approved the final manuscript.

Funding Open Access funding enabled and organized by Projekt DEAL. This article was supported by an intramural funding of the Federal Institute for Drugs and Medical Devices (BfArM).

Availability of data and material The datasets used and/or analyzed during the current study are available from the corresponding author on reasonable request.

Compliance with ethical standards

Conflict of interest The authors declare that they have no conflicting/competing interests.

Ethics approval and consent to participate Human tissue specimens of glioblastoma were provided by the tumor tissue bank of the Clinic of Neurosurgery, University of Cologne. The collection of samples was approved by the University's Institutional Ethical Board. Informed consent of the patients was obtained according to the Helsinki declaration of ethical requirements.

References

Brawanski K et al (2018) Efficacy of d, l-methadone in the treatment of glioblastoma in vitro. CNS Oncol 7:CNS18. https://doi.org/10.2217/cns-2018-0006

Cueni C, Nytko KJ, Thumser-Henner P, Weyland MS, Rohrer Bley C (2020) Methadone does not potentiate the effect of doxorubicin in canine tumour cell lines. Vet Med Sci. https://doi.org/10.1002/vms3.266

Dole VP, Kreek MJ (1973) Methadone plasma level: sustained by a reservoir of drug in tissue. Proc Natl Acad Sci USA 70:10. https://doi.org/10.1073/pnas.70.1.10

Eckstein N et al (2009) Hyperactivation of the insulin-like growth factor receptor I signaling pathway is an essential event for cisplatin resistance of ovarian cancer cells. Cancer Res 69:2996–3003. https://doi.org/10.1158/0008-5472.CAN-08-3153

Fabel K et al (2001) Long-term stabilization in patients with malignant glioma after treatment with liposomal doxorubicin. Cancer 92:1936–1942. https://doi.org/10.1002/1097-0142(20011001)92:7%3c1936::aid-cncr1712%3e3.0.co;2-h

Fanoe S, Jensen GB, Sjogren P, Korsgaard MP, Grunnet M (2009) Oxycodone is associated with dose-dependent QTc prolongation in patients and low-affinity inhibiting of hERG activity in vitro. Br J Clin Pharmacol 67:172–179. https://doi.org/10.1111/j.1365-2125.2008.03327.x

Fiorillo A et al (2004) Second-line chemotherapy with the association of liposomal daunorubicin, carboplatin and etoposide in children with recurrent malignant brain tumors. J Neurooncol 66:179–185. https://doi.org/10.1023/b:neon.0000013471.53015.52

Friesen C, Roscher M, Alt A, Miltner E (2008) Methadone, commonly used as maintenance medication for outpatient treatment of opioid dependence, kills leukemia cells and overcomes chemoresistance. Cancer Res 68:6059–6064. https://doi.org/10.1158/0008-5472.CAN-08-1227

Friesen C et al (2013) Cell death sensitization of leukemia cells by opioid receptor activation. Oncotarget 4:677–690. https://doi.org/10.18632/oncotarget.952

Friesen C et al (2014) Opioid receptor activation triggering downregulation of cAMP improves effectiveness of anti-cancer drugs in treatment of glioblastoma. Cell Cycle 13:1560–1570. https://doi.org/10.4161/cc.28493

Haas B et al (2009) Protein kinase G controls brown fat cell differentiation and mitochondrial biogenesis. Sci Signal 2:ra78. https://doi.org/10.1126/scisignal.2000511

Haas B et al (2018) Inhibition of the PI3K but not the MEK/ERK pathway sensitizes human glioma cells to alkylating drugs. Cancer Cell Int 18:69. https://doi.org/10.1186/s12935-018-0565-4

He Y, Kaina B (2019) Are there thresholds in glioblastoma cell death responses triggered by temozolomide? Int J Mol Sci 20:1562. https://doi.org/10.3390/ijms20071562

Insel PA, Zhang L, Murray F, Yokouchi H, Zambon AC (2012) Cyclic AMP is both a pro-apoptotic and anti-apoptotic second messenger. Acta Physiol (Oxf) 204:277–287. https://doi.org/10.1111/j.1748-1716.2011.02273.x

Inturrisi CE, Colburn WA, Kaiko RF, Houde RW, Foley KM (1987) Pharmacokinetics and pharmacodynamics of methadone in patients with chronic pain. Clin Pharmacol Ther 41:392–401. https://doi.org/10.1038/clpt.1987.47

Kaina B, Beltzig L, Piee-Staffa A, Haas B (2020) Cytotoxic and senolytic effects of methadone in combination with temozolomide in glioblastoma cells. Int J Mol Sci. https://doi.org/10.3390/ijms21197006

Katchman AN, McGroary KA, Kilborn MJ, Kornick CA, Manfredi PL, Woosley RL, Ebert SN (2002) Influence of opioid agonists on cardiac human ether-a-go-go related gene K+ currents. J Pharmacol Exp Ther 303:688–694. https://doi.org/10.1124/jpet.102.038240

Krantz MJ, Mehler PS (2004) Treating opioid dependence. Growing implications for primary care. Arch Intern Med 164:277–288. https://doi.org/10.1001/archinte.164.3.277

Landgraf V, Griessmann M, Roller J, Polednik C, Schmidt M (2019) DL-Methadone as an enhancer of chemotherapeutic drugs in head and neck cancer cell lines. Anticancer Res 39:3633–3639. https://doi.org/10.21873/anticanres.13511

Linares OA, Fudin J, Daly A, Schiesser WE, Boston RC (2015) Methadone recycling sustains drug reservoir in tissue. J Pain Palliat Care Pharmacother 29:261–271. https://doi.org/10.3109/15360288.2015.1047552

Louis DN et al (2016) The 2016 world health organization classification of tumors of the central nervous system: a summary.

Acta Neuropathol 131:803–820. https://doi.org/10.1007/s00401-016-1545-1

Merker PC, Lewis MR, Walker MD, Richardson EP Jr (1978) Neurotoxicity of adriamycin (doxorubicin) perfused through the cerebrospinal fluid spaces of the rhesus monkey. Toxicol Appl Pharmacol 44:191–205. https://doi.org/10.1016/0041-008x(78)90298-3

Michalska M, Schultze-Seemann S, Kuckuck I, Katzenwadel A, Wolf P (2018) Impact of methadone on cisplatin treatment of bladder cancer cells. Anticancer Res 38:1369–1375. https://doi.org/10.21873/anticanres.12360

Neuwelt EA, Pagel M, Barnett P, Glassberg M, Frenkel EP (1981) Pharmacology and toxicity of intracarotid adriamycin administration following osmotic blood-brain barrier modification. Cancer Res 41:4466–4470

Oldendorf WH, Hyman S, Braun L, Oldendorf SZ (1972) Blood–brain barrier: penetration of morphine, codeine, heroin, and methadone after carotid injection. Science 178:984–986. https://doi.org/10.1126/science.178.4064.984

Oppermann H et al (2019) D, l-Methadone does not improve radio- and chemotherapy in glioblastoma in vitro. Cancer Chemother Pharmacol 83:1017–1024. https://doi.org/10.1007/s00280-019-03816-3

Ostrom QT, Gittleman H, Xu J, Kromer C, Wolinsky Y, Kruchko C, Barnholtz-Sloan JS (2016) CBTRUS statistical report: primary brain and other central nervous system tumors diagnosed in the United States in 2009–2013. Neuro Oncol 18:v1–v75. https://doi.org/10.1093/neuonc/now207

Parsons HA, de la Cruz M, El Osta B, Li Z, Calderon B, Palmer JL, Bruera E (2010) Methadone initiation and rotation in the outpatient setting for patients with cancer pain. Cancer 116:520–528. https://doi.org/10.1002/cncr.24754

Perez-Alvarez S et al (2010) Methadone induces necrotic-like cell death in SH-SY5Y cells by an impairment of mitochondrial ATP synthesis. Biochim Biophys Acta 1802:1036–1047. https://doi.org/10.1016/j.bbadis.2010.07.024

Perez-Alvarez S, Iglesias-Guimarais V, Solesio ME, Melero-Fernandez de Mera RM, Yuste VJ, Galindo MF, Jordan J (2011) Methadone induces CAD degradation and AIF-mediated necrotic-like cell death in neuroblastoma cells. Pharmacol Res 63:352–360. https://doi.org/10.1016/j.phrs.2010.12.001

Roos W, Baumgartner M, Kaina B (2004) Apoptosis triggered by DNA damage *O*-6-methylguanine in human lymphocytes requires DNA replication and is mediated by p53 and Fas/CD95/Apo-1. Oncogene 23:359–367. https://doi.org/10.1038/sj.onc.1207080

Sales TT, Resende FFB, Chaves NL, Titze-De-Almeida SS, Bao SN, Brettas ML, Titze-De-Almeida R (2016) Suppression of the Eag1 potassium channel sensitizes glioblastoma cells to injury caused by temozolomide. Oncol Lett 12:2581–2589. https://doi.org/10.3892/ol.2016.4992

Shi L et al (2019) Methadone enhances the effectiveness of 5-aminolevulinic acid-based photodynamic therapy for squamous cell carcinoma and glioblastoma in vitro. J Biophotonics 12:e201800468. https://doi.org/10.1002/jbio.201800468

Shi L et al (2020) MOP-dependent enhancement of methadone on the effectiveness of ALA-PDT for A172 cells by upregulating phosphorylated JNK and BCL2. Photodiagn Photodyn 30:101657. https://doi.org/10.1016/j.pdpdt.2020.101657

Siegel RL, Miller KD, Jemal A (2020) Cancer statistics, 2020 CA Cancer. J Clin 70:7–30. https://doi.org/10.3322/caac.21590

Singh A, Jayanthan A, Farran A, Elwi AN, Kim SW, Farran P, Narendran A (2011) Induction of apoptosis in pediatric acute lymphoblastic leukemia (ALL) cells by the therapeutic opioid methadone and effective synergy with Bcl-2 inhibition. Leukemia Res 35:1649–1657. https://doi.org/10.1016/j.leukres.2011.06.035

Stupp R et al (2005) Radiotherapy plus concomitant and adjuvant temozolomide for glioblastoma. N Engl J Med 352:987–996. https://doi.org/10.1056/NEJMoa043330

Stupp R et al (2009) Effects of radiotherapy with concomitant and adjuvant temozolomide versus radiotherapy alone on survival in glioblastoma in a randomised phase III study: 5-year analysis of the EORTC-NCIC trial. Lancet Oncol 10:459–466. https://doi.org/10.1016/S1470-2045(09)70025-7

Vatter T, Klumpp L, Ganser K, Stransky N, Zips D, Eckert F, Huber SM (2020) Against repurposing methadone for glioblastoma therapy. Biomolecules. https://doi.org/10.3390/biom10060917

Wang XZ, Chen YF, Zhang YH, Guo S, Mo L, An HL, Zhan Y (2017) Eag1 voltage-dependent potassium channels: structure, electrophysiological characteristics, and function in cancer. J Membr Biol 250:123–132. https://doi.org/10.1007/s00232-016-9944-8

Zunkler BJ, Wos-Maganga M (2010) Comparison of the effects of methadone and heroin on human ether-a-go-go-related gene channels. Cardiovasc Toxicol 10:161–165. https://doi.org/10.1007/s12012-010-9074-y

Supplementary Table 1 MGMT and TP53 status of GBM cell lines

Cell Line	MGMT Status (Promotor Methylation)	TP53 Status
A172	Negative (methylated) [1]	wt [2,3]
U87-MG	Negative (methylated) [1]	wt [2,3]
U251-MG	Negative (methylated) [1]	Homozygous Missense Mutation (Arg -> His) [2]
U373-MG	Negative (methylated) [1]	Homozygous Missense Mutation (Arg -> His) [2]

MGMT: methylguanine-DNA methyltransferase, TP53: tumour suppressor p53, wt: wild type

1. Hermisson, M.; Klumpp, A.; Wick, W.; Wischhusen, J.; Nagel, G.; Roos, W.; Kaina, B.; Weller, M. O6- methylguanine DNA methyltransferase and p53 status predict temozolomide sensitivity in human malignant glioma cells. J. Neurochem. 2006, 96, 766–776, doi:10.1111/j.1471-4159.2005.03583.x.

2. Ishii, N.; Maier, D.; Merlo, A.; Tada, M.; Sawamura, Y.; Diserens, A.C.; van Meir, E.G. Frequent coalterations of TP53, p16/CDKN2A, p14ARF, PTEN tumor suppressor genes in human glioma cell lines. Brain Pathol. 1999, 9, 469–479.

3. Michaud, K.; Solomon, D.A.; Oermann, E.; Kim, J.-S.; Zhong, W.-Z.; Prados, M.D.; Ozawa, T.; James, C.D.; Waldman, T. Pharmacologic inhibition of cyclin-dependent kinases 4 and 6 arrests the growth of glioblastoma multiforme intracranial xenografts. Cancer Res. 2010, 70, 3228–3238.

3.5 **Haas B**, Roth I, Sacker L, Wos-Maganga M, Beltzig L, Kaina B. Apoptotic and senolytic effects of hERG/Eag1 channel blockers in combination with temozolomide in human glioblastoma cells. Naunyn Schmiedebergs Arch Pharmacol. 2025;398(9):12267-12278.

Zielsetzung der Arbeit: Eine pharmakologische Hemmung der spannungsaktivierten Kaliumkanäle, *human ether-à-go-go type 1* (Eag1) und *human ether-à-go-go-related gene* (hERG) wird schon länger als Tumortherapie diskutiert (He et al., 2020). In Glioblastom-Patienten ist eine Überexpression der beiden Kanäle mit einer schlechten klinischen Prognose assoziiert (Martinez et al., 2015; Shugg et al., 2021; Zheng et al., 2023) und eine Aktivierung löst in Brustkrebszellen Seneszenz aus (Lansu et al., 2013), was die Kanäle deswegen auch als Therapieziel für Gliome interessant macht (Elias et al., 2023). Darauf aufbauend wurde in dieser Arbeit die Expression von hERG/Eag1 in humanen Glioblastom-Zellen und -Tumorgewebe untersucht und die Auswirkungen einer pharmakologischen Hemmung auf die Apoptose und die zelluläre Seneszenz allein und in Kombination mit TMZ in einer Reihe von humanen Glioblastom-Zelllinien und primären Zellen analysiert.

Methoden und Ergebnisse: Immunfluoreszenz- und Immunoblotting-Experimente zeigten eine vergleichbare hERG- und Eag1-Expression in allen untersuchten Zellen und Glioblastom-Biopsien. Die beiden hERG/Eag1-Blocker Astemizol und Terfenadin waren in MTT-Experimenten bei niedrigen mikromolaren Konzentrationen (IC_{50}: 5–8 µM) zytotoxisch. In Annexin-V-FACS Assays stellte sich heraus, dass Zelltod hauptsächlich (>70%) über Induktion von Apoptose ausgelöst wurde. In Kombination mit TMZ sensitivierten beide Substanzen die Zellen synergistisch für die TMZ-induzierte Apoptose. Darüber hinaus reduzierte Astemizol die TMZ-induzierte Seneszenz signifikant um etwa 50%, was über FACS-Messungen der lysosomalen β-Galaktosidase quantifiziert wurde.

Schlussfolgerung: Diese Arbeit zeigt zum ersten Mal, dass die Blockade von hERG/Eag1-Kanälen in Glioblastom-Zellen die TMZ-induzierte zelluläre Seneszenz verringern und die Zytotoxizität durch die Induktion von Apoptose synergistisch verbessern kann.

Naunyn-Schmiedeberg's Archives of Pharmacology (2025) 398:12267–12278
https://doi.org/10.1007/s00210-025-03955-w

RESEARCH

Apoptotic and senolytic effects of hERG/Eag1 channel blockers in combination with temozolomide in human glioblastoma cells

Bodo Haas[1] · Inken Roth[1,2] · Luisa Säcker[1,2] · Maria Wos-Maganga[1] · Lea Beltzig[3] · Bernd Kaina[3]

Received: 23 January 2025 / Accepted: 18 February 2025 / Published online: 24 March 2025

Abstract

Temozolomide (TMZ) concomitant with radiotherapy is the first-line treatment for glioblastoma. However, treatment resistance is frequently observed in patients. Cellular senescence (CSEN) induced by TMZ has been proposed to be one underlying mechanism resulting in resting cells, causing inflammation and possibly recurrences if senescent cells re-enter the cell cycle after treatment. Inhibition of the K^+ channels human ether-à-go-go type 1 (Eag1) and human ether-à-go-go-related gene (hERG) has shown promising effects in several tumor types including glioblastoma through growth inhibition and induction of apoptosis. In the present study, we analyzed the impact of hERG/Eag1 inhibition on apoptosis and CSEN on its own and in combination with TMZ in a panel of human glioblastoma cell lines and primary glioblastoma cells. hERG/Eag1 protein expression was determined by Western blotting and immunocytochemistry. Cytotoxicity of astemizole and terfenadine alone or in combination with TMZ was assessed by MTT assays. Apoptotic yields were determined by Annexin V/propidium iodide staining, and CSEN was quantified by determining SA-β-galactosidase levels through flow cytometry. We observed a similar protein expression of hERG and Eag1 in all glioblastoma cell lines and primary glioblastoma cells. Astemizole and terfenadine were cytotoxic in glioblastoma cells at low micromolar concentrations (5–10 µM range) through induction of apoptosis. In combination with TMZ, both drugs synergistically sensitized glioblastoma cells to TMZ-induced apoptosis. Moreover, astemizole reduced significantly the TMZ-induced CSEN level, indicating its impact on CSEN induction. Here, we show for the first time that blocking hERG/Eag1 channels in glioblastoma cells can relief TMZ-induced CSEN and synergistically ameliorates cytotoxicity through the induction of apoptosis.

Keywords Glioblastoma · Temozolomide · hERG channel · Eag1 channel · Chemosensitizer

Introduction

Glioblastoma (WHO grade 4) is the most common malignant brain tumor in adulthood and often arises de novo without any clinical history (Komori 2022; Louis et al. 2021). The poor prognosis and the lack of effective therapies, including radiation and drug resistance, is devastating. Beside surgical resection and radiation, adjuvant and concomitant treatment with the alkylating drug temozolomide (TMZ) is the gold standard in glioblastoma therapy (Stupp et al. 2009; Stupp et al. 2005). However, TMZ prolongs the lifespan of patients by only 3 months; the 5-year survival rate is only 6%, and drug resistance is a remaining challenge (Price et al. 2024). All of this indicates that there is a high medical need for new treatment modalities.

We have previously reported that TMZ-resistance of glioblastoma cells might be a consequence of induction of a senescent cell population, which is characterized by resistance to TMZ-induced apoptosis, high level of residual DNA double-strand breaks (DSBs) and a sustained activation of the DNA damage response (DDR) (Aasland et al. 2019; Beltzig, et al. 2022b). Dormant senescent cells were shown to be able to re-enter the cell cycle after treatment cessation and are characterized by a proinflammatory phenotype,

Inken Roth and Luisa Säcker contributed equally.

✉ Bodo Haas
bodo.haas@bfarm.de

[1] Federal Institute for Drugs and Medical Devices (BfArM), Kurt-Georg-Kiesinger-Allee 3, 53175 Bonn, Germany

[2] Faculty of Applied Natural Sciences, TH Köln - University of Applied Sciences, Campus Platz 1, 51379 Leverkusen, Germany

[3] Institute of Toxicology, University Medical Center, Obere Zahlbacher Strasse 67, 55131 Mainz, Germany

which further promotes tumor growth (Riviere-Cazaux et al. 2023; Zhang et al. 2023). Therefore, elimination of the senescent cell population has been suggested as a promising strategy to improve the outcome of glioblastoma therapy (Kaina 2023).

The two members of the KCNH family of voltage-gated potassium ion (K^+) channels, human ether-à-go-go type 1 (Eag1 encoded by *KCNH1*) and human ether-à-go-go-related gene (hERG encoded by *KCNH2*), have been implicated in cancer development (Pardo and Stuhmer 2014; Wang et al. 2017) and hold promise as therapeutic targets (He et al. 2020; Wulff et al. 2009). While hERG is expressed in various tissues such as heart, brain, gastrointestinal tract, urinary bladder, and pancreas, Eag1 is mainly found in the brain (Martin et al. 2008; Vandenberg et al. 2012). However, both KCNH channels have also been shown to be overexpressed in several tumor types, including colon, breast, and cervical cancers, melanoma, neuroblastoma, and glioblastoma (Lastraioli et al. 2015; Meyer and Heinemann 1998; Patt et al. 2004). In patients, overexpression of hERG and Eag1 in glioblastoma results in poor prognosis and reduced survival (Martinez et al. 2015; Shugg et al. 2021; Zheng and Song 2023). KCNH expression is known to be linked to cell cycle phase and essential for cell cycle progression. Increased KCNH channel activity leads to increased proliferation (Pardo et al. 1999). Interestingly, activation of the hERG channel has been shown to activate a senescence program in breast cancer cells, highlighting its role also in senescence development (Lansu and Gentile 2013).

Despite this knowledge, the regulation of proliferation in tumor cells by K^+ channels is not fully understood. It is known that overexpression of K^+ channels in melanoma cells leads to hyperpolarization, which promotes the influx of calcium ions (Ca^{2+}). Ca^{2+} is important for the transition from G1 to S phase in the cell cycle and, therefore, leads to increased proliferation (Nilius et al. 1993; Nilius and Wohlrab 1992). Another mechanism related to increased proliferation is the link between KCNH channels and cell volume. Cell shrinkage is accompanied by high expression of K^+ channels, which deforms the cell and leads to changes in phosphatases and protein kinases, resulting in uncontrolled cell proliferation. Eag1 channel inhibitors keep the cell in G1/S phase and increase cell volume, both of which lead to a decreased proliferation rate (Wonderlin and Strobl 1996). Several studies indicate that inhibition of hERG and/or Eag1 channels with specific inhibitors in cultured glioblastoma cells reduces proliferation and induces apoptosis (Dong et al. 2023; Shugg et al. 2021; Staudacher et al. 2014). The hERG Inhibitor E-4031 was able to inhibit sphere formation in human glioblastoma xenografts in mice (Pointer et al. 2017). Along this line, suppression of Eag1 expression in glioblastoma cells resulted in growth inhibition and sensitization to drug treatment (Bai et al. 2013; Cunha et al. 2013; Sales et al. 2016). Consequently, inhibition of those channels has been proposed as promising treatment strategy for gliomas (Elias et al. 2023), which prompted us to further investigate hERG/Eag1 inhibition in glioblastoma cells in relation to apoptosis induction and impact on cellular senescence (CSEN).

Here, we aimed at disentangling the contribution of hERG/Eag1 inhibition to TMZ-induced cytotoxicity and CSEN, using established human glioblastoma cell lines and primary glioblastoma cells, by applying the potent inhibitors astemizole and terfenadine as model substances (Toplak et al. 2022). We measured concentration–response curves in 3-(4,5-dimethylthiazol-2-yl)−2,5-diphenyltetrazolium bromide (MTT) assays of astemizole and terfenadine either alone or in combination with TMZ, and in a panel of glioblastoma cells, quantified the effects and determined IC_{50} values. We show that astemizole and terfenadine are both cytotoxic to glioblastoma cells by induction of apoptosis. We also report that both drugs synergistically sensitize glioblastoma cells to TMZ, inducing a high yield of apoptosis and reducing the CSEN level.

Materials and methods

Compounds

Temozolomide, astemizole, and terfenadine were dissolved in dimethyl sulfoxide (DMSO). All compounds were purchased from Merck KGaA (Darmstadt, Germany).

Cell culture

U87-MG, U251-MG, and U373-MG (Uppsala) human glioblastoma cell lines were obtained from Sigma-Aldrich (HPA Culture Collections, St. Louis, USA). The A172 and LN229 human glioblastoma cell line were obtained from American Type Culture Collection (ATCC, Manassas, USA). Cell lines were not used beyond passage 20. U251 Cells were cultivated in Roswell Park Memorial Institute (RPMI) 1640 medium containing 10% fetal calf serum (FCS; both from Biochrom, Berlin, Germany), 2 mM L-glutamine, 100 IU/ml penicillin, and 100 µg/ml streptomycin (all from Biowest, Nuaillé, France). Primary cells and all other cell lines were cultivated in Dulbecco's Modified Eagle Medium (DMEM) containing 10% FCS, 2 mM L-glutamine, 100 IU/ml penicillin, and 100 µg/ml streptomycin (all from Biowest, Nuaillé, France). Glioblastoma cells and tissue specimens derived from a human glioblastoma tumor biopsy were obtained from the University Hospital Cologne and characterized as previously described (Haas et al. 2018).

Western blot analysis

To prepare whole cell lysates, cells were washed with ice cold phosphate-buffered saline (PBS; Biowest, Nuaillé, France) and lysed with ice cold RIPA lysis buffer including 1 × HaltTM protease inhibitor cocktail (both from Thermo Fisher Scientific, Waltham, USA) incubated on ice for 30 min, and centrifuged for 20 min at 4 °C. The supernatant was used for protein content determination and subsequent immunoblotting. For immunoblotting, standard procedures using the following antibodies were used as previously described (Haas et al. 2009): anti-KCNH1 (APC-104; 1:250) and anti-KCNH2 (1:250; APC-109; both from Alomone Labs. Ltd., Jerusalem, Israel) combined with goat anti-rabbit Poly-HRP (1:10,000; Thermo Fisher Scientific, Waltham, USA) and β-Actin-HRP (C-4; Santa Cruz Biotechnology, Dallas, USA). Immunoblots were developed with ECL SuperSignal (Thermo Fisher Scientific, Waltham, USA) and densitometric analysis was performed using ImageJ software.

MTT assay

For MTT assays, we followed a published protocol (Eckstein et al. 2009). Briefly, 5000 U251 cells, 7500 U87 and U373 cells, or 15,000 primary glioblastoma cells were plated on 96-wells and grown at 37 °C and 5% CO_2 overnight. Cell survival after exposure to TMZ, astemizole or terfenadine as indicated was determined after 72 h. Final DMSO concentrations in media did not exceed 1%. Absorbance was measured with a Tecan Microplate Reader (Tecan, Hombrechtikon, Switzerland) at 590 nm.

Fluorescence microscopy

150,000 cells were seeded in 2 mL culture medium in small glass bottom dishes (Willco Wells B.V., Amsterdam, Netherlands) and incubated at 37° C and 5% CO_2 for 48 h. Thereafter, cells were washed twice with PBS and fixed with 4% paraformaldehyde/PBS for 10 min. Fixed cells were washed 3-times with PBS and blocked in 2% bovine serum albumin (BSA; Sigma-Aldrich, St. Louis, USA) including 0.2% Triton X-100 for 30 min. Thereafter cells were incubated with Anti-KCNH2-extracellular-FITC (APC-109-F; Alomone Labs Ltd., Jerusalem, Israel.) and Anti-KCNH1 (APC-104; Alomone Labs Ltd., Jerusalem, Israel) in 2% BSA (1:50) at 4° C overnight. The next day cells were washed and Anti-KCNH1 labelled probes were incubated with Anti-rabbit IgG (H + L) Alex Fluor 688 (Life Technologies) in 2% BSA (1:500) for 1 h. All probes were counterstained with NucRed Dead 647 ReadyProbes Reagent (Thermo Fisher Scientific, Waltham, USA) for 5 min. Finally, stained cells were washed for 3 times with PBS and covered with a coverslip by using fluorescent mounting medium (Merck KGaA, Darmstadt, Germany). Cells stained with secondary antibody only were used as negative control. Eag1/hERG expression was visualized by using a Zeiss LSM 780 microscope (Carl Zeiss AG, Oberkochen, Germany) and 40 × magnification.

Annexin V apoptosis assay

For apoptosis measurements, the FITC Annexin V Apoptosis Detection Kit ll (BD Biosciences, Franklin Lakes, USA) was used according to the manufacturer´s protocol. Briefly, cells were seeded into 6-well plates and incubated at 37° C and 5% CO_2 overnight. After compound treatment for 72 h or 120 h, cells were trypsinized and centrifuged for 4 min at 1500 × g. The supernatant was removed and cells were resuspended in 500 µL binding buffer. Five microliter propidium iodide (PI) and 5 µL Annexin V-FITC were mixed with 100 µL of cells in binding buffer. After 15 min of incubation on ice, samples were analyzed by flow cytometry using a FACSCalibur flow cytometer (Becton Dickinson GmbH, Heidelberg, Germany). The CellQuest pro software (Becton Dickinson GmbH, Heidelberg, Germany) was used for data analysis. Annexin V-/PI- cells were defined as living, annexin V + /PI- and annexin V + /PI + cells were defined as apoptotic cells, and annexin V-/PI + cells were defined as necrotic cells.

Quantification of cellular senescence (CSEN)

The percentage of senescent cells within the population was determined by flow cytometry through the senescence-associated β-galactosidase, a marker for senescence, which was quantified by its reaction with the substrate C_{12}FDG. To this end, cells were preincubated with 300 µM chloroquine (Merck KGaA, Darmstadt, Germany) for 30 min at 37 °C and 5% CO_2 to inhibit endogenous β-galactosidase activity and kept in the dark from this point on. C_{12}FDG (Abcam, Cambridge, UK) was added from a 20 mM stock solution to a final concentration of 33 µM to each sample, and cells were incubated for an additional 90 min at 37° C and 5% CO_2. Cells were then collected, washed, resuspended in an adjusted amount of PBS, and stored on ice until measurement. The FACS Canto II flow cytometer (Becton Dickinson GmbH, Heidelberg, Germany) was used for data acquisition using Flowing Software 2.5.1 program (Perttu Terho, Turku Center for Biotechnology, Turku, Finland) for data analysis. Proliferating cells served as control in each experiment as described (Beltzig et al. 2022a).

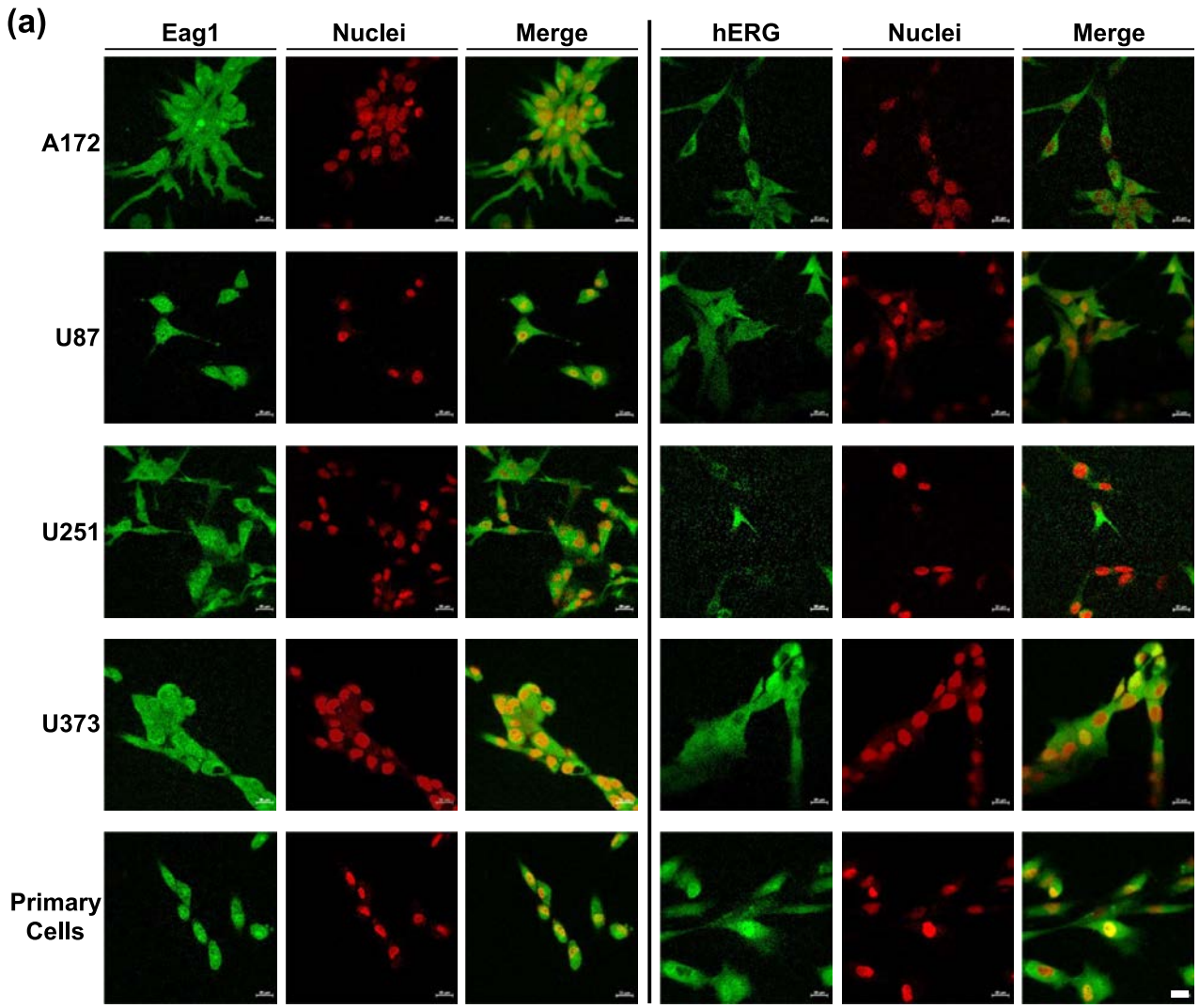
(a)
Eag1
Nuclei
Merge
hERG
Nuclei
Merge
A172
U87
U251
U373
Primary Cells

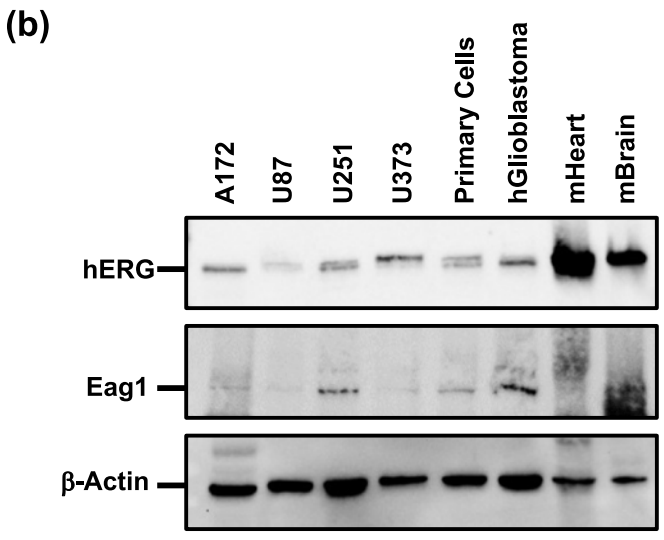
(b)
A172
U87
U251
U373
Primary Cells
hGlioblastoma
mHeart
mBrain
hERG
Eag1
β-Actin

◂**Fig. 1** KCNH protein expression analysis in human glioblastoma cells and tissue. (**a**) Representative immune fluorescence images showing expression of hERG and Eag1 (green fluorescence) in human A172, U87, U251, U373 glioblastoma cell lines and primary human glioblastoma cells. Nuclei are stained in red; scale bar, 20 µm. (**b**) Representative Western blot showing protein expression of hERG and Eag1 in whole cell lysates of human A172, U87, U251, U373 glioblastoma cell lines, primary human glioblastoma cells and human glioblastoma tissue (hGlioblastoma). Murine heart (mHeart) and brain (mBrain) tissues were used as positive controls. β-actin Western blots were performed to control for loading

Data analysis and statistical methods

Concentration effect curves of MTT experiments were fitted to data points by nonlinear regression analysis using the four-parameter logistic equation. Top was set to 100% and bottom to 0% viability (GraphPad Prism, La Jolla, USA). Statistical differences between several groups were determined by ANOVA followed by Tukey's post-hoc test. Data are presented as mean ± SEM. To analyze drug combination effects, the Coefficient of Drug Interaction (CDI) was calculated according to the following equation: $CDI = \frac{A+B-A\times B}{AB}$

When the CDI is under, above or equal to 1, this is indicative of synergy, antagonism or additivity, respectively (Foucquier and Guedj 2015).

Results

Expression analysis of KCNH channels in glioblastoma cells and tissue

Both expression of O^6-methylguanine-DNA methyltransferase (MGMT) and p53 mutations have been linked to TMZ sensitivity of glioblastoma cell lines (Hermisson et al. 2006; Lee 2016). In our study we used cell lines with undetectable MGMT expression. U87, LN229 and A172 are functional p53 wildtype while p53 is mutated in U373 and U251 cells. The mutation status of all used cells can be found in Suppl. Table 1. The expression of hERG and Eag1 in glioblastoma cells and tissues has previously been reported (Masi et al. 2005; Patt et al. 2004). To prove if both channels are actually expressed under the experimental conditions, we determined the protein expression in our panel of glioblastoma cell lines and primary glioblastoma cells. As shown in Fig. 1, hERG and Eag1 channels are expressed to a similar extent in four glioblastoma cell lines (A172, U87, U251, U373) and primary glioblastoma cells, determined by both immunocytochemistry (Fig. 1a) and Western blotting (Fig. 1b and Suppl. Figure 1 a and b). In addition, we confirmed expression of hERG and Eag1 in glioblastoma tissue isolated from a patient biopsy (Fig. 1b).

Blocking hERG/Eag1 induces cytotoxicity in human glioblastoma cells

We next investigated whether inhibition of hERG/Eag1 channels with the well-established and highly potent inhibitors astemizole and terfenadine (Toplak et al. 2022) induces cytotoxicity in selected glioblastoma cells in MTT experiments. We recorded very similar IC_{50} values in all cell lines in the range from 4 to 9 µM after 72 h treatment (Fig. 2a and b). Both drugs displayed a very steep concentration response in all cell lines (Hill slopes ranging from −5.02 to −5.37, Suppl. Table 2). The lowest IC_{50} of 5.8 µM for astemizole was obtained for primary glioblastoma cells (Fig. 2a) and the lowest IC_{50} of 4.8 µM for terfenadine in U373 cells (Fig. 2b). U251 appeared to be the most resistant cell line to both drugs (IC_{50s} of 9.5 µM and 6.2 µM for astemizole and terfenadine, respectively, Fig. 2a and b). In order to test if cell death is driven by apoptosis or necrosis, we performed Annexin V/PI staining followed by flow cytometry of selected cell lines treated with astemizole concentrations close to the previously determined IC_{50} values in comparison to TMZ. Representative plots are shown in Fig. 2c. The experiments revealed that > 70% of cell deaths accounted for apoptosis (Fig. 2d).

Astemizole and terfenadine sensitize human glioblastoma cells to TMZ treatment

It has been reported that astemizole was capable of sensitizing U87 cells to TMZ when given at fixed concentrations at a 72 h treatment schedule (Sales et al. 2016). To determine a concentration relationship in a panel of cell lines, we treated three different glioblastoma cell lines and primary glioblastoma cells with ascending TMZ concentrations combined with respective astemizole concentrations close to the IC_{50} values obtained in previous experiments and performed MTT assays. In addition, we also treated primary cells with TMZ and terfenadine using the same experimental set up. We observed left-shifts of the MTT concentration–response curves after astemizole/TMZ co-treatment and a reduction in TMZ IC_{50} values in all cell lines and primary glioblastoma cells (Fig. 3a–d), indicative of a sensitization. The respective IC_{50} values are displayed in Table 1.

While the observed reduction in TMZ IC_{50} values after co-treatment was low in U251 and U373 cells, the TMZ IC_{50} was approximately reduced by twofold in U87 and primary glioblastoma cells. A similar strong sensitization was observed with terfenadine in primary glioblastoma cells (Suppl. Figure 2a and Table 1).

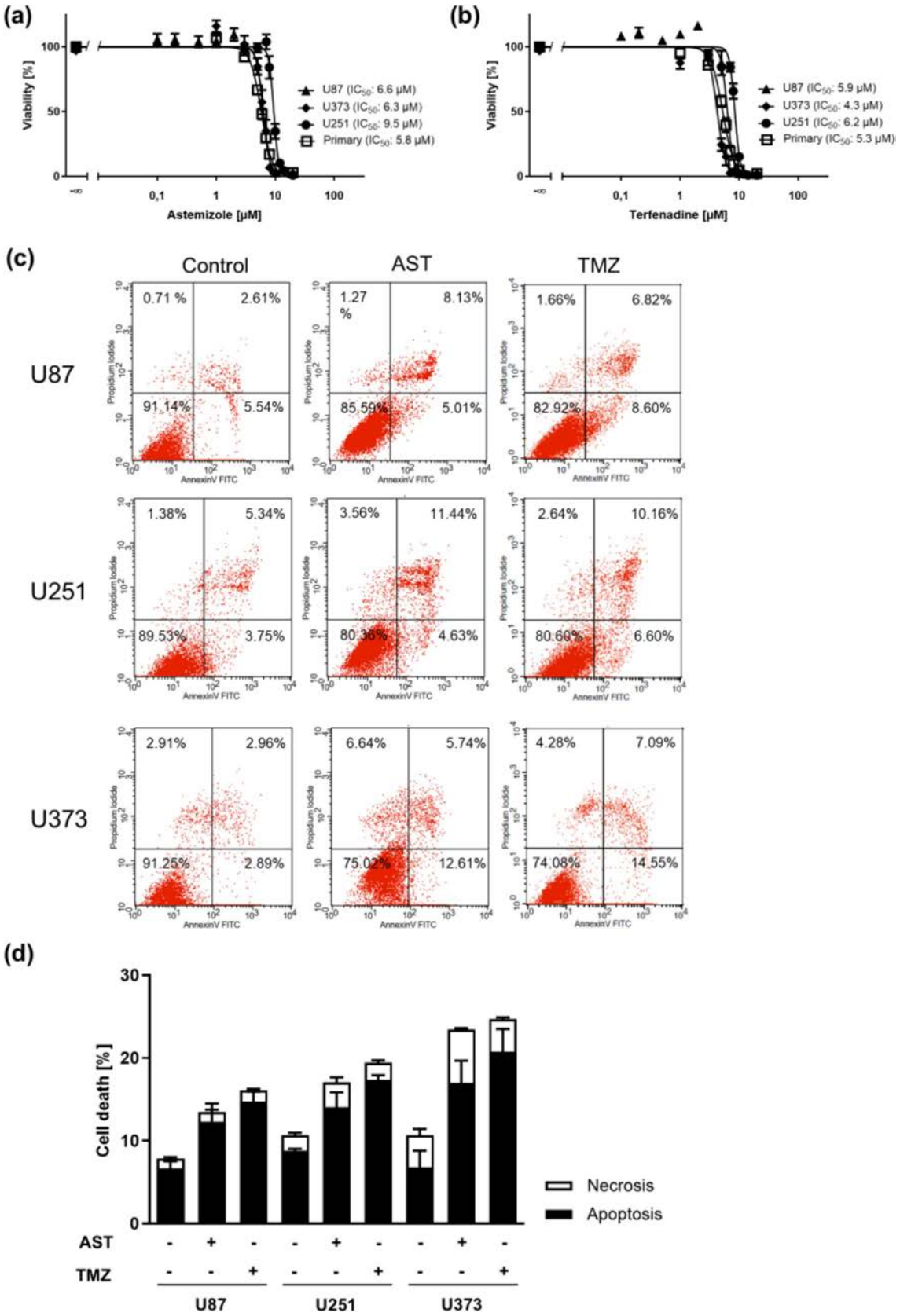
(a)
Viability [%]
Astemizole [µM]
U87 (IC50: 6.6 µM)
U373 (IC50: 6.3 µM)
U251 (IC50: 9.5 µM)
Primary (IC50: 5.8 µM)
(b)
Viability [%]
Terfenadine [µM]
U87 (IC50: 5.9 µM)
U373 (IC50: 4.3 µM)
U251 (IC50: 6.2 µM)
Primary (IC50: 5.3 µM)
(c)
Control
AST
TMZ
U87
0.71 %
2.61%
91.14%
5.54%
1.27 %
8.13%
85.59%
5.01%
1.66%
6.82%
82.92%
8.60%
U251
1.38%
5.34%
89.53%
3.75%
3.56%
11.44%
80.36%
4.63%
2.64%
10.16%
80.60%
6.60%
U373
2.91%
2.96%
91.25%
2.89%
6.64%
5.74%
75.02%
12.61%
4.28%
7.09%
74.08%
14.55%
Propidium Iodide
AnnexinV FITC
(d)
Cell death [%]
Necrosis
Apoptosis
AST
TMZ
U87
U251
U373

◂**Fig. 2** Cytotoxic effects of astemizole and terfenadine in glioblastoma cells. 3-(4,5-dimethylthiazol-2-yl)−2,5-diphenyltetrazolium bromide (MTT) assays of three human glioblastoma cell lines and primary glioblastoma cells treated with increasing concentrations of astemizole (**a**) and terfenadine (**b**) for 72 h, as indicated. (**c**) Representative AnnexinV/propidium iodide (PI) FACS analysis of glioblastoma cell lines U87, U251, and U373 treated with the respective astemizole (AST) IC_{50} or 1 mM temozolomide (TMZ) for 72 h. (**d**) Percent cell death induced via apoptosis or necrosis after AST and TMZ treatment. Annexin V positive cells were considered apoptotic and PI positive/Annexin V negative cells necrotic. Values are displayed as mean ± SEM ($n = 3–4$)

hERG/Eag1 inhibition synergistically increases TMZ-induced apoptosis

We extended the experiment of TMZ and subsequent astemizole treatment by determining the apoptotic rates in several glioblastoma cell lines. Treatment with an astemizole IC_{50} and a fixed TMZ concentration (1 mM) significantly enhanced TMZ-induced apoptosis induction by approximately two- to threefold, with the exception of U251 cells, where no effect of astemizole was detected (Fig. 4a). Importantly, the coefficient of drug interaction (CDI) was < 1 for the A172, U87 and U373 cell lines, which indicates a synergistic effect (Table 2, column Apoptosis, TMZ high, 72 h).

Similar synergistic effects were observed in U87 cells treated with terfenadine and TMZ (CDI < 0.60; Suppl. Figure 2b). While astemizole and terfenadine induce apoptosis early (i.e., 2–3 days) after treatment, TMZ needs a much longer time for lesion processing and cell death pathway induction (5 to 8 days in glioblastoma cells, depending on the respective cell cycle progression) (He and Kaina 2019). Consequently, much lower and physiologically more relevant TMZ concentrations can be applied to effectively kill glioblastoma cells. Therefore, we repeated the experiment with an extended panel of glioblastoma cell lines and treated for 120 h with 50 µM TMZ. This occurred without and with a low astemizole concentration (2 µM) that was not yet cytotoxic when applied alone. In A172, U87 and LN229, but not U251 and U373, we observed a statistically significant and synergistic (CDIs < 1) effect of astemizole on TMZ-induced apoptosis levels (Fig. 4b and Table 2, column Apoptosis, TMZ low, 120 h).

Astemizole reduces TMZ-induced CSEN

Previously, we have shown that TMZ induces CSEN in functionally p53 wildtype LN229 and A172 glioblastoma cells, with a yield of up to 80% over time (Beltzig et al. 2022b). As senescent cells exhibit a proinflammatory phenotype, which is discussed to promote tumor growth (Aasland et al. 2019), strategies are desired to prevent or reduce the level of CSEN induction. To address if Eag1/hERG inhibition impacts CSEN, we determined the senescence level of A172 and LN229 cells following treatment with TMZ alone or in combination with astemizole for 120 h. As previously reported (Aasland et al. 2019; Beltzig et al. 2022b), TMZ significantly induced senescence in both cell lines, while astemizole (2 µM) was ineffective. Interestingly, when TMZ and astemizole were given concomitantly, the senescent cell population was significantly reduced by approximately 50% in both cell lines (Fig. 5 and Suppl. Figure 3). This was reflected by an CDI > 1 indicative of an antagonistic effect of astemizole on TMZ-induced CSEN (Table 2, column CSEN, TMZ low, 120 h).

Discussion

A hallmark of glioblastoma is resistance to radio- and chemotherapy resulting in dismal prognosis. This is also reflected by the fact that about 70% of glioblastoma patients do not show a benefit following TMZ, which stresses the need to further explore mechanisms to enhance the cytotoxic activity of the drug (Chamberlain 2010). In this context it is of interest that the KCNH channels, hERG and Eag1, have been reported to impact glioblastoma proliferation, apoptosis and progression (Elias et al. 2023; He et al. 2020). Moreover, overexpression of both channels in glioma tissues was shown to be correlated with reduced survival and poor prognosis (Martinez et al. 2015; Shugg et al. 2021; Zheng and Song 2023). While several studies revealed that blocking hERG or Eag1 with inhibitors or a genetic knock-down induces cell cycle arrest and apoptosis in glioblastoma cells (Elias et al. 2023), only one study has proposed a sensitizing potential of Eag1 blockade to TMZ treatment in U87 cells (Sales et al. 2016). This prompted us to quantitatively investigate the chemosensitizing effects of hERG/Eag1 inhibition in a panel of human glioblastoma cell lines and patient-derived primary glioblastoma cells. We found that both channels were similarly expressed in all the cells rendering them suitable for further investigations.

Initially, we tested the two hERG/Eag1 blocker astemizole and terfenadine alone and found that both are cytotoxic in all glioblastoma cells to a similar extent (IC_{50} values for both, astemizole and terfenadine, were in the range of 5–8 µM after 72 h-treatment). Cytotoxicity was related to the induction of apoptosis (> 70%), which appeared to be the main cause of cell death. This is in line with what was reported after hERG/Eag1 inhibition in other tumor cell lines (Jehle et al. 2011). As both compounds already induced cytotoxicity after 72 h, we initially used this time to investigate a sensitizing potential on TMZ treatment in concentration–response experiments. Astemizole and terfenadine induced a systematic left shift of the concentration–response curves and reduced the TMZ IC_{50} by around twofold in U87 and primary human glioblastoma cells indicative of a strong

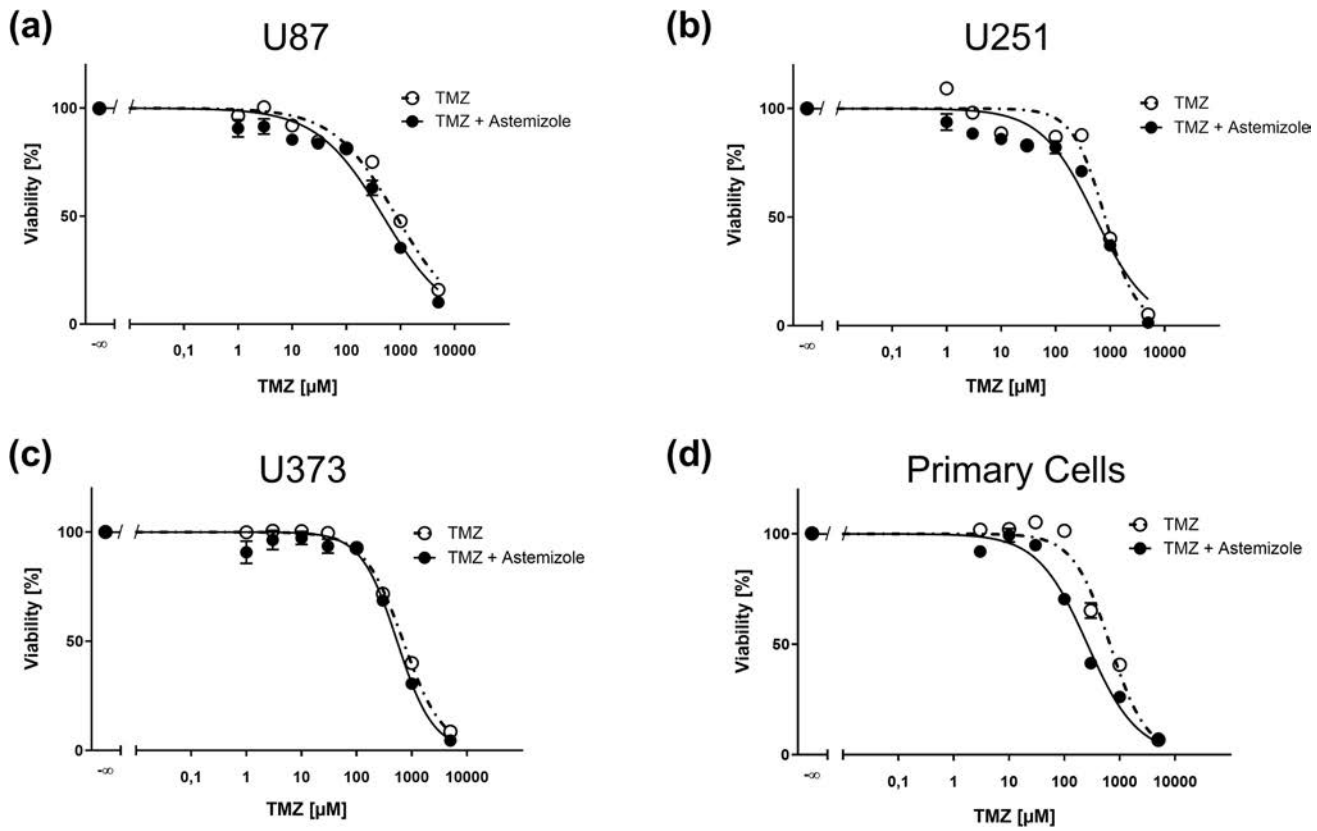

Fig. 3 Astemizole sensitizes glioblastoma cells to temozolomide (TMZ) treatment. MTT assays of U87 (**a**), U251 (**b**), U373 (**c**), and primary glioblastoma cells (**d**) treated with increasing concentrations of TMZ for 72 h alone or in combination with astemizole (5–7 µM). Values are displayed as mean ± SEM ($n = 3$)

Table 1 Temozolomide (TMZ) IC_{50} values derived from MTT assays of TMZ treated (Ctr.) glioblastoma cells with or without astemizole (AST) or terfenadine (TERF). Values are displayed as mean ($n = 3$). The 95% confidence interval (CI) is shown in brackets. ND, not determined

	TMZ IC_{50} (95% CI), [µM]			
Cells	U87	U251	U373	Primary
Ctr	836 (713 – 980)	805 (694 – 935)	700 (637 – 769)	584 (525 – 661)
AST	476 (384 – 590)	533 (434 – 656)	542 (467 – 628)	261 (231 – 294)
TERF	ND	ND	ND	188 (144 – 244)

sensitizing effect across various TMZ concentrations. In U251 and U373 cells, the concentration–response curves largely overlapped and reductions in TMZ IC_{50} values after co-treatment were smaller. In terms of apoptosis induction synergistic effects of astemizole on TMZ treatment at different experimental conditions (e.g., high concentrations for 72 h vs. low concentrations for 120 h) were observed in most cell lines. Again, the U251 cell appeared to be non-responsive towards astemizole treatment in combination with TMZ (CDI > 1). The reasons for these differences remain speculative as all cell lines express hERG and Eag1 channels. But differences might be related to the mutation patterns of the cells. While all used cell lines are IDH wildtype and the MGMT promoter is methylated (Haas et al. 2018; Perazzoli et al. 2015), they differ in the p53 mutation status. U87, A172 and LN229 cells are functionally p53 wildtype and displayed a good response towards combination treatment. In contrast, U251 and U373 cells are p53-mutated (Beltzig et al. 2022b; Hermisson et al. 2006; Lee et al. 2020) and had a lower response rate. This suggests that the p53 status plays a role in the sensitivity of glioblastoma cells towards hERG/Eag1 inhibition, which needs however further and more detailed mechanistic studies.

Recent studies revealed that glioblastoma cells respond to TMZ treatment with the induction of senescence, a phenomenon observed in many cancers upon treatment and described as therapy-induced senescence (TIS). TMZ-induced senescent cells go into a mitotic arrest and display an altered transcriptional, metabolic and secretory phenotype (Aasland et al. 2019; Beltzig et al. 2022b; Tchkonia et al. 2013). Moreover, it was proposed that CSEN might

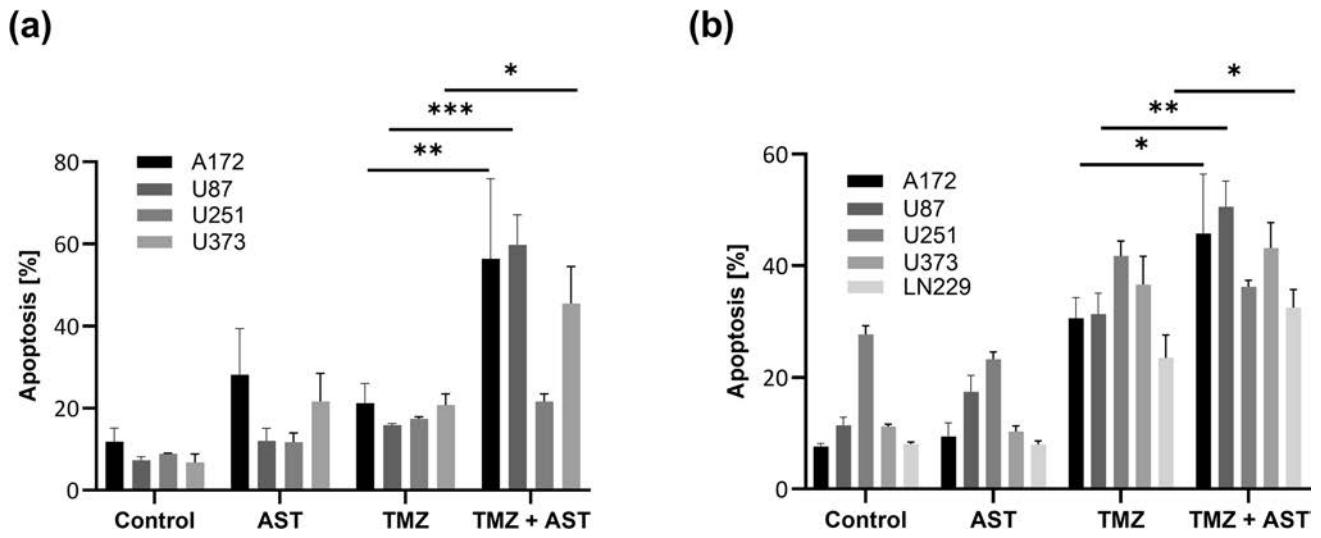

Fig. 4 Sensitization of glioblastoma cells to temozolomide (TMZ)-induced apoptosis by astemizole (AST) at different treatment schedules. AnnexinV/propidium iodide FACS analysis of glioblastoma cell lines treated with a high TMZ concentration (1 mM) for 72 h alone or in combination with astemizole (5–7 µM) (**a**), or a low TMZ concentration (50 µM) for 120 h alone or in combination with 2 µM astemizole (**b**). Values are displayed as mean ± SEM ($n = 3$); *, $p < 0.05$, ** $p < 0.01$, *** $p < 0.001$. One-way Anova with Tukey's post-hoc test

Table 2 Coefficient of drug interaction (CDI) for apoptosis and cellular senescence (CSEN) of temozolomide (TMZ) and astemizole co-treatment at different time points and TMZ concentrations in various glioblastoma cell lines. ND, not determined

Coefficient of drug interaction (CDI)			
	Apoptosis		CSEN
Cells	***TMZ high, 72 h***	***TMZ low, 120 h***	***TMZ low, 120 h***
A172	0.86	0.81	1.89
LN229	ND	0.93	2.18
U87	0.86	0.46	ND
U251	1.25	1.52	ND
U373	0.83	0.91	ND

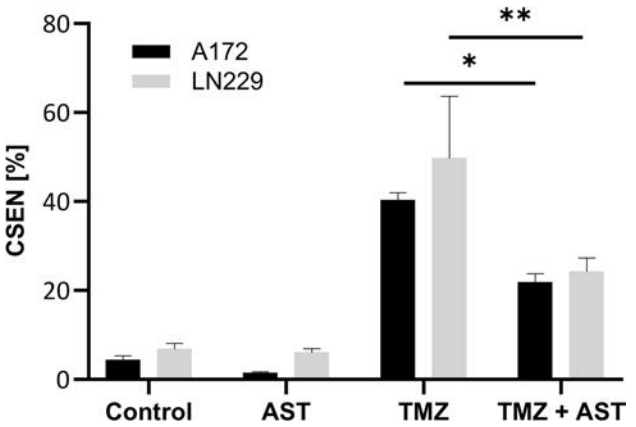

Fig. 5 Effect of astemizole (AST) on temozolomide (TMZ)-induced cellular senescence (CSEN) in two glioblastoma cell lines. C_{12}FDG analysis of LN229 and A172 cells treated with 20 µM TMZ for 120 h alone or in combination with 2 µM astemizole. Values are displayed as mean ± SEM of at least three independent experiments; *, $p < 0.05$, ** $p < 0.01$. One-way Anova with Tukey's post-hoc test

be a driver of tumor recurrence as senescent cells could re-enter the cell cycle after termination of treatment (Milanovic et al. 2018; Ouchi et al. 2016). Furthermore, senescent cells are characterized by a proinflammatory phenotype, which favors tumor growth (Aasland et al. 2019). Novel approaches aim at targeting CSEN by senolytic agents, and for glioblastoma some compounds have been identified so far (Riviere-Cazaux et al. 2023). An alternative strategy rests on inhibition of CSEN induction. TMZ is highly effective in inducing CSEN. Thus, the level of CSEN is raising 3 days after treatment and 8 days later about 80% of the population is in the senescent state (Beltzig et al. 2022b). In this context it is also interesting to note that hERG activation has been implicated in the induction of CSEN in breast cancer cells (Lansu and Gentile 2013). Here, we show for the first time that inhibition of hERG/Eag1 by concomitant treatment of glioblastoma cells with TMZ and astemizole significantly reduced TMZ-induced CSEN (by about 50%). This was accompanied by an increase in the apoptotic cell death level, which indicates that hERG/Eag1 inhibition has the potential to inhibit the CSEN pathway and pushing cells into the death pathway. We did not mechanistically follow up on our findings and clearly further research is needed to investigate the underlying mechanisms. However, our results are encouraging and might pave the way for further experimentation. Importantly, studies have shown that astemizole

has good brain permeability (Di et al. 2003; Rojo et al. 2010) and, therefore, is proposed as treatment modality in Alzheimer's and Parkinson's disease (Rojo et al. 2010; Sun et al. 2016). One shortcoming of many hERG blocking agents like astemizole and terfenadine is their proarrhythmic and torsadogenic potential by the inhibition of hERG channels in cardiomyocytes (Zunkler 2006). But there are several other commercial drugs available (e.g., amitriptyline, haloperidol or fluoxetine) with good hERG/Eag1 blocking activity, but rather moderate proarrhythmic effects in patients. Most importantly, glioblastoma patients with a high hERG expression level who took those drugs in conjunction with TMZ/radiation had a better survival rate (Pointer et al. 2017).

Overall, we conclude that blocking hERG/Eag1 channels in glioblastoma is a promising strategy to overcome TMZ-induced senescence and drug resistance. Further in vitro and in vivo studies are required to define the mode of action and proof the efficacy in animal models before clinical use can be envisioned.

Supplementary Information The online version contains supplementary material available at https://doi.org/10.1007/s00210-025-03955-w.

Acknowledgements We thank M Timmer for providing primary human glioblastoma cells and tissue specimens. We are grateful to J Altmaier for support and N Eckstein (RIP) and BJ Zünkler for expert scientific advice.

Authors' contributions B.H. and B.K. conceived and designed research. B.H., B.K., I.R., L.B., L.K. and M.W.-M. conducted experiments. B.H., B.K., I.R., L.B. and L.K. analyzed data. B.H. prepared figures and wrote the manuscript. All authors read and approved the manuscript. The authors declare that all data were generated in-house and that no paper mill was used.

Funding Open Access funding enabled and organized by Projekt DEAL.

Data availability All source data for this work (or generated in this study) are available upon reasonable request.

Declarations

Competing interests The authors declare no competing nor financial and non-financial interests.

Disclaimer The opinions mentioned throughout the following article are personal views of the authors and do not reflect an official position of the Federal Institute for Drugs and Medical Devices (BfArM).

References

Aasland D et al (2019) Temozolomide Induces Senescence and Repression of DNA Repair Pathways in Glioblastoma Cells via Activation of ATR-CHK1, p21, and NF-kappaB. Cancer Res 79:99–113. https://doi.org/10.1158/0008-5472.CAN-18-1733

Bai Y et al (2013) MiR-296–3p regulates cell growth and multi-drug resistance of human glioblastoma by targeting ether-a-go-go (EAG1). Eur J Cancer 49:710–724. https://doi.org/10.1016/j.ejca.2012.08.020

Beltzig L, Christmann M, Kaina B (2022a) Abrogation of Cellular Senescence Induced by Temozolomide in Glioblastoma Cells: Search for Senolytics. Cells 11:2588. https://doi.org/10.3390/cells11162588

Beltzig L et al (2022b) Senescence Is the Main Trait Induced by Temozolomide in Glioblastoma Cells. Cancers (Basel) 14:2233. https://doi.org/10.3390/cancers14092233

Chamberlain MC (2010) Temozolomide: therapeutic limitations in the treatment of adult high-grade gliomas. Expert Rev Neurother 10:1537–1544. https://doi.org/10.1586/ern.10.32

Cunha LC, Del Bel E, Pardo L, Stuhmer W, Titze DEAR (2013) RNA interference with EAG1 enhances interferon gamma injury to glioma cells in vitro. Anticancer Res 33:865–870

Di L, Kerns EH, Fan K, McConnell OJ, Carter GT (2003) High throughput artificial membrane permeability assay for blood-brain barrier. Eur J Med Chem 38:223–232. https://doi.org/10.1016/s0223-5234(03)00012-6

Dong W et al (2023) A designer peptide against the EAG2-Kvbeta2 potassium channel targets the interaction of cancer cells and neurons to treat glioblastoma. Nat Cancer 4:1418–1436. https://doi.org/10.1038/s43018-023-00626-8

Eckstein N et al (2009) Hyperactivation of the insulin-like growth factor receptor I signaling pathway is an essential event for cisplatin resistance of ovarian cancer cells. Cancer Res 69:2996–3003. https://doi.org/10.1158/0008-5472.CAN-08-3153

Elias AF, Lin BC, Piggott BJ (2023) Ion Channels in Gliomas-From Molecular Basis to Treatment. Int J Mol Sci 24. https://doi.org/10.3390/ijms24032530

Foucquier J, Guedj M (2015) Analysis of drug combinations: current methodological landscape. Pharmacol Res Perspect 3:e00149. https://doi.org/10.1002/prp2.149

Haas B et al (2009) Protein kinase G controls brown fat cell differentiation and mitochondrial biogenesis. Sci Signal 2:ra78. https://doi.org/10.1126/scisignal.2000511

Haas B et al (2018) Inhibition of the PI3K but not the MEK/ERK pathway sensitizes human glioma cells to alkylating drugs. Cancer Cell Int 18:69. https://doi.org/10.1186/s12935-018-0565-4

He Y, Kaina B (2019) Are There Thresholds in Glioblastoma Cell Death Responses Triggered by Temozolomide? Int J Mol Sci 20:1562. https://doi.org/10.3390/ijms20071562

He S et al (2020) HERG channel and cancer: A mechanistic review of carcinogenic processes and therapeutic potential Biochim Biophys Acta Rev. Cancer 1873:188355. https://doi.org/10.1016/j.bbcan.2020.188355

Hermisson M et al (2006) O6-methylguanine DNA methyltransferase and p53 status predict temozolomide sensitivity in human malignant glioma cells. J Neurochem 96:766–776. https://doi.org/10.1111/j.1471-4159.2005.03583.x

Jehle J, Schweizer PA, Katus HA, Thomas D (2011) Novel roles for hERG K(+) channels in cell proliferation and apoptosis. Cell Death Dis 2:e193. https://doi.org/10.1038/cddis.2011.77

Kaina B (2023) Temozolomide, Procarbazine and Nitrosoureas in the Therapy of Malignant Gliomas: Update of Mechanisms, Drug Resistance and Therapeutic Implications. J Clin Med 12:744. https://doi.org/10.3390/jcm12237442

Komori T (2022) [The 2021 WHO Classification of Tumors, 5th edition, Central Nervous System Tumors: A Short Review]. Brain Nerve 74:803–809. https://doi.org/10.11477/mf.1416202124

Lansu K, Gentile S (2013) Potassium channel activation inhibits proliferation of breast cancer cells by activating a senescence program. Cell Death Dis 4:e652. https://doi.org/10.1038/cddis.2013.174

Lastraioli E, Iorio J, Arcangeli A (2015) Ion channel expression as promising cancer biomarker. Biochim Biophys Acta 1848:2685–2702. https://doi.org/10.1016/j.bbamem.2014.12.016

Lee SY (2016) Temozolomide resistance in glioblastoma multiforme. Genes Dis 3:198–210. https://doi.org/10.1016/j.gendis.2016.04.007

Lee YJ, Seo HW, Baek JH, Lim SH, Hwang SG, Kim EH (2020) Gene expression profiling of glioblastoma cell lines depending on TP53 status after tumor-treating fields (TTFields) treatment. Sci Rep 10:12272. https://doi.org/10.1038/s41598-020-68473-6

Louis DN et al (2021) The 2021 WHO Classification of Tumors of the Central Nervous System: a summary. Neuro Oncol 23:1231–1251. https://doi.org/10.1093/neuonc/noab106

Martin S, Lino de Oliveira C, Mello de Queiroz F, Pardo LA, Stuhmer W, Del Bel E (2008) Eag1 potassium channel immunohistochemistry in the CNS of adult rat and selected regions of human brain. Neuroscience 155:833–844. https://doi.org/10.1016/j.neuroscience.2008.05.019

Martinez R, Stuhmer W, Martin S, Schell J, Reichmann A, Rohde V, Pardo L (2015) Analysis of the expression of Kv10.1 potassium channel in patients with brain metastases and glioblastoma multiforme: impact on survival. BMC Cancer 15:839. https://doi.org/10.1186/s12885-015-1848-y

Masi A et al (2005) hERG1 channels are overexpressed in glioblastoma multiforme and modulate VEGF secretion in glioblastoma cell lines. Br J Cancer 93:781–792. https://doi.org/10.1038/sj.bjc.6602775

Meyer R, Heinemann SH (1998) Characterization of an eag-like potassium channel in human neuroblastoma cells. J Physiol 508(Pt 1):49–56. https://doi.org/10.1111/j.1469-7793.1998.049br.x

Milanovic M et al (2018) Senescence-associated reprogramming promotes cancer stemness. Nature 553:96–100. https://doi.org/10.1038/nature25167

Nilius B, Wohlrab W (1992) Potassium channels and regulation of proliferation of human melanoma cells. J Physiol 445:537–548. https://doi.org/10.1113/jphysiol.1992.sp018938

Nilius B, Schwarz G, Droogmans G (1993) Control of intracellular calcium by membrane potential in human melanoma cells. Am J Physiol 265:C1501-1510. https://doi.org/10.1152/ajpcell.1993.265.6.C1501

Ouchi R, Okabe S, Migita T, Nakano I, Seimiya H (2016) Senescence from glioma stem cell differentiation promotes tumor growth. Biochem Biophys Res Commun 470:275–281. https://doi.org/10.1016/j.bbrc.2016.01.071

Pardo LA, Stuhmer W (2014) The roles of K(+) channels in cancer. Nat Rev Cancer 14:39–48. https://doi.org/10.1038/nrc3635

Pardo LA, del Camino D, Sanchez A, Alves F, Bruggemann A, Beckh S, Stuhmer W (1999) Oncogenic potential of EAG K(+) channels. EMBO J 18:5540–5547. https://doi.org/10.1093/emboj/18.20.5540

Patt S et al (2004) Expression of ether a go-go potassium channels in human gliomas. Neurosci Lett 368:249–253. https://doi.org/10.1016/j.neulet.2004.07.001

Perazzoli G et al (2015) Temozolomide Resistance in Glioblastoma Cell Lines: Implication of MGMT, MMR, P-Glycoprotein and CD133 Expression. PLoS One 10:e0140131. https://doi.org/10.1371/journal.pone.01401314

Pointer KB, Clark PA, Eliceiri KW, Salamat MS, Robertson GA, Kuo JS (2017) Administration of Non-Torsadogenic human Ether-a-go-go-Related Gene Inhibitors Is Associated with Better Survival for High hERG-Expressing Glioblastoma Patients. Clin Cancer Res 23:73–80. https://doi.org/10.1158/1078-0432.CCR-15-3169

Price M et al (2024) CBTRUS Statistical Report: Primary Brain and Other Central Nervous System Tumors Diagnosed in the United States in 2017–2021. Neuro Oncol 26:vi1–vi85. https://doi.org/10.1093/neuonc/noae145

Riviere-Cazaux C et al (2023) An untapped window of opportunity for glioma: targeting therapy-induced senescence prior to recurrence NPJ Precis. Oncol 7:126. https://doi.org/10.1038/s41698-023-00476-8

Rojo LE, Alzate-Morales J, Saavedra IN, Davies P, Maccioni RB (2010) Selective interaction of lansoprazole and astemizole with tau polymers: potential new clinical use in diagnosis of Alzheimer's disease. J Alzheimers Dis 19:573–589. https://doi.org/10.3233/JAD-2010-1262

Sales TT, Resende FF, Chaves NL, Titze-De-Almeida SS, Bao SN, Brettas ML, Titze-De-Almeida R (2016) Suppression of the Eag1 potassium channel sensitizes glioblastoma cells to injury caused by temozolomide. Oncol Lett 12:2581–2589. https://doi.org/10.3892/ol.2016.4992

Shugg T, Dave N, Amarh E, Assiri AA, Pollok KE, Overholser BR (2021) Letrozole targets the human ether-a-go-go-related gene potassium current in glioblastoma. Basic Clin Pharmacol Toxicol 128:357–365. https://doi.org/10.1111/bcpt.13515

Staudacher I et al (2014) HERG K+ channel-dependent apoptosis and cell cycle arrest in human glioblastoma cells. PLoS One 9:e88164. https://doi.org/10.1371/journal.pone.0088164

Stupp R et al (2005) Radiotherapy plus concomitant and adjuvant temozolomide for glioblastoma. N Engl J Med 352:987–996. https://doi.org/10.1056/NEJMoa043330

Stupp R et al (2009) Effects of radiotherapy with concomitant and adjuvant temozolomide versus radiotherapy alone on survival in glioblastoma in a randomised phase III study: 5-year analysis of the EORTC-NCIC trial. Lancet Oncol 10:459–466. https://doi.org/10.1016/S1470-2045(09)70025-7

Sun AG, Lin AQ, Huang SY, Huo D, Cong CH (2016) Identification of potential drugs for Parkinson's disease based on a sub-pathway method. Int J Neurosci 126:318–325. https://doi.org/10.3109/00207454.2014.986673

Tchkonia T, Zhu Y, van Deursen J, Campisi J, Kirkland JL (2013) Cellular senescence and the senescent secretory phenotype: therapeutic opportunities. J Clin Invest 123:966–972. https://doi.org/10.1172/JCI64098

Toplak Z et al (2022) Overcoming challenges of HERG potassium channel liability through rational design: Eag1 inhibitors for cancer treatment. Med Res Rev 42:183–226. https://doi.org/10.1002/med.21808

Vandenberg JI, Perry MD, Perrin MJ, Mann SA, Ke Y, Hill AP (2012) hERG K(+) channels: structure, function, and clinical significance. Physiol Rev 92:1393–1478. https://doi.org/10.1152/physrev.00036.2011

Wang X, Chen Y, Zhang Y, Guo S, Mo L, An H, Zhan Y (2017) Eag1 Voltage-Dependent Potassium Channels: Structure, Electrophysiological Characteristics, and Function in Cancer. J Membr Biol 250:123–132. https://doi.org/10.1007/s00232-016-9944-8

Wonderlin WF, Strobl JS (1996) Potassium channels, proliferation and G1 progression. J Membr Biol 154:91–107. https://doi.org/10.1007/s002329900135

Wulff H, Castle NA, Pardo LA (2009) Voltage-gated potassium channels as therapeutic targets. Nat Rev Drug Discov 8:982–1001. https://doi.org/10.1038/nrd2983

Zhang L, Pitcher LE, Prahalad V, Niedernhofer LJ, Robbins PD (2023) Targeting cellular senescence with senotherapeutics: senolytics and senomorphics. FEBS J 290:1362–1383. https://doi.org/10.1111/febs.16350

Zheng Z, Song Y (2023) Integrated analysis of the voltage-gated potassium channel-associated gene KCNH2 across cancers. BMC Bioinformatics 24:51. https://doi.org/10.1186/s12859-023-05180-9

Zunkler BJ (2006) Human ether-a-go-go-related (HERG) gene and ATP-sensitive potassium channels as targets for adverse drug effects. Pharmacol Ther 112:12–37. https://doi.org/10.1016/j.pharmthera.2006.03.002

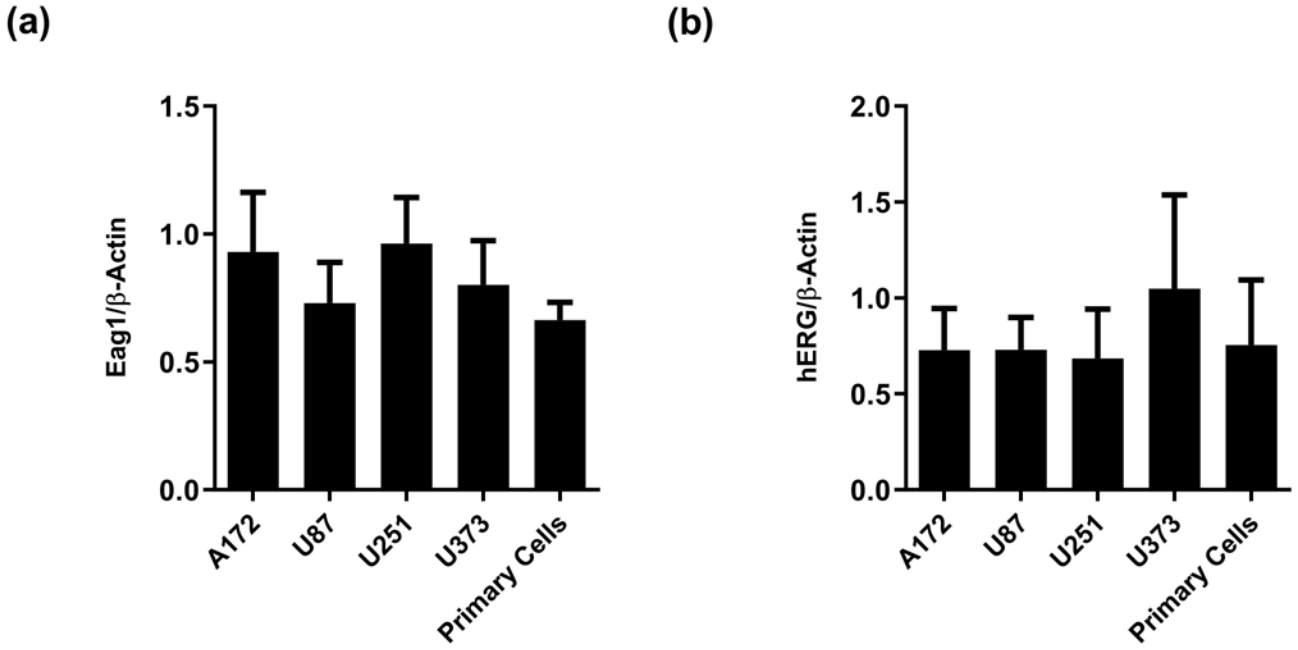

Suppl. Fig. 1 Quantification of Eag1 (**a**) and hERG (**b**) protein expression in A172, U87, U251, U373 and primary glioblastoma cells. Western Blot bands were analyzed by densitometric analysis and values for Eag1 and hERG were normalized to β-Actin. Values are displayed as mean +/- SEM (n = 3).

Supplementary Table 1: Genetic status of investigated cells.

Cells	p53	IDH	MGMT promoter status	PTEN
LN229	wt	wt	methylated	wt
A172	wt	wt	methylated	mut
U251	mut	wt	methylated	mut
U373	mut	wt	methylated	mut
U87	wt	wt	methylated	mut
Primary cells	unknown	wt	methylated	unknown

Abbreviations: IDH, isocitrate dehydrogenase; MGMT, O^6-methylguanine-DNA methyltransferase, PTEN, phosphatase and tensin homolog; Sources: Beltzig et al. 2022; Furnari et al. 1997; Haas et al. 2018; Hermisson et al. 2006; Lee et al. 2020; Perazzoli et al. 2015; American Type Culture Collection (https://www.atcc.org/)

References

Beltzig L et al. (2022) Senescence Is the Main Trait Induced by Temozolomide in Glioblastoma Cells Cancers (Basel) 14 doi:10.3390/cancers14092233

Furnari FB, Lin H, Huang HS, Cavenee WK (1997) Growth suppression of glioma cells by PTEN requires a functional phosphatase catalytic domain Proc Natl Acad Sci U S A 94:12479-12484 doi:10.1073/pnas.94.23.12479

Haas B et al. (2018) Inhibition of the PI3K but not the MEK/ERK pathway sensitizes human glioma cells to alkylating drugs Cancer Cell Int 18:69 doi:10.1186/s12935-018-0565-4

Hermisson M et al. (2006) O6-methylguanine DNA methyltransferase and p53 status predict temozolomide sensitivity in human malignant glioma cells J Neurochem 96:766-776 doi:10.1111/j.1471-4159.2005.03583.x

Lee YJ, Seo HW, Baek JH, Lim SH, Hwang SG, Kim EH (2020) Gene expression profiling of glioblastoma cell lines depending on TP53 status after tumor-treating fields (TTFields) treatment Sci Rep 10:12272 doi:10.1038/s41598-020-68473-6

Perazzoli G et al. (2015) Temozolomide Resistance in Glioblastoma Cell Lines: Implication of MGMT, MMR, P-Glycoprotein and CD133 Expression PLoS One 10:e0140131 doi:10.1371/journal.pone.0140131

Supplementary Table 2: Hill slopes and IC_{50} values from MTT assays of glioblastoma cells treated with astemizole or terfenadine for 72 h.

	Astemizole			**Terfenadine**		
	Hill slope	**Log IC_{50}**	**IC_{50} [µM]**	**Hill slope**	**Log IC_{50}**	**IC_{50} [µM]**
U87	- 12.79 +/- 1.622	- 5.182 +/- 0.00503	6.6	- 22.54 +/- 6.856	- 5.23 +/- 0.00442	5.9
U251	- 10.61 +/- 1.395	- 5.02 +/- 0.00672	9.5	- 12.71 +/- 1.471	- 5.21 +/- 0.00428	6.2
U373	- 7.94 +/- 1.176	- 5.20 +/- 0.00852	6.3	- 6.156 +/- 0.744	- 5.37 +/- 0.0132	4.3
Primary Cells	- 4.689 +/- 0.3013	- 5.236 +/- 0.00548	5.8	- 4.434 +/- 0.4086	- 5.279 +/- 0.00912	5.3

(a)

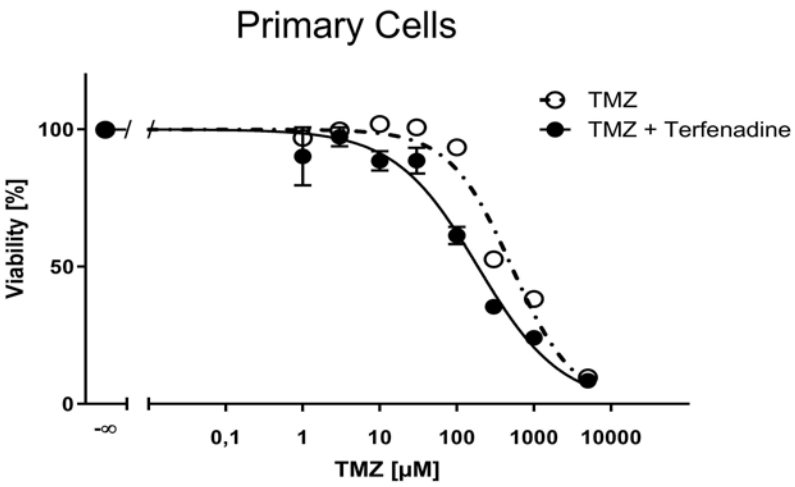

(b)

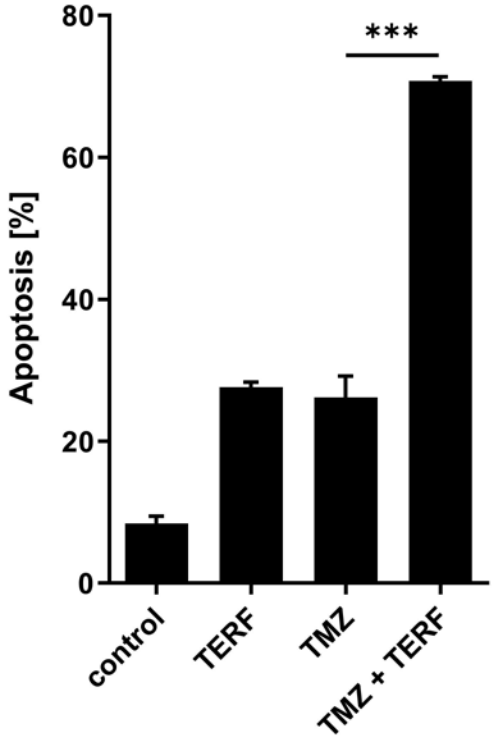

Coefficient of drug interaction (CDI)

Cells	*U87*
CDI	0.59

Suppl. Fig. 2 (**a**) MTT assay of primary glioblastoma cells treated with increasing concentrations of temozolomide (TMZ) for 72 h alone or in combination with 5 µM terfenadine (TERF). (**b**) AnnexinV/propidium iodide FACS analysis (left) of U87 glioblastoma cell line treated with 1 mM TMZ for 72 h alone or in combination with 5 µM terfenadine. The table (right) shows the Coefficient of Drug Interaction (CDI) indicating a strong synergistic effect of terfenadine on TMZ-induced apoptosis induction. Values are displayed as mean +/- SEM (n = 3); *** $p < 0.001$. One-way Anova with Tukey's post-hoc test.

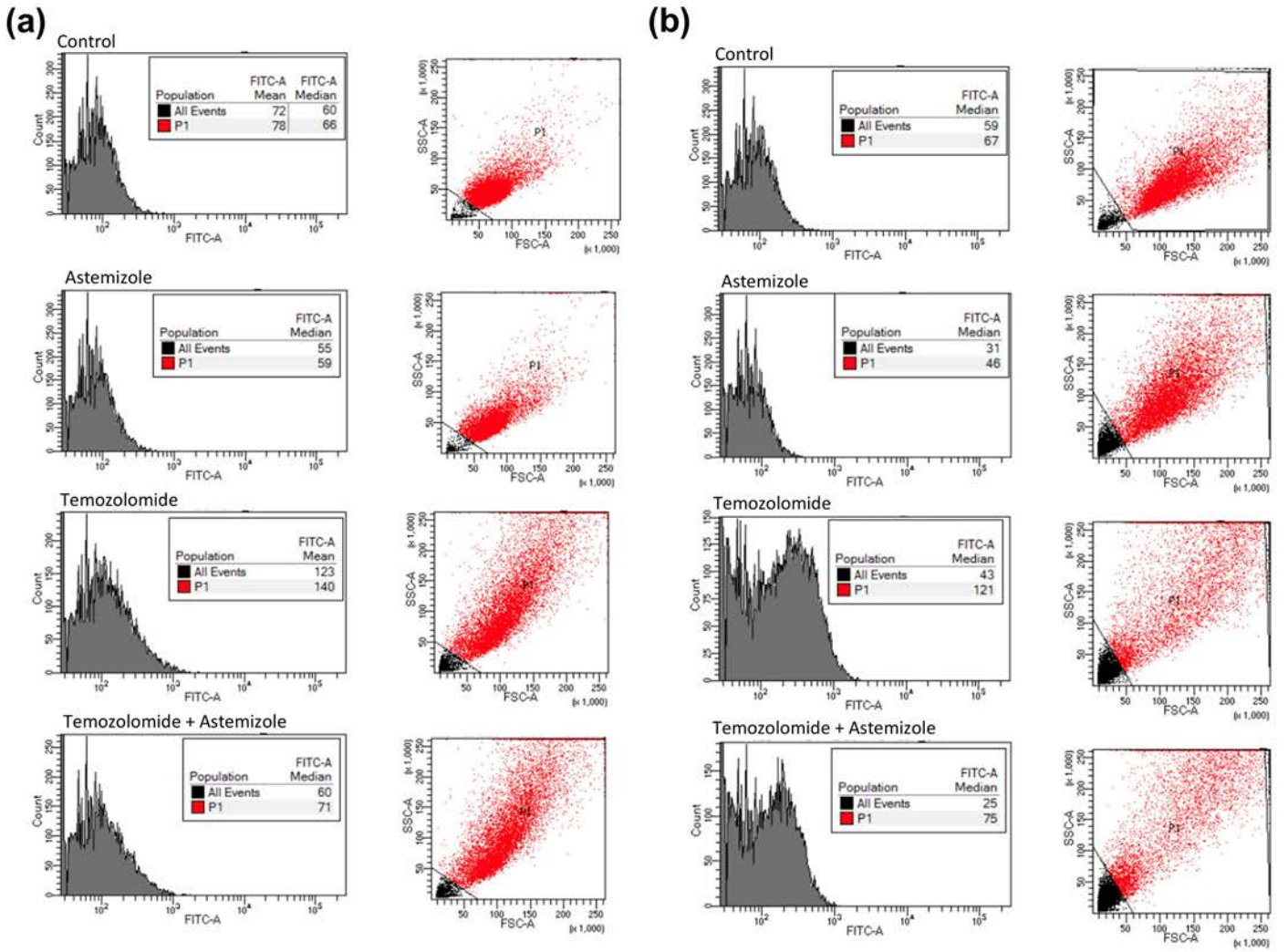

Suppl. Fig. 3 Representative blots of senescence measured by C_{12}FDG flow cytometry. LN229 cells (**a**) and A172 cells (**b**) treated with Astemizole, Temozolomide and Temozolomide + Astemizole (from top to bottom).

4 Diskussion

Glioblastome gehören zu den tödlichsten Tumorentitäten überhaupt. Dies liegt zum einen daran, dass Glioblastome infiltrativ wachsen und keinen abgekapselten Tumor bilden, sodass die komplette chirurgische Resektion kaum möglich ist. Zum anderen sprechen sie sehr schlecht auf die Strahlen- und Chemotherapie an, was zur Folge hat, dass die 5-Jahres-Überlebensrate trotz Therapie bei nur etwa 6% liegt (Price et al., 2024). Seit der Studie von Stupp et al. vor 20 Jahren ist TMZ adjuvant zur Bestrahlung bis heute der Goldstandard in der Therapie (Stupp et al., 2005). Es gibt Daten einer Phase III Studie, die eine Verlängerung des progressionsfreien Gesamtüberlebens nach der Behandlung mit elektrischen Wechselfeldern zusätzlich zur Standardtherapie zeigen (Stupp et al., 2017). Eine allgemeine Empfehlung zur Aufnahme in die Behandlungsleitlinie ist aber bisher nicht erfolgt (Wick et al., 2021). Sowohl der Nitrosoharnstoff Lomustin als auch der monoklonale VEGF-Antikörper Bevacizumab zeigten in klinischen Studien in Kombination mit der Standardtherapie ein verlängertes progressionsfreies Überleben. Beide hatten jedoch keinen nennenswerten Einfluss auf das Gesamtüberleben (Herrlinger et al., 2019; Chinot et al., 2014; Gilbert et al., 2014), weshalb sie bisher nicht für die Behandlung von Glioblastomen zugelassen sind.

Der Grund für das schlechte Ansprechen der Therapie ist die ausgeprägte intrinsische Resistenz des Glioblastoms auf Grund von Mutationen und einer veränderten Aktivitzät von DNA-Reparaturenzymen und Tumorsuppressorgenen gepaart mit einer Überaktivierung von Rezeptortyrosinkinase-Signalwegen. Insbesondere der PI3K-Signalweg ist in Glioblastomen häufig überaktiviert, entweder durch die vorgeschalteten Rezeptortyrosinkinasen wie EGFR oder durch Mutationen in *PTEN*, was mit einer schlechten klinischen Prognose einhergeht (Chakravarti et al., 2004). Es gibt ausreichend Daten an verschiedenen Tumoren einschließlich Glioblastomen, die belegen, dass eine Hemmung des Signalweges der Chemoresistenz entgegenwirken kann (He et al., 2021; Colardo et al., 2021). Allerdings sind die Erfolge auf präklinische Studien beschränkt und ein klinischer Erfolg blieb bisher aus. Häufig spielen pharmakokinetische Gründe für die ausbleibende klinische Wirkung eine Rolle, da die Arzneimittel Blut-Hirn-Schranken gängig sein müssen, um ausreichende Spiegel im Tumorgewebe zu erreichen. Weiterhin ist der PI3K-Signalweg ubiquitär und an vielen metabolischen Prozessen beteiligt, sodass eine Blockade häufig auch zu unerwünschten Wirkungen und zum Abbruch der klinischen Studien führt. Es wird

auch diskutiert, dass die alleinige Hemmung nur eines Signalweges möglicherweise nicht ausreicht, da im Gegenzug andere Signalwege, wie zum Beispiel der RAS-Signalweg oder übergeordnete Rezeptortyrosinkinasen hochreguliert werden und somit die Hemmung umgangen wird (Westhoff et al., 2014). Diese Hypothese war der Ausgangspunkt für die erste Arbeit (3.1; Haas et al., 2018a), die zunächst den genauen Aktivierungsstatus in Glioblastom-Biopsien und *PTEN*-mutierten Zellen untersuchte und durch gezielte Hemmung der Signalwege den Einfluss auf die Resistenz gegenüber Alkylanzien aufklären sollte. Wir hatten die Möglichkeit seltene Proben von sekundären Glioblastomen (*IDH*-mutiert) vor Therapie (n=4) und nach Auftreten eines Rezidivs nach Therapie (n=4) derselben Patienten untersuchen zu können. Während Proteine der RAS-Signalkaskade in allen Proben gleich überaktiviert waren, zeigte sich eine reduzierte Phosphorylierung von AKT und des nachgeschalteten Transkriptionsfaktors CREB in den Rezidiven. Dies deutet darauf hin, dass die Behandlung einen Einfluss auf den PI3K-Signalweg hat und bei der Resistenzentwicklung eine Rolle zu spielen scheint. Ebenfalls fand sich eine verminderte Expression von Pro-Caspase 3, was belegt, dass die Apoptose in den Rezidiven reduziert ist. Es ist jedoch anzumerken, dass die hier untersuchten Tumorproben von sekundären Glioblastomen stammten, die zwar histologisch vergleichbar zu primären Glioblastomen sind, sich aber im *IDH*-Mutationsstatus unterscheiden. Des Weiteren war uns der *MGMT*-Promotormethylierungsstatus nicht bekannt, sodass sich die Ergebnisse nicht eins zu eins auf die klinische Situation übertragen lassen. Die untersuchten *PTEN*-mutierten Glioblastom-Zelllinien waren schon vor einer Behandlung mit Cisplatin, welches zunächst als alkylierende Modellsubstanz verwendet wurde, vergleichbar resistent (vergleichbare Cisplatin IC_{50}-Werte) wie Cisplatin-adaptierte Brustkrebszellen (MCF-7 CisR) und Ovarialkarzinomzellen (A2780 CisR), die in einer vorangegangenen Arbeit von den Kooperationspartnern generiert worden waren (Eckstein et al., 2008). Cisplatin-Behandlungszyklen von 24 Wochen verringerten das Ansprechen der Glioblastom-Zelllinien nicht weiter. In immer wieder gleich durchgeführten MTT-Versuchen veränderten sich die IC_{50}-Werte für Cisplatin über 24 Wochen kaum. Dies zeigt insgesamt, dass die Zellen ihren maximalen Resistenzgrad bereits vor Behandlung erreicht haben. Eine Hemmung der übergeordneten Rezeptortyrosinkinasen EGFR, IGFR und PDGFR, die in den Zellen intrinsisch aktiviert waren, blieb erfolglos in der Beeinflussung der Chemotherapie. Wie sich mittlerweile gezeigt hat, haben

Rezeptortyrosinkinase-Inhibitoren zur Behandlung von Glioblastomen auch klinische kaum eine Wirkung (Alexandru et al., 2020). Ein wichtiger Aspekt dieser Arbeit ist, dass nur eine Hemmung der PI3K die Sensitivität der Zellen gegenüber TMZ verbessern konnte, eine Hemmung von MEK mit zwei verschiedenen Inhibitoren reduzierte sogar das Ansprechen auf TMZ. Dies lässt sich damit erklären, dass eine MEK-Hemmung die Zellproliferation der Zellen so stark reduziert, dass TMZ, das auf Proliferation zur Entfaltung seiner DNA-schädigenden und zytotoxischen Wirkung angewiesen ist, nicht mehr wirken kann. Dies passt auch zu Ergebnissen einer Studie, die zeigte, dass der RAF-Inhibitor Sorafenib zwar die Zellproliferation von Glioblastom-Zellen reduzierte, aber keinen Einfluss auf die Sensitivität gegenüber einer Chemotherapie hatte (Riedel et al., 2016). Der PI3K-Signalweg reguliert in Glioblastomen unter anderem Apoptose und DNA-Reparaturmechanismen (Westhoff et al., 2014). AKT inhibiert die MMR, die benötigt wird, um die durch TMZ ausgelösten O^6meG-Läsionen zu prozessieren und Apoptose auszulösen. Zusätzlich aktiviert AKT die BER und steigert so die Reparatur der zytotoxischen N^3meA- und N^7meG-Läsionen (Liu et al., 2014). Dies könnte miterklären, warum ein überaktivierter PI3K-Signalweg das Ansprechen der Zellen auf TMZ verringert. Im Umkehrschluss lässt eine PI3K-Hemmung die MMR wieder arbeiten und reduziert die BER, wodurch TMZ wirksamer wird (vergleiche hierzu Abbildung 2 in Abschnitt 2.3.3.1). In unseren Versuchen zeigte sich dies in einer Zunahme von DNA-Schäden nach Kombination von TMZ mit dem PI3K-Inhibitor LY294002 und gesteigerten Apoptoseraten. Die Fülle an präklinischen Arbeiten zur Beeinflussung des PI3K-Signalweges in Glioblastomen, die in den letzten Jahren publiziert wurden, gepaart mit der Tatsache, dass sich einige Kandidaten in klinischen Prüfungen befinden (Zhao et al., 2017; Hashemi et al., 2023), belegen, dass es sich um einen lohnenden therapeutischen Angriffspunkt handelt.

Auf diese Ergebnisse aufbauend führten wir weitere Untersuchungen durch (3.2; Haas et al., 2018b). AKT inhibiert auch die *Apoptosis Signal-regulated Kinase 1* (ASK1), die über die *c-Jun N-terminal Kinase* (JNK) and *p38 Mitogen-activated Protein Kinase* (p38 MAPK) Apoptose auslöst (Ichijo et al., 1997; Saitoh et al., 1998). ASK1 wird zusätzlich durch Trx negativ reguliert. Bei Trx handelt es sich um eine kleine, ubiquitär exprimierte Oxidoreduktase mit zwei Cysteinen im katalytischen Zentrum, die in die zelluläre Redox-Homöostase involviert ist. Nach Oxidation durch zum Beispiel oxidativen Stress wird Trx über die *Thioredoxin Reductase* (TrxR) rekuperiert. Zusätzlich wird Trx noch durch das *Trx-interacting Protein* (TXNIP), ein Tumorsuppressorprotein das auch unter

dem Namen *Vitamin-D3-upregulated Protein 1* (VDUP1) bekannt ist, in seiner Funktion gehemmt. Trx bindet und inaktiviert ASK1, unter oxidativem Stress jedoch wird ASK1 freigesetzt und löst Apoptose aus. Zusätzlich ist auch beschrieben, dass Trx PTEN inhibieren kann und somit die PI3K- und AKT-Aktivität steigert (Meuillet et al., 2004). Sowohl eine verringerte TXNIP- als auch eine erhöhte Trx-Expression findet man nur in höher gradigen Gliomen. Beides ist mit einem kürzerem Gesamtüberleben der Patienten assoziiert ist (Gollapalli et al., 2017; Zhang et al., 2017b; Yao et al., 2020). Es war also anzunehmen, dass sowohl durch eine Hemmung von Trx als auch der PI3K, die ASK1-Hemmung aufgehoben und Apoptose ausgelöst wird. Unsere Untersuchungen zeigten, dass eine Trx-Hemmung mit dem spezifischen Inhibitor PX-12 in Glioblastom-Zellen Apoptose induzierte und die Phosphorylierung von AKT und somit seine Aktivität reduzierte, was auf ein Zusammenspiel der Signalkaskaden hindeutete. Dies wurde weiter dadurch untermauert, dass die Kombination von PX-12 mit nicht zytotoxischen Konzentrationen des PI3K Inhibitor LY294002, fast alle Zellen komplett abtötete. Ähnlich wie die PI3K-Hemmung, die in der vorangegangenen Arbeit untersucht worden war (3.1; Haas et al., 2018a), führte sowohl die pharmakologische Hemmung von Trx als auch die genetische Überexpression von TXNIP zu einem besseren Ansprechen der Zellen auf Cisplatin und TMZ. Diese synergistischen Effekte waren, zum Zeitpunkt als die Arbeit durchgeführt wurde, für Glioblastom-Zellen noch nicht beschrieben. Neuere Publikationen mit TrxR-Inhibitoren bestätigen aber mittlerweile unsere Ergebnisse (Jovanovic et al., 2020; Martinez-Jaramillo et al., 2024). In diesem Zusammenhang ist es von Interesse, dass der TrxR-Inhibitor Auranofin in verschiedenen klinischen Studien als Tumortherapeutikum, unter anderem auch in Kombination mit TMZ zur Behandlung des rezidivierten Glioblastoms (Halatsch et al., 2021), untersucht wird (NCT01419691, NCT03456700, NCT01737502, NCT01747798, NCT02770378)[3]. Auronafin ist ein organischer Goldkomplex, der eigentlich in der Rheumatherapie eingesetzt wird. Durch seine hemmende Wirkung auf die TrxR in Tumorzellen erhöht sich der oxidierte, nicht funktionsfähige Anteil an Trx. Dies wiederum steigert unter anderem das oxidative Stresslevel der Zellen und verringert die AKT-Aktivität, was schlussendlich zu Apoptose führt (Abdalbari et al., 2021).

Während der Durchführung der ersten beiden oben beschriebenen Arbeiten, erlangte das Opioid Methadon mediale Aufmerksamkeit als mögliche adjuvante Therapieoption

[3] Die Studien sind zu finden unter: https://clinicaltrials.gov/

zur Behandlung des Glioblastoms (Hübner et al., 2017). Hintergrund für die mediale Berichterstattung waren Studien, die positive Effekte von Methadon auf die Apoptose-induzierende Wirkung von Doxorubicin in Glioblastom-Zellen und in einem Mausmodell zeigten (Friesen et al., 2014). Diesen Studien waren weitere Publikationen der Arbeitsgruppe vorausgegangen, die über ähnliche Effekte von Methadon in Leukämiezellen berichteten (Friesen et al., 2008; Friesen et al., 2013). Der postulierte Mechanismus war eine Aktivierung des μ-Opioidrezeptors und anschließende Unterdrückung der Aktivität der Proteinkinase A (PKA), was schließlich Apoptose induziert. Zusätzlich wurde gezeigt, dass Methadon die intrazellulären Doxorubicin-Konzentrationen erhöht, indem es den Effluxtransporter P-Glykoprotein (P-gp) inhibiert. Allerdings widersprach sich die Studienlage, so berichteten einige nachfolgende Studien von keinem oder nur geringen Effekten von Methadon in Kombination mit Chemotherapeutika auf Glioblastom-Zellen (Brawanski et al., 2018; Oppermann et al., 2019; Vatter et al., 2020; Cueni et al., 2020). Ein weiterer Kritikpunkt an den Studien von Friesen et al. war die Verwendung von Doxorubicin, welches in der Glioblastom-Therapie nicht indiziert ist und zudem eine schlechte Blut-Hirn-Schranken-Gängigkeit hat. Um dem weiter nachzugehen, fokussierten sich zwei der hier beschriebenen Arbeiten darauf, den Effekt von Methadon im Zusammenspiel mit dem Therapie-Goldstandard TMZ in einer Reihe von Glioblastom-Zellen zu untersuchen (3.3; Kaina et al., 2020 und 3.4; Haas et al., 2021). Wir konnten eine hohe Expression des μ-Opioidrezeptors in allen untersuchten Zelllinien und primären Glioblastom-Zellen nachweisen. Allerdings war eine zytotoxische Wirkung nur durch Methadon zu beobachten, nicht aber durch die ebenfalls potenten μ-Opioidrezeptor-Agonisten Oxycodon und Morphin. Auch der Antagonist Naloxon konnte die Methadon-Wirkung nicht aufheben. Die Ergebnisse sprechen eher dafür, dass Methadon über andere molekulare Angriffspunkte seine Zytotoxizität vermittelt. Obwohl in beiden Studien Glioblastom-Zelllinien verwendet wurden, die Unterschiede im *MGMT*- und *TP53*-Mutationsstatus aufwiesen, waren die in MTT- und Apoptose-Versuchen ermittelten zytotoxischen Konzentrationen recht ähnlich (IC_{50}: 60 – 130 μM). Dies zeigt zunächst, dass die Methadon-induzierte Zytotoxizität unabhängig von der DNA-Reparaturkapazität der Zellen ist und nicht über einen genotoxischen Mechanismus zustande kommt, was zusätzlich durch Comet- und γH2AX-Assays belegt wurde. Zum anderen zeigen die Versuche aber auch, dass die benötigten Methadon-Konzentrationen in einem Bereich liegen, der klinisch ohne Auslösung einer

Atemdepression nicht erreicht werden kann. Die getesteten Konzentrationen (10 – 100 µM) reichten auch nicht aus, die Zellen gegenüber TMZ zu sensitivieren. Die Plasmakonzentration von Schmerzpatienten liegt nach Verabreichung von 10 – 30 mg Methadon im Bereich von 1 µM (Inturrisi et al., 1987). Wir konnten die zuvor gefunden Effekte von Methadon auf die Zytotoxizität von Doxorubicin bestätigen (Friesen et al., 2014), allerdings waren auch hier Konzentrationen im Bereich von 60 µM notwendig und die Effekte waren stark von der Zelllinie und der Doxorubicin-Konzentration abhängig. Die beste Wirkung von Methadon auf die Doxorubicin-induzierte Zytotoxizität wurde in A172-Zellen erreicht, während Methadon in U87-Zellen keinen Effekt hatte. Dies könnte auf Unterschiede in der P-gp Expression zurückzuführen sein, die als möglicher Mechanismus für die Methadon-Wirkung diskutiert wird (Friesen et al., 2014). In der ersten Arbeit (3.1; Haas et al., 2018a) wurden mehrere Zelllinien auf ihre P-gp-Expression hin untersucht. In U87-Zellen konnte auch nach längerer Chemotherapie kein P-gp Protein nachgewiesen werden. Die A172-Zellen waren nicht Teil der Untersuchungen, es gibt aber Literaturdaten, die eine Hochregulierung der P-gp-Expression durch eine Chemotherapie belegen (Perazzoli et al., 2015). Das könnte das verbesserte Ansprechen der Zellen auf Doxorubicin in Kombination mit Methadon erklären. Allerdings ist TMZ ebenfalls ein P-gp-Substrat (Munoz et al., 2015) und eine potenzielle Hemmung durch Methadon sollte die intrazelluläre Konzentration vergleichbar zu Doxorubicin erhöhen und die Zellen effektiver abtöten, was wir allerdings nicht beobachten konnten. Somit ist die Frage des Mechanismus der Methadon-Wirkung auf Glioblastom-Zellen weiterhin nicht eindeutig geklärt. Ein weiterer Aspekt, der in dieser Arbeit untersucht wurde, war ein Einfluss von Methadon auf die zelluläre Seneszenz. In Vorarbeiten konnten unser Kooperationspartner zeigen, dass TMZ in Glioblastom-Zellen nach längeren Behandlungsdauern Seneszenz induziert und die Apoptoseraten zurückgehen. Dies könnte erklären, warum TMZ über die Zeit seine Wirkung verliert (Aasland et al., 2019; Beltzig et al., 2022b). Lange Zeit wurde postuliert, dass der seneszente Zustand irreversibel ist und die Zellen die Fähigkeit verlieren, erneut zu proliferieren. Neuere Arbeiten zeigen jedoch, dass die schlafenden Zellen auch wieder reaktiviert werden können und Tumore erneut anfangen zu wachsen. Zusätzlich produzieren die Zellen pro-inflammatorische Zytokine, die die Tumorprogression weiter fördern (Saleh et al., 2019). Untersuchungen an Biopsien von Glioblastom-Rezidiven zeigten eine Erhöhung der seneszenten Zellpopulation bei gleichzeitiger Reduktion der

Apoptoserate und eine gesteigerte Il-6 und IL-8 Expression (Beltzig et al., 2022b). Somit erscheint es plausibel, dass Seneszenz auch bei der TMZ-Resistenz und dem Rezidivieren von Glioblastomen eine Rolle zu spielen scheint (Chojak et al., 2023). Daraus ergibt sich ein neuer Behandlungsansatz, der zum Ziel hat, seneszente Zellen selektiv abzutöten. Arzneistoffe, die diese Eigenschaft haben, werden auch als Senolytika bezeichnet (Zhang et al., 2023; Kaina, 2023). Für Methadon konnten wir allerdings keine relevanten Effekte auf die Seneszenz nachweisen. Die Suche nach weiteren Senolytika führte uns zu den KCHN-Kanälen, Eag1 and hERG, die schließlich in der letzten Arbeit untersucht wurden (3.5; Haas et al., 2025). Beide Kanäle sind strukturell eng miteinander verwandt und unter anderem im Gehirn exprimiert. Der hERG-Kanal ist zudem stark in Kardiomyozyten exprimiert und spielt dort eine wichtige physiologische Rolle in der Repolarisation des Herzens und der Länge des QTc-Intervalls (Zunkler, 2006). Die Funktion des Eag1 ist auf das Gehirn beschränkt, wo er die Neurotransmitterfreisetzung beeinflusst (Whicher et al., 2016). Neben diesen Effekten sind die beiden Kanäle aber auch in der Regulation der Zellproliferation und der Apoptose von Tumorzellen involviert und werden mit der Tumorentstehung in Verbindung gebracht (Pardo et al., 2014; Wang et al., 2017). Eine Hemmung der Kanäle ist schon seit längerem als potenzieller therapeutischer Angriffspunkt auch für Gliome im Gespräch (He et al., 2020; Wulff et al., 2009; Elias et al., 2023). Beide Kanäle werden in Glioblastomen exprimiert und eine Überexpression korreliert mit einer schlechten klinischen Prognose und einem verringerten Gesamtüberleben (Martinez et al., 2015; Shugg et al., 2021; Zheng et al., 2023). Interessanterweise induzieren aktivierte hERG-Kanäle Seneszenz in Brustkrebszellen (Lansu et al., 2013). Dies veranlasste uns, die Rolle einer hERG/Eag1-Blockade auf die Apoptose und Seneszenz in Glioblastom-Zellen zu untersuchen. Dazu verwendeten wir die beiden H1-Antihistaminika Astemizol und Terfenadin, die beide potente hERG/Eag1-Blocker sind (Toplak et al., 2022). Expressionsanalysen zeigten eine gleichmäßige Expression beider Kanäle sowohl in humanen Glioblastom-Zelllinien als auch in primären Zellen und Glioblastom-Gewebe, das aus Biopsien gewonnen wurde. Beide Arzneistoffe töteten die Zellen über Induktion von Apoptose, was auch für andere Tumorzellen bereits beschrieben war (Jehle et al., 2011). Allerdings hatten sie keinen Einfluss auf die seneszente Zellpopulation, wenn Zellen alleine mit ihnen inkubiert wurden. In Kombination mit TMZ kam es jedoch zu synergistischen Effekten auf die Apoptoseinduktion vor allem in p53-exprimierenden U87-, A172- und LN229-Zellen,

während in *TP53*-mutierten U251- und U373-Zellen kaum Effekte beobachtet wurden. Der p53-Status scheint also eine Rolle in der Sensitivität der Zellen gegenüber der Wirkung einer hERG/Eag1-Blockade zu spielen. Dies wurde in der vorliegenden Arbeit allerdings mechanistisch nicht weiterverfolgt und muss in weiteren Studien geklärt werden. Bei Glioblastom-Zellen steigt nach 3 Tagen TMZ-Inkubation die seneszente Zellpopulation an und nach 10 Tagen sind fast 90% der Zellen seneszent (Beltzig et al., 2022b). Durch gleichzeitige Inkubation von TMZ und Astemizol konnten wir bereits nach 5 Tagen Behandlung die seneszente Zellpopulation um etwa 50% reduzieren. Solche Effekte von hERG/Eag1-Blockern auf die Hemmung der Therapie-induzierten Seneszenz waren bis dahin in der Literatur noch nicht beschrieben. Diese Daten geben Anlass zur Hoffnung, dass eine hERG/Eag1-Blockade auch in Patienten positive Effekte auf die TMZ-Therapie haben könnte. Astemizol passiert die Blut-Hirn-Schranke und wird zur Behandlung von Alzheimer und Parkinson erforscht (Di et al., 2003; Rojo et al., 2010; Sun et al., 2016). Allerdings ist beim Einsatz von hERG-Kanalblockern Vorsicht geboten, denn sie hemmen auch die Repolarisation im Herzen, was zur QTc-Intervallverlängerung und gefürchteten, tödlichen *Torsade-de-Points*-Arrhythmien führen kann, weshalb Astemizol als Antihistaminikum vom Markt genommen wurde. Allerdings gibt es einige zugelassene Arzneimittel, die zwar die Kanäle blockieren, dabei aber nur moderate Effekte auf die QT-Zeit der behandelten Patienten haben. Hierzu gehören zum Beispiel die Antipsychotika Amitriptylin, Haloperidol und Fluoxetin oder das Antimykotikum Ketoconazol. Interessanterweise zeigte eine Studie, dass Glioblastom-Patienten, bei denen eine hohe hERG-Expression im Tumorgewebe nachgewiesen wurde und die parallel zur Standardtherapie diese Arzneimittel einnahmen, eine höhere Überlebenswahrscheinlichkeit hatten (Pointer et al., 2017). Unsere Ergebnisse unterstützen somit die Hypothese, dass hier ein kausaler Zusammenhang zwischen der Einnahme der Arzneimittel, einer hERG/Eag1-Hemmung und der Überlebenswahrscheinlichkeit bestehen könnte.

Zusammenfassend lässt sich sagen, dass in den fünf zugrundeliegenden Arbeiten dieser Habilitationsschrift mehrere molekular-pharmakologische Angriffspunkte zur Sensitivierung von Glioblastom-Zellen gegenüber der TMZ-Therapie gefunden wurden. Diese *in vitro* Ergebnisse können zum Anlass genommen werden, weitere präklinische *in vivo* Studien anzustoßen und Arzneistoffkandidaten zu entwickeln, die diese molekularen Strukturen zum Ziel haben. In diesem Zusammenhang ist auch zu

erwähnen, dass seit einigen Jahren klinische Studien mit dem sogenannten CUSP9v3-Protokoll[4] laufen, in denen Glioblastom-Patienten einen Medikamentencocktail bestehend aus neun für andere Indikationen zugelassene Arzneimittel zusätzlich zu TMZ erhalten (Kast et al., 2013). Dieser Cocktail enthält drei Wirkstoffe, die die hier untersuchten Angriffspunkte das Trx-System (Auranofin) und die hERG-Kanäle (Sertralin, Itraconazol) zum Ziel haben. Die ersten Ergebnisse sind vielversprechend, das Tumorwachstum konnte durch das Protokoll etwa bei der Hälfte der Patienten nach der ersten Auswertungsphase gestoppt werden (Halatsch et al., 2021).

[4] CUSP9v3 steht für ***C**oordinated **U**ndermining of **S**urvival **P**aths combining **9** repurposed non-oncological drugs with metronomic temozolomide-**v**ersion **3***. Das Protokoll wurde unter anderem von dem Ulmer Mediziner Prof. Dr. Halatsch entwickelt und vom Netzwerk *International Initiative for Accelerated Improvement of Glioblastoma Care* (IIAIGC) begleitet.

5 Zusammenfassung

Glioblastome gehören zu den aggressivsten Tumoren des Gehirns und sind durch ein infiltratives Wachstum, Nekrose und mikrovaskuläre Proliferation gekennzeichnet. Seit nunmehr 20 Jahren besteht die Therapie aus Operation, Strahlentherapie und adjuvanter TMZ-Therapie. Bis heute gab es keine substanziellen Fortschritte in der Therapie, weshalb die 5-Jahresüberlebensrate immer noch bei nur etwa 6% liegt. Ein Hauptproblem der Chemotherapie ist eine intrinsische Resistenz der Tumore gegenüber TMZ. Ein wichtiger Marker für das Ansprechen auf die Therapie ist das DNA-Reparaturenzym MGMT, das in etwa 60% der Glioblastome aktiv ist und somit das Ansprechen auf TMZ verringert. Daneben sind in Glioblastomen aber auch andere DNA-Reparaturenzyme dereguliert und die Tumore tragen Mutationen in Genen von Tumorsuppressor- und Rezeptortyrosinkinase-Signalwegen, die einen Einfluss auf die TMZ-Resistenz haben können. Das Ziel dieser Arbeit war es, die Expression und den Aktivierungsstatus der für die TMZ-Resistenz relevanten Signalwege in Glioblastom-Biopsien und -Zellen zu untersuchen und durch gezielte pharmakologische Beeinflussung der aktivierten Signalwege ein verbessertes Ansprechen der Zellen auf TMZ zu erreichen. In zwei Arbeiten konnten der PI3K-Signalweg als lohnendes Therapieziel identifiziert werden. Die gesamte Signalkaskade war in Glioblastom-Gewebe und -Zellen überaktiviert und eine pharmakologische Hemmung der PI3K sensitivierte die Zellen gegenüber der TMZ-Therapie. Im Zusammenspiel mit der PI3K wurde auch das in der Redox-Homöostase involvierte Trx-System als möglicher Angriffspunkt identifiziert. Eine Hemmung beider Signalwege induzierte synergistisch Apoptose in Glioblastom-Zellen und verbesserte das Ansprechen auf TMZ. Eine Hemmung des Trx-Systems auf die Wirkung von TMZ war zum Zeitpunkt der Studiendurchführung in der Literatur noch nicht beschrieben. Nachfolgende präklinische Untersuchungen anderer Arbeitsgruppen belegen die Relevanz unserer Ergebnisse, was zusätzlich durch aktuell laufende klinische Studien mit PI3K- und TrxR-Inhibitoren untermauert wird. Neben der Verwendung adjuvanter Arzneimittel zur Verringerung der TMZ-Resistenz hat sich in den letzten Jahren auch die Hemmung der zellulären Seneszenz durch Senolytika als therapeutischer Angriffspunkt herauskristallisiert. Insbesondere TMZ induziert über die Zeit effektiv Seneszenz in Glioblastom-Zellen, wodurch sie Therapie-resistent und aggressiver werden. In einer der vorgelegten Arbeiten wurden die beiden spannungsaktivierten Kaliumkanäle

hERG und Eag1 als potenzieller Angriffspunkt zur Reduzierung der Seneszenz identifiziert. Durch eine Hemmung der Kanäle mit dem Antihistaminikum Astemizol wurde eine synergistische Steigerung der Apoptoseraten in Kombination mit TMZ beobachtet bei gleichzeitiger Reduktion der seneszenten Zellpopulation um etwa 50%. Der Einfluss einer hERG/Eag1-Hemmung auf die Therapie-induzierte Seneszenz von Glioblastomen ist in der Literatur bisher noch nicht beschrieben worden. Unsere Ergebnisse werden unterstützt durch klinische Daten, die zeigen, dass Glioblastom-Patienten, die im Tumorgewebe hERG überexprimieren von einer adjuvanten Therapie mit Arzneistoffen profitieren, die den Kanal hemmen. Das durch extensive mediale Berichterstattung bekannt gewordene Opioid Methadon als adjuvante Therapieoption beim Glioblastom zeigte in unseren Studien weder Effekte auf die Seneszenz noch verbesserte es das Ansprechen der Glioblastom-Zellen auf TMZ. Die Ergebnisse der zwei hier vorgelegten Arbeiten unterstützen die Verwendung von Methadon in der Glioblastom-Therapie nicht. Zurzeit laufen klinische Studien mit dem sogenannten CUSP9v3-Protokoll, indem neun für andere Indikationen zugelassene Arzneimittel in einem Cocktail in Kombination mit TMZ zur Behandlung des Glioblastoms zum Einsatz kommen. Drei der verwendeten neun Arzneimittel beeinflussen die hier identifizierten Signalwege, was auch die klinische Relevanz unserer Befunde unterstreicht.

6 Überlappung durch geteilte Autorenschaften

Die vorliegende Habilitationsschrift hat fünf publizierte Originalarbeiten zur Grundlage. Vier der Arbeiten habe ich als alleiniger Erstautor veröffentlicht (Haas et al., 2018a; Haas et al., 2018b; Haas et al., 2021; Haas et al., 2025). Diese Arbeiten wurden durch mich initiiert und konzipiert, weiterhin wurden die Daten durch mich und die Koautoren akquiriert, analysiert und interpretiert. Die Entwürfe und finalen Korrekturen der Publikationen erfolgten durch mich. Eine der Arbeiten habe ich als Letztautor veröffentlicht (Kaina et al., 2020). Diese Arbeit entstand in enger Kooperation mit Prof. emer. Dr. Kaina, ehemaliger Direktor des Instituts für Toxikologie der Universitätsmedizin Mainz. Die Arbeit wurde durch Prof. Kaina und mich initiiert und konzipiert. Ein Großteil der Versuche fand am Institut für Toxikologie unter Prof. Kainas Aufsicht statt. Die finalen Korrekturen der Publikationen erfolgten durch Prof. Kaina und mich.
Eine Überlappung mit anderen Habilitationsschriften ist nicht gegeben.

7 Bibliographie

Aasland, D., Reich, T. R., Tomicic, M. T., Switzeny, O. J., Kaina, B., and Christmann, M. (2018). Repair gene O(6) -methylguanine-DNA methyltransferase is controlled by SP1 and up-regulated by glucocorticoids, but not by temozolomide and radiation. J Neurochem 144, 139-51.

Aasland, D., Gotzinger, L., Hauck, L., Berte, N., Meyer, J., Effenberger, M., Schneider, S., Reuber, E. E., Roos, W. P., Tomicic, M. T., Kaina, B., and Christmann, M. (2019). Temozolomide Induces Senescence and Repression of DNA Repair Pathways in Glioblastoma Cells via Activation of ATR-CHK1, p21, and NF-kappaB. Cancer Res 79, 99-113.

Abdalbari, F. H., and Telleria, C. M. (2021). The gold complex auranofin: new perspectives for cancer therapy. Discov Oncol 12, 42.

Agnihotri, S., Gajadhar, A. S., Ternamian, C., Gorlia, T., Diefes, K. L., Mischel, P. S., Kelly, J., McGown, G., Thorncroft, M., Carlson, B. L., Sarkaria, J. N., Margison, G. P., Aldape, K., Hawkins, C., Hegi, M., and Guha, A. (2012). Alkylpurine-DNA-N-glycosylase confers resistance to temozolomide in xenograft models of glioblastoma multiforme and is associated with poor survival in patients. J Clin Invest 122, 253-66.

Alexandru, O., Horescu, C., Sevastre, A. S., Cioc, C. E., Baloi, C., Oprita, A., and Dricu, A. (2020). Receptor tyrosine kinase targeting in glioblastoma: performance, limitations and future approaches. Contemp Oncol (Pozn) 24, 55-66.

Baker, S. D., Wirth, M., Statkevich, P., Reidenberg, P., Alton, K., Sartorius, S. E., Dugan, M., Cutler, D., Batra, V., Grochow, L. B., Donehower, R. C., and Rowinsky, E. K. (1999). Absorption, metabolism, and excretion of 14C-temozolomide following oral administration to patients with advanced cancer. Clin Cancer Res 5, 309-17.

Beltzig, L., Christmann, M., and Kaina, B. (2022a). Abrogation of Cellular Senescence Induced by Temozolomide in Glioblastoma Cells: Search for Senolytics. Cells 11.

Beltzig, L., Schwarzenbach, C., Leukel, P., Frauenknecht, K. B. M., Sommer, C., Tancredi, A., Hegi, M. E., Christmann, M., and Kaina, B. (2022b). Senescence Is the Main Trait Induced by Temozolomide in Glioblastoma Cells. Cancers (Basel) 14.

Brawanski, K., Brockhoff, G., Hau, P., Vollmann-Zwerenz, A., Freyschlag, C., Lohmeier, A., Riemenschneider, M. J., Thome, C., Brawanski, A., and Proescholdt, M. A. (2018). Efficacy of D,L-methadone in the treatment of glioblastoma in vitro. CNS Oncol 7, CNS18.

Brennan, C.W., Verhaak, R.G., McKenna, A., Campos, B., Noushmehr, H., Salama, S.R., Zheng, S., Chakravarty, D., Sanborn, J.Z., Berman, S.H., Beroukhim, R., Bernard, B., Wu, C.J., Genovese, G., Shmulevich, I., Barnholtz-Sloan, J., Zou, L., Vegesna, R., Shukla, S.A., Ciriello, G., Yung, W.K., Zhang, W., Sougnez, C., Mikkelsen, T., Aldape, K., Bigner, D.D., Van Meir, E.G., Prados, M., Sloan, A., Black, K.L., Eschbacher, J., Finocchiaro, G., Friedman, W., Andrews, D.W., Guha, A., Iacocca, M., O'Neill, B.P., Foltz, G., Myers, J., Weisenberger, D.J., Penny, R., Kucherlapati, R., Perou, C.M., Hayes, D.N., Gibbs, R., Marra, M., Mills, G.B., Lander, E., Spellman, P., Wilson, R., Sander, C., Weinstein, J., Meyerson, M., Gabriel, S., Laird, P.W., Haussler, D., Getz, G., and Chin, L. (2013). The somatic genomic landscape of glioblastoma. Cell 155, 462-77.

Cahill, D. P., Levine, K. K., Betensky, R. A., Codd, P. J., Romany, C. A., Reavie, L. B., Batchelor, T. T., Futreal, P. A., Stratton, M. R., Curry, W. T., Iafrate, A. J., and

Louis, D. N. (2007). Loss of the mismatch repair protein MSH6 in human glioblastomas is associated with tumor progression during temozolomide treatment. Clin Cancer Res 13, 2038-45.
Chakravarti, A., Zhai, G., Suzuki, Y., Sarkesh, S., Black, P.M., Muzikansky, A., and Loeffler, J.S. (2004). The prognostic significance of phosphatidylinositol 3-kinase pathway activation in human gliomas. J. Clin. Oncol 22, 1926-33.
Chinot, O. L., Wick, W., Mason, W., Henriksson, R., Saran, F., Nishikawa, R., Carpentier, A. F., Hoang-Xuan, K., Kavan, P., Cernea, D., Brandes, A. A., Hilton, M., Abrey, L., and Cloughesy, T. (2014). Bevacizumab plus radiotherapy-temozolomide for newly diagnosed glioblastoma. N Engl J Med 370, 709-22.
Chojak, R., Fares, J., Petrosyan, E., and Lesniak, M. S. (2023). Cellular senescence in glioma. J Neurooncol 164, 11-29.
Christmann, M., and Kaina, B. (2019). Epigenetic regulation of DNA repair genes and implications for tumor therapy. Mutat Res Rev Mutat Res 780, 15-28.
Colardo, M., Segatto, M., and Di Bartolomeo, S. (2021). Targeting RTK-PI3K-mTOR Axis in Gliomas: An Update. Int J Mol Sci 22.
Comprehensive genomic characterization defines human glioblastoma genes and core pathways (2008). Nature 455, 1061-68.
Coppe, J. P., Desprez, P. Y., Krtolica, A., and Campisi, J. (2010). The senescence-associated secretory phenotype: the dark side of tumor suppression. Annu Rev Pathol 5, 99-118.
Cuddapah, V. A., Robel, S., Watkins, S., and Sontheimer, H. (2014). A neurocentric perspective on glioma invasion. Nat Rev Neurosci 15, 455-65.
Cueni, C., Nytko, K. J., Thumser-Henner, P., Weyland, M. S., and Rohrer Bley, C. (2020). Methadone does not potentiate the effect of doxorubicin in canine tumour cell lines. Vet Med Sci.
Dakal, T. C., Kakde, G. S., and Maurya, P. K. (2024). Genomic, epigenomic and transcriptomic landscape of glioblastoma. Metab Brain Dis 39, 1591-611.
Denny, B. J., Wheelhouse, R. T., Stevens, M. F., Tsang, L. L., and Slack, J. A. (1994). NMR and molecular modeling investigation of the mechanism of activation of the antitumor drug temozolomide and its interaction with DNA. Biochemistry 33, 9045-51.
Di, L., Kerns, E. H., Fan, K., McConnell, O. J., and Carter, G. T. (2003). High throughput artificial membrane permeability assay for blood-brain barrier. Eur J Med Chem 38, 223-32.
Dosch, J., Christmann, M., and Kaina, B. (1998). Mismatch G-T binding activity and MSH2 expression is quantitatively related to sensitivity of cells to methylating agents. Carcinogenesis 19, 567-73.
Eckstein, N., Servan, K., Girard, L., Cai, D., von, Jonquieres G., Jaehde, U., Kassack, M.U., Gazdar, A.F., Minna, J.D., and Royer, H.D. (2008). Epidermal growth factor receptor pathway analysis identifies amphiregulin as a key factor for cisplatin resistance of human breast cancer cells. J Biol. Chem 283, 739-50.
Elias, A. F., Lin, B. C., and Piggott, B. J. (2023). Ion Channels in Gliomas-From Molecular Basis to Treatment. Int J Mol Sci 24.
Esteller, M., Garcia-Foncillas, J., Andion, E., Goodman, S. N., Hidalgo, O. F., Vanaclocha, V., Baylin, S. B., and Herman, J. G. (2000). Inactivation of the DNA-repair gene MGMT and the clinical response of gliomas to alkylating agents. N Engl J Med 343, 1350-4.
Faget, D. V., Ren, Q., and Stewart, S. A. (2019). Unmasking senescence: context-dependent effects of SASP in cancer. Nat Rev Cancer 19, 439-53.

Feldheim, J., Kessler, A. F., Monoranu, C. M., Ernestus, R. I., Lohr, M., and Hagemann, C. (2019). Changes of O(6)-Methylguanine DNA Methyltransferase (MGMT) Promoter Methylation in Glioblastoma Relapse-A Meta-Analysis Type Literature Review. Cancers (Basel) 11.

Friesen, C., Roscher, M., Alt, A., and Miltner, E. (2008). Methadone, commonly used as maintenance medication for outpatient treatment of opioid dependence, kills leukemia cells and overcomes chemoresistance. Cancer Res 68, 6059-64.

Friesen, C., Roscher, M., Hormann, I., Fichtner, I., Alt, A., Hilger, R. A., Debatin, K. M., and Miltner, E. (2013). Cell death sensitization of leukemia cells by opioid receptor activation. Oncotarget 4, 677-90.

Friesen, C., Hormann, I., Roscher, M., Fichtner, I., Alt, A., Hilger, R., Debatin, K. M., and Miltner, E. (2014). Opioid receptor activation triggering downregulation of cAMP improves effectiveness of anti-cancer drugs in treatment of glioblastoma. Cell Cycle 13, 1560-70.

Furnari, F. B., Fenton, T., Bachoo, R. M., Mukasa, A., Stommel, J. M., Stegh, A., Hahn, W. C., Ligon, K. L., Louis, D. N., Brennan, C., Chin, L., DePinho, R. A., and Cavenee, W. K. (2007). Malignant astrocytic glioma: genetics, biology, and paths to treatment. Genes Dev 21, 2683-710.

Gilbert, M. R., Dignam, J. J., Armstrong, T. S., Wefel, J. S., Blumenthal, D. T., Vogelbaum, M. A., Colman, H., Chakravarti, A., Pugh, S., Won, M., Jeraj, R., Brown, P. D., Jaeckle, K. A., Schiff, D., Stieber, V. W., Brachman, D. G., Werner-Wasik, M., Tremont-Lukats, I. W., Sulman, E. P., Aldape, K. D., Curran, W. J., Jr., and Mehta, M. P. (2014). A randomized trial of bevacizumab for newly diagnosed glioblastoma. N Engl J Med 370, 699-708.

Gollapalli, K., Ghantasala, S., Atak, A., Rapole, S., Moiyadi, A., Epari, S., and Srivastava, S. (2017). Tissue Proteome Analysis of Different Grades of Human Gliomas Provides Major Cues for Glioma Pathogenesis. OMICS 21, 275-84.

Gorgoulis, V., Adams, P. D., Alimonti, A., Bennett, D. C., Bischof, O., Bishop, C., Campisi, J., Collado, M., Evangelou, K., Ferbeyre, G., Gil, J., Hara, E., Krizhanovsky, V., Jurk, D., Maier, A. B., Narita, M., Niedernhofer, L., Passos, J. F., Robbins, P. D., Schmitt, C. A., Sedivy, J., Vougas, K., von Zglinicki, T., Zhou, D., Serrano, M., and Demaria, M. (2019). Cellular Senescence: Defining a Path Forward. Cell 179, 813-27.

Haas, B., Klinger, V., Keksel, C., Bonigut, V., Kiefer, D., Caspers, J., Walther, J., Wos-Maganga, M., Weickhardt, S., Rohn, G., Timmer, M., Frotschl, R., and Eckstein, N. (2018a). Inhibition of the PI3K but not the MEK/ERK pathway sensitizes human glioma cells to alkylating drugs. Cancer Cell Int 18, 69.

Haas, B., Schutte, L., Wos-Maganga, M., Weickhardt, S., Timmer, M., and Eckstein, N. (2018b). Thioredoxin Confers Intrinsic Resistance to Cytostatic Drugs in Human Glioma Cells. Int J Mol Sci 19.

Haas, B., Ciftcioglu, J., Jermar, S., Weickhardt, S., Eckstein, N., and Kaina, B. (2021). Methadone-mediated sensitization of glioblastoma cells is drug and cell line dependent. J Cancer Res Clin Oncol 147, 779-92.

Haas, B., Roth, I., Sacker, L., Wos-Maganga, M., Beltzig, L., and Kaina, B. (2025). Apoptotic and senolytic effects of hERG/Eag1 channel blockers in combination with temozolomide in human glioblastoma cells. Naunyn Schmiedebergs Arch Pharmacol 398, 12267-12278.

Halatsch, M. E., Kast, R. E., Karpel-Massler, G., Mayer, B., Zolk, O., Schmitz, B., Scheuerle, A., Maier, L., Bullinger, L., Mayer-Steinacker, R., Schmidt, C., Zeiler, K., Elshaer, Z., Panther, P., Schmelzle, B., Hallmen, A., Dwucet, A., Siegelin, M. D., Westhoff, M. A., Beckers, K., Bouche, G., and Heiland, T. (2021). A phase

Ib/IIa trial of 9 repurposed drugs combined with temozolomide for the treatment of recurrent glioblastoma: CUSP9v3. Neurooncol Adv 3, vdab075.
Hashemi, M., Etemad, S., Rezaei, S., Ziaolhagh, S., Rajabi, R., Rahmanian, P., Abdi, S., Koohpar, Z. K., Rafiei, R., Raei, B., Ahmadi, F., Salimimoghadam, S., Aref, A. R., Zandieh, M. A., Entezari, M., Taheriazam, A., and Hushmandi, K. (2023). Progress in targeting PTEN/PI3K/Akt axis in glioblastoma therapy: Revisiting molecular interactions. Biomed Pharmacother 158, 114204.
He, S., Moutaoufik, M. T., Islam, S., Persad, A., Wu, A., Aly, K. A., Fonge, H., Babu, M., and Cayabyab, F. S. (2020). HERG channel and cancer: A mechanistic review of carcinogenic processes and therapeutic potential. Biochim Biophys Acta Rev Cancer 1873, 188355.
He, Y., Sun, M. M., Zhang, G. G., Yang, J., Chen, K. S., Xu, W. W., and Li, B. (2021). Targeting PI3K/Akt signal transduction for cancer therapy. Signal Transduct Target Ther 6, 425.
Hegi, M. E., Diserens, A. C., Gorlia, T., Hamou, M. F., de Tribolet, N., Weller, M., Kros, J. M., Hainfellner, J. A., Mason, W., Mariani, L., Bromberg, J. E., Hau, P., Mirimanoff, R. O., Cairncross, J. G., Janzer, R. C., and Stupp, R. (2005). MGMT gene silencing and benefit from temozolomide in glioblastoma. N Engl J Med 352, 997-1003.
Herrlinger, U., Tzaridis, T., Mack, F., Steinbach, J. P., Schlegel, U., Sabel, M., Hau, P., Kortmann, R. D., Krex, D., Grauer, O., Goldbrunner, R., Schnell, O., Bahr, O., Uhl, M., Seidel, C., Tabatabai, G., Kowalski, T., Ringel, F., Schmidt-Graf, F., Suchorska, B., Brehmer, S., Weyerbrock, A., Renovanz, M., Bullinger, L., Galldiks, N., Vajkoczy, P., Misch, M., Vatter, H., Stuplich, M., Schafer, N., Kebir, S., Weller, J., Schaub, C., Stummer, W., Tonn, J. C., Simon, M., Keil, V. C., Nelles, M., Urbach, H., Coenen, M., Wick, W., Weller, M., Fimmers, R., Schmid, M., Hattingen, E., Pietsch, T., Coch, C., Glas, M., and Neurooncology Working Group of the German Cancer, Society (2019). Lomustine-temozolomide combination therapy versus standard temozolomide therapy in patients with newly diagnosed glioblastoma with methylated MGMT promoter (CeTeG/NOA-09): a randomised, open-label, phase 3 trial. Lancet 393, 678-88.
Huang, Y., Che, X., Wang, P. W., and Qu, X. (2024). p53/MDM2 signaling pathway in aging, senescence and tumorigenesis. Semin Cancer Biol 101, 44-57.
Hübner, Jutta, Hartmann, Michael, Wedding, Ulrich, Gießler, Wolfgang, Schuler, Ulrich, and Hochhaus, Andreas (2017). Methadon in der Onkologie: „Strohhalmfunktion“ ohne Evidenz. Dtsch Arztebl International 114, -8470-.
Ichijo, H., Nishida, E., Irie, K., ten Dijke, P., Saitoh, M., Moriguchi, T., Takagi, M., Matsumoto, K., Miyazono, K., and Gotoh, Y. (1997). Induction of apoptosis by ASK1, a mammalian MAPKKK that activates SAPK/JNK and p38 signaling pathways. Science 275, 90-4.
Inturrisi, C. E., Colburn, W. A., Kaiko, R. F., Houde, R. W., and Foley, K. M. (1987). Pharmacokinetics and pharmacodynamics of methadone in patients with chronic pain. Clin Pharmacol Ther 41, 392-401.
Jehle, J., Schweizer, P. A., Katus, H. A., and Thomas, D. (2011). Novel roles for hERG K(+) channels in cell proliferation and apoptosis. Cell Death Dis 2, e193.
Jovanovic, M., Dragoj, M., Zhukovsky, D., Dar'in, D., Krasavin, M., Pesic, M., and Podolski-Renic, A. (2020). Novel TrxR1 Inhibitors Show Potential for Glioma Treatment by Suppressing the Invasion and Sensitizing Glioma Cells to Chemotherapy. Front Mol Biosci 7, 586146.
Kaina, B., Ziouta, A., Ochs, K., and Coquerelle, T. (1997). Chromosomal instability, reproductive cell death and apoptosis induced by O6-methylguanine in Mex-,

Mex+ and methylation-tolerant mismatch repair compromised cells: facts and models. Mutat Res 381, 227-41.
Kaina, B., Beltzig, L., Piee-Staffa, A., and Haas, B. (2020). Cytotoxic and Senolytic Effects of Methadone in Combination with Temozolomide in Glioblastoma Cells. Int J Mol Sci 21.
Kaina, B. (2023). Temozolomide, Procarbazine and Nitrosoureas in the Therapy of Malignant Gliomas: Update of Mechanisms, Drug Resistance and Therapeutic Implications. J Clin Med 12.
Kang, T. W., Yevsa, T., Woller, N., Hoenicke, L., Wuestefeld, T., Dauch, D., Hohmeyer, A., Gereke, M., Rudalska, R., Potapova, A., Iken, M., Vucur, M., Weiss, S., Heikenwalder, M., Khan, S., Gil, J., Bruder, D., Manns, M., Schirmacher, P., Tacke, F., Ott, M., Luedde, T., Longerich, T., Kubicka, S., and Zender, L. (2011). Senescence surveillance of pre-malignant hepatocytes limits liver cancer development. Nature 479, 547-51.
Kast, R. E., Boockvar, J. A., Bruning, A., Cappello, F., Chang, W. W., Cvek, B., Dou, Q. P., Duenas-Gonzalez, A., Efferth, T., Focosi, D., Ghaffari, S. H., Karpel-Massler, G., Ketola, K., Khoshnevisan, A., Keizman, D., Magne, N., Marosi, C., McDonald, K., Munoz, M., Sassoon, D., Pourgholami, M. H., Sardi, I., Sella, A., Srivenugopal, K. S., Tuccori, M., Wang, W., Wirtz, C. R., and Halatsch, M. E. (2013). A conceptually new treatment approach for relapsed glioblastoma: coordinated undermining of survival paths with nine repurposed drugs (CUSP9) by the International Initiative for Accelerated Improvement of Glioblastoma Care. Oncotarget 4, 502-30.
Knizhnik, A. V., Roos, W. P., Nikolova, T., Quiros, S., Tomaszowski, K. H., Christmann, M., and Kaina, B. (2013). Survival and death strategies in glioma cells: autophagy, senescence and apoptosis triggered by a single type of temozolomide-induced DNA damage. PLoS One 8, e55665.
Knobbe, C.B., Reifenberger, J., and Reifenberger, G. (2004). Mutation analysis of the Ras pathway genes NRAS, HRAS, KRAS and BRAF in glioblastomas. Acta Neuropathol 108, 467-70.
Knudsen, E. S., Witkiewicz, A. K., and Rubin, S. M. (2024). Cancer takes many paths through G1/S. Trends Cell Biol 34, 636-45.
Komori, T. (2022). [The 2021 WHO Classification of Tumors, 5th edition, Central Nervous System Tumors: A Short Review]. Brain Nerve 74, 803-09.
Koul, D. (2008). PTEN signaling pathways in glioblastoma. Cancer Biol. Ther 7, 1321-25.
Lamba, N., Wen, P. Y., and Aizer, A. A. (2021). Epidemiology of brain metastases and leptomeningeal disease. Neuro Oncol 23, 1447-56.
Lansu, K., and Gentile, S. (2013). Potassium channel activation inhibits proliferation of breast cancer cells by activating a senescence program. Cell Death Dis 4, e652.
Lee, S. Y. (2016). Temozolomide resistance in glioblastoma multiforme. Genes Dis 3, 198-210.
Liu, Q., Turner, K. M., Alfred Yung, W. K., Chen, K., and Zhang, W. (2014). Role of AKT signaling in DNA repair and clinical response to cancer therapy. Neuro Oncol 16, 1313-23.
Louis, D. N., Perry, A., Wesseling, P., Brat, D. J., Cree, I. A., Figarella-Branger, D., Hawkins, C., Ng, H. K., Pfister, S. M., Reifenberger, G., Soffietti, R., von Deimling, A., and Ellison, D. W. (2021). The 2021 WHO Classification of Tumors of the Central Nervous System: a summary. Neuro Oncol 23, 1231-51.
Marenco-Hillembrand, L., Wijesekera, O., Suarez-Meade, P., Mampre, D., Jackson, C., Peterson, J., Trifiletti, D., Hammack, J., Ortiz, K., Lesser, E., Spiegel, M.,

Prevatt, C., Hawayek, M., Quinones-Hinojosa, A., and Chaichana, K. L. (2020). Trends in glioblastoma: outcomes over time and type of intervention: a systematic evidence based analysis. J Neurooncol 147, 297-307.

Martinez-Jaramillo, E., Jamali, F., Abdalbari, F. H., Abdulkarim, B., Jean-Claude, B. J., Telleria, C. M., and Sabri, S. (2024). Pro-Oxidant Auranofin and Glutathione-Depleting Combination Unveils Synergistic Lethality in Glioblastoma Cells with Aberrant Epidermal Growth Factor Receptor Expression. Cancers (Basel) 16.

Martinez, R., Stuhmer, W., Martin, S., Schell, J., Reichmann, A., Rohde, V., and Pardo, L. (2015). Analysis of the expression of Kv10.1 potassium channel in patients with brain metastases and glioblastoma multiforme: impact on survival. BMC Cancer 15, 839.

McFaline-Figueroa, J. L., Braun, C. J., Stanciu, M., Nagel, Z. D., Mazzucato, P., Sangaraju, D., Cerniauskas, E., Barford, K., Vargas, A., Chen, Y., Tretyakova, N., Lees, J. A., Hemann, M. T., White, F. M., and Samson, L. D. (2015). Minor Changes in Expression of the Mismatch Repair Protein MSH2 Exert a Major Impact on Glioblastoma Response to Temozolomide. Cancer Res 75, 3127-38.

Meuillet, E. J., Mahadevan, D., Berggren, M., Coon, A., and Powis, G. (2004). Thioredoxin-1 binds to the C2 domain of PTEN inhibiting PTEN's lipid phosphatase activity and membrane binding: a mechanism for the functional loss of PTEN's tumor suppressor activity. Arch Biochem Biophys 429, 123-33.

Mojas, N., Lopes, M., and Jiricny, J. (2007). Mismatch repair-dependent processing of methylation damage gives rise to persistent single-stranded gaps in newly replicated DNA. Genes Dev 21, 3342-55.

Munoz, J. L., Walker, N. D., Scotto, K. W., and Rameshwar, P. (2015). Temozolomide competes for P-glycoprotein and contributes to chemoresistance in glioblastoma cells. Cancer Lett 367, 69-75.

Newlands, E. S., Stevens, M. F., Wedge, S. R., Wheelhouse, R. T., and Brock, C. (1997). Temozolomide: a review of its discovery, chemical properties, pre-clinical development and clinical trials. Cancer Treat Rev 23, 35-61.

Ohgaki, H., and Kleihues, P. (2009). Genetic alterations and signaling pathways in the evolution of gliomas. Cancer Sci 100, 2235-41.

Oppermann, H., Matusova, M., Glasow, A., Dietterle, J., Baran-Schmidt, R., Neumann, K., Meixensberger, J., and Gaunitz, F. (2019). D,L-Methadone does not improve radio- and chemotherapy in glioblastoma in vitro. Cancer Chemother Pharmacol 83, 1017-24.

Pardo, L. A., and Stuhmer, W. (2014). The roles of K(+) channels in cancer. Nat Rev Cancer 14, 39-48.

Park, Y. W., Vollmuth, P., Foltyn-Dumitru, M., Sahm, F., Ahn, S. S., Chang, J. H., and Kim, S. H. (2023). The 2021 WHO Classification for Gliomas and Implications on Imaging Diagnosis: Part 1-Key Points of the Fifth Edition and Summary of Imaging Findings on Adult-Type Diffuse Gliomas. J Magn Reson Imaging 58, 677-89.

Pegg, A. E. (2000). Repair of O(6)-alkylguanine by alkyltransferases. Mutat Res 462, 83-100.

Pelloski, C.E., Lin, E., Zhang, L., Yung, W.K., Colman, H., Liu, J.L., Woo, S.Y., Heimberger, A.B., Suki, D., Prados, M., Chang, S., Barker, F.G., III, Fuller, G.N., and Aldape, K.D. (2006). Prognostic associations of activated mitogen-activated protein kinase and Akt pathways in glioblastoma. Clin Cancer Res 12, 3935-41.

Perazzoli, G., Prados, J., Ortiz, R., Caba, O., Cabeza, L., Berdasco, M., Gonzalez, B., and Melguizo, C. (2015). Temozolomide Resistance in Glioblastoma Cell Lines:

Implication of MGMT, MMR, P-Glycoprotein and CD133 Expression. PLoS One 10, e0140131.
Pointer, K. B., Clark, P. A., Eliceiri, K. W., Salamat, M. S., Robertson, G. A., and Kuo, J. S. (2017). Administration of Non-Torsadogenic human Ether-a-go-go-Related Gene Inhibitors Is Associated with Better Survival for High hERG-Expressing Glioblastoma Patients. Clin Cancer Res 23, 73-80.
Powis, G., and Montfort, W. R. (2001). Properties and biological activities of thioredoxins. Annu Rev Pharmacol Toxicol 41, 261-95.
Price, M., Ballard, C., Benedetti, J., Neff, C., Cioffi, G., Waite, K. A., Kruchko, C., Barnholtz-Sloan, J. S., and Ostrom, Q. T. (2024). CBTRUS Statistical Report: Primary Brain and Other Central Nervous System Tumors Diagnosed in the United States in 2017-2021. Neuro Oncol 26, vi1-vi85.
Quiros, S., Roos, W. P., and Kaina, B. (2010). Processing of O6-methylguanine into DNA double-strand breaks requires two rounds of replication whereas apoptosis is also induced in subsequent cell cycles. Cell Cycle 9, 168-78.
Ray, P. D., Huang, B. W., and Tsuji, Y. (2012). Reactive oxygen species (ROS) homeostasis and redox regulation in cellular signaling. Cell Signal 24, 981-90.
Riedel, M., Struve, N., Muller-Goebel, J., Kocher, S., Petersen, C., Dikomey, E., Rothkamm, K., and Kriegs, M. (2016). Sorafenib inhibits cell growth but fails to enhance radio- and chemosensitivity of glioblastoma cell lines. Oncotarget 7, 61988-95.
RKI, 2023. Krebs in Deutschland für 2019/2020. 14. Ausgabe. Robert Koch-Institut (Hrsg) und die Gesellschaft der epidemiologischen Krebsregister in Deutschland e.V. (Hrsg). Berlin, 2023.
Rojo, L. E., Alzate-Morales, J., Saavedra, I. N., Davies, P., and Maccioni, R. B. (2010). Selective interaction of lansoprazole and astemizole with tau polymers: potential new clinical use in diagnosis of Alzheimer's disease. J Alzheimers Dis 19, 573-89.
Roos, W. P., Batista, L. F., Naumann, S. C., Wick, W., Weller, M., Menck, C. F., and Kaina, B. (2007). Apoptosis in malignant glioma cells triggered by the temozolomide-induced DNA lesion O6-methylguanine. Oncogene 26, 186-97.
Roos, W. P., Thomas, A. D., and Kaina, B. (2016). DNA damage and the balance between survival and death in cancer biology. Nat Rev Cancer 16, 20-33.
Ruhland, M. K., Loza, A. J., Capietto, A. H., Luo, X., Knolhoff, B. L., Flanagan, K. C., Belt, B. A., Alspach, E., Leahy, K., Luo, J., Schaffer, A., Edwards, J. R., Longmore, G., Faccio, R., DeNardo, D. G., and Stewart, S. A. (2016). Stromal senescence establishes an immunosuppressive microenvironment that drives tumorigenesis. Nat Commun 7, 11762.
Ruscetti, M., Leibold, J., Bott, M. J., Fennell, M., Kulick, A., Salgado, N. R., Chen, C. C., Ho, Y. J., Sanchez-Rivera, F. J., Feucht, J., Baslan, T., Tian, S., Chen, H. A., Romesser, P. B., Poirier, J. T., Rudin, C. M., de Stanchina, E., Manchado, E., Sherr, C. J., and Lowe, S. W. (2018). NK cell-mediated cytotoxicity contributes to tumor control by a cytostatic drug combination. Science 362, 1416-22.
Saitoh, M., Nishitoh, H., Fujii, M., Takeda, K., Tobiume, K., Sawada, Y., Kawabata, M., Miyazono, K., and Ichijo, H. (1998). Mammalian thioredoxin is a direct inhibitor of apoptosis signal-regulating kinase (ASK) 1. EMBO J 17, 2596-606.
Salam, R., Saliou, A., Bielle, F., Bertrand, M., Antoniewski, C., Carpentier, C., Alentorn, A., Capelle, L., Sanson, M., Huillard, E., Bellenger, L., Guegan, J., and Le Roux, I. (2023). Cellular senescence in malignant cells promotes tumor progression in mouse and patient Glioblastoma. Nat Commun 14, 441.

Saleh, T., Tyutyunyk-Massey, L., and Gewirtz, D. A. (2019). Tumor Cell Escape from Therapy-Induced Senescence as a Model of Disease Recurrence after Dormancy. Cancer Res 79, 1044-46.

Shugg, T., Dave, N., Amarh, E., Assiri, A. A., Pollok, K. E., and Overholser, B. R. (2021). Letrozole targets the human ether-a-go-go-related gene potassium current in glioblastoma. Basic Clin Pharmacol Toxicol 128, 357-65.

Stupp, R., Mason, W.P., van den Bent, M.J., Weller, M., Fisher, B., Taphoorn, M.J., Belanger, K., Brandes, A.A., Marosi, C., Bogdahn, U., Curschmann, J., Janzer, R.C., Ludwin, S.K., Gorlia, T., Allgeier, A., Lacombe, D., Cairncross, J.G., Eisenhauer, E., and Mirimanoff, R.O. (2005). Radiotherapy plus concomitant and adjuvant temozolomide for glioblastoma. N. Engl. J. Med 352, 987-96.

Stupp, R., Hegi, M.E., Mason, W.P., van den Bent, M.J., Taphoorn, M.J., Janzer, R.C., Ludwin, S.K., Allgeier, A., Fisher, B., Belanger, K., Hau, P., Brandes, A.A., Gijtenbeek, J., Marosi, C., Vecht, C.J., Mokhtari, K., Wesseling, P., Villa, S., Eisenhauer, E., Gorlia, T., Weller, M., Lacombe, D., Cairncross, J.G., and Mirimanoff, R.O. (2009). Effects of radiotherapy with concomitant and adjuvant temozolomide versus radiotherapy alone on survival in glioblastoma in a randomised phase III study: 5-year analysis of the EORTC-NCIC trial. Lancet Oncol 10, 459-66.

Stupp, R., Taillibert, S., Kanner, A., Read, W., Steinberg, D., Lhermitte, B., Toms, S., Idbaih, A., Ahluwalia, M. S., Fink, K., Di Meco, F., Lieberman, F., Zhu, J. J., Stragliotto, G., Tran, D., Brem, S., Hottinger, A., Kirson, E. D., Lavy-Shahaf, G., Weinberg, U., Kim, C. Y., Paek, S. H., Nicholas, G., Bruna, J., Hirte, H., Weller, M., Palti, Y., Hegi, M. E., and Ram, Z. (2017). Effect of Tumor-Treating Fields Plus Maintenance Temozolomide vs Maintenance Temozolomide Alone on Survival in Patients With Glioblastoma: A Randomized Clinical Trial. JAMA 318, 2306-16.

Sun, A. G., Lin, A. Q., Huang, S. Y., Huo, D., and Cong, C. H. (2016). Identification of potential drugs for Parkinson's disease based on a sub-pathway method. Int J Neurosci 126, 318-25.

Switzeny, O. J., Christmann, M., Renovanz, M., Giese, A., Sommer, C., and Kaina, B. (2016). MGMT promoter methylation determined by HRM in comparison to MSP and pyrosequencing for predicting high-grade glioma response. Clin Epigenetics 8, 49.

Tentori, L., Portarena, I., Torino, F., Scerrati, M., Navarra, P., and Graziani, G. (2002). Poly(ADP-ribose) polymerase inhibitor increases growth inhibition and reduces G(2)/M cell accumulation induced by temozolomide in malignant glioma cells. Glia 40, 44-54.

Teraiya, M., Perreault, H., and Chen, V. C. (2023). An overview of glioblastoma multiforme and temozolomide resistance: can LC-MS-based proteomics reveal the fundamental mechanism of temozolomide resistance? Front Oncol 13, 1166207.

Toplak, Z., Hendrickx, L. A., Abdelaziz, R., Shi, X., Peigneur, S., Tomasic, T., Tytgat, J., Peterlin-Masic, L., and Pardo, L. A. (2022). Overcoming challenges of HERG potassium channel liability through rational design: Eag1 inhibitors for cancer treatment. Med Res Rev 42, 183-226.

Toso, A., Revandkar, A., Di Mitri, D., Guccini, I., Proietti, M., Sarti, M., Pinton, S., Zhang, J., Kalathur, M., Civenni, G., Jarrossay, D., Montani, E., Marini, C., Garcia-Escudero, R., Scanziani, E., Grassi, F., Pandolfi, P. P., Catapano, C. V., and Alimonti, A. (2014). Enhancing chemotherapy efficacy in Pten-deficient

prostate tumors by activating the senescence-associated antitumor immunity. Cell Rep 9, 75-89.
Vatter, T., Klumpp, L., Ganser, K., Stransky, N., Zips, D., Eckert, F., and Huber, S. M. (2020). Against Repurposing Methadone for Glioblastoma Therapy. Biomolecules 10.
Wang, X., Chen, Y., Zhang, Y., Guo, S., Mo, L., An, H., and Zhan, Y. (2017). Eag1 Voltage-Dependent Potassium Channels: Structure, Electrophysiological Characteristics, and Function in Cancer. J Membr Biol 250, 123-32.
Weller, M., van den Bent, M., Preusser, M., Le Rhun, E., Tonn, J. C., Minniti, G., Bendszus, M., Balana, C., Chinot, O., Dirven, L., French, P., Hegi, M. E., Jakola, A. S., Platten, M., Roth, P., Ruda, R., Short, S., Smits, M., Taphoorn, M. J. B., von Deimling, A., Westphal, M., Soffietti, R., Reifenberger, G., and Wick, W. (2021). EANO guidelines on the diagnosis and treatment of diffuse gliomas of adulthood. Nat Rev Clin Oncol 18, 170-86.
Weller, M., Wen, P. Y., Chang, S. M., Dirven, L., Lim, M., Monje, M., and Reifenberger, G. (2024). Glioma. Nature Reviews Disease Primers 10.
Weller, Michael, Knobbe-Thomsen, Christiane B., Le Rhun, Emilie, and Reifenberger, Guido (2022). Die WHO-Klassifikation der Tumoren des zentralen Nervensystems 2021. Der Onkologe 28, 155-63.
Westhoff, M.A., Karpel-Massler, G., Bruhl, O., Enzenmuller, S., La Ferla-Bruhl, K., Siegelin, M.D., Nonnenmacher, L., and Debatin, K.M. (2014). A critical evaluation of PI3K inhibition in Glioblastoma and Neuroblastoma therapy. Mol. Cell Ther 2, 32.
Whicher, J. R., and MacKinnon, R. (2016). Structure of the voltage-gated K(+) channel Eag1 reveals an alternative voltage sensing mechanism. Science 353, 664-9.
Wick W. et al., Gliome, S2k-Leitlinie, 2021, in: Deutsche Gesellschaft für Neurologie (Hrsg.), Leitlinien für Diagnostik und Therapie in der Neurologie. Online: www.dgn.org/leitlinien (abgerufen am 23.02.2025).
Wiewrodt, D., Nagel, G., Dreimuller, N., Hundsberger, T., Perneczky, A., and Kaina, B. (2008). MGMT in primary and recurrent human glioblastomas after radiation and chemotherapy and comparison with p53 status and clinical outcome. Int J Cancer 122, 1391-9.
Wirsching, H. G., Galanis, E., and Weller, M. (2016). Glioblastoma. Handb Clin Neurol 134, 381-97.
Witkiewicz, A. K., Knudsen, K. E., Dicker, A. P., and Knudsen, E. S. (2011). The meaning of p16(ink4a) expression in tumors: functional significance, clinical associations and future developments. Cell Cycle 10, 2497-503.
Wulff, H., Castle, N. A., and Pardo, L. A. (2009). Voltage-gated potassium channels as therapeutic targets. Nat Rev Drug Discov 8, 982-1001.
Xue, W., Zender, L., Miething, C., Dickins, R. A., Hernando, E., Krizhanovsky, V., Cordon-Cardo, C., and Lowe, S. W. (2007). Senescence and tumour clearance is triggered by p53 restoration in murine liver carcinomas. Nature 445, 656-60.
Yao, A., Storr, S. J., Al-Hadyan, K., Rahman, R., Smith, S., Grundy, R., Paine, S., and Martin, S. G. (2020). Thioredoxin System Protein Expression Is Associated with Poor Clinical Outcome in Adult and Paediatric Gliomas and Medulloblastomas. Mol Neurobiol 57, 2889-901.
Yoshimoto, S., Loo, T. M., Atarashi, K., Kanda, H., Sato, S., Oyadomari, S., Iwakura, Y., Oshima, K., Morita, H., Hattori, M., Honda, K., Ishikawa, Y., Hara, E., and Ohtani, N. (2013). Obesity-induced gut microbial metabolite promotes liver cancer through senescence secretome. Nature 499, 97-101.

Zhang, J., Li, X., Han, X., Liu, R., and Fang, J. (2017a). Targeting the Thioredoxin System for Cancer Therapy. Trends Pharmacol Sci 38, 794-808.
Zhang, L., Pitcher, L. E., Prahalad, V., Niedernhofer, L. J., and Robbins, P. D. (2023). Targeting cellular senescence with senotherapeutics: senolytics and senomorphics. FEBS J 290, 1362-83.
Zhang, P., Gao, J., Wang, X., Wen, W., Yang, H., Tian, Y., Liu, N., Wang, Z., Liu, H., Zhang, Y., and Tu, Y. (2017b). A novel indication of thioredoxin-interacting protein as a tumor suppressor gene in malignant glioma. Oncol Lett 14, 2053-58.
Zhao, H. F., Wang, J., Shao, W., Wu, C. P., Chen, Z. P., To, S. T., and Li, W. P. (2017). Recent advances in the use of PI3K inhibitors for glioblastoma multiforme: current preclinical and clinical development. Mol Cancer 16, 100.
Zheng, Z., and Song, Y. (2023). Integrated analysis of the voltage-gated potassium channel-associated gene KCNH2 across cancers. BMC Bioinformatics 24, 51.
Zunkler, B. J. (2006). Human ether-a-go-go-related (HERG) gene and ATP-sensitive potassium channels as targets for adverse drug effects. Pharmacol Ther 112, 12-37.

8 Danksagung

Es gibt zwei Personen in meinem wissenschaftlichen Leben, die mich sehr positiv geprägt haben und denen ich meinen besonderen Dank ausdrücken möchte. An erster Stelle wäre hier Prof. Dr. Alexander Pfeifer zu nennen, der bereits mein Doktorvater war und mich auch jetzt bei der Erstellung dieser Arbeit als Fachvertreter immer unterstützt hat. Von ihm habe ich lernen dürfen, was akkurates, wissenschaftliches Arbeiten heißt und es sich lohnt hartnäckig zu bleiben und ein Ziel zu verfolgen, auch wenn es manchmal aussichtslos erscheint. Die wohl wichtigste, wissenschaftliche Weisheit, die er mir mit auf dem Weg gegeben hat, beherzige ich bis heute: „Qualität setzt sich am Ende durch!“

Nach meiner Zeit am Institut für Pharmakologie und Toxikologie lernte ich Prof. Dr. Niels Eckstein als geschätzten Kollegen und Freund am BfArM kennen. Er war es, der mich dazu motiviert hat, am BfArM weiter in der Forschung am Ball zu bleiben, zu publizieren, meine Lehrtätigkeit zu intensivieren und schlussendlich das Projekt Habilitation in Angriff zu nehmen. Niels ist leider viel zu früh im Alter von 52 Jahren verstorben und hat uns und insbesondere seine Frau und seine beiden Söhne in tiefer Trauer hinterlassen. Ich möchte Niels diese Arbeit widmen und ihm auf diesem Wege meine Dankbarkeit ausdrücken für all das, was er mir ermöglicht hat.

Ein großer Dank geht auch an Prof. Dr. Jochen Zünkler und Prof. emer. Dr. Bernd Kaina, die mich beide wissenschaftlich immer motiviert haben und jederzeit verlässliche Kollegen und Kooperationspartner in vielen gemeinsamen Projekten waren. Daneben möchte ich meinen Dank auch PD Dr. Elke Röhrdanz und Dr. Roland Frötschl aussprechen, die mir am BfArM gute Kollegen/Innen und Vorgesetzte sind und waren und mich bei allen wissenschaftlichen Projekten immer unterstützt und gefördert haben.

Zu guter Letzte gilt der größte Dank meiner Frau und meinen beiden Kindern, die immer als ruhender Pol und ausgleichende Kraft an meiner Seite stehen.